STILL WATCHING TREES GROW:

A MULTISPECIES AND CROSS-SCALE EXAMINATION OF THE RADIAL GROWTH, CLIMATE, AND CARBON INTERFACE

A Thesis Submitted to the
College of Graduate and Postdoctoral Studies
In Partial Fulfillment of the Requirements
For the Degree of Doctor of Philosophy
In the School of Environment and Sustainability
University of Saskatchewan
Saskatoon

By

JASON MAILLET

© Copyright Jason Maillet, September 2020. All rights reserved.

PERMISION TO USE

In presenting this thesis/dissertation in partial fulfillment of the requirements for a Postgraduate degree from the University of Saskatchewan, I agree that the Libraries of this University may make it freely available for inspection. I further agree that permission for copying of this thesis/dissertation in any manner, in whole or in part, for scholarly purposes may be granted by the professor or professors who supervised my thesis/dissertation work or, in their absence, by the Head of the Department or the Dean of the College in which my thesis work was done. It is understood that any copying or publication or use of this thesis/dissertation or parts thereof for financial gain shall not be allowed without my written permission. It is also understood that due recognition shall be given to me and to the University of Saskatchewan in any scholarly use which may be made of any material in my thesis/dissertation.

Requests for permission to copy or to make other uses of materials in this thesis/dissertation in whole or part should be addressed to:

School of Environment and Sustainability

University of Saskatchewan

Room 323 Kirk Hall, 117 Science Place

Saskatoon, Saskatchewan, S7N 5C8, Canada

OR

Dean

College of Graduate and Postdoctoral Studies

University of Saskatchewan

116 Thorvaldson Building, 110 Science Place

Saskatoon, Saskatchewan, S7N 5C9, Canada

ABSTRACT

Climate change is progressing at a rapid pace, especially in northern regions, where the most dramatic land surface warming is occurring. Boreal ecosystems are therefore situated in an area which is particularly susceptible to the impacts of climate change. This dissertation represents a comprehensive assessment of the interactions between tree growth, climate, and carbon at multiple temporal scales in the southern boreal forest. The goal of this work is to better understand the potential impacts of climate change on boreal forest growth and carbon dynamics in this region. The collection of research contained herein took place at the Boreal Ecosystem Research and Monitoring Sites (BERMS), Old Jack Pine (OJP), Old Black Spruce (OBS), and Old Aspen (OA). Located in the southern boreal forest of Saskatchewan, these sites represent one of the most comprehensive collections of long-term high-resolution carbon (C) flux data, alongside of which comes an equally impressive suite of meteorological data. To supplement these data, I collected high-resolution stem size data of the dominant and co-dominant tree species at these sites: jack pine (*Pinus banksiana*), black spruce (*Picea mariana*), eastern larch (*Larix laricina*), and trembling aspen (*Populus tremuloides*) between 2015 and 2018 (the short-term observation period). I also collected tree cores from jack pine, black spruce, and trembling aspen, to extend the radial growth record backwards to stand establishment (~ 100 years; the long-term observation period), and contributed the latest in a series of repeated inventory style measurements which make up a two-decade long record (1994 – 2016) of forest C stocks and fluxes at OJP and OA (the medium-term observation period).

Chapter 2 presents a multiscale dendroclimatological assessment of jack pine, black spruce, eastern larch, and trembling aspen. I find shifting growth/climate relationships at annual-scale resolution over the long term (~100 years), including a weakening of the relationship between radial growth and precipitation and an enhanced positive relationship between radial growth and spring and summer air temperature over time. Like the divergence problem, which highlights issues of non-stationarity in the growth/climate relationship in trees further north, I attribute the cause of this dynamic relationship to shifting limitations. In this case, the change likely signals a decrease in moisture limitations and a positive response to recent warming. Over intra-annual scales, during the short-term observation period (2015 – 2018), I find evidence of a positive relationship between daily stem radius change (ΔR) and air temperature within the

growing season. However, this relationship was only significant when moisture requirements were met, calling reference to the importance of moisture and its role in supporting the relationship between radial growth, or tracheid cell production, and temperature.

Changes in moisture conditions in the Canadian boreal forest, both historically and moving forward, are spatially variable across the landscape. In Prince Albert, Saskatchewan, where the nearest and most complete long-term record of climate is recorded, conditions have been warming and wetting since 1890 (Appendix D). It is likely that the BERMS sites are situated in a region where an increase in evaporative demand in response to recent warming has, to date, been successfully offset by a co-occurring increase in precipitation, resulting in a net increase in available moisture. This is likely having a positive impact on tree growth in this region, but one which is unlikely to persist as rates of evapotranspiration are expected to overshadow any gains in moisture related to an increase in precipitation over the long term.

In Chapter 3, I apply analytical techniques analogous to those from the dendroclimatological assessment completed in Chapter 2, in this case they are applied to the study of radial growth and stem radius change, and its relationship with ecosystem C-flux over the medium- and short-terms. Overall my findings are similar to those from other recent studies. At annual scale resolution, only the radial growth of jack pine was significantly and positively correlated with ecosystem production (net ecosystem production; NEP) over the medium term (~20 years). Comparatively, black spruce and trembling aspen are more likely to rely situationally on stored carbohydrates, introducing the potential for inconsistency in the relationship between ecosystem production (uptake) and radial growth (allocation). During the observation period (2000 – 2018), the annual radial growth of jack pine benefited from non-structural carbohydrate storage from the previous fall and from elevated levels of NEP during the current spring. Over intra-annual scales, there was effectively no evidence of a relationship between stem size and measures of ecosystem C-flux during the short-term observation period (2015 – 2018). Perceived relationships between these variables over fine temporal scales were likely spurious, driven by a combination of factors, including but not limited to precipitation and soil temperature.

In Chapter 4, I identify large-scale changes in the distribution of carbon across the landscape at OJP and OA over the medium term (between 1994 – 2016). The most notable stock

changes occurred during periods of enhanced tree mortality, likely resulting from moisture stress at OA, and windthrow at OJP. There is evidence that ecosystem level production was also impacted during periods of enhanced tree mortality, however this differed between the two sites. Tree level net primary production (NPP_{Tree}) decreased at OJP in response to enhanced mortality, yet it was maintained at a relatively stable level at OA regardless of the mortality rate. The deciduous trees here were likely more capable of taking advantage of holes in the canopy by increasing their production efficiency. As for eddy covariance based net ecosystem production (NEP_{EC}), the opposite pattern was observed. NEP_{EC} was maintained at a stable level at OJP, and was notably depressed during a period of increased mortality at OA.

In summary, over the near term, warming and wetting may continue to benefit the radial growth of several tree species in the southern boreal forest of Saskatchewan, where moisture has long represented the main limiting factor. However, in mature trembling aspen dominated stands, an increase in available moisture may contribute to moderate disturbance, resulting in enhanced tree mortality and a significant flux of carbon from biomass to necromass. Moving forward, rates of evapotranspiration are expected to overshadow any gains in moisture related to an increase in precipitation. Under these circumstances, species in the southern boreal forest will need to rely more heavily on effective precipitation and root-zone soil moisture to support their growth. Under extreme water limitations, we are likely to see a negative response to warm air temperature, reduced growth rates, and enhanced tree mortality. Lastly, wind likely represents an important agent of change in mature jack pine stands. An increase in the incidence and intensity of extreme storms and high winds due to climate change will likely lead to more frequent high-impact disturbance in the boreal forest. While mature jack pine stands may be particularly vulnerable to this type of disturbance, this is likely to have widespread impacts in a range of boreal forest stands.

While the findings from this and other studies help to improve our understanding of the impacts of climate change on boreal forest trees, more work is needed. Relationships between radial-tree growth and climate in the Canadian boreal forest are regionally defined and species specific, requiring widespread and comprehensive study. In the meantime, when forecasting change in the boreal forest, we must be careful not to paint this diverse biome with too wide a brush.

ACKNOWLEDGEMENTS

Well it's been a long haul. I feel it's been longer than five years, but simply because of all the amazing experiences I've collected in that time. I've spent countless hours in the field, on the road, on campus, and in the lab with some truly amazing people. I've spent time in the classroom, coming into my own as an educator; on stage, growing as a performer and supporter of local live music; in the climbing gym, scrambling up walls; and in the coffee shop, as a tweaked out graduate student hammering out this document.

There are so many people who have helped me along the way that I need to thank. But most of all, I need to thank Noel, for supporting me in every sense of the word. You've been there every step of the way, and for this I can never repay you. Thank you for believing in me, for encouraging me, for pushing me, for putting up with me, and for loving me. I love you right back. Also, thanks for picking up random cats on the sidewalk against my better judgement (Love and miss you Fisher), for spearheading the adoption of another furdude (Love you Frappuccino-man), for going on adventures with me, for putting up with me again, and for being my sugar momma when my funding ran out. I look forward to seeing what the future has in store for us. Love you lots.

A huge thank you to my friend and mentor Dr. Colin Laroque, for bankrolling our lunches from Safeway in Prince Albert, for dealing with the fallout after I decided to ramp the quad off the back of the truck, and for dealing with the fallout after I decided to have one too many drinks at Steamworks or Blue on Whyte. In all seriousness, I would not be where I am today if it wasn't for you, and for this I am forever grateful. Thank you for your unconditional support and for everything you've done for me.

Thank you to my friends and family here in Saskatoon, and back home in New Brunswick. Most importantly, to my Mom, Dad, and Mémère for being my biggest supporters back home while only barely understanding what I do. Granted, I'm often in the same boat. I love you guys.

Thank you to my committee members, Alan Barr, Barrie Bonsal, Andrew Ireson, and Warren Helgason for your guidance and support.

Thank you to the people I've dragged through the hazelnut at Old Aspen, or ridden bikes with on the sketchy boardwalk at Old Black Spruce, or shared mayonnaise based salads with at Old Jack Pine, or been miserable with / gotten lost with / walked barefoot with / nearly frozen to death with at Fen. Namely, Magali Nehemy, Scott Wood, Gary Beckhusen, Beckett Stark, Owen Laroque, Inge Verbeek, Nia Perron, Megan Horachek, Brooke Howat, Rafaella Mayrinck, Tiara Jackle, and Ben Nykiforuk.

And finally, a big thanks to the MAD Lab family, new and old. To those who have helped me out throughout this process or who have simply shared the lab with me: Bryan, Zach, Lindsey, Sheri, Teagan, Chloe, Annette, Reanna, Cassidy, Nicole, Victoria, Aaron, and Kristi.

TABLE OF CONTENTS

LIST OF TABLES

LIST OF FIGURES

LIST OF ABBREVIATIONS

IPCC	Intergovernmental Panel on Climate Change
NOAA	National Oceanic and Atmospheric Administration
C	Carbon
CO_2	Carbon Dioxide
EC	Eddy Covariance
NEE	Net Ecosystem Exchange
GEP	Gross Ecosystem Production
R_E	Ecosystem Respiration
NEP	Net Ecosystem Production
R_A	Autotrophic Respiration
R_H	Heterotrophic Respiration
NPP	Net Primary Production
GPP	Gross Primary Production
NSCs	Non-Structural Carbohydrates
DR	Stem Radius Change

BOREAS	Boreal Ecosystems Atmosphere Study
NSA	Northern Study Area
SSA	Southern Study Area
BERMS	Boreal Ecosystem Research and Monitoring Sites
OJP	Old Jack Pine
OBS	Old Black Spruce
OA	Old Aspen
VWC	Volumetric Water Content
m	Meter
cm	Centimeter
mm	Millimeter
µm	Micrometer
ΔR	Stem Radius Change
ECCC	Environment and Climate Change Canada
Rmean	Mean Stem Radius
Rmin	Minimum Stem Radius
Rmax	Maximum Stem Radius
ITRDB	International Tree Ring Databank
MAD Lab	Mistik Askiwin Dendrochronology Laboratory
C stock	Carbon Stock
NPP_{Tree}	Tree Level Net Primary Production

NEP_{EC}	Eddy Covariance Based Measure of Net Ecosystem Production
NEP_{Bio}	Biometric Measure of Net Ecosystem Production
VPD	Vapor Pressure Deficit
yr	Year
gC/m^2yr	Grams of Carbon per Meter Square per Year
tC/ha	Tons of Carbon per Hectare
Pg	Petagrams
PET	Potential Evapotranspiration
EC	Eddy Covariance
B	Living Biomass
SD	Standing Dead
DBH	Diameter at Breast Height
DWD	Downed Woody Debris
V	Volume
FF	Forest Floor
ΔC	Change in Total Ecosystem Carbon
LA	Eastern Larch

CHAPTER 1

INTRODUCTION

1.1 Boreal Forest Extent

Spanning approximately 1.2 billion hectares, the circumpolar boreal forest comprises about one third (33%) of global forests (Ruckstuhl et al., 2008; FAO 2015) and almost three quarters (73%) of the earth's coniferous forests (Kuusela, 1992). A little over one quarter (25%-28%) of the circumpolar boreal is located within Canada (Kuusela, 1992; Brandt, 2009; FAO 2015), covering just under a third (30%) of the entire Canadian landscape (Brandt, 2009). Despite a significant amount of industrial activity in the Canadian boreal forest, with over half (54%) classified as managed for commercial use (Brandt et al., 2013), much of the boreal forest in Canada remains relatively unfragmented by roads or settlement (Ruckstuhl et al., 2008), thus providing substantial opportunity for conservation and adaptive management moving forward.

Forest stand composition in the Canadian boreal is relatively simple, limited to a little over a dozen tree species (Soja et al., 2007; Brandt, 2009). Tree species with the greatest relative abundance include white spruce (Picea glauca), black spruce (Picea mariana), eastern larch (Larix laricina), jack pine (Pinus banksiana), and trembling aspen (Populous tremuloides). These five species are most widely distributed across the Canadian boreal forest and often dominate the canopy (Brandt, 2009). Their distribution is based on complex interactions between several factors including climate, site characteristics, and disturbance (Soja et al., 2007). In the north, stand assemblage and distribution is governed primarily by temperature and growing season length, with tree line coinciding approximately with the 6°C isotherm for mean temperature during the growing season, or the 10°C isotherm for mean temperature during the warmest month (Sellers et al., 1995; Körner, 2003). Along the southern edge of the boreal forest, in central and western Canada, main drivers include the moisture regime, natural disturbance, and land use change (Sellers et al., 1995; Ireson et al., 2015). The location of treeline at the southern edge of the boreal forest is in large part governed by moisture. South of the boreal forest in Saskatchewan, where there is insufficient moisture to naturally support more diverse forest assemblages, we find the aspen parkland (a transitional ecozone), and grassland ecosystems.

1.2 Climate Change and its Impacts

Despite the ongoing spread of misinformation, and accusations of climate "alarmism" directed towards the scientific community, it has been suggested that scientists are in fact more likely to present conservative estimates when discussing rates of climate change (Brysse et al., 2013). It is therefore unsurprising that a wide range of climatic changes are occurring more rapidly than originally anticipated (Soja et al., 2007). The most cited of which is the observed increase in land surface and ocean temperature (IPCC 2013). It has been suggested that, as a society, we have likely already committed to over 1.5°C of mean land surface warming regardless of the actions taken today to avoid this outcome (Huntingford and Mercado, 2016). The most significant warming is expected in the north, above 50 degrees latitude (IPCC, 2013; Xia et al., 2014; Huntingford and Mercado, 2016). The Canadian boreal forest is therefore likely already committed to land surface warming well above 2°C (Huntingford and Mercado, 2016). The most recent data collected by the National Oceanic and Atmospheric Administration (NOAA) show that eight of the ten warmest years on record since 1880 occurred within the last decade (prior to 2019), and the last four years, 2015, 2016, 2017, and 2018, ranked 2nd, 1st, 3rd, and 4th, respectively (NOAA, 2019a). According to these data, global surface temperature anomalies, compared with a base period of 1901 – 2000, are already approaching 1°C over land and ocean, and 1.5°C over land only (NOAA, 2019b). Meanwhile, much of northern Canada has already experienced an increase in annual average temperature surpassing 2°C since 1948 (Bush and Lemmen, 2019).

Trends in moisture conditions over the last several decades are spatially variable across the Canadian boreal, with a marked drying trend across much of central and western Canada, while northeastern Canada appears to be trending towards wetter conditions (Wang et al., 2014; Bush and Lemmen, 2019). Moving forward, mean annual precipitation is projected to increase across the Canadian boreal, with the most notable changes to occur over the winter and spring months (Henderson and Sauchyn 2008; Jeong et al., 2014). However, gains in precipitation are likely to be offset by an increase in evapotranspiration over the long term, leading to a net increase in the frequency and severity of drought, especially in central and western Canada (Wang et al., 2014).

In response to this expected intensification of drought, reduced growth rates and widespread tree mortality are expected worldwide (Allen et al., 2010). In Canada, such impacts are already being felt. A significant increase in mortality rates has been reported in a wide range of forest ecosystems across the country, with the most pervasive effects being felt in western Canada (Peng et al., 2011; Michaelian et al., 2011). Tree mortality in western Canada is occurring at 2.6 times the rate observed in eastern Canada, and is significantly correlated with increasing temperature and moisture deficit (Peng et al., 2011).

An increase in atmospheric CO_2 and the resulting land surface warming could have some positive impacts on the Canadian boreal forest. In controlled experiments, it has been shown that CO_2 fertilization can lead to a moderate increase in tree growth and water use efficiency (Field et al., 1995; Ainsworth and Long, 2005; Norby et al., 2005). However, field-based studies on this subject are far less conclusive, often reporting little to no measurable impact of CO_2 fertilization (Huang et al., 2007; Gedalof and Berg, 2010; Girardin et al., 2011). Several studies have reported on a measurable lengthening of the growing season due to the recent warming trend (Linderholm, 2006; Piao et al., 2007). In response, boreal forest vegetation exhibits general trends towards earlier greening, later dormancy, and enhanced productivity, all contributing to a measurable increase in annual primary production (Piao et al., 2007). It has been suggested that a further lengthening of the growing season could lead to a measurable increase in the annual-radial growth of several boreal forest trees (Huang et al., 2010). With warmer temperatures in the north also comes an expected change in boreal forest species distribution and a northward advance of treeline (Overpeck et al., 1991). In a more recent global-scale meta-analysis, undertaken by Harsch et al. (2009), treeline advance was recorded in just over half of the surveyed sites.

Beyond the direct physiological response of trees to changes in climate, there exists several other factors that influence boreal forest health in Canada. The fire regime is often cited as the most significant factor controlling ecological processes and structure in the boreal forest (Weber and Flannigan 1997; Tardif et al., 2016). Climate change is expected to significantly alter the fire regime in Canada, with an expected lengthening of the fire season, and an increase in both fire frequency and severity (Weber and Flannigan, 1997). It is further suggested that the greatest increase in fire weather severity is likely to occur in the Boreal Plains of Saskatchewan

and Alberta (Wang et al., 2015). Wind represents another agent of disturbance with potential to be exaserbated by climate change, due to an expected increase in the incidence and intensity of extreme storms and high winds (IPCC, 2013). This will lead to more frequent high impact disturbance in vulnerable stands across the boreal forest. Jack pine and trembling aspen dominated stands are identified as being particularly susceptible to windthrow (Rich et al., 2007). Insect outbreak is also expected to increase in both incidence and intensity, in large part due to warming during the spring and winter (Volney and Fleming, 2000). While insect outbreak is ecologically damaging in and of itself, at times accounting for over one-third of annual forest loss in Canada (Volney and Fleming, 2000), trees are more susceptible to wildfire post-outbreak, representing one of many positive feedbacks capable of further intensifying the impacts of climate change.

Another example of a positive feedback occurring in the Canadian boreal is the decrease in albedo associated with advancing treeline in the north (Soja et al., 2007; Ruckstuhl et al., 2008). Replacing lighter more reflective tundra ground cover (lichens, mosses, and shrubs), with darker forest cover will increase the amount of incidental solar radiation absorbed by the earth, further amplifying the warming effect. Meanwhile, above the discontinuous permafrost line, local topography and soil composition will dictate whether permafrost thaw will lead to flooding, deforestation, and the establishment of mosses and sedges, or drying, afforestation, and the decomposition and release of soil organic carbon (Camill, 2005; Baltzer et al., 2014). It should be noted that, due to the size and complexity of the boreal forest biome, the impacts of climate change are numerous and often inconsistent across space.

1.3 Importance of the Boreal Forest

The boreal forest plays an important role in governing global-scale processes (Bonan, 2008), many of which contribute to the earth's radiative equilibrium. As mentioned, changes in boreal forest distribution and extent can have a significant impact on the earth's energy balance, through changes in surface and cloud albedo (Betts, 2000; Spracklen et al., 2008). The boreal forest is also an extremely important component of the global carbon cycle, as it represents the single largest reservoir of global terrestrial carbon (Sellers et al., 1995; Soja et al., 2007; Bradshaw and Warkentin 2015). Capable of storing nearly twice as much carbon as tropical forests (Carlson et al., 2009), the boreal forest currently contains an estimated 1041.5 Pg C ±

674.2 of stored carbon, equivalent to at least half of the carbon currently present in our atmosphere (Gower et al., 2001; Bradshaw and Warkentin 2015). If even a small portion of boreal carbon stocks were to be rereleased to the atmosphere, it would undoubtedly have severe consequences on the global climate system.

On an annual basis, the boreal forest has long been regarded as an overall sink for carbon. There is evidence suggesting that the strength of this sink is decreasing significantly in response to rapid climate change, with some regions approaching carbon neutrality, and others expected to become an overall source of carbon in the foreseeable future (Kurz et al., 2008; Peng et al., 2011; Bradshaw and Warkentin 2015). In a recent spatial analysis of carbon flux across the circumpolar boreal zone, Canada yielded the lowest mean annual carbon flux overall, with a value just above, but near zero. Temporally, there was an observed declining trend in annual carbon uptake since 1980 and projected persistent negative annual fluxes in Canada by 2050 (Bradshaw and Warkentin 2015). It is also likely that some regions (e.g. western Canada) are already emitting more carbon than they are storing in response to rapid changes in the disturbance regime (Bradshaw and Warkentin 2015).

An earlier study undertaken by Kurz et al. (2008) examined sink-source dynamics in Canada's managed forest, where much of the empirical data regarding forest carbon in Canada is collected. Canada's managed forest represents 65% of Canada's total forested land, including a large portion of the Canadian boreal forest (Brandt et al., 2013; NRCan 2017; ECCC 2017). The results from this study show that Canada's managed forest was a net sink for carbon in 2000 and 2001. Following this two-year period, the forest shifted to a net source for carbon in 2002, where it is projected to remain for the next 20 years, through 2022 (Kurz et al., 2008). The authors of this paper also provided more explicit predictions concerning the actual magnitude of forest carbon emissions. They predicted that the managed Canadian forests would be a source of approximately 30 to 245 Mt of Carbon between 2008 and 2012, in large part due to the increasing impact of natural disturbance on forest carbon stocks (Kurz et al., 2008). Thanks to the passage of time, these predictions can now be validated, and according to published data, they were in fact correct. The managed forest in Canada has not been a sink for carbon since 2001, and it can be said that they were conservative with their estimates of carbon emissions between 2008 – 2012, since approximately 330 Mt of carbon were emitted from the managed

forest during this period, 35% more than the upper limit of their prediction (NRCan 2017; ECCC 2017).

1.4 Carbon Distribution and Measurement

Much of the storage capacity of boreal forests is attributable to the ability of peatland and permafrost soils to accumulate and store carbon over hundreds or even thousands of years. It is estimated that boreal soils can contain up to 85% of the total C stock, with the remaining 15% being allocated to overstory and understory vegetation (Lal, 2005; Carlson et al., 2009). This is a big picture estimate at the whole-biome level, but there is much regional variability when working over smaller spatial scales. A regional study of carbon stocks by Banfield et al. (2002) focused on a 12 Mha region in the cordilleran-boreal transition zone in western Alberta. Using a few different observation methods and models, the authors identified a slightly lower proportion for soil carbon (between 60% and 77% of the total C stock), with some disagreement between measurement methods. These two studies provided an overview of forest carbon stocks with coarse spatial and temporal resolution. Scale is extremely important when trying to identify or better understand the main processes driving the distribution (stock), and the movement of carbon from one pool to another (flux). As resolution increases, carbon dynamics become increasingly dominated by regional or stand level processes (Misson et al., 2007; Litton et al., 2007; Chen et al., 2013).

The most accurate way to measure forest carbon flux at the stand or ecosystem level is with the eddy covariance (EC) method, which provides a measure of gas exchange between the forest ecosystem and the atmosphere (Baldocchi, 2003). This method provides a representation of the ebb and flow of carbon into and out of an ecosystem, measured as the net ecosystem exchange (NEE). Depending on the level of detail required by a given study, it is often required to redefine or partition the flux into some of its component parts. In terms of flux partitioning, there exist reliable models used to separate NEE into gross ecosystem production (GEP), and total ecosystem respiration (R_E), built on the notion that nighttime NEE = R_E (Stoy et al., 2006; Richardson et al., 2012). Net ecosystem production (NEP) is relatively easy to resolve. NEP represents the net uptake of CO_2 by the ecosystem, including losses from both plant-based autotrophic respiration (R_A) and decomposition-based heterotrophic respiration (R_H), the sum of

which is equal to R_E. While NEE is positive when CO_2 is emitted, NEP = -NEE and is positive when CO_2 is absorbed (Reichstein et al., 2012). Net primary production (NPP) is more difficult to quantify. Like NEP, NPP also represents the net uptake of CO_2 by the ecosystem, but accounting only for autotrophic respiration (NPP = GEP - R_A), it therefore more accurately represents the net assimilation of photosynthetic carbon by a forest. Quantifying NPP often requires complementary field-based techniques to directly measure, either biometrically or allometrically, R_A and R_H, to break R_E down into its discrete components (Law et al., 2000; Ohtsuka et al., 2009).

It is also important to understand where carbon is being allocated within a forest ecosystem. To do so, the forest can be compartmentalized into layers (e.g. crown, overstory, understory, soil), or further into individual constituents (e.g. foliage, wood, roots), to assess how each component contributes to overall forest primary production. Carbon allocation is measured or inferred in a few different ways, either from physical measurements in the field, or with gas-exchange flux measurements, scaled to an appropriate level (Gower et al., 2001; Litton et al., 2007; Chen et al., 2013). A study by Misson et al. (2007) used eddy covariance to assess the contribution of forest understory, including soil level processes, to the overall annual flux. The authors of this paper report that the understory can account for up to 39% of the total gross primary production (GPP), an analogous measure to GEP (Stoy et al., 2006), yet across the studied sites, understory contributes on average about 14% to total GPP. Furthermore, understory can account for around half of total ecosystem respiration, with a higher proportion in deciduous forests (62%), when compared with coniferous forests (44%) (Misson et al., 2007). A study by Litton et al. (2007), working across a wide range of forest types, reports that carbon allocation to foliage remains remarkably constant year to year. Further, above ground NPP is found to be significantly and positively correlated with annual GPP (Litton et al., 2007; Chen et al., 2013). With regards to allocation of total above ground NPP in the Canadian boreal forest, wood accounts for between 50% - 61%, foliage between 25% - 42%, and understory between 4% - 22% (Gower et al., 2001). Contributions to below ground NPP (coarse and fine root) are highly dependent on forest type, with the highest relative values associated with jack pine forests, and the lowest with aspen forests. The magnitude of below ground NPP varies between 12% - 87% when compared with the total magnitude of above ground NPP across the studied sites (Gower et al., 2001).

1.5 Dendrochronology

While eddy covariance may represent the most accurate method for measuring carbon exchange between an ecosystem and the atmosphere, it is limited in its ability to offer a breakdown of the flux beyond its main components of GEP, R_E, and NEP (or NEE) (Baldocchi 2003). Furthermore, the equipment necessary to measure eddy covariance flux is costly to deploy and must be maintained over long periods. Detailed eddy covariance flux data are therefore sparse and often limited in length (Gea-Izquierdo et al., 2014). These limitations restrict the development of a detailed and mechanistic understanding of carbon allocation across a wide range of forest ecosystems, which is required to accurately anticipate the impacts of climate change on forest biogeochemical cycling (Litton et al., 2007; Chen et al., 2013)

Biometric based measurements regarding the growth of individual forest components can be used to partition annual production into some of its component parts. One of the main challenges of better understanding forest production and carbon allocation may be a lack of reliable and consistent biometric measurement techniques to supplement eddy covariance based flux data (Babst et al., 2014a; Babst et al., 2014b). In this context, tree-rings hold great potential. Tree-rings have several characteristics that make them attractive as a potential proxy for ecosystem production. Firstly, they are an in-situ representation of forest wood production over time. This is significant considering that carbon stored in woody biomass represents the largest component of forest ecosystem production (Gower et al., 2001; Chen et al., 2013) and is the most significant and persistent annual sink for atmospheric carbon (Ilvesniemi et al., 2009), responsible for offsetting an estimated 15% of anthropogenic carbon emissions annually (Pan et al., 2011). While other components of ecosystem production, including annual contributions from understory growth, foliage, coarse and fine root, may be difficult to extrapolate from tree rings, proportions of carbon allocated to different components of total NPP are remarkably consistent across geographic regions (Gower et al., 2001). Therefore, total NPP may be reliably estimated from measures of above ground NPP (Gower et al., 2001). Above ground NPP and total NPP were significantly correlated with an r^2 of 0.66-0.68 across boreal forest stands, and above ground NPP was positively correlated with the mean annual biomass increment, meaning it can be calculated from ring-widths (Gower et al., 2001; Rocha et al., 2006). Tree ring data are also easily accessible and often inexpensive to collect, and there already exists an extensive

international repository of tree ring data. Yet to date, tree-ring data have been underutilized in the context of forest carbon research (Babst et al., 2014b).

For these reasons, there are several studies that attempt to quantify the relationship between radial growth and forest ecosystem production. These represent a relatively new area of study, and so far have yielded mixed results. When assessing this relationship on an annual scale, several studies report significant correlations between ring-widths, or values of woody biomass accumulation derived from stem measurements, and several eddy covariance based measures of ecosystem production (Rocha et al., 2006; Zweifel et al., 2010; Babst et al., 2014a; Gea-Izquierdo et al., 2014; Lempereur et al., 2015). Some of these studies identified no relationship between tree growth and GEP (Rocha et al., 2006; Zweifel et al., 2010), while others report the opposite (Gea-Izquierdo et al., 2014; Lempereur et al., 2015). Interestingly, all these studies identified a positive relationship between the annual radial increment and same-year annual NEP (Rocha et al., 2006; Zweifel et al., 2010; Babst et al., 2014a; Gea-Izquierdo et al., 2014; Lempereur et al., 2015). The persistence in the observed relationship between annual radial growth and NEP is surprising considering that annual ring-width measurements are simply representative of the biomass increment – the portion of carbon allocated and stored within a discrete pool over a discrete period. Measurements of NEP are far more complex, relating to integrated, ecosystem wide processes of carbon uptake and partitioning across several pools. For this reason, there is substantial variability in the strength of this relationship between species, between sites, and across the temporal scale (Zweifel et al., 2010; Babst et al., 2014a; Gea-Izquierdo et al., 2014; Lempereur et al., 2015). This is not surprising considering that these characteristics would influence the distribution of carbon across the landscape. In fact, there are several reasons to expect a decoupling of the relationship between the radial growth increment and ecosystem production. These are explored in detail in the subsequent sections.

1.6 Potential Disconnection Between Tree Rings and Carbon Flux

Lempereur et al. (2015) identified a strong relationship between the annual biomass increment and components of ecosystem production (GPP, NEP) at coarse temporal scales. This relationship decreased in significance with increasing temporal resolution. It is suggested that the breakdown in this relationship could be due to differences in how radial growth and ecosystem production interact with growing season conditions. For example, due to differences in their

response and threshold tolerances to extremes in temperature and moisture stress (Lempereur et al., 2015). Under limiting temperature and moisture conditions, values for ecosystem production remained positive while the cell production responsible for radial growth had ceased (Lempereur et al., 2015). Therefore, while growth ceases in response to a certain level of temperature and moisture stress, photosynthesis and the assimilation of carbohydrates persist to a higher threshold limit. Perhaps the non-structural carbohydrates (NSCs) that are produced under these conditions are allocated to the maturation of existing tracheid cells, or stored for when growth reinitiates, or used to proliferate roots in search for deeper water. What is know is learned from Deslauriers et al. (2016) who suggested that without sufficient moisture to provide the required turgor pressure, cells would be stuck in the radial enlargement phase of tracheid differentiation. Thus, growth is ceased under water limitations. Under these conditions, NSCs are diverted from growth processes and used for osmoregulation, to maintain cell turgor pressure (Deslauriers et al., 2016).

Large amounts of carbohydrate storage, or significant allocation from stored carbohydrates to support growth, could theoretically result in a decoupling of ecosystem production from the annual biomass increment, resulting in autoregression or time lags in the relationship between carbon assimilation and allocation (Richardson et al., 2013). The magnitude of carbon flux in and out of internal storage pools are also species specific, with some species relying more heavily on stored carbohydrates to maintain cellular respiration or support growth (Richardson et al., 2013). Gea-Izquierdo et al. (2014) found that there was a stronger relationship between ecosystem production and radial growth in jack pine then there was in black spruce. Jack pine growth maintained a relatively strong relationship with ecosystem production across the temporal scale, while black spruce growth was only related to ecosystem production on an annual scale (Gea-Izquierdo et al., 2014). It is hypothesized that these differences could be due to different carbon allocation strategies between the two species. If black spruce were to have significant carbohydrate storage capacity, a beneficial characteristic for stress-tolerant trees, it would not only explain the discrepancies seen here, but it would also help explain the observed decoupling between black spruce ring-width and annual GEP in the study by Rocha et al. (2006).

A recent study by Cuny et al. (2015) has helped improve our understanding of the phenology and physiology of active ring formation and annual carbon accumulation in the stem, which further explains observed discrepancies between forest ecosystem production and woody

biomass production over the short term. Only about 20% of total annual ring-width can be attributed to the production of new tracheid cells; the radial enlargement of these newly formed xylem cells accounts for the remaining 80% (Cuny et al., 2015). The peak rate at which stem size increases therefore coincides with the time during which the most tracheid cells are in the radial enlargement phase during earlywood production. In contrast, about 90% of woody biomass production occurs during cell wall thickening, a later stage of tracheid development (Cuny et al., 2015). Peak carbon sequestration in woody biomass therefore loosely coincides with the production of transition wood, just before the start of latewood production. Cuny et al. (2015) observed that by early-August, 90% of the final ring-width was realized, while only 70% of the carbon to be stored in woody biomass that year was present within the actively developing ring. Much of the asynchrony between peak ring-width and peak carbon storage can therefore be attributed to the discrepancy in time required to complete each of the phases of tracheid cell development. The radial cell enlargement phase, largely responsible for controlling peak ring-width, took approximately 12 and 6 days for earlywood and latewood cells respectively, while cell wall thickening, largely responsible for peak carbon storage in woody biomass, took 22 and 50 days respectively (Cuny et al., 2015). Note that the approximate length of time required to complete each phase is applicable only to this study. However, an analysis of data from other forest ecosystems reveals a similar time lag between peak radial expansion and peak carbon storage in woody biomass, to the order of approximately 1-month, 27 ± 6 days in boreal ecosystems (Cuny et al., 2015).

One final reason for discrepancy between the biomass increment and ecosystem production is unique to fine scale stem increment data and is due to the nature of this data and how it is typically measured, as water related variability increases with temporal resolution (Zweifel et al., 2010; Lempereur et al., 2015). Automatic dendrometers provide high-resolution data regarding one of the most important components of carbon assimilation, the production of new wood. However, high-resolution dendrometer data also contains variability related to reversible changes in stem size associated with tree water relations, mainly influencing phloem cells (Zweifel et al., 2010). There is therefore a hypothesized decrease in explanatory power of the stem increment at sub-annual scales, as tree water begins to play a more defining role in biometric stem size data (Zweifel et al., 2010). This provides another possible explanation for the observed breakdown in the relationship between the stem increment and ecosystem production at

fine temporal resolutions observed by Lempereur et al. (2015). Nonetheless, the authors of Zweifel et al. (2010) identify an unexpectedly strong relationship between stem radius change (DR) and whole ecosystem NEP across the temporal scale, from half-hourly to annual resolution. NEP and stem radius were positively correlated on annual ($R^2 = 0.85$), and monthly scales, and negatively correlated at half-hourly scale resolution during days when average daily temperature is above zero (Zweifel et al., 2010). The reason for the negative correlation between DR and NEP on a half hourly scale in the summer is clear. Warm sunny conditions lead to increasing transpiration and dehydration of the stem, these conditions are also favorable for photosynthetic activity. It is therefore reasonable to assume that periods of peak stem dehydration during clear sunny summer days, would correspond with periods of elevated photosynthetic activity and carbon assimilation. Hence, half-hourly correlations were most significant during sunny summer days (Zweifel et al., 2010). Water relations also played a role in the correlation between stem size and NEP on a monthly scale resolution. Shrinking values for stem size associated with winter dehydration corresponded well with ecosystem losses to winter respiration. Moreover, between February and March, the rehydration period began, followed shortly by the onset of ecosystem photosynthesis (Zweifel et al., 2010). May was an exception in terms of the relationship between monthly values of NEP and stem size. During the month of May, stem rehydration was still ongoing, while NEP had already reached relatively high values (Zweifel et al., 2010). Therefore, due to the nature of dendrometer data, correlations were spurious at sub-annual resolution, as the processes governing stem size and ecosystem production were not causally linked.

Only when assessing the relationship between radial growth, climate, and ecosystem production across the temporal scale can we begin to disentangle some of the complexity inherent in this relationship. Monitoring stem radius change over intra-annual scales provides vital information regarding the phenology of active ring development and any associated time lags between carbon assimilation and allocation (Richardson et al., 2013; Babst et al., 2014a; Cuny et al., 2015). To better understand the processes of forest carbon allocation, further comparisons between eddy covariance and biometric based measures of carbon flux are needed across a wide range of forest ecosystems (Zweifel et al., 2010; Babst et al., 2014a).

1.7 A Note on Tree Ring Sampling and the International Tree Ring Databank

Though there is an extensive repository of tree ring data that could be of potential use, there are several potential issues with traditional tree ring sampling and its ability to yield data that are useful in answering questions regarding carbon dynamics at the ecosystem level (Babst et al., 2014b). Traditional tree ring studies often employ sampling schemes designed to fulfill individual project objectives, frequently targeted at old, vulnerable, or stressed individuals and stands (Babst et al., 2014b). While the resulting data may prove useful in addressing specific research questions, utilizing these data out of context can introduce significant bias. Because dendrochronological methods have only recently been applied to the study of forest carbon, there lacks a unified standard technique for the quantification of above ground biomass accumulation from tree rings, and there remains much inconsistency across studies (Babst et al., 2014b). Comparing radial growth data with measures of forest production requires an unbiased ring-width chronology that is scalable to the stand level. This renders the existing tree ring database of little use in the study of forest productivity.

1.8 Conclusion and Research Gap

Considering the importance of the boreal forest in terms of its ability to sequester atmospheric carbon, it is imperative that we develop a comprehensive understanding of the processes governing carbon flux across a diverse set of boreal forest stands. To fully appreciate the intricate nature of carbon balance in the boreal forest, we must, perhaps most importantly, gain an understanding of the mechanisms driving the allocation and storage of photosynthetic carbon in the tree stem. The stem represents the single most important repository of above ground carbon in the boreal forest (Lal et al., 2005; Chen et al., 2013) and while the recent application of dendrochronology in carbon cycle research has helped to improve our understanding of the role of stem-level biomass in forest carbon storage (Rocha et al., 2006; Ilvesniemi et al., 2009; Zweifel et al., 2010; Babst et al., 2014; Cuny et al., 2015), there remains much work to be done. Our lack of understanding regarding the mechanisms of photosynthate storage and allocation, including its role in active ring development, translate to significant gaps in our understanding of forest carbon dynamics, and hinders our ability to precisely partition the measured carbon flux. Our understanding of these processes directly limits the accuracy of the current carbon cycle, and climate-carbon feedback models (Gower et al., 2001; Litton et al.,

2007; Misson et al., 2007; Zweifel et al., 2010; Chen et al., 2013). A more thorough understanding of forest carbon flux and storage will not only improve our ability to accurately model the impact of climate change on the carbon cycle, it is also needed to help inform the decision-making process, which can lead to more informed and sustainable forest management policy, and strategies for climate change mitigation (Bradshaw and Warkentin, 2015). To my knowledge, the proposed research will be the first to apply a cross-scale approach to the study of stem-level carbon allocation in the North American boreal forest. It will also be the first to simultaneously assess the radial growth/climate relationship across the same temporal scales, which has further implications in helping to better understand the direct impacts of climate change on the Canadian boreal forest. In short, the goal of this research is to better understand the interface between radial growth, climate, and carbon in the southern boreal forests of Canada.

1.9 Study Sites

In 1993, the Boreal Ecosystems Atmosphere Study (BOREAS) was launched, representing one of the most comprehensive investigations of boreal forest dynamics at the ecosystem level (Sellers et al., 1995). The main goal of this international effort was to improve our collective understanding of boreal ecosystem-atmosphere interactions in the face of significant global change (Sellers et al., 1995). Long-term study sites were established in several representative North American boreal forest stands, split between a Northern Study Area (NSA) and a Southern Study Area (SSA). Within both, a trembling aspen dominated stand, a black spruce stand, a jack pine stand, as well as a wetland fen were instrumented (Sellers et al., 1995; Sellers et al., 1997). Each of the sites were equipped with an extensive array of equipment to collect meteorological, biometeorological, and eddy covariance flux data, mounted on flux towers tall enough to measure gas exchange from a mature forest (Sellers et al., 1995; Sellers et al., 1997). BOREAS was indeed successful in substantially improving our understanding of boreal forest ecosystem processes. A comprehensive assessment of the forests radiation and energy balance allowed for significant advancements in climate modeling, while cross-scale carbon flux studies helped to better define sink/source dynamics in the Canadian boreal forest (Sellers et al., 1997).

1.9.1 A Legacy Continued

As the BOREAS project came to a close, the Boreal Ecosystem Research and Monitoring Sites (BERMS) program assumed responsibility for maintaining the sites within the SSA, located north of Prince Albert, Saskatchewan. The SSA spans approximately 11,700 km^2 (Sellers et al., 1995). Land cover within the SSA can be broken down as follows: Wet conifer stands (often dominated by black spruce), cover the largest proportion of the SSA, accounting for 46% of the total land area, followed by dry conifer stands (often dominated by jack pine), and aspen dominated stands, covering approximately 20% and 13% of the SSA respectively (Kljun et al., 2007). It can therefore be said that the study sites within the SSA, Old Jack Pine (OJP), Old Black Spruce (OBS), and Old Aspen (OA) are appropriately representative of the area overall. This area is ideal for the study of climate change impacts on the Canadian boreal forest. Based on the literature reviewed, this area is particularly vulnerable to climatic change, with enhanced sensitivity to drought (Michaelian et al., 2011; Peng et al., 2011), fire weather severity (Wang et al., 2015), and insect outbreak (Volney and Fleming 2000). We can therefore expect to see measurable changes occur here before elsewhere in Canada. Furthermore, the BERMS continue to represent one of the most comprehensive collections of long-term high-resolution carbon flux data (Kljun et al., 2007), alongside of which comes an equally impressive suite of meteorological data. This powerful dataset provides a significant opportunity to further advance our understanding of carbon cycling in the boreal forest.

1.10 Site Descriptions

This study was conducted at three of the Boreal Ecosystem Research and Monitoring Sites (BERMS), located near the southern edge of the boreal forest in the Boreal Plains Ecozone of central Saskatchewan (Figure 1.1). Site characteristics are given in Table 1.1. The climate of the study area is characterized by short, warm, dry summers and long, cold winters.

The Old Jack Pine (OJP) site, located northeast of Candle Lake, Saskatchewan, is an even-aged stand of jack pine, naturally established post-fire in 1914 (Barr et al., 2012). The understory is composed of clumps of green alder (*Alnus crispa*), and the dominant ground cover includes some bearberry (*Arctostaphylos uva-ursi*), and a nearly continuous cover of reindeer lichen (*Cladina mitis*). The soil is a well-drained Orthic Eutric Brunisol (loamy sand).

The Old Black Spruce (OBS) site is located due north of Candle Lake, and is a black spruce dominated forest with co-dominant eastern larch comprising approximately 10% of the stand's makeup (Pappas et al., 2018). The stand was established post-fire in approximately 1879 (Barr et al., 2012). The understory is mainly comprised of wild rose (*Rosa Woodsii)* and Labrador tea (*Ledum groenlandieum*). The groundcover is comprised of a mixture of feather mosses, sphagnum moss, and lichen. The soil is poorly drained, with a thick layer of peat (~20 cm) over waterlogged sand.

The BERMS Old Aspen (OA) site in Prince Albert National Park, is an even-aged stand of trembling aspen, naturally established after a forest fire in 1919 (Barr et al., 2012). The understory is mainly hazelnut (*Corylus cornuta*) with a few other shrubs. The topography is relatively level, with uniform fetch of at least 3 km in each direction from the tower. The soil is an Orthic Gray Luvisol (loam to clay loam).

1.11 Meteorological Conditions Within the Short-Term Observation Period

An array of high-resolution meteorological variables are collected at the BERMS sites. These include precipitation, volumetric water content (VWC) in the root zone, air temperature measured above the canopy, and soil temperature measured at 2, 5, 10, 20, 50 and 100cm depth, all recorded over the 22-year period between 1997 – 2018 (21-years, 1997 – 2017, at OA). From these high-resolution data, daily average temperatures, VWC, and daily precipitation totals were computed for the short-term observation period (2015 – 2018). These were compared with average daily temperatures, and average monthly precipitation totals from the 22-year record to assess how conditions within the observation period compare to the norm. The following description of trends are depicted in Figures 1.2A, 1.2B, and 1.2C.

2015

Air and soil temperature during the 2015 growing season were quite average overall. Precipitation was similar at all three sites, with below average rainfall during the late spring months (May and June), and above average precipitation throughout the summer months (July, August, and September). Compared to the 22-year average, the precipitation deficit in the spring (May and June) was in the range of approximately (~) 70 – 75 mm at OJP and OBS, and -58 mm at OA. This deficit was made up for during the rest of the growing season (July, August, and

September), with rainfall that amounted to ~ 60 – 70 mm above the average at OJP and OBS, and +109 mm at OA. VWC followed a similar pattern, with depletion of water in the root zone from about mid-May to mid-July, and replenishment of soil water following mid-July.

2016

Beyond a brief cold spell during the second week of May 2016, air temperature tended to be above average from the beginning of the growing season until about the end of June, when it fell back towards the average. This resulted in warmer than average soil temperatures (by approximately 1 – 2 °C) until about mid-August at all three sites. In terms of precipitation; May and June were below average at all three sites (~ 35 – 50 mm deficit); July was very wet at OJP and OBS (+89 mm and +132 mm, respectively), and average at OA; August was wet at OJP (+32 mm), and average at OBS and OA; and September had below average precipitation at all three sites (~ 10 mm deficit). VWC was average during much of the growing season at OJP, except in late-May and June when it fell below the average. At OBS, VWC was above average in May below average in late-June, and around average to slightly above average during the rest of the growing season. OA had below average VWC during the whole 2016 growing season.

2017

During the 2017 growing season, air temperature flipped from below average in early- to mid-May, to above average from about mid-May to mid-June, and again below average during the second half of June. This resulted in below average soil temperatures from May to early-July at all three sites, except during the warm spell from mid-May to mid-June, which caused soil temperatures to approach or surpass the average for a brief period. Soil temperature trended around the average for the rest of the growing season, from about early-July to end-September. May of 2017 was much wetter than usual, receiving about twice the average amount of precipitation for this month at all three sites (~ 40 mm surplus). June was slightly dry at OJP (-20 mm) and slightly wet at OBS and OA (+14 mm and +23 mm, respectively). The rest of the growing season (July – September) received below average amounts of precipitation, except during the month of September at OA, which received precipitation amounting to almost exactly the average for this site. During this period (July – September), OJP was driest, with a 101 mm precipitation deficit, OBS was second driest (-74 mm), and OA had only a 39 mm deficit. Over

the course of the 2017 growing season, VWC displayed a declining trend at OJP and OBS growing season, going from above average from May to mid-July, to below average from mid-July to October. At OA, VWC was about average during the first half of the growing season (May – mid-July), then falling below the average during the second half (mid-July – October).

2018

Overall trends in air temperature during the 2018 growing season were generally above average from the beginning of May to the end of June, near average from early-July to about mid-August, and significantly below average from about late-August to end-September. Trends in soil temperatures were similar to the described trends in air temperature. Rainfall varied significantly between OJP and OBS. At OJP, there was below average precipitation every month except for September, which received only 5 mm above the average. At OBS, precipitation was slightly above average for May (+5 mm), below average for June (-26 mm), above average for July (+23 mm), below average for August (-36 mm), and above average for September (+10 mm). Over the course of the whole growing season, OBS received only 6 mm less than the 22-year average, while OJP recorded a 78 mm deficit compared with the average for this site. VWC was about average at OJP and below average at OBS.

1.12 References

Ainsworth, E. A., & Long, S. P. (2005). What have we learned from 15 years of free-air CO2 enrichment (FACE)? A meta-analytic review of the responses of photosynthesis, canopy properties and plant production to rising CO2. *New Phytologist*, *165*(2), 351–372.

Allen, C. D., Macalady, A. K., Chenchouni, H., Bachelet, D., McDowell, N., Vennetier, M., Kitzberger, T., Rigling, A., Breshears, D. D., Hogg, E. T., Gonzalez, P., Fensham, R., Zhang, Z., Castro, J., Demidova, N., Lim, J-H., Allard, G., Running, S. W., & Cobb, N. (2010). A global overview of drought and heat-induced tree mortality reveals emerging climate change risks for forests. *Forest Ecology and Management*, *259*(4), 660–684.

Babst, F., Bouriaud, O., Alexander, R., Trouet, V., & Frank, D. (2014). Toward consistent measurements of carbon accumulation: A multi-site assessment of biomass and basal area increment across Europe. *Dendrochronologia*, *32*(2), 153–161.

Babst, F., Bouriaud, O., Papale, D., Gielen, B., Janssens, I. A., Nikinmaa, E., Ibrom, A., Wu, J., Bernhofer, C., & Köstner, B. (2014). Above-ground woody carbon sequestration measured from tree rings is coherent with net ecosystem productivity at five eddy-covariance sites. *New Phytologist*, *201*(4), 1289–1303.

Baldocchi, D. D. (2003). Assessing the eddy covariance technique for evaluating carbon dioxide exchange rates of ecosystems: Past, present and future. *Global Change Biology*, *9*(4), 479–492.

Baltzer, J. L., Veness, T., Chasmer, L. E., Sniderhan, A. E., & Quinton, W. L. (2014). Forests on thawing permafrost: Fragmentation, edge effects, and net forest loss. *Global Change Biology*, *20*(3), 824–834.

Banfield, G. E., Bhatti, J. S., Jiang, H., & Apps, M. J. (2002). Variability in regional scale estimates of carbon stocks in boreal forest ecosystems: Results from West-Central Alberta. *Forest Ecology and Management*, *169*(1), 15–27.

Barr, A. G., van der Kamp, G., Black, T. A., McCaughey, J. H., & Nesic, Z. (2012). Energy balance closure at the BERMS flux towers in relation to the water balance of the White Gull Creek watershed 1999–2009. *Agricultural and Forest Meteorology*, *153*, 3–13.

Betts, R. A. (2000). Offset of the potential carbon sink from boreal forestation by decreases in surface albedo. *Nature*, *408*(6809), 187–190.

Bonan, G. B. (2008). Forests and Climate Change: Forcings, Feedbacks, and the Climate Benefits of Forests. *Science*, *320*(5882), 1444–1449.

Bradshaw, C. J., & Warkentin, I. G. (2015). Global estimates of boreal forest carbon stocks and flux. *Global and Planetary Change*, *128*, 24–30.

Brandt, J. P., Flannigan, M. D., Maynard, D. G., Thompson, I. D., & Volney, W. J. A. (2013). An introduction to Canada's boreal zone: Ecosystem processes, health, sustainability, and environmental issues 1. *Environmental Reviews*, *21*(4), 207–226.

Brandt, J. P. (2009). The extent of the North American boreal zone. *Environmental Reviews*, *17*(NA), 101–161.

Brysse, K., Oreskes, N., O'Reilly, J., & Oppenheimer, M. (2013). Climate change prediction: Erring on the side of least drama? *Global Environmental Change*, *23*(1), 327–337.

Bush, E. & Lemmen, D.S, editors (2019). Canada's changing climate report. *Government of Canada, Ottawa, ON,* 444p.

Camill, P. (2005). Permafrost thaw accelerates in boreal peatlands during late-20th century climate warming. *Climatic Change*, *68*(1), 135–152.

Carlson, M., Wells, J., & Roberts, D. (2009). *The carbon the world forgot: Conserving the capacity of Canada's Boreal Forest region to mitigate and adapt to climate change.* Boreal Songbird Initiative and Canadian Boreal Initiative, Seattle, WE, USA and Ottawa, Canada.

Chen, G., Yang, Y., & Robinson, D. (2013). Allocation of gross primary production in forest ecosystems: Allometric constraints and environmental responses. *New Phytologist*, *200*(4), 1176–1186.

Cuny, H. E., Rathgeber, C. B., Frank, D., Fonti, P., Mäkinen, H., Prislan, P., Rossi, S., del Castillo, E. M., Campelo, F., Varvcik, H., Camarero, J. J., Bryunkhanova, M. V., Jyske, T., Gricar, J., Gryc, V., De Luis, M., Vieira, J., Cufar, K., Kirdyanov, A. V., Oberhuber, W., Tremill, V., Huang, J. G., Li, X., Swidrak, I., Deslauriers, A., Liang, E., Nojd, P., Gruber, A., Nabais, C., Morin, H., Krause, C., King, & G., Fournier, M.(2015). Woody biomass production lags stem-girth increase by over one month in coniferous forests. *Nature Plants*, *1*, 15160.

Deslauriers, A., Huang, J.-G., Balducci, L., Beaulieu, M., & Rossi, S. (2016). The contribution of carbon and water in modulating wood formation in black spruce saplings. *Plant Physiology*, pp–01525.

Environment and Climate Change Canada (ECCC). (2017). *National Inventory Report 1990–2015: Greenhouse Gas Sources and Sinks in Canada*. The Pollutant Inventories and Reporting Division.

Field, C. B., Jackson, R. B., & Mooney, H. A. (1995). Stomatal responses to increased CO2: Implications from the plant to the global scale. *Plant, Cell & Environment*, *18*(10), 1214–1225.

Food and Agriculture Organization of the UN (FAO). (2015). *Global Forest Resources Assessment 2015: How Are the World's Forests Changing?*

Gea-Izquierdo, G., Bergeron, Y., Huang, J.-G., Lapointe-Garant, M.-P., Grace, J., & Berninger, F. (2014). The relationship between productivity and tree-ring growth in boreal coniferous forests. *Boreal Environment Research*.

Gedalof, Z., & Berg, A. A. (2010). Tree ring evidence for limited direct CO2 fertilization of forests over the 20th century. *Global Biogeochemical Cycles*, *24*(3).

Girardin, M. P., Bernier, P. Y., Raulier, F., Tardif, J. C., Conciatori, F., & Guo, X. J. (2011). Testing for a CO2 fertilization effect on growth of Canadian boreal forests. *Journal of Geophysical Research: Biogeosciences*, *116*(G1).

Gower, S. T., Krankina, O., Olson, R. J., Apps, M., Linder, S., & Wang, C. (2001). Net primary production and carbon allocation patterns of boreal forest ecosystems. *Ecological Applications*, *11*(5), 1395–1411.

Harsch, M. A., Hulme, P. E., McGlone, M. S., & Duncan, R. P. (2009). Are treelines advancing? A global meta-analysis of treeline response to climate warming. *Ecology Letters*, *12*(10), 1040–1049.

Henderson, N., & Sauchyn, D. (2008). Climate change impacts on Canada's Prairie Provinces: A summary of our state of knowledge. *Prairie Adaptation Research Collaborative: Summary Document*, *08–01*, 20.

Huang, J., Tardif, J. C., Bergeron, Y., Denneler, B., Berninger, F., & Girardin, M. P. (2010). Radial growth response of four dominant boreal tree species to climate along a latitudinal gradient in the eastern Canadian boreal forest. *Global Change Biology*, *16*(2), 711–731.

Huntingford, C., & Mercado, L. M. (2016). High chance that current atmospheric greenhouse concentrations commit to warmings greater than 1.5° C over land. *Scientific Reports*, *6*.

Ilvesniemi, H., LevuIa, J., Ojansuu, R., KoIari, P., KuImaIa, L., Pumpanen, J., Launiainen, S., VesaIa, T., & Nikinmaa, E. (2009). Long-term measurements of the carbon balance of a boreal Scots pine dominated forest ecosystem. *Boreal Environment Research*, *14*(4).

Ireson, A. M., Barr, A. G., Johnstone, J. F., Mamet, S. D., van der Kamp, G., Whitfield, C. J., Michel, N. L., North, R. L., Westbrook, C. J., DeBeer, C., Chun, K. P., Nazemi, A., & Sagin, J. (2015). The changing water cycle: The Boreal Plains ecozone of Western Canada. *Wiley Interdisciplinary Reviews: Water*, *2*(5), 505–521.

Jeong, D. I., Sushama, L., & Khaliq, M. N. (2014). The role of temperature in drought projections over North America. *Climatic Change*, *127*(2), 289–303.

Kljun, N., Black, T. A., Griffis, T. J., Barr, A. G., Gaumont-Guay, D., Morgenstern, K., McCaughey, J. H., & Nesic, Z. (2007). Response of net ecosystem productivity of three boreal forest stands to drought. *Ecosystems*, *10*(6), 1039–1055.

Körner, C. (2003). *Alpine plant life: Functional plant ecology of high mountain ecosystems; with 47 tables*. Springer Science & Business Media.

Kurz, W. A., Stinson, G., Rampley, G. J., Dymond, C. C., & Neilson, E. T. (2008). Risk of natural disturbances makes future contribution of Canada's forests to the global carbon cycle highly uncertain. *Proceedings of the National Academy of Sciences*, *105*(5), 1551–1555.

Kuusela, K. (1992). [The boreal forests: An overview]. *Unasylva (FAO)*.

Lal, R. (2005). Forest soils and carbon sequestration. *Forest Ecology and Management*, *220*(1), 242–258.

Law, B. E., Waring, R. H., Anthoni, P. M., & Aber, J. D. (2000). Measurements of gross and net ecosystem productivity and water vapour exchange of a Pinus ponderosa ecosystem, and an evaluation of two generalized models. *Global Change Biology*, *6*(2), 155–168.

Lempereur, M., Martin-StPaul, N. K., Damesin, C., Joffre, R., Ourcival, J.-M., Rocheteau, A., & Rambal, S. (2015). Growth duration is a better predictor of stem increment than carbon supply in a Mediterranean oak forest: Implications for assessing forest productivity under climate change. *New Phytologist*, *207*(3), 579–590.

Linderholm, H. W. (2006). Growing season changes in the last century. *Agricultural and Forest Meteorology*, *137*(1), 1–14.

Litton, C. M., Raich, J. W., & Ryan, M. G. (2007). Carbon allocation in forest ecosystems. *Global Change Biology*, *13*(10), 2089–2109.

Michaelian, M., Hogg, E. H., Hall, R. J., & Arsenault, E. (2011). Massive mortality of aspen following severe drought along the southern edge of the Canadian boreal forest. *Global Change Biology*, *17*(6), 2084–2094.

Misson, L., Baldocchi, D. D., Black, T. A., Blanken, P. D., Brunet, Y., Yuste, J. C., Dorsey, J. R., Falk, M., Granier, A., Irvine, M. R., Jarosz, N., Lamaud, E., Launiainen S., Law, B. E., Longdoz, B., Loustau, D., McKay, M., Paw U, K. T., & Goldstein, A. H. (2007). Partitioning forest carbon fluxes with overstory and understory eddy-covariance measurements: A synthesis based on FLUXNET data. *Agricultural and Forest Meteorology*, *144*(1), 14–31.

National Centers for Environmental Information (NOAA). (2019a). State of the Climate: Global Climate Report for Annual 2018. published online January 2019, retrieved on January 1, 2020 from https://www.ncdc.noaa.gov/sotc/global/201813

National Centers for Environmental Information (NOAA). (2019b). Climate at a Glance: Global Time Series. (2019b) published December 2019, retrieved on January 1, 2020 from https://www.ncdc.noaa.gov/cag/

Norby, R. J., DeLucia, E. H., Gielen, B., Calfapietra, C., Giardina, C. P., King, J. S., Ledford, J., McCarthy, H. R., Moore, D. J. P., Ceulemans, R., De Angelis, P., Finzi, A. C., Karnosky, D. F., Kubiske, M. E., Lukac, M., Pregitzer, K. S., Scarascla-Mugnozza G. E., Schlesinger, W. H., & Oren, R. (2005). Forest response to elevated CO2 is conserved across a broad range of productivity. *Proceedings of the National Academy of Sciences of the United States of America*, *102*(50), 18052–18056.

NRCan. (2017). *Indicator: Forest carbon emissions and removals*. http://www.nrcan.gc.ca/forests/report/disturbance/16552

Ohtsuka, T., Saigusa, N., & Koizumi, H. (2009). On linking multiyear biometric measurements of tree growth with eddy covariance-based net ecosystem production. *Global Change Biology*, *15*(4), 1015–1024.

Overpeck, Johnathan T., Bartlein, Patrick J., & Webb, Thompson III. (1991). Potential magnitude of future vegetation change in eastern North America: Comparisons with the past. *Science*, *254*(5032), 692–695.

Pan, Y., Birdsey, R. A., Fang, J., Houghton, R., Kauppi, P. E., Kurz, W. A., Phillips, O. L., Shvidenko, A., Lewis, S. L., Canadell, J. G., Ciais, P., Jackson, R. B., Pacala, S. W., McGuire, A. D., Piao, S., Rautiainen, A., Sitch, S., & Hayes, D. (2011). A Large and Persistent Carbon Sink in the World's Forests. *Science*, *333*(6045), 988–993.

Pappas, C., Matheny, A. M., Baltzer, J. L., Barr, A. G., Black, T. A., Bohrer, G., Detto, M., Maillet, J., Roy, A., Sonnentag, O., & Stephens, J. (2018). Boreal tree hydrodynamics: Asynchronous, diverging, yet complementary. *Tree Physiology*, *38*(7), 953–964.

Peng, C., Ma, Z., Lei, X., Zhu, Q., Chen, H., Wang, W., Liu, S., Li, W., Fang, X., & Zhou, X. (2011). A drought-induced pervasive increase in tree mortality across Canada's boreal forests. *Nature Climate Change*, *1*(9), 467–471.

Piao, S., Friedlingstein, P., Ciais, P., Viovy, N., & Demarty, J. (2007). Growing season extension and its impact on terrestrial carbon cycle in the Northern Hemisphere over the past 2 decades. *Global Biogeochemical Cycles*, *21*(3).

Reichstein, M., Stoy, P. C., Desai, A. K., Lasslop, G., & Richardson, A.D. (2012). Chapter 9: Partitioning of Net Fluxes in M., Aubinet, T., Vesala, D., Papale, (Eds.) *Eddy Covariance: A Practical Guide to Measurement and Data Analysis.* Springer Atmospheric Sciences.

Rich, R. L., Frelich, L. E., & Reich, P. B. (2007). Wind-throw mortality in the southern boreal forest: Effects of species, diameter and stand age. *Journal of Ecology*, *95*(6), 1261–1273.

Richardson, A. D., Carbone, M. S., Keenan, T. F., Czimczik, C. I., Hollinger, D. Y., Murakami, P., Schaberg, P. G., & Xu, X. (2013). Seasonal dynamics and age of stemwood nonstructural carbohydrates in temperate forest trees. *New Phytologist*, *197*(3), 850–861.

Rocha, A. V., Goulden, M. L., Dunn, A. L., & Wofsy, S. C. (2006). On linking interannual tree ring variability with observations of whole-forest CO2 flux. *Global Change Biology*, *12*(8), 1378–1389.

Ruckstuhl, K. E., Johnson, E. A., & Miyanishi, K. (2008). Introduction. The boreal forest and global change. *Philosophical Transactions of the Royal Society of London B: Biological Sciences*, *363*(1501), 2243–2247.

Sellers, P., Hall, F., Ranson, K. J., Margolis, H., Kelly, B., Baldocchi, D., den Hartog, G., Cihlar, J., Ryan, M. G., & Goodison, B. (1995). The Boreal Ecosystem–Atmosphere Study (BOREAS): An overview and early results from the 1994 field year. *Bulletin of the American Meteorological Society*, *76*(9), 1549–1577.

Sellers, P. J., Hall, F. G., Kelly, R. D., Black, A., Baldocchi, D., Berry, J., Ryan, M., Ranson, K. J., Crill, P. M., & Lettenmaier, D. P. (1997). BOREAS in 1997: Experiment overview, scientific results, and future directions. *Journal of Geophysical Research: Atmospheres*, *102*(D24), 28731–28769.

Soja, A. J., Tchebakova, N. M., French, N. H., Flannigan, M. D., Shugart, H. H., Stocks, B. J., Sukhinin, A. I., Parfenova, E. I., Chapin, F. S., & Stackhouse, P. W. (2007). Climate-induced boreal forest change: Predictions versus current observations. *Global and Planetary Change*, *56*(3), 274–296.

Spracklen, D. V., Bonn, B., & Carslaw, K. S. (2008). Boreal forests, aerosols and the impacts on clouds and climate. *Philosophical Transactions of the Royal Society A: Mathematical, Physical and Engineering Sciences*, *366*(1885), 4613–4626.

Stocker, T. F., Qin, D., Plattner, G. K., Tignor, M., Allen, S. K., Boschung, J., Nauels, A., Xia, Y., Bex, B., & Midgley, B. M. (IPCC). (2013). *IPCC, 2013: Climate change 2013: the physical science basis. Contribution of working group I to the fifth assessment report of the intergovernmental panel on climate change*.

Stoy, P. C., Katul, G. G., Siqueira, M. B., Juang, J.-Y., Novick, K. A., Uebelherr, J. M., & Oren, R. (2006). An evaluation of models for partitioning eddy covariance-measured net ecosystem exchange into photosynthesis and respiration. *Agricultural and Forest Meteorology*, *141*(1), 2–18.

Tardif, J. C., Cornelsen, S., Conciatori, F., Hodgin, E. B., & Pellatt, M. G. (2016). Fire Regime in Marginal Jack Pine Populations at Their Southern Limit of Distribution, Riding Mountain National Park, Central Canada. *Forests*, *7*(10), 219.

Volney, W. J. A., & Fleming, R. A. (2000). Climate change and impacts of boreal forest insects. *Agriculture, Ecosystems & Environment*, *82*(1), 283–294.

Wang, X., Thompson, D. K., Marshall, G. A., Tymstra, C., Carr, R., & Flannigan, M. D. (2015). Increasing frequency of extreme fire weather in Canada with climate change. *Climatic Change*, *130*(4), 573–586.

Wang, Y., Hogg, E. H., Price, D. T., Edwards, J., & Williamson, T. (2014). Past and projected future changes in moisture conditions in the Canadian boreal forest. *The Forestry Chronicle*, *90*(5), 678–691.

Weber, M. G., & Flannigan, M. D. (1997). Canadian boreal forest ecosystem structure and function in a changing climate: Impact on fire regimes. *Environmental Reviews*, *5*(3–4), 145–166.

Xia, J. Y., Chen, J. Q., Piao, S. L., Ciais, P., Luo, Y. Q., & Wan, S. Q. (2014). Terrestrial carbon cycle affected by non-uniform climate warming. *Nature Geoscience, 7.*

Zweifel, R., Eugster, W., Etzold, S., Dobbertin, M., Buchmann, N., & Häsler, R. (2010). Link between continuous stem radius changes and net ecosystem productivity of a subalpine Norway spruce forest in the Swiss Alps. *New Phytologist*, *187*(3), 819–830.

1.13 Tables and Figures

Table 1.1: Various site characteristics. Stand age is approximated from site descriptions in Barr et al. (2012) and correspond well with core samples taken in 2016 at OBS and in 2018 at OJP and OA. Stand density is calculated from measurements taken in 2016, at OJP and OA for Chapter 4 and at OBS for Pappas et al. (2018). The uncertainty value associated with stand density is the standard error between sample plots. The elevated value for standard error associated with stand density at OBS results from a large discrepancy in the number of individuals between the two circular plots.

	OJP	OBS	OA
Latitude (decimal ^{o}N)	53.92	53.99	53.63
Longitude (decimal ^{o}W)	104.69	105.12	106.19
Stand age (years, 2018)	~105	~140	~100
Stand density (stem ha^{-1}, 2016)	887 ± 99	5921 ± 2431	473 ± 47

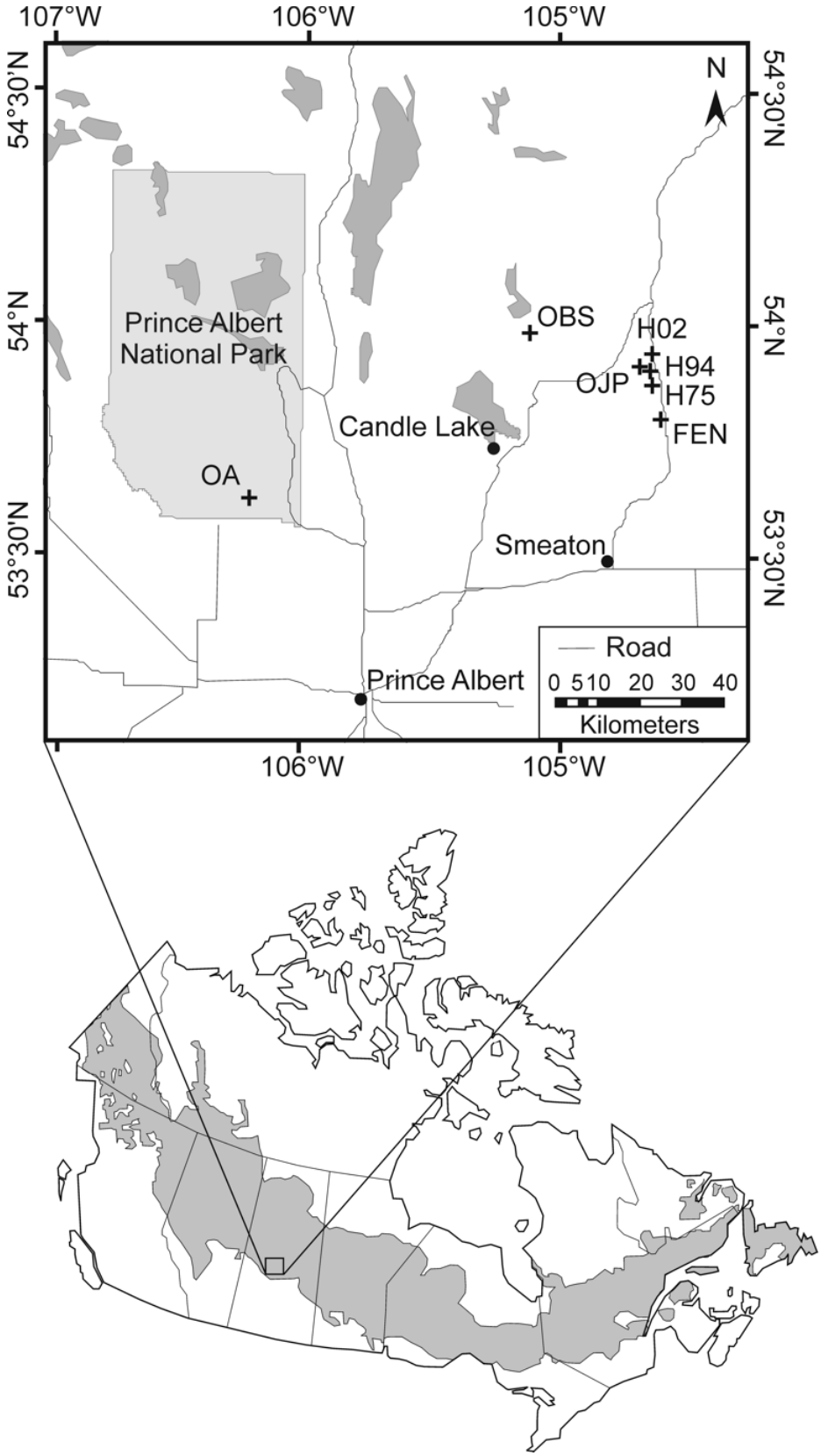

Figure 1.1: A map showing the location of the BERMS study sites. The extent of the Canadian boral forest is shown in gray.

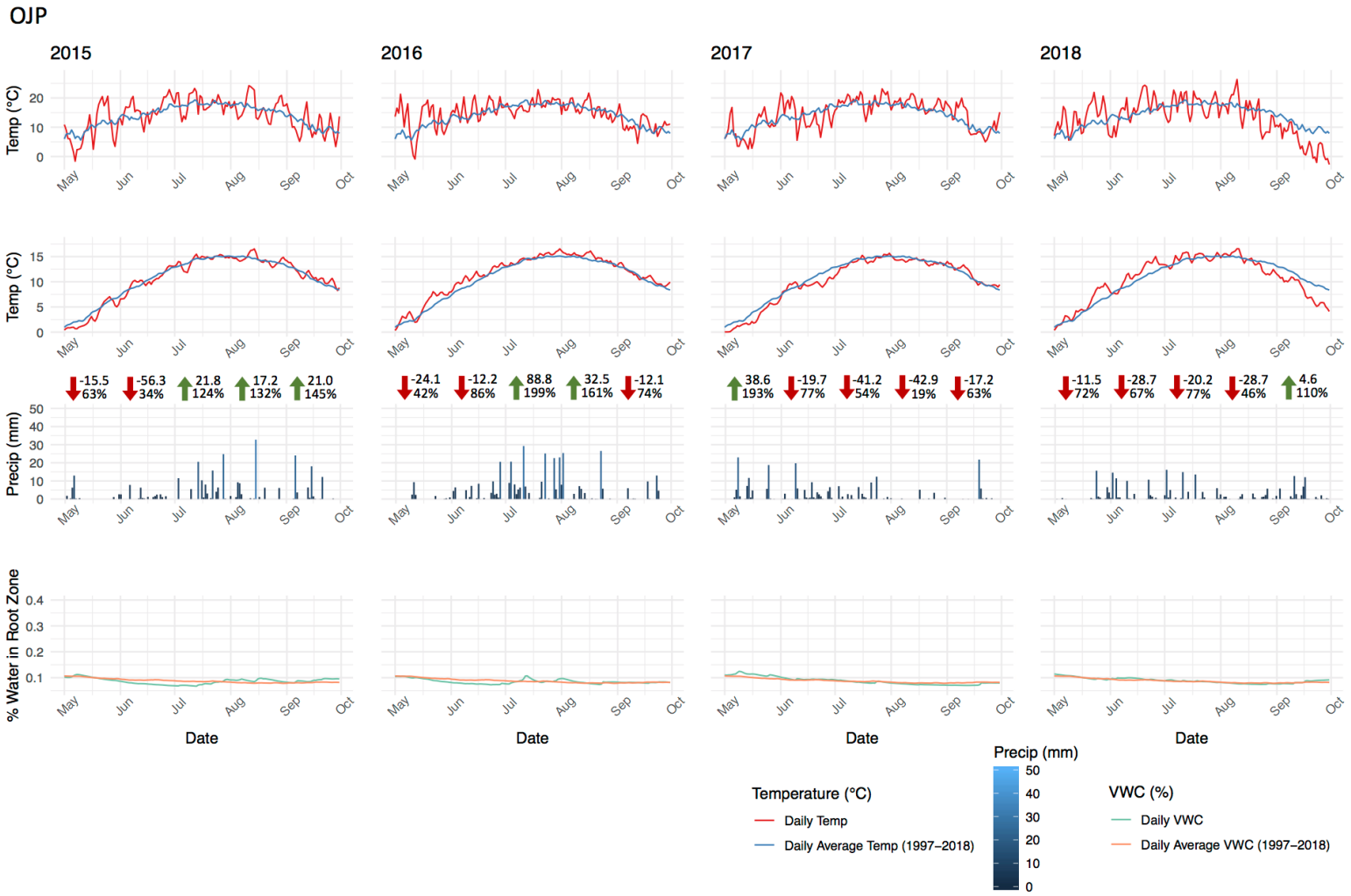

Figure 1.2A: Conditions within the observation period at OJP. From top to bottom, daily mean air temperature (red line), daily mean soil temperature measured at 20cm depth (red line), daily precipitation totals (blue columns), and daily mean VWC (green line). Trends within each growing season can be compared to the norm, calculated from the 22-year record (1997 – 2018). Average daily temperatures (blue lines), and average daily VWC (orange line). Monthly precipitation totals can be compared to the norm with arrows indicating above or below average, mm above or below average, and % precip compared with the monthly average.

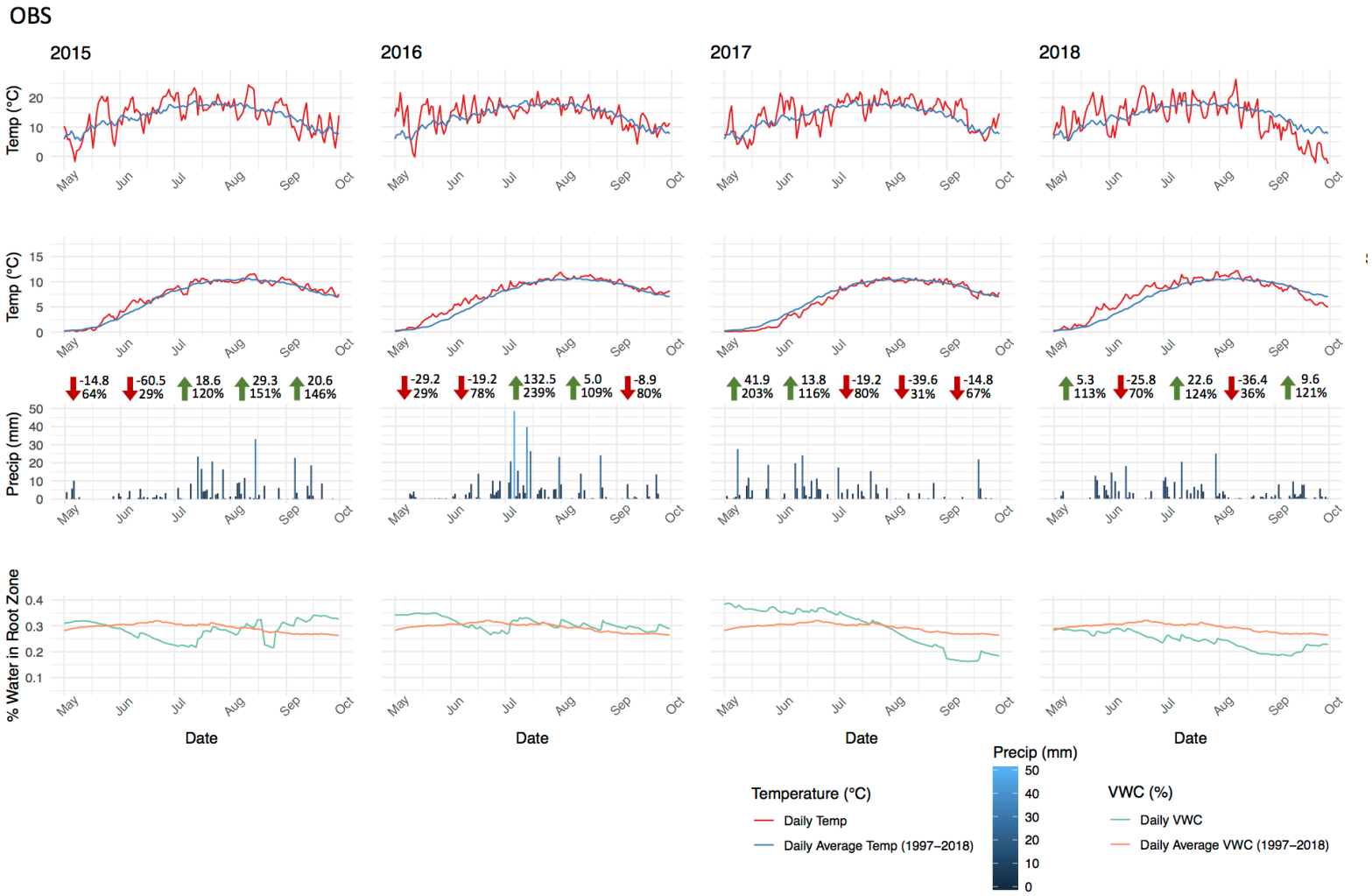

Figure 1.2B: Conditions within the observation period at OBS. From top to bottom, daily mean air temperature (red line), daily mean soil temperature measured at 2cm depth (red line), daily precipitation totals (blue columns), and daily mean VWC (green line). Trends within each growing season can be compared to the norm, calculated from the 22-year record (1997 – 2018). Average daily temperatures (blue lines), and average daily VWC (orange line). Monthly precipitation totals can be compared to the norm with arrows indicating above or below average, mm above or below average, and % precip compared with the monthly average.

Figure 1.2C: Conditions within the observation period at OA. From top to bottom, daily mean air temperature (red line), daily mean soil temperature measured at 2cm depth (red line), daily precipitation totals (blue columns), and daily mean VWC (green line). Trends within each growing season can be compared to the norm, calculated from the 22-year record (1997 – 2018). Average daily temperatures (blue lines), and average daily VWC (orange line). Monthly precipitation totals can be compared to the norm with arrows indicating above or below average, mm above or below average, and % precip compared with the monthly average.

CHAPTER 2

RECENT WARMING AND WETTING IS LIKELY HAVING A SHORT-TERM POSITIVE IMPACT ON SOUTHERN BOREAL FORESTS IN SASKATCHEWAN

2.1 Abstract

Climate change is causing a notable impact on the boreal forest, with projected further increases in temperature, precipitation, and evapotranspiration. In this study, a comprehensive assessment of the tree growth/climate relationship was undertaken to better understand the potential impacts of climate change on four widespread boreal tree species (*Pinus banksiana*, *Picea mariana*, *Larix laricina*, and *Populus tremuloides*) located at the southern limits of the western Canadian boreal forest. At annual resolution, the growth/climate relationship changed over the lifetime of each forest stand. Over the last several decades, the relationship between precipitation and annual-radial tree growth has weakened, while positive relationships between spring and summer air temperature and annual-radial tree growth have emerged, likely signaling a decrease in moisture limitations, and a positive response to spring warming. Over finer temporal scales, precipitation is likely the main driver of stem radius change (ΔR), with jack pine radius having the most consistent positive relationship. Precipitation had a stronger relationship with stem radius variation in black spruce and eastern larch during periods of low volumetric water content (VWC) in the root zone, pointing to the likelihood that certain species rely more heavily on available moisture in the uppermost layers of the soil column to replenish stem water, especially during extended dry periods. It was also found that warm air temperatures had an immediate negative impact on stem water content due to transpiration. This was most marked during periods of reduced moisture availability, when trees are more susceptible to net water volume loss. During periods when moisture was not limiting, a positive relationship between lagged air temperature and ΔR was detected. Warm air temperatures may therefore play an important role in stimulating tracheid cell production when moisture requirements are met. The findings from this study support the conclusion that boreal forest tree species may benefit from spring and summer warming over the near term, providing there is sufficient moisture to support growth. However, over the long term, rates of evapotranspiration are expected to overshadow gains in moisture related to an increase in precipitation. Under these circumstances, we are likely to see reduced growth rates and an increasingly negative response to warm air temperature.

2.2 Introduction

Despite a few accusations of climate "alarmism" directed towards the scientific community, recent observations have shown that climate change, and its impacts, have in fact been underestimated (Brysse et al., 2013). It is therefore unsurprising that the rate of climate change is faster than anticipated, especially in northern regions (Soja et al., 2007; Bush and Lemmen, 2019), where the most dramatic and rapid land surface warming is expected to occur (IPCC 2013; Huntingford and Mercado, 2016). This warming is already having an observable impact on trees in northern forests. For example, there is evidence of treeline advance and shifting ecosystem boundaries, of tree growth decline and mortality, and of an intensification of wildfire and insect outbreak across a range of boreal forest ecosystems (Soja et al., 2007; Harsch et al., 2009). These impacts are also quite prevalent across the boreal forest in Canada (Hogg et al., 2002; Kasischke and Turetsky, 2006; Michaelian et al., 2011; Peng et al., 2011; Wang et al., 2015). Trends in moisture conditions over the last several decades are spatially variable across the Canadian boreal, with a marked drying trend across much of central and western Canada, while northeastern Canada appears to be trending towards wetter conditions (Wang et al., 2014). Moving forward, mean-annual total precipitation is projected to increase across the Canadian boreal, with the most notable changes to occur over the winter and spring months (Henderson and Sauchyn 2008; Jeong et al., 2014; Zhang et al., 2019). However, gains in precipitation are likely to be offset by an increase in evapotranspiration over the long term, leading to a net increase in the frequency and severity of drought, especially in central and western Canada (Wang et al., 2014; Tam et al., 2018).

The boreal forest plays an important role in governing global-scale processes (Bonan, 2008). For example, changes in boreal forest distribution and extent can have a significant impact on earth's radiative balance, through changes in surface and cloud albedo (Betts, 2000; Spracklen et al., 2008). The boreal forest is also an extremely important component of the global carbon cycle, as it represents the largest reservoir of global terrestrial carbon (Sellers et al., 1995; Soja et al., 2007; Bradshaw and Warkentin 2015). Detailed assessments of the radial growth/climate relationship of dominant boreal tree species help predictions regarding how the boreal forest will respond to further changes in climate (Charney et al., 2016). Traditionally this is done using dendroclimatological methods. The standard analysis, developed by Fritts et al.

(1971), and later revised by Blasing et al. (1984) and Guiot (1991), involves using a bootstrapped response or correlation functions to assess linear relationships between standardized annual-ring widths and monthly-climate variables, most often mean temperature and total precipitation. The main assumption is that the relationship between climate and radial growth remains relatively static over the course of the growth period, a tenet which is increasingly unlikely with ongoing rapid climate changes (Biondi, 2000; D'Arrigo et al., 2008). In this environment, a tree's relationship with climate is likely to evolve over the course of its lifetime (e.g., if limitations suddenly become fulfilled, or if tolerances are exceeded) (Jacoby and D'Arrigo, 1995). Alternatively, we can compute correlation and response functions over a moving or evolving window, to address possible non-stationarity in the growth/climate relationship, and to assess how the relationship changes over time (Biondi, 1997). Thanks to advances in computing and the recent widespread adoption of R statistical software, this type of analysis is common, replicable, and easy to compute (Biondi and Waikul, 2004; Zang and Biondi, 2015).

Over the last few decades, several researchers have turned to automatic dendrometers to help examine the tree growth/climate relationship in more detail (Deslauriers, 2003; Bouriaud et al., 2005; Gruber et al, 2009; Duchesne et al., 2011; Cocozza et al., 2016; Cocozza et al., 2018; Güney et al., 2019; Gao et al., 2019) These studies highlight the potential for dendrometers to provide a unique perspective into the mechanisms of tree ring development and its relationship with meteorological conditions within the growing season. However, this method of collecting high-resolution stem size data is not without challenges. The main one relates to disentangling the growth signal from the water signal (Zweifel and Hasler, 2001, Mäkinen et al., 2003; Deslauriers et al., 2007a). Dendrometers measure both reversible and irreversible changes in stem size. Reversible changes are related to daily tree water relations (Herzog et al., 1995) and irreversible changes are associated with radial growth (Deslauriers et al., 2003), which is driven in large part by the expansion of newly formed xylem cells (Cuny et al., 2015). For slow growing trees, it can be difficult to draw conclusions about the relationship between stem radius change and local meteorological variables outside of the main period of stem expansion (Deslauriers et al., 2007a). This is the period during which there is the greatest number of earlywood cells being produced and undergoing radial enlargement (Deslauriers et al., 2003). Further additions to stem size occur beyond this period, as new xylem cells (often latewood cells) continue to be produced and existing tracheids enter later stages of development, including cell wall thickening and

lignification (Samuels et al., 2006). However, these latter processes have a smaller impact on the overall width of the actively developing growth ring (Cuny et al., 2015), and can more easily be overshadowed by water-related variability in stem size (Deslauriers et al., 2007a).

The goal of this study is to comprehensively assess the radial growth/climate relationship of four dominant boreal forest species, jack pine (*Pinus banksiana),* black spruce (*Picea mariana*), eastern larch (*Larix laricina*), and trembling aspen (*Populus tremuloides*) in the southern boreal forest of Saskatchewan. This includes the application of different dendroclimatological approaches to determine how the relationship is expressed at different temporal scales (daily, weekly, and monthly), and whether it varies across species and over time. Note that over fine temporal scales, the term radial growth is no longer used, and instead I discuss relationships between stem radius change (ΔR) and weather. These relationships nonetheless provide additional information regarding potential responses of tree growth (or stem size) to local environmental variables in the southern boreal forest. Intra-annual relationships are assessed over four individual growing seasons between 2015 and 2018, while the observation period for the examination of inter-annual relationships extends back to stand establishment (approx. 100 years).

2.3 Study Sites

This study was conducted at three of the Boreal Ecosystem Research and Monitoring Sites (BERMS), located near the southern edge of the boreal forest in the Boreal Plains Ecozone of central Saskatchewan (Figure 1.1). Site characteristics are given in Table 1.1. The climate of the study area is characterized by short, warm, dry summers and long, cold winters. Mean annual temperature In Prince Albert (PA), Saskatchewan, where the nearest and most complete long term record of climate is recorded, is currently 1.7°C (1989 – 2018). This represents a 1.9°C increase in annual average temperature over the last century, when compared to the 1890 – 1919 reference period (-0.2°C). Annual average precipitation in PA is 517 mm (1983 – 2012), a 60 mm increase since the 1890 – 1919 reference period (457 mm) (Appendix D).

The Old Jack Pine (OJP) site, located northeast of Candle Lake, Saskatchewan, is an even-aged stand of jack pine, naturally established post-fire in 1914 (Barr et al., 2012). The understory is composed of clumps of green alder (*Alnus crispa*), and the dominant ground cover

includes some bearberry (*Arctostaphylos uva-ursi*), and a nearly continuous cover of reindeer lichen (*Cladina mitis*). The soil is a well-drained Orthic Eutric Brunisol (loamy sand). Water table depth is approximately ~6-7 m below the ground surface, and often decoupled from the root zone.

The Old Black Spruce (OBS) site is located due north of Candle Lake, and is a black spruce dominated forest with co-dominant eastern larch comprising approximately 10% of the stands makeup (Pappas et al., 2018). The stand was established post-fire in approximately 1879 (Barr et al., 2012). The understory is mainly comprised of wild rose (*Rosa Woodsii)* and Labrador tea (*Ledum groenlandieum*). The groundcover consists of a mixture of feather mosses, sphagnum moss, and lichen. The soil is poorly drained, with a thick layer of peat (~20 cm) over waterlogged sand. Water table is near or at the ground surface during most of the year, often impinging on the root zone.

The BERMS Old Aspen (OA) site in Prince Albert National Park, is an even-aged stand of trembling aspen, naturally established after a forest fire in 1919 (Barr et al., 2012). The understory is mainly hazelnut (*Corylus cornuta*) with a few other shrubs. The soil is an Orthic Gray Luvisol (loam to clay loam). Water table may be as deep as 4 m below the soil surface, at times impinging on the root zone.

2.4 Methods

2.4.1 Climate and Meteorological data

Several meteorological variables recorded with 30-minute resolution are collected at the BERMS sites. These include precipitation, volumetric water content (VWC) in the root zone, air temperature measured above the canopy, and soil temperature measured at 2, 5, 10, 20, 50 and 100 cm. These are all recorded over the 22-year period 1997 – 2018 (21-years, 1997 – 2017, at OA). From these high temporal-resolution data, daily- and weekly-average temperature, VWC, and precipitation totals were calculated for the short-term observation period (2015 – 2018). To assess lag in the relationship between the meteorological variables and daily ΔR, additional datasets were created by lagging daily temperature, precipitation, and VWC backwards from the stem radius data by 0 to 11 days. Conditions within the short-term observation period (2015 – 2018) are compared to the average in Section 1.11 and Figures 1.2 A, B, and C (Chapter 1).

Long-term (100+ year) climate records were acquired from the Environment and Climate Change Canada (ECCC) climate stations in Prince Albert (station #4056240 and #4056241) and Waskesiu Lake (station #4068559). Regression determined the relationship between conditions at the ECCC stations and those at the BERMS sites. Long-term climate records for each of the BERMS sites were modeled from these observed relationships, however the Prince Albert dataset showed a good relationship with BERMS sites overall (Appendix A). Therefore, rather than introducing uncertainty into the analysis by using modeled climate data, the Prince Albert dataset, which provided an almost continuous record of homogenized mean-, minimum-, and maximum-monthly temperature from 1890 – 2018 and adjusted monthly precipitation totals from 1890 to 2012 was used.

2.4.2 Dendrometer data

DC2 type circumference band dendrometers (Ecomatik, 2019) were affixed to four individuals of each study species in 2015, trembling aspen at OA, jack pine at OJP, and black spruce and eastern larch at OBS. The four dendrometers assigned to each species were split into pairs and fed to two HOBO UX120-006M data loggers, for a total of 16 bands, and eight data loggers. In 2016, to increase sample depth and cover a wider spatial area within each site, an additional 12 individuals of each species were instrumented (DC3 type dendrometers; Ecomatik, 2019). Over the short-term observation period (2015 – 2018), the sites were visited regularly during the growing season (May to October), to ensure the smooth running of the instruments, and when necessary, to replace or repair dendrometers. Following the expansion of data collection efforts in 2016, between 12 and 16 individual trees of each species were instrumented at any given time.

Raw data were collected with 30-minute resolution, at equal time steps as the meteorological data collected at BERMS. An R-script, based on calculations provided by Ecomatik, was used to convert the raw dendrometer output to a measure of radius change from a starting point of 0µm. The resulting data were checked for errors relating to sensor failure, or wildlife activity, and data were omitted accordingly. At our study sites, the dendrometers recorded synchronous variations in stem size between individuals. Species averages were therefore calculated and used as site- and species-specific records of radius change. The only exception was for eastern larch in 2016. This species produced two distinct records of ΔR which

were dependent on where the banded individuals were located in the site. Half of the individuals being located in a wetter section of OBS, and the other half in an area with less standing water. Two species averages were therefore produced for eastern larch in 2016, larch-wet and larch-dry.

To determine which method would be most appropriate for the extraction of the growth signal from the high-resolution dendrometer data, a comparison of the four most common extraction methods (stem cycle, Rmean, Rmin, and Rmax) was made in Appendix B. It became apparent that the stem cycle approach had a tendency of over-representing large pulses in stem size relating to moisture inputs, resulting in increased variability (Appendix B). The "daily mean approach" is known to produce similar results as the stem cycle approach and is similarly effective at extracting the growth signal (Deslauriers et al., 2007a). Daily and weekly-resolved records of mean stem radius were therefore constructed before calculating the difference between each value of mean stem radius and the preceding one, resulting in records of stem radius change (ΔR) over the short-term observation period (2015 – 2018).

2.4.3 Core Samples

Core samples were extracted from trees at OJP and OA using a 5.1 mm increment borer following the 2018 growing season. A plot-based sampling scheme was employed based on the findings from Babst et al. (2014). This sampling protocol is designed to yield ring-width data appropriate for the reconstruction of stand-level above-ground biomass accumulation. The appropriate sample size is determined by stand density, with dense stands requiring a greater sample size to achieve an accurate reconstruction of biomass accumulation (Babst et al., 2014). Existing permanent sampling plots at OJP and OA (Gower, 2001) were examined and the one which most accurately represented overall stand density at each of the sites was chosen. Every living individual within these two plots were sampled and their length was extended on a randomly chosen side to accommodate additional individuals and reach the required sample size based on stand density. OJP Gower plot 4 was extended by 2.5 m (27.5 m x 25 m), and OA Gower plot 2 by 15 m (40 m x 25 m). In total, a single core was extracted from 54 and 46 individuals at OJP and OA respectively.

OBS was sampled in 2015 (Pappas et al.; 2020). Here, a single core was extracted from >90 black spruce and eastern larch trees located in two 5 m-radius circular plots in random

locations within the site. Because of the limited sample size, eastern larch cores were excluded from study, along with black spruce cores which contained missing or heavily fragmented segments. The final master chronology included 73 black spruce trees (ITRDB site code CANA610; https://www.ncdc.noaa.gov/paleo-search/study/29612).

All samples were processed using standard dendrochronological techniques (Speer, 2010) in the Mistik Askiwin Dendrochronology (MAD) Lab. After being mounted to slotted boards and sanded with progressively finer grits of sandpaper, each ring was measured with 0.001 mm precision on a Velmex stage system, under a Nikon 63X stereomicroscope using ProjectJ2X software (VoorTech, 2017). The resulting ring-width series were crossdated using COFECHA software (Holmes, 1983; Speer, 2010), and remeasurements were made to account for human error and minimize the amount of flagged problematic segments (Table 2.1). The resulting crossdated series were standardized using the detrend function in the dplR (Bunn, 2008). A negative exponential curve was fit to each series, before species specific master chronologies were built.

2.4.4 Statistical Analysis

All data analysis and preliminary visualization was done in R. Moving-window correlations at both the daily and annual scale, were done using the treeclim package (Zang and Biondi, 2015). Bootstrapped Pearson's correlations were computed over a 30-day/year moving window offset by 1-day/year. The resulting relationships were "flagged" if statistically significant at the 99% confidence level. The treeclim package was also utilized to undertake a lag analysis, computing bootstrapped Pearson's correlations between variations in stem radius and lagged meteorological variables, offset from the records of ΔR by 0 to 11 days. In the case of precipitation, which returned errors in two instances when Pearson's correlations were bootstrapped, a non-bootstrapped version was computed. In this instance, significance was flagged at the 99% confidence level but based on a critical r-value rather than the bootstrapped confidence intervals. Since this type of analysis is not often undertaken at the daily scale, the data were tested for normality across each of the 30-day intervals using the Shapiro-Wilk test (Appendix C). To further ensure Pearson's correlations are appropriate for use with these datasets, results from the moving-window Pearson's correlation were also compared to equivalent analyses using non-parametric tests, Kendall's tau and Spearman's rank correlations

(Appendix C). Static-correlation analyses at weekly and annual scales are also undertaken using the treeclim package, with statistical significance once again flagged at the 99% confidence level.

2.5 Results

2.5.1 Inter-annual Growth/Climate Relationships

An assessment of the static relationships between standardized annual-ring widths and monthly climate variables over the long term (n = 94 to 122 years) yielded generally weak correlations, with few instances of statistical significance at the 99% confidence level. Black spruce radial growth had a negative association with current spring maximum monthly temperatures, including a statistically significant negative relationship with maximum-June temperature (Figure 2.1-A-i.). The relationship between aspen radial growth and temperature during the late-spring and summer months, both from the current and previous growing season was generally positive, including a positive correlation with mean-July temperature from the current growing season (Figure 2.1-B-i.). There were no statistically significant relationships between the radial growth of the study species and minimum monthly temperature, however those between aspen radial growth and minimum monthly temperature during the late-spring and summer months were once again generally positive (Figure 2.1-C-i.). Black spruce was the only species whose annual radial growth was significantly related to monthly precipitation totals (Figure 2.1-D-i.). Current spring precipitation (April-June), as well as previous-May and previous-August precipitation (year n-1), was positively correlated with black spruce radial growth. Relationships between jack pine radial growth and the monthly climate variables were generally weak, with no instances of statistical significance. However, perhaps the only climate variable of note was May precipitation from the current growing season, which had a relatively strong positive correlation with jack pine radial growth (Figure 2.1).

2.5.2 Non-Stationary Growth/Climate Relationships

Considering the possibility of non-stationarity in the long-term growth/climate relationship, a 30-year moving-window correlation analysis revealed a changing relationship between annual-radial growth and climate (Figure 2.1-ii.). Black spruce radial growth was negatively correlated with monthly temperature during the spring and summer (March-August)

from the mid-1910s to the mid-1960s (Figure 2.1-ii.). Previous July temperature also had a negative relationship with black spruce radial growth over this same period. Beginning in the mid- to late-1940s, there was a long period where previous September temperature had a negative relationship with black spruce radial growth (Figure 2.1-ii.). Overall, there were very few intervals during which there were significant positive correlations between black spruce growth and monthly temperature variables. Mean and maximum July and September temperature had a positive relationship with black spruce radial growth for a few decades during the early-1900s, and more recently, a positive relationship with current summer temperatures, notably minimum September temperature, has emerged (Figure 2.1-C-ii.).

Compared with black spruce, jack pine and aspen radial growth had weaker relationships with monthly temperature, and most were positive (Figure 2.1-ii.). Only recently, since about 1980, has there been significant positive correlations between monthly temperature variables and jack pine radial growth. These emergent positive relationships occur during the early-spring (April) and winter (November, December) from the previous growing season, as well as January, early-spring (April), and late-summer (July, August, September) from the current growing season (Figure 2.1-ii.).

The strongest and most persistent relationships between aspen radial growth and monthly temperature occurred during the beginning and end of the growth record (Figure 2.1-ii.). Early in the growth record, from about 1925 to the late 1950s, mean- and minimum-monthly temperature had a positive association with aspen radial growth during July of the previous year, and during May, June, July, and September of the current year (Figure 2.1-B and C-ii.). In recent decades, since about the 1970s and 80s, positive relationships between aspen radial growth and previous growing season temperatures have again emerged, including a significant positive correlation with mean and maximum September temperature (year n-1) (Figure 2.1-A and B-ii.), and with minimum May and June temperature (year n-1) (Figure 2.1-C-ii.).

The relationship between annual-radial growth and precipitation was most often positive (Figure 2.1-D). There were however a few periods of negative correlations with previous June and current March for jack pine, and previous October and December for black spruce. Persistent positive relationships occurred in May for jack pine, both from the previous and current growing season. Current June and August precipitation also had a significant positive relationship with

jack pine radial growth, but during only a few 30-year intervals (Figure 2.1-D-ii.). There were several instances over the course of the growth record where black spruce radial growth was positively associated with monthly precipitation. There were sporadic instances of statistical significance in this relationship during May, July, and August of the previous year, and over the spring and summer months of the current year (March-August) (Figure 2.1-D-ii.). There were only two months during which there were significant relationships between precipitation and aspen radial growth. The strongest and most persistent relationship between these two variables occurred in September of the previous year, which was positive from the early-1930s to the mid-1970s. Precipitation during April of the previous year also had a significant positive correlation with aspen growth, but over only two intervals (Figure 2.1-D-ii.). It should also be noted that relationships between precipitation and radial growth appear to be weakening in recent decades. There are no significant correlations between radial growth and precipitation since the mid-1950s for aspen, and since the late 1970s for jack pine and black spruce (Figure 2.1-D-ii.).

2.5.3 Intra-Annual Drivers of Stem Radius Change

In contrast to Figure 2.1, which relates annual radial growth to monthly climate variables over the life of the stands (~ 100 years), Figures 2.2 to 2.6 show the relationships between ΔR and meteorological variables at weekly and daily scales during four individual growing seasons within the short-term observation period (2015 – 2018). Of the seven meteorological variables examined, precipitation was the only one that had a significant correlation with ΔR at weekly scale resolution (Figure 2.2). Relationships between weekly precipitation totals and weekly ΔR were generally positive for all species assessed in 2017 (jack pine, black spruce, eastern larch, and aspen), and in 2018 (jack pine, black spruce, and eastern larch), with statistically significant results for jack pine, eastern larch, and black spruce in both years. The relationship between weekly jack pine ΔR and precipitation was also moderately positive in 2016. Beyond precipitation, VWC was the only other meteorological variable that had noteworthy relationships with the weekly ΔR of the study species. Aspen ΔR had a stronger positive correlation with weekly VWC in 2017, and jack pine ΔR had a stronger negative correlation with VWC in 2015. A lag analysis at weekly resolution showed no significant results.

At daily resolution, precipitation and air temperature had the most important relationships with ΔR. This assessment is based on the strength (r-values) and persistence (consecutive

instances of statistical significance) of correlations at the 99% confidence level. Shallow soil temperature (measured at 2, 5, and 10 cm) also had a significant relationship with the ΔR of the study species, but only for comparatively brief periods of time during the 2016, 2017, and 2018 growing seasons (Figure 2.3).

The relationship between ΔR and precipitation was generally weakest for aspen, most persistent (longest running statistical significance) for jack pine, and strongest for black spruce and eastern larch (Figures 2.3 and 2.4). In Figure 2.4, relationships between daily precipitation and ΔR at lag = 0 provide information regarding the correlation between rainfall and the change in mean stem radius since the last 24h cycle. This correlation was always positive, and was generally stronger towards the beginning and end of the growing seasons. Correlations between ΔR and precipitation at lag = -1 day were also positive and generally strongest near the beginning and end of each growing season. Beginning at lag = -2 days, the relationship transitions from positive to negative. Therefore, precipitation frequently corresponded with an increase in stem radius compared to the previous day, or by the next day and a decrease during subsequent days, most frequently during the subsequent two days. These three modes can exist simultaneously, during the same 30-day interval, or over distinct periods throughout different parts of the growing season. The bootstrapping technique resulted in errors and missing data regarding the relationship between daily precipitation totals and daily variations in jack pine and aspen stem radius in 2017. This particular correlation analysis, shown in figure 2.4, was therefore done without bootstrapping. Results at lag = 0 in Figure 2.4 can be compared to bootstrapped versions of these same correlations in Figure 2.3 (except for jack pine and aspen in 2017) and the results were unaffected.

Air temperature had a negative relationship with variations in mean daily stem radius of the study species at lag = 0 (Figure 2.5). This shows that warm air temperatures often corresponded with a decrease in stem radius since the previous day. This relationship transitioned to positive at lag = -1, -2, and -3 days, with the strongest and most persistent positive correlations at lag = -2 days. Therefore, warm air temperatures at times corresponded with a decrease in the stem radius of the study species compared to the previous day and a subsequent increase in stem radius within the next three consecutive days, most frequently during the following two consecutive days. Again, these modes can exist simultaneously (e.g. during

intervals with start dates in May and June 2016 and 2017), but more frequently occured over distinct periods during the growing season (Figure 2.5). These two modes alternated in 2018, from positive (lag = -2 and -3 days) for intervals with start dates in May to about mid- June, to negative (lag = 0) for intervals with start dates during the second half of June, back to positive (lag = -1 and -2 days) for intervals with start dates in July, and again to negative (lag = 0) for intervals with start dates in August.

The relationship between daily soil temperature and ΔR was weak and inconsistent when compared with precipitation and air temperature (Figure 2.3). Relationships between soil temperature and ΔR were most often positive, and only statistically significant for brief periods of time, primarily during the 2016, 2017, and 2018 growing seasons. Soil temperature was measured at multiple depths, and the shallowest depths (2, 5, and 10 cm) had the most important relationship with the ΔR of the study species. Beyond a few sporadic instances, the only period of note during which there were stronger correlations between ΔR and deep soil temperature (below 10 cm) was near the end of the 2017 growing season (Figure 2.3). During this period, there were significant negative correlations between variations in black spruce, eastern larch, and aspen stem radius, and deep soil temperature. Relationships between soil temperature and ΔR that were strong at lag = 0 often weakened when lag was introduced. One of the few exceptions was again the negative correlation between shallow soil temperature and ΔR towards the end of the 2017 growing season, which increased in strength and significance when soil temperature was lagged by 1 to 5 days (Figure 2.6). Only the lag analysis for soil temperature at 2 cm was shown because patterns remained the same for soil temperature taken deeper in the soil column, the only difference being that relationships were weaker.

Overall, the coniferous study species (jack pine, black spruce, and eastern larch) had similar relationships with meteorological conditions within each of the growing seasons. This can be seen by comparing the first three (or four in 2016) rows of graphs in Figures 2.3, 2.4, 2.5, or 2.6, during any of the growing seasons within the observation period (2015 – 2018). Trembling aspen too, at times, exhibited a somewhat similar relationship with meteorological conditions. However, there were several potential issues regarding the dataset of aspen stem radius that must be considered when interpreting these data. Firstly, due to issues with site access, the record of aspen stem radius was quite limited in 2015, both in terms of length and

sample depth. Secondly, during the following growing season (2016), there was a severe forest tent caterpillar outbreak, which resulted in a near complete defoliation and two separate leaf out events (Stephens et al., 2018). This undoubtedly had a severe impact on radial growth, and likely altered how these trees reacted to meteorological conditions over the course of this growing season. The 2017 growing season was a recovery year, and it was also likely impacted by the 2016 outbreak. The 2016 and 2017 growth years are therefore not representative of normal growing seasons. Furthermore, the aspen time series ends in 2017 due to the decommissioning of the Old Aspen site in 2018. Thus, great caution should be exercised when interpreting results from OA at daily and weekly resolution.

2.6 Discussion

2.6.1 Traditional Dendroclimatological Analysis

Important relationships that were identified following static dendroclimatological analyses are not necessarily those that had the strongest impact on radial growth. When the long-term radial-growth record was broken down into 30-year segments, and relationships were reassessed over a moving window, the monthly climate variables that had the strongest associations with radial growth over the long term often showed weak associations over the medium term. For example, the relationship between maximum-June temperature and black spruce radial growth, which was strong negative over the full length of the growth record, was rather weak when the growth record was broken down into 30-year intervals (Figure 2.1-A-i. and A-ii.). Similarly, the relationship between mean-July temperature and aspen radial growth, which was strong positive over the long term, was again weak over the medium term, with a single 30-year interval showing a statistically significant result (Figure 2.1-B-i. and B-ii). The static correlations that were strongest over the long term are those that were most consistent in terms of their quality, with the direction of their relationship remaining the same over time. Therefore, the static correlation analysis was only successful in highlighting the relationships that were most consistent over time, not necessarily those that were most meaningful in terms of their overall influence on radial growth.

For the entire growth record, relationships between black spruce radial growth and monthly temperature during the current and previous growing season (April-September) have in

large part been negative, most significantly between the mid-1910s and 1960s. Huang et al. (2010) attributed negative correlations between black spruce radial growth and growing season temperatures to enhanced water-stress due to increased rates of respiration and evapotranspiration under warm conditions. Earlier studies by Dang & Lieffers, (1989) and Hofgaard et al. (1999) reported similar relationships, and the timeframe of these studies may overlap more closely with the period of enhanced negative correlations between black spruce radial growth and growing season temperatures observed in this study. The sensitivity of black spruce to water-stress also explains its significant positive relationship with growing season precipitation, an association which is more important in this species than it is in jack pine and aspen. In this study, jack pine was generally insensitive to the monthly climate variables assessed. Over the course of the growth record, May precipitation, both from the current and previous growing season is the climate variable that had the most persistent relationship with jack pine radial growth, a relationship which is significantly positive from about the mid-1930s to the mid-1980s. May precipitation was also found to enhance the radial growth of jack pine in Huang et al. (2010), due to the potential importance of spring precipitation for replenishing water supply at latitudes north of 52°. Aspen radial growth had generally positive relationships with spring temperature in this study, primarily during the current growing season. A positive correlation between aspen radial growth and May temperature was also identified in Chen et al. (2017), and is attributed to the enhancement of aspen growth in response to early leaf emergence and photosynthesis.

The moving-window correlation analysis also helped to reveal some emergent trends in the growth/climate relationship. Emergent relationships between radial growth and temperature include: positive correlations between radial growth and current summer temperatures for jack pine and black spruce (Figure 2.1-ii.); positive correlations between jack pine radial growth and April temperatures (both current and previous), as well as previous-winter temperatures (November, December, and current January) (Figure 2.1-ii.); and positive correlations between aspen radial growth and previous-growing-season temperatures (April to September). Relationships between radial growth and precipitation have also decreased in significance in recent decades, since the mid-1950s for aspen, and since the late 1970s for jack pine and black spruce (Figure 2.1-D-ii.). Non-stationarity in the growth-climate relationship has been observed by many, and is widely discussed in D'Arrigo et al. (2008). However, in contrast to studies

which report weakening relationships with temperature (D'Arrigo et al., 2008), the results from this study show an enhanced positive relationship with temperature and weakening relationships with precipitation. The main difference is that the BERMS sites are located at lower latitudes than those reporting a reduction in sensitivity to temperature. In Prince Albert, Saskatchewan, where the nearest and most complete long-term record of climate is recorded, there is an overall trend towards warmer and wetter conditions since at least the mid-1940s, especially during the spring and summer months (Chen et al., 1999; also see Appendix D). Non-stationarity in the radial growth/climate relationship is often attributed to shifting limitations (D'Arrigo et al., 2008), and in this case, it is likely signaling a decrease in moisture limitations, and a positive response to warming.

2.6.2 Assessment of Relationships over Intra-Annual Scales

As stated earlier, dendrometers produce data containing both reversible and irreversible changes in stem size from the competing signals of tree-water relations and radial growth. Furthermore, beyond the main period of stem expansion, from late-spring to mid-summer, it is more likely for the reversible changes in stem size, caused by the hydration and dehydration of the stem, to overshadow any irreversible changes in stem size related to the addition and expansion of latewood cells, or to cell wall thickening and lignification late in the growing season (Deslauriers et al., 2007a). It is difficult to precisely identify the onset of xylem cell production from dendrometer data, as it often overlaps and is easily confused with spring rehydration (Deslauriers et al., 2007a; Duchesne et al., 2011). However, based on a preliminary analysis of weekly microcore data (not shown), and according to the data of cumulative stem radius (Figure 2.7), the main period of stem expansion for the study species runs from approximately late-May to mid-July. This is the period during which the dendrometer data are most heavily influenced by the radial growth signal. Due to the variable influence of radial growth on the dendrometer data, it is common practice to offer a breakdown of the growing season, or to isolate the main period of growth, prior to an examination of relationships (Gruber et al., 2009; Duchesne et al., 2011). The moving-window correlation analysis is not often applied to the study of relationships over fine temporal resolution. However, this technique offers a high-resolution breakdown of the growing season, allowing for an examination of relationships between stem radius variations and meteorological variables, as they evolve during different

points in the process of ring development, and in response to changing growing season conditions.

The observed relationship between daily and weekly precipitation and the ΔR of the study species (Figures 2.2 and 2.3) was likely related to the influence of stem water content on variations in stem radius rather than the influence of radial growth. At daily resolution, a pulse in moisture often corresponded with an increase in stem radius either since the previous day, or by the next day, most frequently beyond the main period of stem expansion. An increase in stem size following a rain event has been observed by many others (Mäkinen et al., 2003; Deslauriers et al., 2007b; Turcotte et al., 2011; King et al., 2013; Güney et al., 2019) and is likely driven by daily changes in stem water storage. During the day, when transpiration is taking place, water storages in elastic tissues (i.e. bark, phloem, cambium) are depleted, resulting in stem shrinkage (Steppe et al., 2006; Zweifel et al., 2000; Zweifel et al., 2001). This is less likely to occur during rain events, under cloudy conditions and low vapour pressure deficit (VPD). Overnight when transpiration is low or ceased, water stores are replenished resulting in stem radius expansion. A net increase in stem size is therefore more likely to occur following days when VPD is low, when stem water recharge overnight can more easily surpass the volume of stem water depleted during the day. Daily changes in stem water storage is therefore dependent on environmental conditions such as precipitation, due to its influence on atmospheric demand and moisture availability (Zweifel et al. 2005; Drew et al., 2011).

The link between stem size and stem moisture content was present at the BERMS sites regardless of speciation, yet based on the strength and persistence of relationships between ΔR and precipitation, jack pine appeared to be most susceptible to stem radius fluctuations in response to precipitation (Figure 2.3). This is perhaps unsurprising, considering that this species, compared to the other study species, has lesser access to water in the root zone (Figure 1.2 VWC), and must be more efficient at uptake when water is made available. Similarly, black spruce and eastern larch stem radius were more strongly correlated with precipitation during periods of depressed VWC in the root zone, towards the end of the 2017 growing season and during the main period of growth in 2018 (Figures 1.2 VWC and 2.3). It is believed that jack pine is restricted in terms of water availability, whereas black spruce and eastern larch may change the depth at which they are uptaking water according to shifting availability. Jack pine is

located over well drained sandy soil and while the roots extend deep into the soil column, most roots are concentrated near the surface. Conversely, the high water-table at OBS limits the rooting depth of black spruce and eastern larch but allows for increased water availability in the root zone (Figure 1.2). Jack pine must therefore take advantage of water in the shallow soils when it is replenished by precipitation, while black spruce and eastern larch may rely on water table resources during wet periods and shift to shallow soil resources when water table depth drops well below the root zone. There are reports of similar shifts in the depth of water uptake in the literature. Ellsworth and Sternberg (2015) investigated intra-seasonal water use in a dry plant community in Florida, USA, and showed that during the dry season the depth of water uptake changed according to water availability. Furthermore, Nehemy et al. (2019) used a controlled experiment to show that water uptake shifted from shallow to deep water resources in response to changes in plant water status. Species ability to quickly acquire transient water sources and shift the depth of water uptake under limited supply is an ecological trait (Ehleringer et al., 1991; Volkman et al., 2016).

It is likely that, during periods of reduced moisture, instances of stem water replenishment were immediately followed by water loss, as it is more difficult for trees to maintain high levels of water storage in the stem under these conditions. This is evidenced by the observation that negative relationships between precipitation and stem radius variations (strongest at lag = -2 days) were strongest during periods with below average precipitation (e.g. May – June, 2016) (Figure 2.4).

In this study, warm air temperatures corresponded with either a decrease in stem radius since the previous day (negative correlations at lag = 0), or an increase in stem radius during subsequent days (positive correlations at lag = -1, -2, and -3 days) (Figure 2.4). Negative relationships between air temperature and stem radius variations over daily to sub-daily scales are well documented and are attributed to an increase in transpiration rates and a decrease in stem water volume in response to warm air temperatures (Peng et al., 2017; Cocozza et al., 2018; Güney et al., 2019; Gao et al., 2019). Moisture availability also plays a role in governing this relationship, since net volume loss is more likely to occur during periods with limited moisture, when daily water loss is not easily offset by stem water replenishment overnight (Mäkinen et al., 2003; Turcotte et al., 2011). This ultimately results in a persistent reduction in amplitude of the

diurnal stem size cycle as dryness persists (King et al., 2013). Furthermore, it has been found that xylem cell production may cease in response to water limitations (Deslauriers et al., 2016), making it more likely for the data of stem radius to be dominated by the stem-water signal during periods of water deficit (Zweifel et al., 2016). The observations from this study support these findings. It is likely for these reasons that negative relationships between the ΔR of the study species and air temperature at lag = 0 are most prevalent during periods with little precipitation (Figures 1.2 and 2.5).

Conversely, air temperature, within an optimal range, may play an important role in stimulating xylogenesis (Gruber et al., 2009; Oberhuber et al., 2014; Cocozza et al., 2016), perhaps most importantly towards the beginning of the growing season, where air temperature exerts significant control over the onset of xylem cell production (Rossi et al., 2007; Rossi et al., 2008). There is evidence of this at the BERMS sites, but only during periods of increased moisture availability. Under these conditions, observations suggest that elevated air temperature may result in a stimulation of the processes contributing to radial growth in the study species over the next 1 to 3 days, resulting in a positive correlation with lagged air temperature (lag = -1, -2, and -3 days) (Figure 2.5). Positive relationships between lagged-air temperature and variations in stem radius occured during the main period of stem expansion in 2016, during intervals with start dates in early to mid-July, corresponding with a period of increased moisture availability (Figures 1.2 and 2.5). The spring of 2017 was also extremely wet, with about twice the average amount of precipitation during the month of May (Figure 1.2). Following this input of moisture, around the time one would expect the onset of radial growth for the season, there were strong positive relationships between the ΔR of the four study-species and air temperature (lag = -2 days) (Figure 2.5), pointing to the importance of temperature in stimulating radial growth when moisture requirements have been met.

A good illustration of the dual nature of the relationship between temperature and daily stem radius variations can be seen in 2018. There was below-average precipitation during much of the 2018 growing season, with pulses of moisture in late-May to early-June, and in July (Figure 1.2). It is during these periods of increased moisture that the strongest positive correlations between lagged air temperature and variations in stem radius are observed (Figure

2.5). Negative relationships with air temperature at lag = 0 occurred intermittently in 2018, during the driest periods, in late-June and August (Figure 2.5).

Observed correlations between stem radius variations and soil temperature, which were weak compared to correlations with precipitation and air temperature, were likely spurious, due to a co-occurring positive relationship with air temperature. Periods during which the positive relationship between ΔR and soil temperature were strongest include early in the growing season in 2016 and 2017, during intervals with start dates in mid-May, towards the end of the main period of stem expansion, during intervals with start dates in July 2016 and 2018, and beyond the main period of stem expansion, during intervals with start dates in August 2017 (Figure 2.6). These examples co-occur with the most marked positive relationships with air temperature (Figure 2.5), except with a reduction in lag time; likely the time required for warmth to penetrate the uppermost layers of the soil.

Negative relationships with daily air and soil temperature observed late during the 2017 growing season initiate almost synchronously across the four study-species immediately following a rain event (Figures 2.5 and 2.6). This is likely indicative of a response to the input of moisture late in the growing season, during a time when air and soil temperature are falling naturally. Following the main period of stem expansion in 2017, there was a steady decline in the stem radius of the study-species, indicative of stem dehydration, which lasted from about late-July to mid-September (Figure 2.8). This was a very dry period, especially at OJP and OBS, which received very little precipitation during this time (Figures 1.2, and 2.8C). There was a late pulse in stem radius beginning on September 19th, in response to a rainfall event that occurred this same day (Figure 2.8A and C). Over a period of only a few days, the study species recuperated water volume lost during the dry period, and with the exception of aspen, which received a bit of a reprieve from this dry spell with an input of moisture on August 5th (Figure 1.2), extend past their maximum recorded stem radius (Figure 2.8). Beginning around interval 233-262 (August 21st – September 19th), two relationships emerged: a strong negative relationship with air and soil temperature for all species (Figures 2.5 and 2.6), and a strong positive relationship with precipitation (lag = -1 day) for jack pine, black spruce, and eastern larch (Figure 2.4).

2.7 Conclusion

It is important to acknowledge that the tree growth/climate relationship is often not static through time. This relationship has been shown to evolve over the short- and long-term in response to changes in weather, stand dynamics, and climate. In this study, the most common dendroclimatological analysis, a static bootstrapped correlation function analysis between annual-ring width and monthly climate variables, was only successful in identifying the growth/climate relationships which were most consistent over time, not necessarily those that had the most meaningful impact on the growth of the study species, especially in recent years. This type of analysis may therefore become increasingly inappropriate during this era of climatic change. To account for the dynamic nature of the growth/climate relationship, I computed bootstrapped response or correlation functions over a moving or evolving window. In doing so, I identified a general increase in the strength of positive relationships between spring and summer air temperature and radial growth, and a weakening of the relationship between precipitation and radial growth over time, likely signaling a positive response to spring warming, and a decrease in moisture limitations in this region. These findings provide evidence that non-stationarity in the growth-climate relationship may be more widespread than originally anticipated, or perhaps that these issues are becoming far reaching as climate change progresses. The identification of dynamic growth/climate relationships in the southern boreal forest has implications for researchers using tree rings for paleoclimate reconstruction and for projections of future climate.

The ΔR of the study species at daily and weekly scales often had a strong correlation with precipitation, likely calling reference to the importance of stem water dynamics in driving intra-annual variations in stem radius. Bearing in mind the limitations associated with the record of aspen stem radius, I identified a response to moisture input that was common among the four study-species. Furthermore, the relationship between precipitation and ΔR in black spruce and eastern larch was enhanced during periods of low VWC in the root zone. This points to the likelihood that certain species in the southern boreal forest rely more heavily on available moisture in the uppermost layers of the soil column during periods when moisture in the root zone is limiting. This information would be of interest to those conducting ongoing research regarding tree-water relations in the southern boreal forest.

I also observed that warm air temperatures have an immediate negative impact on stem water content. This occurred most frequently at the BERMS sites during periods of reduced moisture availability, when the stem radius data are more likely to be dominated by the water signal, and when trees are more susceptible to net volume loss due to high evaporative demand. When moisture requirements are met however, warm air temperatures may have the opposite effect, playing a role in stimulating radial growth and resulting in an increase in stem radius during subsequent days. It should be noted that this interpretation of results is based on detailed observation over a limited timeframe. Continued observation and alternative methods of analysis are required to test this hypothesis, and to determine whether these results persist over a longer period.

It has been suggested that some boreal forest trees may end up benefitting from spring warming over the near term, providing there is sufficient moisture to support growth (Boisvenue & Running, 2006; Zhang et al., 2008; D'Orangeville et al., 2018). In response to the recent wetting trend, trees in the southern boreal forest may be particularly well positioned to take advantage of this short-term benefit, considering that moisture is the dominant limiting factor controlling the distribution and growth of trees in this region (Sellers et al., 1995; Ireson et al., 2015) and considering that the dominant species in this region may benefit from moderate climate warming (D'Orangeville et al., 2018). The results from this study help to support this hypothesis and build on our understanding of a potential response of common boreal forest trees to changing environmental conditions in the southern boreal forest. It is likely that the recent warming and wetting trend has contributed to a decrease in moisture limitations and an enhanced positive response to spring and summer air temperature over the last several decades at the BERMS sites. There is evidence of this at annual temporal resolution, in the shifting growth/climate relationships, and in the more nuanced response of daily variations in stem radius to environmental conditions within the growing season. It is recommended that high-resolution stem-size data should continue to be collected at these sites to establish a proper baseline for active ring development and its response to meteorological conditions within the growing season. Moving forward, rates of evapotranspiration are expected to overshadow any gains in moisture related to an increase in precipitation (Wang et al, 2014), a trend which is likely already occurring further north (Walker & Johnstone 2014). Under these circumstances, and based on my results, species in the southern boreal forest will need to rely more heavily on effective

precipitation to support their growth, until a point when water becomes extremely limiting, in which case we are likely to see reduced growth rates, and a negative response to warm air temperature (Barber et al., 2000; Walker & Johnstone 2014).

2.8 References

Babst, F., Bouriaud, O., Alexander, R., Trouet, V., & Frank, D. (2014). Toward consistent measurements of carbon accumulation: A multi-site assessment of biomass and basal area increment across Europe. *Dendrochronologia*, *32*(2), 153–161.

Barber, V. A., Juday, G. P., & Finney, B. P. (2000). Reduced growth of Alaskan white spruce in the twentieth century from temperature-induced drought stress. *Nature*, *405*(6787), 668–673.

Barr, A. G., van der Kamp, G., Black, T. A., McCaughey, J. H., & Nesic, Z. (2012). Energy balance closure at the BERMS flux towers in relation to the water balance of the White Gull Creek watershed 1999–2009. *Agricultural and Forest Meteorology*, *153*, 3–13.

Betts, R. A. (2000). Offset of the potential carbon sink from boreal forestation by decreases in surface albedo. *Nature*, *408*(6809), 187–190.

Biondi, F. (1997). Evolutionary and moving response functions in dendroclimatology. *Dendrochronologia*, *15*, 139–150.

Biondi, F. (2000). Are Climate-Tree Growth Relationships Changing in North-Central Idaho, U.S.A.? *Arctic, Antarctic, and Alpine Research*, *32*(2), 111–116.

Biondi, F., & Waikul, K. (2004). DENDROCLIM2002: A C++ program for statistical calibration of climate signals in tree-ring chronologies. *Computers & Geosciences*, *30*(3), 303–311.

Blasing, T. J., Solomon, A. M., & Duvick, D. N. (1984). Response Functions Revisited. *Tree-Ring Bulletin, 44.*

Boisvenue, C., & Running, S. W. (2006). Impacts of climate change on natural forest productivity – evidence since the middle of the 20th century. *Global Change Biology*, *12*(5), 862–882.

Bonan, G. B. (2008). Forests and Climate Change: Forcings, Feedbacks, and the Climate Benefits of Forests. *Science*, *320*(5882), 1444–1449.

Bouriaud, O., Leban, J.-M., Bert, D., & Deleuze, C. (2005). Intra-annual variations in climate influence growth and wood density of Norway spruce. *Tree Physiology*, *25*(6), 651–660.

Bradshaw, C. J., & Warkentin, I. G. (2015). Global estimates of boreal forest carbon stocks and flux. *Global and Planetary Change*, *128*, 24–30.

Brysse, K., Oreskes, N., O'Reilly, J., & Oppenheimer, M. (2013). Climate change prediction: Erring on the side of least drama? *Global Environmental Change*, *23*(1), 327–337.

Bunn, A. G. (2008). A dendrochronology program library in R (dplR). *Dendrochronologia*, *26*(2), 115–124.

Bush, E. & Lemmen, D.S, editors (2019). Canada's changing climate report. *Government of Canada, Ottawa, ON,* 444p.

Charney, N. D., Babst, F., Poulter, B., Record, S., Trouet, V. M., Frank, D., Enquist, B.J., & Evans, M. E. K. (2016). Observed forest sensitivity to climate implies large changes in 21st century North American forest growth. *Ecology Letters*, *19*(9), 1119–1128.

Chen, W. J., Black, T. A., Yang, P. C., Barr, A. G., Neumann, H. H., Nesic, Z., Blanken, P.D., Novak, M.D., Eley, J., & Ketler, R. J. (1999). Effects of climatic variability on the annual carbon sequestration by a boreal aspen forest. *Global Change Biology*, *5*(1), 41–53.

Chen, L., Huang, J.-G., Alam, S. A., Zhai, L., Dawson, A., Stadt, K. J., & Comeau, P. G. (2017). Drought causes reduced growth of trembling aspen in western Canada. *Global Change Biology*.

Cocozza, C., Palombo, C., Tognetti, R., La Porta, N., Anichini, M., Giovannelli, A., & Emiliani, G. (2016). Monitoring intra-annual dynamics of wood formation with microcores and dendrometers in Picea abies at two different altitudes. *Tree Physiology*, *36*(7), 832–846.

Cocozza, C., Tognetti, R., & Giovannelli, A. (2018). High-Resolution Analytical Approach to Describe the Sensitivity of Tree–Environment Dependences through Stem Radial Variation. *Forests*, *9*(3), 134.

Cuny, H. E., Rathgeber, C. B., Frank, D., Fonti, P., Mäkinen, H., Prislan, P., Rossi, S., del Castillo, E. M., Campelo, F., Varvcik, H., Camarero, J. J., Bryunkhanova, M. V., Jyske, T., Gricar, J., Gryc, V., De Luis, M., Vieira, J., Cufar, K., Kirdyanov, A. V., Oberhuber, W., Tremill, V., Huang, J. G., Li, X., Swidrak, I., Deslauriers, A., Liang, E., Nojd, P., Gruber, A., Nabais, C., Morin, H., Krause, C., King, G., & Fournier, M.(2015). Woody biomass production lags stem-girth increase by over one month in coniferous forests. *Nature Plants*, *1*, 15160.

D'Arrigo, R., Wilson, R., Liepert, B., & Cherubini, P. (2008). On the 'Divergence Problem' in Northern Forests: A review of the tree-ring evidence and possible causes. *Global and Planetary Change*, *60*(3), 289–305.

D'Orangeville, L., Houle, D., Duchesne, L., Phillips, R. P., Bergeron, Y., & Kneeshaw, D. (2018). Beneficial effects of climate warming on boreal tree growth may be transitory. *Nature Communications*, *9*.

Dang, Q. L., & Lieffers, V. J. (1989). Climate and annual ring growth of black spruce in some Alberta peatlands. *Canadian Journal of Botany*, *67*(6), 1885–1889.

Deslauriers, A., Morin, H., Urbinati, C., & Carrer, M. (2003). Daily weather response of balsam fir (Abies balsamea (L.) Mill.) stem radius increment from dendrometer analysis in the boreal forests of Québec (Canada). *Trees*, *17*(6), 477–484.

Deslauriers, A., Rossi, S., & Anfodillo, T. (2007a). Dendrometer and intra-annual tree growth: What kind of information can be inferred? *Dendrochronologia*, *25*(2), 113–124.

Deslauriers, A., Anfodillo, T., Rossi, S., & Carraro, V. (2007b). Using simple causal modeling to understand how water and temperature affect daily stem radial variation in trees. *Tree Physiology*, *27*(8), 1125–1136.

Drew, D. M., Richards, A. E., Downes, G. M., Cook, G. D., & Baker, P. (2011). The development of seasonal tree water deficit in Callitris intratropica. *Tree Physiology*, *31*(9), 953–964.

Duchesne, L., & Houle, D. (2011). Modelling day-to-day stem diameter variation and annual growth of balsam fir (Abies balsamea (L.) Mill.) from daily climate. *Forest Ecology and Management*, *262*(5), 863–872.

Ecomatik. (2019). Circumference DC2, DC3. Retrieved October 25, 2019, from Ecomatik website: https://ecomatik.de/en/products/dendrometer/circumference-dc2-dc3/

Ehleringer, J. R., Phillips, S. L., Schuster, W. S. F., & Sandquist, D. R. (1991). Differential utilization of summer rains by desert plants. *Oecologia*, *88*(3), 430–434.

Ellsworth, P. Z., & Sternberg, L. S. L. (2015). Seasonal water use by deciduous and evergreen woody species in a scrub community is based on water availability and root distribution. *Ecohydrology*, *8*(4), 538–551.

Fritts, H. C., Blasing, T. J., Hayden, B. P., & Kutzbach, J. E. (1971). Multivariate Techniques for Specifying Tree-Growth and Climate Relationships and for Reconstructing Anomalies in Paleoclimate. *Journal of Applied Meteorology*, *10*(5), 845–864.

Gao, J., Yang, B., He, M., & Shishov, V. (2019). Intra-annual stem radial increment patterns of Chinese pine, Helan Mountains, Northern Central China. *Trees*, *33*(3), 751–763.

Gower, S. T., Krankina, O., Olson, R. J., Apps, M., Linder, S., & Wang, C. (2001). Net primary production and carbon allocation patterns of boreal forest ecosystems. *Ecological Applications*, *11*(5), 1395–1411.

Gruber, A., Zimmermann, J., Wieser, G., & Oberhuber, W. (2009). Effects of climate variables on intra-annual stem radial increment in Pinus cembra (L.) along the alpine treeline ecotone. *Annals of Forest Science*, *66*(5).

Guiot, J. (1991). *The Bootstrapped Response Function*. *Tree-Ring Bulletin, 51.*

Güney, A., Gülsoy, S., Şentürk, Ö., Niessner, A., & Küppers, M. (2019). Environmental control of daily stem radius increment in the montane conifer Cedrus libani. *Journal of Forestry Research*.

Harsch, M. A., Hulme, P. E., McGlone, M. S., & Duncan, R. P. (2009). Are treelines advancing? A global meta-analysis of treeline response to climate warming. *Ecology Letters*, *12*(10), 1040–1049.

Henderson, N., & Sauchyn, D. (2008). Climate change impacts on Canada's Prairie Provinces: A summary of our state of knowledge. *Prairie Adaptation Research Collaborative: Summary Document*, (08–01), 20.

Herzog, K. M., Häsler, R., & Thum, R. (1995). Diurnal changes in the radius of a subalpine Norway spruce stem: Their relation to the sap flow and their use to estimate transpiration. *Trees*, *10*(2), 94–101.

Hofgaard, A., Tardif, J., & Bergeron, Y. (1999). Dendroclimatic response of Picea mariana and Pinus banksiana along a latitudinal gradient in the eastern Canadian boreal forest. *Canadian Journal of Forest Research*, *29*(9), 1333–1346.

Hogg, E. H., Brandt, J. P., & Kochtubajda, B. (2002). Growth and dieback of aspen forests in northwestern Alberta, Canada, in relation to climate and insects. *Canadian Journal of Forest Research*, *32*(5), 823–832.

Holmes, R. L. (1983). Computer-assisted quality control in tree-ring dating and measurement. *Tree-Ring Bulletin*, *43*(1), 69–78.

Huang, J., Tardif, J. C., Bergeron, Y., Denneler, B., Berninger, F., & Girardin, M. P. (2010). Radial growth response of four dominant boreal tree species to climate along a latitudinal gradient in the eastern Canadian boreal forest. *Global Change Biology*, *16*(2), 711–731.

Huntingford, C., & Mercado, L. M. (2016). High chance that current atmospheric greenhouse concentrations commit to warmings greater than 1.5 °C over land. *Scientific Reports*, *6*, 30294.

IPCC (2013) Climate Change 2013: The Physical Science Basis. *Working Group I Contribution to the Fifth Assessment Report of the Intergovernmental Panel on Climate Change.* Cambridge University Press, Cambridge, UK.

Ireson, A. M., Barr, A. G., Johnstone, J. F., Mamet, S. D., van der Kamp, G., Whitfield, C. J., Michel, N. L., North, R. L., Westbrook, C. J., DeBeer, C., & others. (2015). The changing water cycle: The Boreal Plains ecozone of Western Canada. *Wiley Interdisciplinary Reviews: Water*, *2*(5), 505–521.

Jacoby, G. C., & D'Arrigo, R. D. (1995). Tree ring width and density evidence of climatic and potential forest change in Alaska. *Global Biogeochemical Cycles*, *9*(2), 227–234.

Jeong, D. I., Sushama, L., & Khaliq, M. N. (2014). The role of temperature in drought projections over North America. *Climatic Change*, *127*(2), 289–303.

Kasischke, E. S., & Turetsky, M. R. (2006). Recent changes in the fire regime across the North American boreal region—Spatial and temporal patterns of burning across Canada and Alaska. *Geophysical Research Letters*, *33*(9).

King, G., Fonti, P., Nievergelt, D., Büntgen, U., & Frank, D. (2013). Climatic drivers of hourly to yearly tree radius variations along a 6° C natural warming gradient. *Agricultural and Forest Meteorology*, *168*, 36–46.

Mäkinen, H., Nöjd, P., & Saranpää, P. (2003). Seasonal changes in stem radius and production of new tracheids in Norway spruce. *Tree Physiology*, *23*(14), 959–968.

Michaelian, M., Hogg, E. H., Hall, R. J., & Arsenault, E. (2011). Massive mortality of aspen following severe drought along the southern edge of the Canadian boreal forest. *Global Change Biology*, *17*(6), 2084–2094.

Nehemy, M. F., Benettin, P., Asadollahi, M., Pratt, D., Rinaldo, A., & McDonnell, J. J. (2019). How plant water status drives tree source water partitioning. *Hydrology and Earth System Sciences Discussions*, 1–26.

Oberhuber, W., Gruber, A., Kofler, W., & Swidrak, I. (2014). Radial stem growth in response to microclimate and soil moisture in a drought-prone mixed coniferous forest at an inner Alpine site. *European Journal of Forest Research*, *133*(3), 467–479.

Pappas C., Maillet, J., Rakowski, S., Baltzer, J.L., Barr, A.G., Black, A., Fatichi, S., Matheny, A.M, Roy, A., Sonnentag, O., & Zha, T. (2020). Aboveground tree growth is a minor and decoupled fraction of boreal forest carbon input. *Agricultural and Forest Meteorolog,*. 290.

Pappas, C., Matheny, A. M., Baltzer, J. L., Barr, A. G., Black, T. A., Bohrer, G., Detto, M., Maillet, J., Roy, A., Sonnentag, O., & Stephens, J. (2018). Boreal tree hydrodynamics: Asynchronous, diverging, yet complementary. *Tree Physiology*, *38*(7), 953–964.

Peng, C., Ma, Z., Lei, X., Zhu, Q., Chen, H., Wang, W., Liu, S., Li, W., Fang, X., & Zhou, X. (2011). A drought-induced pervasive increase in tree mortality across Canada's boreal forests. *Nature Climate Change*, *1*(9), 467–471.

Peng, X., Xiao, S., Cheng, G., Tian, Q., & HongLang, X. (2017). Microcoring and dendrometer-detected intra-annual wood formation of Populus euphratica in the Ejina Oasis, northwestern China. *Sciences in Cold and Arid Regions, 9(1),* 54-66.

Rossi, S., Deslauriers, A., Anfodillo, T., & Carraro, V. (2007). Evidence of threshold temperatures for xylogenesis in conifers at high altitudes. *Oecologia*, *152*(1), 1–12.

Rossi, S., Deslauriers, A., Griçar, J., Seo, J.-W., Rathgeber, C. B., Anfodillo, T., Morin, H., Levanic, T., Oven, P., & Jalkanen, R. (2008). Critical temperatures for xylogenesis in conifers of cold climates. *Global Ecology and Biogeography*, *17*(6), 696–707.

Samuels, A. L., Kaneda, M., & Rensing, K. H. (2006). The cell biology of wood formation: From cambial divisions to mature secondary xylem This review is one of a selection of papers published in the Special Issue on Plant Cell Biology. *Botany*, *84*(4), 631–639.

Sellers, P., Hall, F., Margolis, H., Kelly, B., Baldocchi, D., den Hartog, G., Cihlar, J., Ryan M. G., Goodison, B., Crill, P., Ranson, K. J., Lettenmaier, D., & Wickland, D. E., (1995). The boreal ecosystem-atmosphere study (BOREAS): An overview and early results from the 1994 field year. *Bulletin of the American Meteorological Society*, *76*(9), 1549–1577.

Soja, A. J., Tchebakova, N. M., French, N. H., Flannigan, M. D., Shugart, H. H., Stocks, B. J., Sukhinin, A. I., Parfenova, E. I., Chapin, F. S., & Stackhouse, P. W. (2007). Climate-induced boreal forest change: Predictions versus current observations. *Global and Planetary Change*, *56*(3), 274–296.

Speer, J. H. (2010). *Fundamentals of Tree-ring Research*. University of Arizona Press.

Spracklen, D. V., Bonn, B., & Carslaw, K. S. (2008). Boreal forests, aerosols and the impacts on clouds and climate. *Philosophical Transactions of the Royal Society A: Mathematical, Physical and Engineering Sciences*, *366*(1885), 4613–4626.

Stephens, J. J., Black, T. A., Jassal, R. S., Nesic, Z., Grant, N. J., Barr, A. G., Helgason, W.D., Richardson, A.D., Johnson, M.S., & Christen, A. (2018). Effects of forest tent caterpillar defoliation on carbon and water fluxes in a boreal aspen stand. *Agricultural and Forest Meteorology*, *253–254*, 176–189.

Steppe, K., De Pauw, D. J. W., Lemeur, R., & Vanrolleghem, P. A. (2006). A mathematical model linking tree sap flow dynamics to daily stem diameter fluctuations and radial stem growth. *Tree Physiology*, *26*(3), 257–273.

Tam, B., Szeto, K., Bonsal, B., Flato, G., Cannon, A.J., & Rong, R. (2018). CMIP5 drought projections in Canada based on the Standardized Precipitation Evapotranspiration Index. *Canadian Water Resources Journal*, **44**, 90-107.

Turcotte, A., Rossi, S., Deslauriers, A., Krause, C., & Morin, H. (2011). Dynamics of Depletion and Replenishment of Water Storage in Stem and Roots of Black Spruce Measured by Dendrometers. *Frontiers in Plant Science*, *2*.

van der Maaten, E., van der Maaten-Theunissen, M., Smiljanic, M., Rossi, S., Simard, S., Wilmking, M., Deslauriers, A., Fonti, P., von Arx, G., & Bouriaud, O. (2016). dendrometeR: Analyzing the pulse of trees in R. *Dendrochronologia*, 40.

Volkmann, T. H. M., Haberer, K., Gessler, A., & Weiler, M. (2016). High-resolution isotope measurements resolve rapid ecohydrological dynamics at the soil–plant interface. *New Phytologist*, *210*(3), 839–849.

VoorTech. (2017). The Tree Ring Measuring Program Project J2X. Retrieved October 25, 2019, from http://www.voortech.com/projectj2x/

Walker, X., & Johnstone, J. F. (2014). Widespread negative correlations between black spruce growth and temperature across topographic moisture gradients in the boreal forest. *Environmental Research Letters*, *9*(6), 064016.

Wang, X., Thompson, D. K., Marshall, G. A., Tymstra, C., Carr, R., & Flannigan, M. D. (2015). Increasing frequency of extreme fire weather in Canada with climate change. *Climatic Change*, *130*(4), 573–586.

Wang, Y., Hogg, E. H., Price, D. T., Edwards, J., & Williamson, T. (2014). Past and projected future changes in moisture conditions in the Canadian boreal forest. *The Forestry Chronicle*, *90*(5), 678–691.

Zang, C., & Biondi, F. (2015). treeclim: An R package for the numerical calibration of proxy-climate relationships. *Ecography*, *38*(4), 431–436.

Zhang, K., Kimball, J. S., Hogg, E. H., Zhao, M., Oechel, W. C., Cassano, J. J., & Running, S. W. (2008). Satellite-based model detection of recent climate-driven changes in northern high-latitude vegetation productivity. *Journal of Geophysical Research: Biogeosciences*, *113*(G3).

Zhang, X., Flato, G., Kirchmeier-Young, M., Vincent, L., Wan, H., Wang, X., Rong, R., Fyfe, J., Li, G., Kharin, V.V. (2019). Changes in Temperature and Precipitation Across Canada; Chapter 4 *in* Bush, E. and Lemmen, D.S. (Eds.) Canada's Changing Climate Report. *Government of Canada*, *Ottawa, Ontario*, 112-193.

Zweifel, R., & Häsler, R. (2001). Dynamics of water storage in mature subalpine Picea abies: Temporal and spatial patterns of change in stem radius. *Tree Physiology*, *21*(9), 561–569.

Zweifel, R., Zimmermann, L., & Newbery, D. M. (2005). Modeling tree water deficit from microclimate: An approach to quantifying drought stress. *Tree Physiology*, *25*(2), 147–156.

Zweifel, R., Haeni, M., Buchmann, N., & Eugster, W. (2016). Are trees able to grow in periods of stem shrinkage? *New Phytologist*, *211*(3), 839–849.

Zweifel, R., Item, H., & Häsler, R. (2000). Stem radius changes and their relation to stored water in stems of young Norway spruce trees. *Trees*, *15*(1), 50–57.

2.9 Tables and Figures

Table 2.1: Characteristics of annual radial growth chronologies built from core samples taken at OJP and OA in the fall of 2018, and at OBS in the spring of 2016 for Pappas et al. (2018).

	OJP	OBS	OA
Number of Individuals in Chronology	54	73	46
Series Intercorrelation	0.632 critical value 0.366	0.548 critical value 0.328	0.692 critical value 0.366
Chronology Length	1923-2018 96 years	1894-2015 122 years	1925-2018 94 years
Number of Flagged Segments	6 of 215	13 of 279	5 of 179
Segment Length	40-year segments 20-year overlap	50-year segments 25-year overlap	40-year segments 20-year overlap

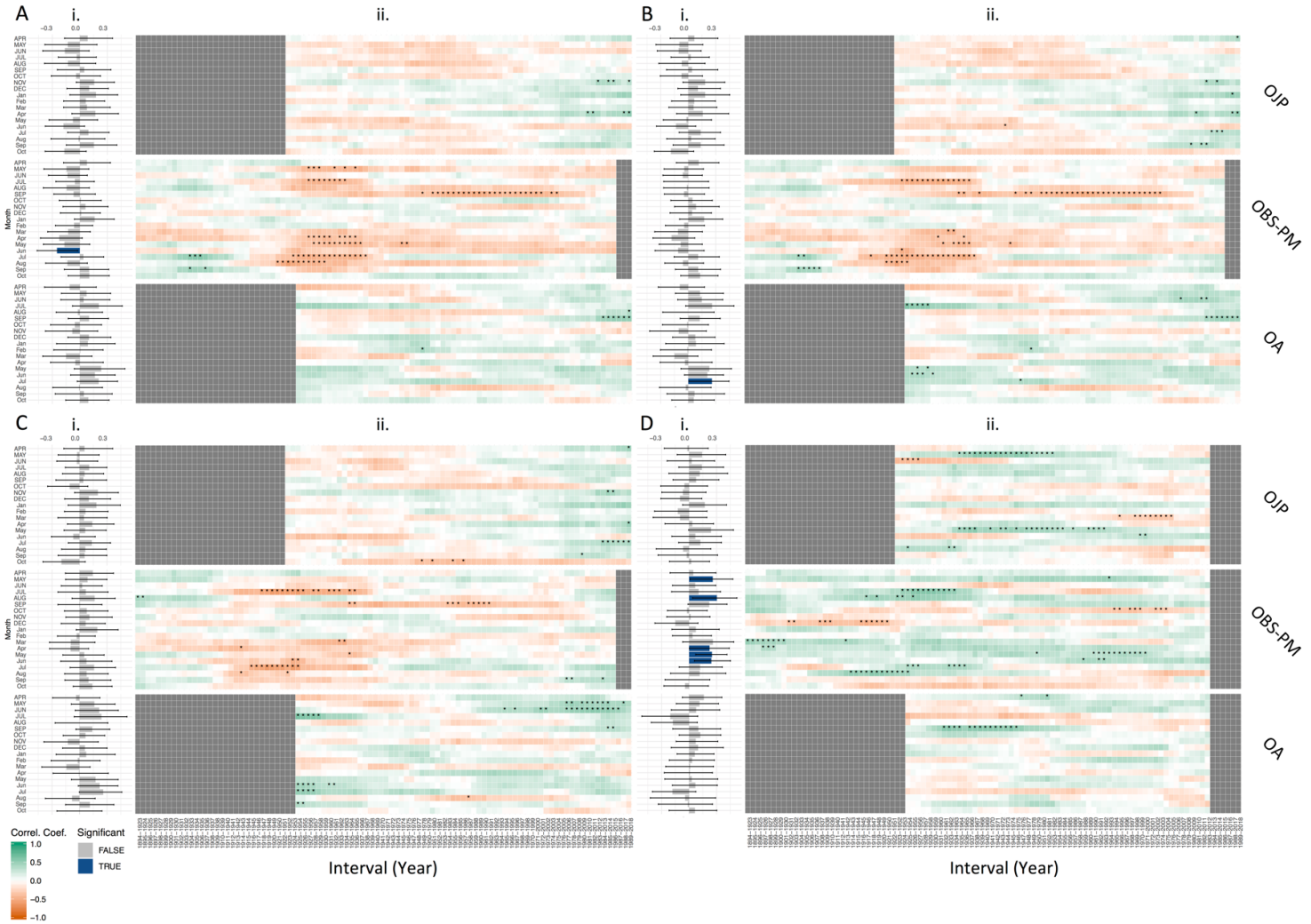

Figure 2.1: Static (i.) and moving window (ii.) correlation analyses between annual radial growth and monthly maximum (A), mean (B), and minimum (C) monthly temperature, and total monthly precipitation (D). Pearson's correlations were computed 1000 times with random resampling. Significance at the 99% confidence level is based on the bootstrapped confidence intervals and is highlighted in blue (i.), or flagged with * (ii.).

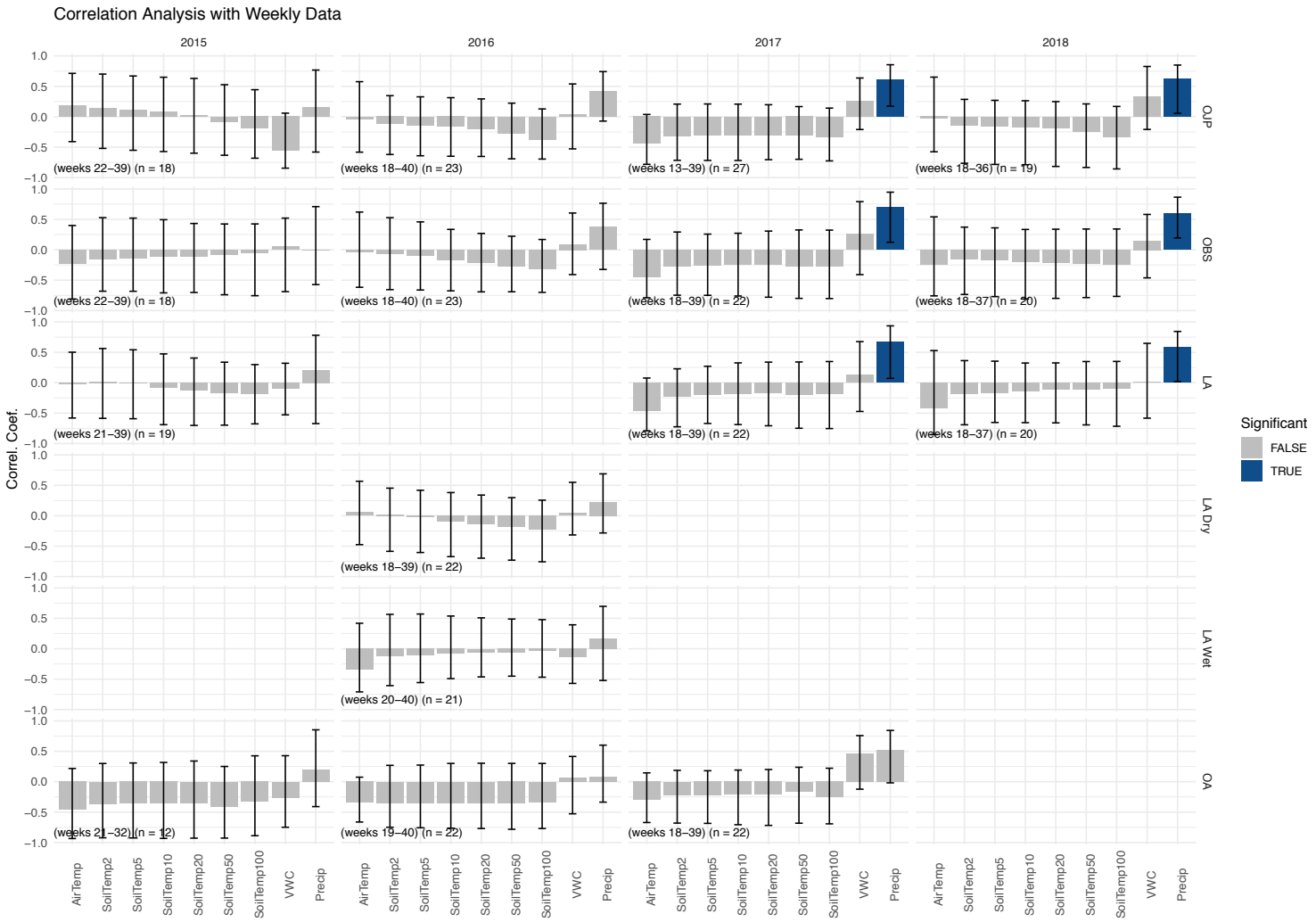

Figure 2.2: Correlation analysis between weekly variations in stem radius and local meteorological variables (x-axis). Relationships were assessed within each growing season from 2015 – 2018. The height of each column represents Pearson's correlation r-value from -1 to 1. Bootstrapped confidence intervals (99%) are depicted by each error bar, and instances of statistical significance are highlighted in blue. Graphs are arranged in a two-dimensional matrix with growing season year listed above each column, and site/species names labeled to the right of each row.

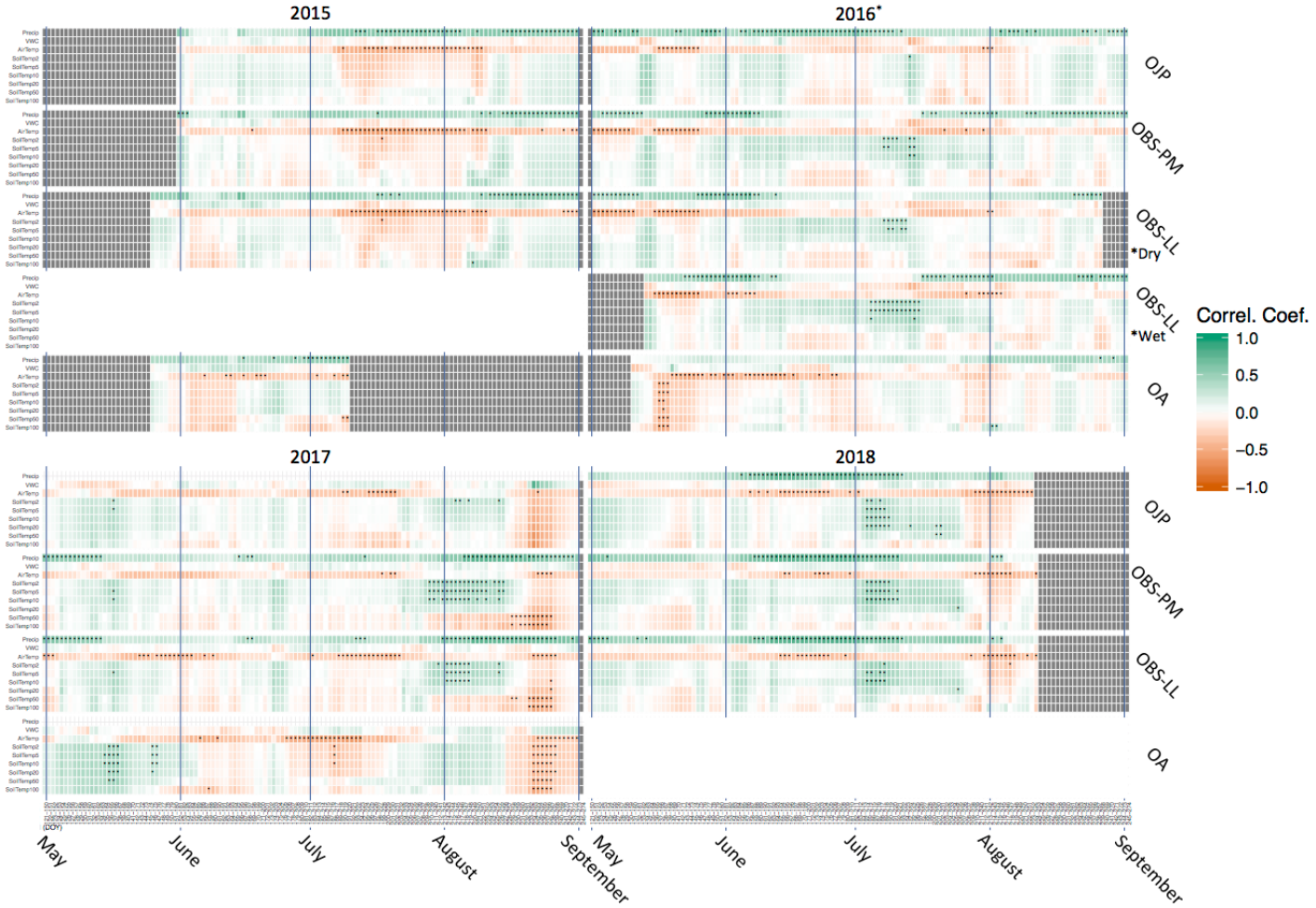

Figure 2.3: Moving window correlation functions of the relationship between daily resolved variations in stem radius and local meteorological variables within each of the four growing seasons during the observation period (2015 – 2018). Relationships were assessed over a 30-day moving window, jogged by 1-day, using bootstrapped Pearson's correlations (1000 iterations). The labels on the x-axis correspond with the start date of each 30-day interval. For example, intervals with start dates in May are found between the May and June x-axis labels. Significance at the 99% confidence level is flagged with *.

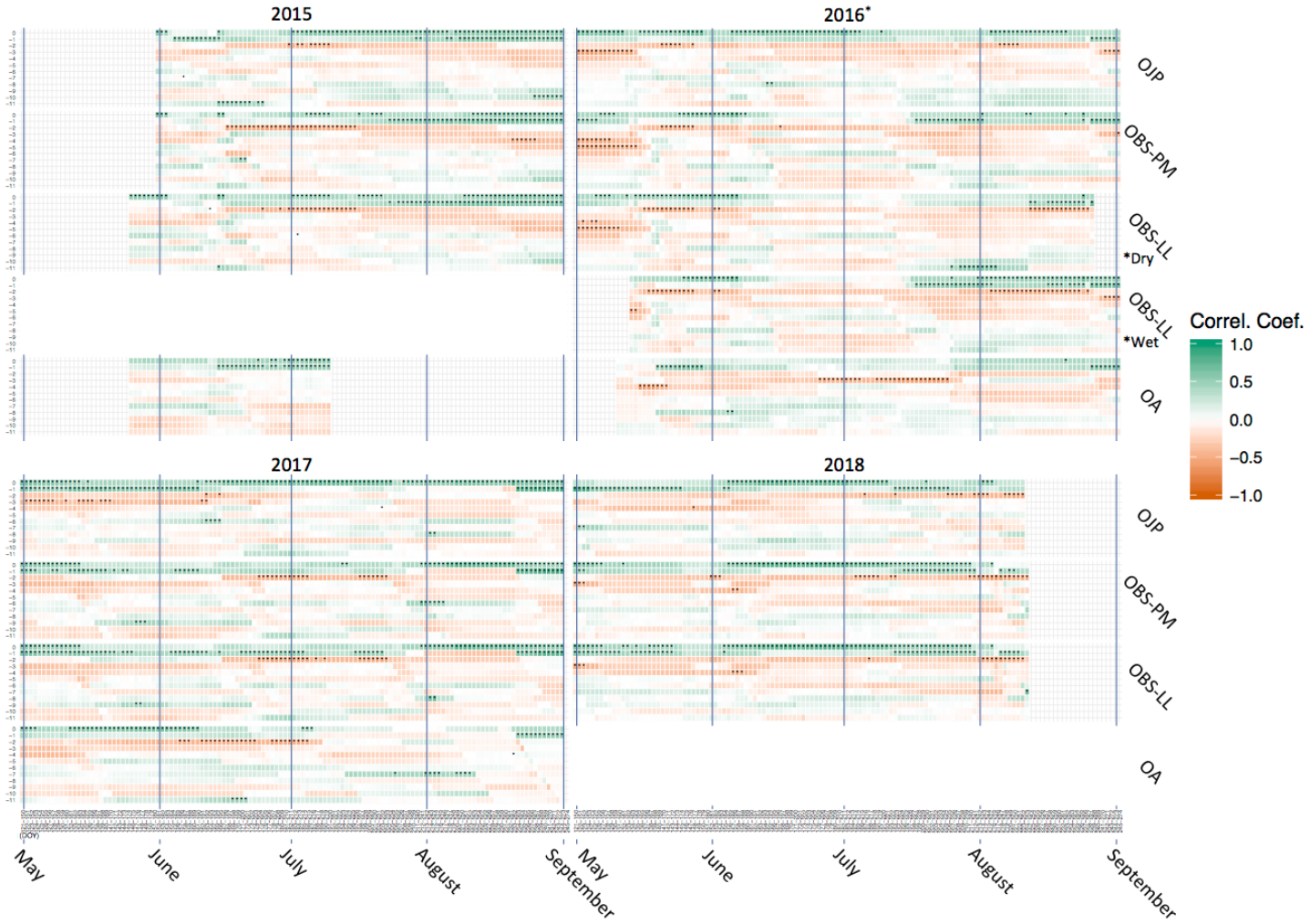

Figure 2.4: Moving window correlation functions assessing lag in the relationship between daily variations in stem radius and precipitation, which is lagged from the stem radius data by 0 to 11-days (y-axis). As above, relationships were assessed over a 30-day moving window, jogged by 1-day, using bootstrapped Pearson's correlations. The labels on the x-axis correspond with the start date of each 30-day interval. Significance at the 99% confidence level is flagged with *.

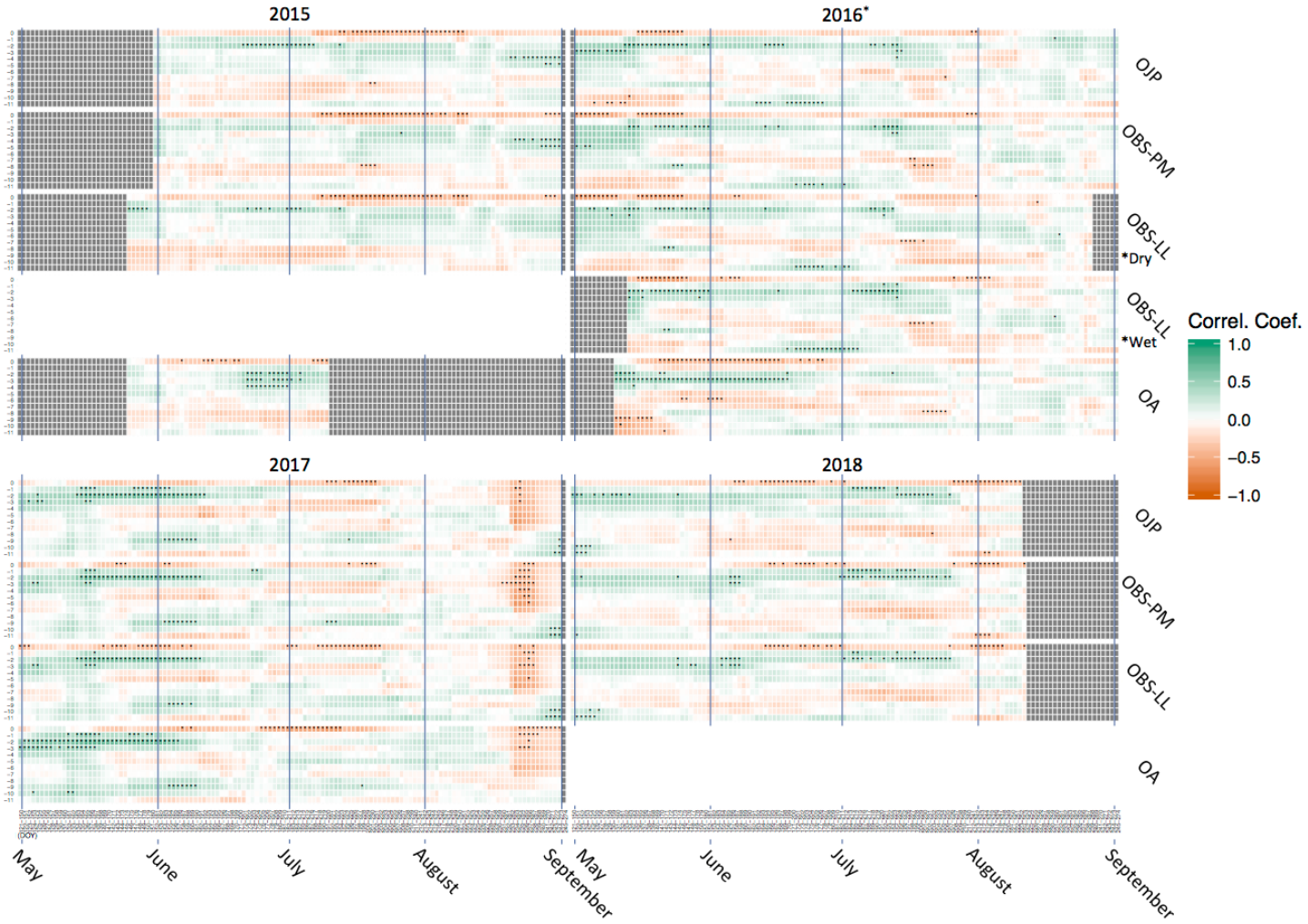

Figure 2.5: Moving window correlation functions assessing lag in the relationship between daily variations in stem radius and mean air temperature, which is lagged from the stem radius data by 0 to 11-days (y-axis). As above, relationships were assessed over a 30-day moving window, jogged by 1-day, using bootstrapped Pearson's correlations. The labels on the x-axis correspond with the start date of each 30-day interval. Significance at the 99% confidence level is flagged with *.

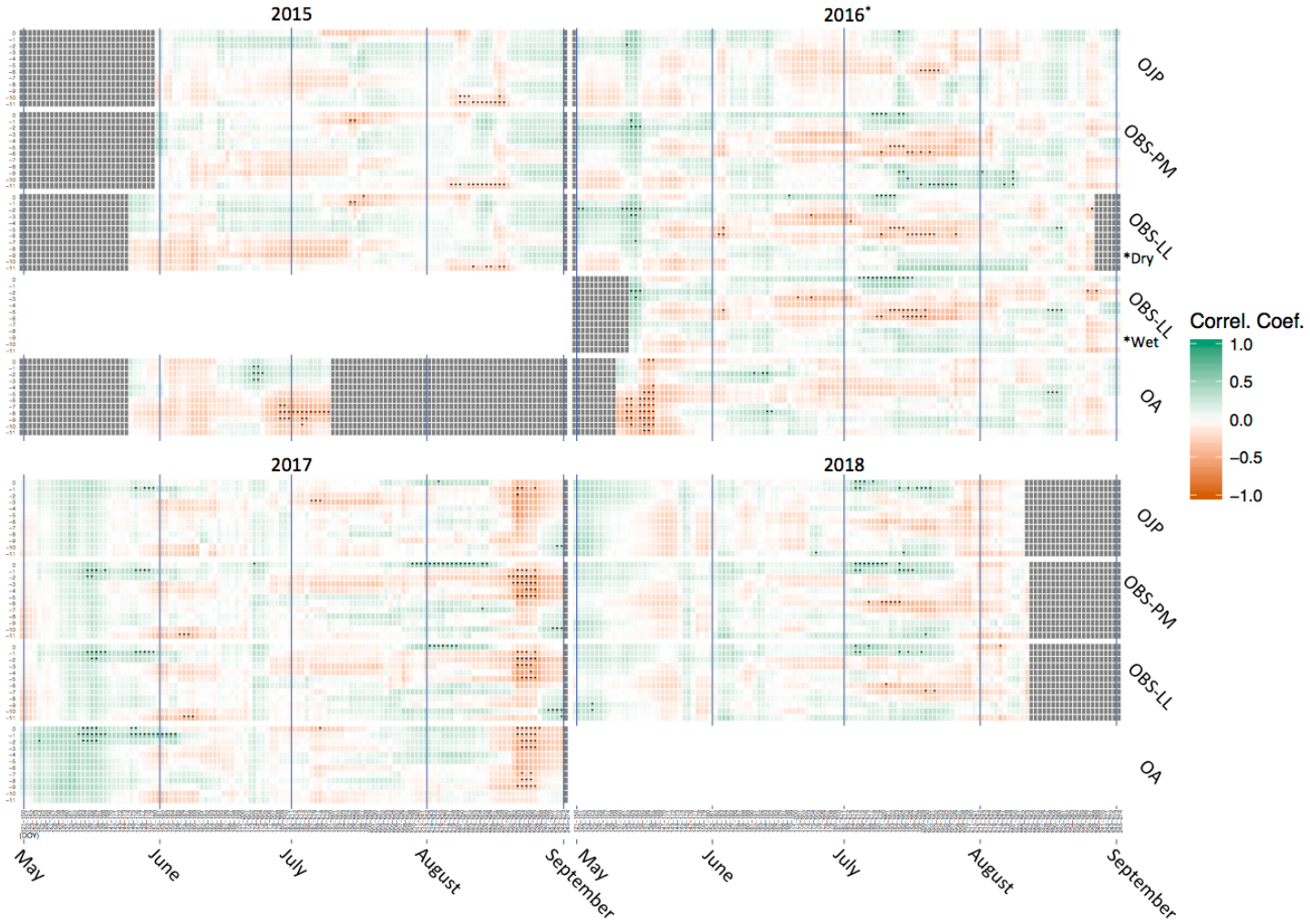

Figure 2.6: Moving window correlation functions assessing lag in the relationship between daily variations in stem radius and shallow soil temperature (2cm depth), which is lagged from the stem radius data by 0 to 11-days (y-axis). As above, relationships were assessed over a 30-day moving window, jogged by 1-day, using bootstrapped Pearson's correlations. The labels on the x-axis correspond with the start date of each 30-day interval. Significance at the 99% confidence level is flagged with *.

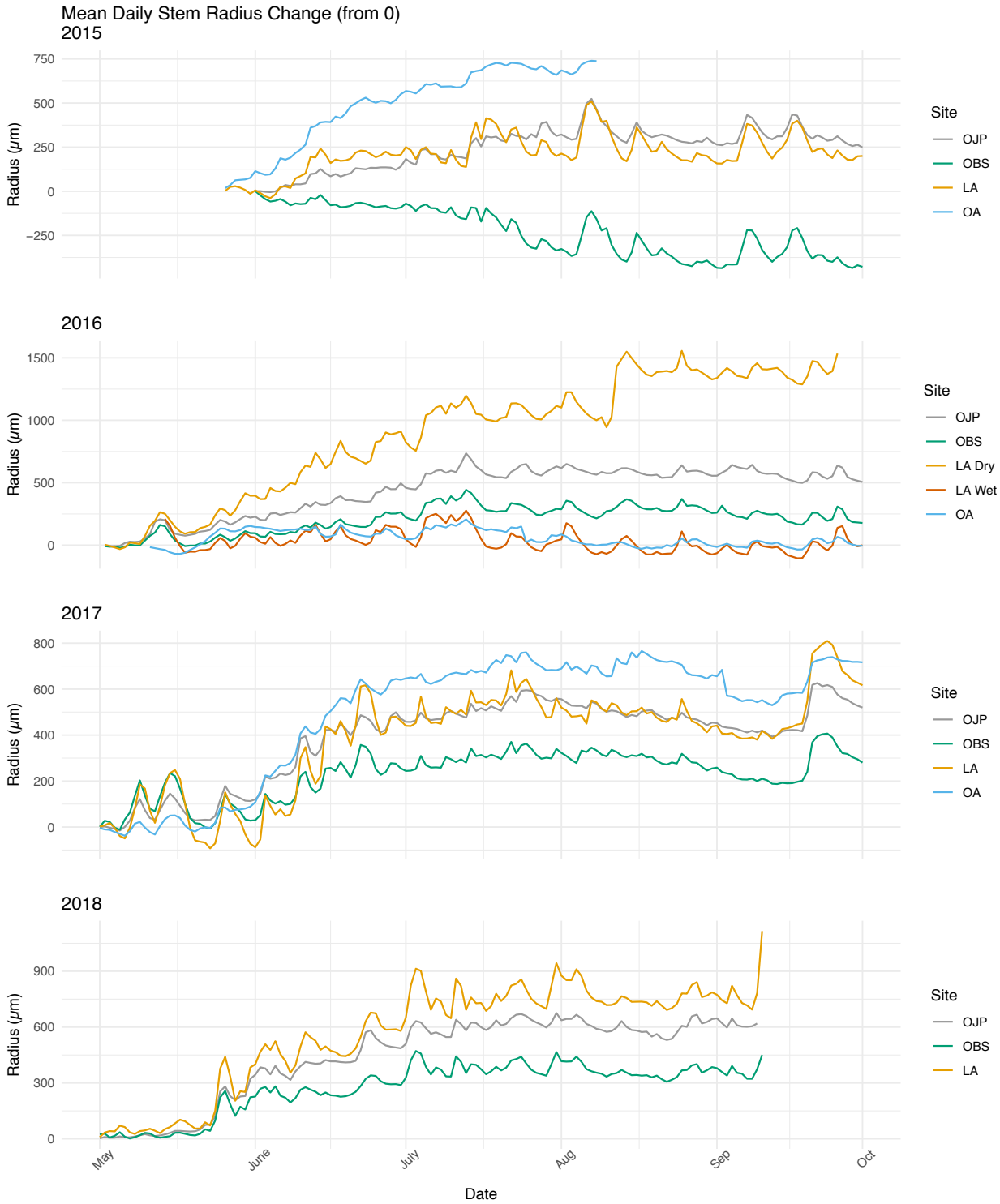

Figure 2.7: Dendrometer graphs depicting cumulative stem radius (from 0) each growing season (2015 – 2018).

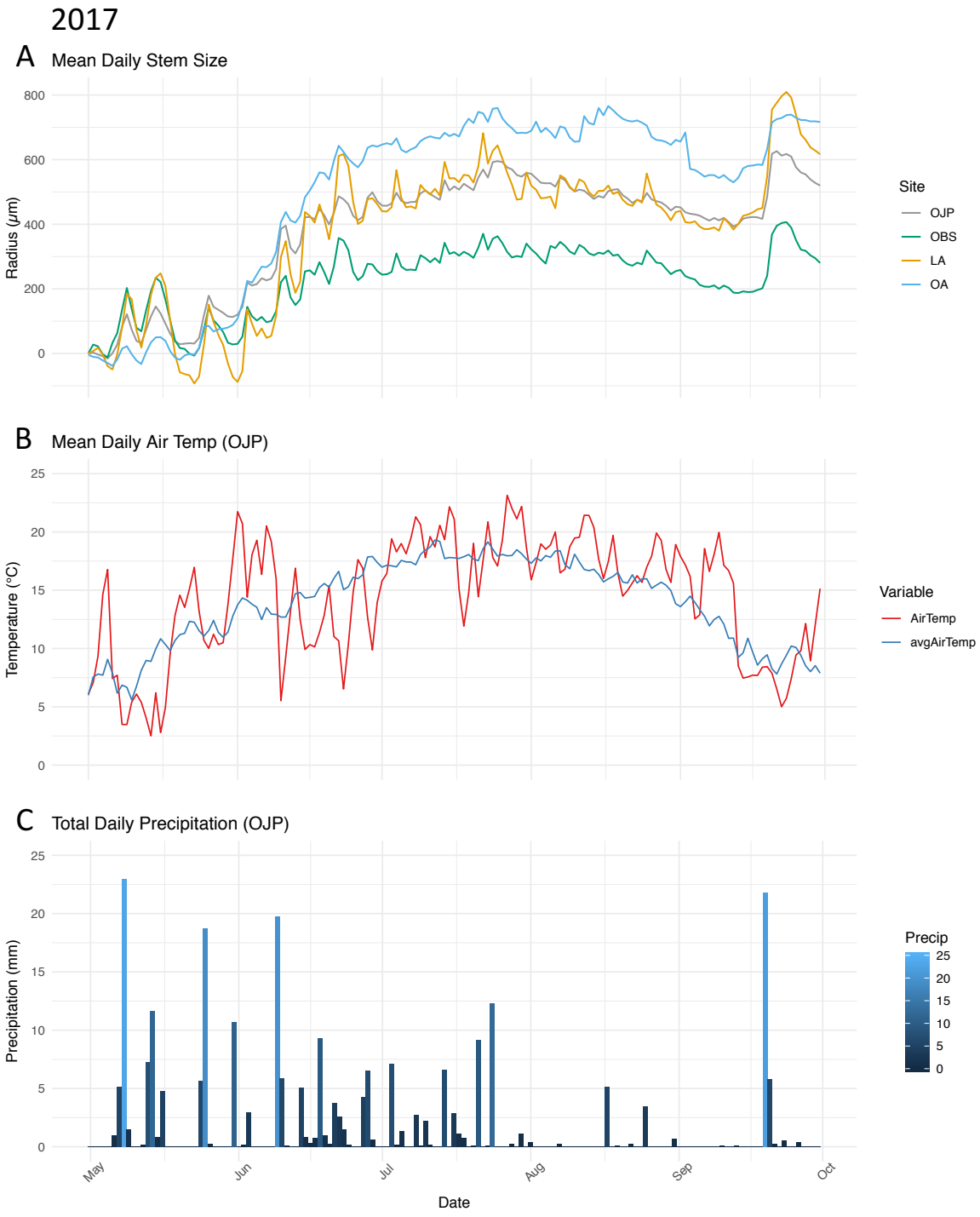

Figure 2.8: Case study of the 2017 growing season, comparing daily records of cumulative stem radius (A), mean air temperature (B), and total precipitation (C).

CHAPTER 3

SPURIOUS CORRELATION INFLUENCES RELATIONSHIPS BETWEEN RADIAL GROWTH AND ECOSYSTEM CARBON FLUX AT DAILY TEMPORAL RESOLUTION

3.1 Abstract

Tree rings hold great potential to improve our still fragmented understanding of carbon (C) allocation across a wide range of forest ecosystems. To date, tree rings remain underutilized in the context of forest carbon research and those pioneering this work have produced mixed, sometimes conflicting results. Further examination of the relationship between stem radial growth and forest carbon is required across a wide range of forest ecosystems. This study assesses relationships between stem radial growth and ecosystem C exchange in three southern boreal forest stands at annual, monthly, weekly, and daily resolutions over the medium- to short-term. At annual resolution, jack pine (*Pinus banksiana*) was the only species among those studied whose radial growth was significantly related to measures of ecosystem C-flux, with a significant positive relationship between annual-ring width and net ecosystem production (NEP). More specifically, based on a detailed assessment of relationships between 1999 – 2018, the annual-radial growth of jack pine benefited from elevated levels of NEP during the previous fall (August and October) and the current spring (May). Based on these findings, it is likely that radial growth had more of a consistent relationship with NEP for jack pine than black spruce (*Picea mariana*) or trembling aspen (*Populus tremuloides*). A correlation analysis at weekly resolution failed to provide any reliable information regarding the relationship between stem radius change (ΔR) and ecosystem C-fluxes. Correlations between the ΔR of all study species and ecosystem production (both gross and net) at daily resolution (2015 – 2018) were likely spurious, because of the confounding influence of stem water content on daily variations in stem radius. To improve results over fine temporal resolutions, more work is needed to develop a standardized method that more effectively disentangles the growth from the water signal in dendrometer data. Overall, the findings from this study agree with recent research, thus helping to broaden our understanding of the numerous and complex processes that govern both radial growth and ecosystem C-flux in a diverse set of forest ecosystems and climates across the globe.

3.2 Introduction

Eddy covariance is a standard and accurate method for measuring carbon exchange between an ecosystem and the atmosphere (Baldocchi 2003). While this method is often quite effective at directly measuring net ecosystem exchange (NEE) or net ecosystem production (NEP), eddy covariance is limited in its ability to offer a breakdown of the flux beyond its main components of gross ecosystem production (GEP) and total ecosystem respiration (R_E) (Baldocchi 2003). Furthermore, the equipment necessary to measure eddy covariance flux is costly and must be maintained over long periods. Detailed eddy covariance flux data are therefore sparse and often limited in length (Gea-Izquierdo et al., 2014). These limitations restrict the development of a detailed and mechanistic understanding of carbon allocation across a wide range of forest ecosystems, which is required to accurately anticipate the impacts of climate change on forest biogeochemical cycling (Litton et al., 2007; Chen et al., 2013)

One of the main challenges of better understanding forest production and carbon allocation may be a lack of reliable and consistent biometric measurement techniques to supplement eddy covariance based flux data (Babst et al., 2014a; Babst et al., 2014b). Biometric based measurements regarding the growth of individual forest components can be used to partition annual production into some of its component parts. In this context, tree rings hold great potential since they have several characteristics that make them attractive as a potential proxy for ecosystem production. Firstly, they are an *in situ* representation of forest wood production over time. This is significant considering that carbon stored in woody biomass often represents the largest component of forest ecosystem production (Gower et al., 2001; Chen et al., 2013) and the most significant and persistent annual sink for atmospheric carbon (Ilvesniemi et al., 2009), responsible for offsetting an estimated 15% of anthropogenic carbon emissions annually (Pan et al., 2011). While other components of ecosystem production, including contributions from understory growth, foliage, coarse and fine root, may be difficult to extrapolate from tree rings, proportions of carbon allocated to different components of total NPP were remarkably consistent across geographic regions (Gower et al., 2001). Furthermore, above ground NPP and total NPP were significantly correlated across boreal forest stands (Gower et al., 2001) leading to the assumption that total NPP may be reliably estimated from measures of above ground NPP, which can be extrapolated from ring widths (Bakker et al., 2005; Babst et al., 2014a; Papas et al., 2020

in review). Tree-ring data are also easily accessible and often inexpensive to collect, and there already exists an extensive international repository of tree-ring data. Yet to date, tree rings have been underutilized in the context of forest carbon research (Babst et al., 2014a).

For these reasons, there are several recent studies that attempted to quantify the relationship between radial growth and forest ecosystem production that have yielded mixed results. On seasonal to annual scales, several studies reported significant correlation between ring widths or values of above ground woody biomass accumulation derived from ring widths, and several eddy covariance based measures of ecosystem exchange (Rocha et al., 2006; Zweifel et al., 2010; Babst et al., 2014b; Gea-Izquierdo et al., 2014; Lempereur et al., 2015; Delpierre et al., 2016; Teets et al., 2018). Some identified no relationship between ring width and GEP (Rocha et al., 2006; Zweifel et al., 2010; Delpierre et al., 2016), while others found the opposite (Babst et al., 2014b; Gea-Izquierdo et al., 2014; Lempereur et al., 2015). Interestingly, most identified a positive relationship between the annual-radial increment and same-year annually or seasonally resolved measures of NEP (Rocha et al., 2006; Zweifel et al., 2010; Babst et al., 2014b; Gea-Izquierdo et al., 2014; Lempereur et al., 2015; Delpierre et al., 2016; Teets et al., 2018). Persistence in the observed relationship between annual-radial growth and NEP is surprising considering that annual ring-width measurements are simply representative of the biomass increment – a portion of carbon allocated and stored within a discrete pool, over a discrete period, while measurements of NEP relate to integrated, ecosystem wide processes of carbon uptake and partitioning across several pools.

Studies that assessed the relationship between ecosystem C-flux and radial growth over finer temporal resolution (half-hourly, daily, weekly, and monthly) revealed substantial variability in the strength and persistence of this relationship between species, between sites, and across the temporal scale (Granier et al., 2008; Zweifel et al., 2010; Gea-Izquierdo et al., 2014; Lempereur et al., 2015). Lempereur et al. (2015) identified a significant decrease in the strength and significance of the relationship between radial growth and components of ecosystem flux with increasing temporal resolution, while Granier et al. (2008) and Zweifel et al. (2010) observed the opposite. Zweifel et al. (2010) identified an unexpectedly strong relationship between stem size fluctuations and whole ecosystem NEP across the temporal scale, which changed from positive at annual and monthly scales to negative at half hourly scale resolution.

Inconsistency in these findings highlights the complexity inherent in this relationship, with changing allocation patterns of photosynthetic carbon to different storage pools, which varies between species (Richardson et al., 2013; Gea-Izquierdo et al., 2014), between sites (Babst et al., 2014b; Gea-Izquierdo et al., 2014), in response to environmental conditions (Lempereur et al., 2015; Deslauriers et al., 2016), and with the seasonal cycle (Richardson et al., 2013; Babst et al., 2014b; Cuny et al., 2015).

The possibility of time lags between the assimilation of photosynthetic carbon and its allocation to the production of stem level woody biomass must also be considered. Newly assimilated carbon can be applied directly to active growth or stored in photosynthate reserves to be used when needed. The role and relative contribution of these two pools in fueling active growth is still a subject of current research (Deslauriers et al., 2016). Significant allocation of photosynthetic carbon to carbohydrate storage pools, or from storage pools to maintain growth processes would result in a decoupling of radial growth from ecosystem production (Richardson et al., 2013; Deslauriers et al., 2016). Furthermore, the magnitude of C flux in and out of internal storage pools are species specific, with some relying more heavily on stored non-structural carbohydrates (NSCs) to maintain cellular respiration or to support growth (Richardson et al., 2013). Increased lags between measures of ecosystem C-flux and radial growth are expected in deciduous trees (Richardson et al., 2013) and in slow growing or stress tolerant trees (Rocha et al., 2006; Gea-Izquierdo et al., 2014).

Rather than being causally linked, correlations between stem size and ecosystem C exchange may be driven by a common response variable (Delpierre et al., 2016). Because photosynthesis responds to environmental conditions almost instantaneously, while stem size or radial growth may take far longer to react to the same input, there is also potential for lag in a spurious correlation between these two variables. Furthermore, it is suggested that radial growth and ecosystem production have different threshold tolerances to extremes in temperature and moisture stress (Lempereur et al., 2015). While growth ceases in response to a certain level of temperature and moisture stress, photosynthesis persists to a higher threshold limit (Lempereur et al., 2015; Deslauriers et al., 2016). Under these conditions, NSCs are diverted from growth processes to meet other requirements, such as osmoregulation, to maintain cell turgor pressure during drought (Deslauriers et al., 2016). Unfavourable environmental conditions may therefore

result in a temporary disruption in the relationship between ecosystem production and radial growth or stem size over finer temporal scales.

While the recent application of dendrochronology in carbon cycle research has improved our understanding of the role of stem-level biomass in forest carbon storage (Rocha et al., 2006; Granier et al., 2008; Ilvesniemi et al., 2009; Zweifel et al., 2010; Babst et al., 2014b; Gea-Izquierdo et al., 2014; Cuny et al., 2015; Lempereur et al., 2015; Delpierre et al., 2016; Teets et al., 2018), there remain numerous uncertainties. Our lack of understanding regarding the causal link between measures of radial growth and ecosystem C-flux, as well as the mechanisms of photosynthate storage and allocation, including its role in active ring development in different forest types and under changing environmental conditions, translate to significant gaps in our understanding of forest carbon dynamics. This directly limits the accuracy of the current carbon cycle and climate-carbon feedback models (Gower et al., 2001; Litton et al., 2007; Misson et al., 2007; Zweifel et al., 2010; Chen et al., 2013). To better understand the processes of forest carbon allocation, further comparisons between eddy covariance and biometric based measures of carbon uptake are needed across a wide range of forest ecosystems (Zweifel et al., 2010; Babst et al., 2014b).

Central Saskatchewan is a prime location for this type of work. This is an area that is particularly susceptible to many of the impacts of climate change (Henderson and Sauchyn 2008; Bush and Lemmen, 2019), and where one of the most comprehensive collections of long-term high-resolution carbon flux data resides (Kljun et al., 2007). These carbon flux data are being collected at the Boreal Ecosystem Research and Monitoring Sites (BERMS), alongside an equally impressive suite of meteorological data, since the mid-1990s. This study assesses the relationship between radial growth and ecosystem carbon flux across the temporal scale in three common southern boreal forest stands. High resolution stem radius data were collected over four growing seasons (from 2015 – 2018) and radial growth measured from ring widths extends the record of annual tree growth back to stand establishment, allowing for an assessment of relationships at multiple temporal scales over the short (2015 – 2018) and medium (1997 – 2018) terms. This powerful collection of data provides a significant opportunity to further advance our understanding of carbon dynamics in the boreal forest.

3.3 Study Sites

This study was conducted at three of the BERMS sites, located near the southern edge of the boreal forest in the Boreal Plains Ecozone of central Saskatchewan (Figure 1.1). Site characteristics are given in Table 1.1. The climate of the study area is characterized by short, warm, dry summers and long, cold winters.

The Old Jack Pine (OJP) site, located northeast of Candle Lake, Saskatchewan, is an even-aged stand of jack pine, naturally established post-fire in 1914 (Barr et al., 2012). The understory is composed of clumps of green alder (*Alnus crispa*), and the dominant ground cover includes some bearberry (*Arctostaphylos uva-ursi*) and a nearly continuous cover of reindeer lichen (*Cladina mitis*). The soil is a well-drained Orthic Eutric Brunisol (loamy sand).

The Old Black Spruce (OBS) site is located due north of Candle Lake and is a black spruce dominated forest with co-dominant eastern larch comprising approximately 10% of the stands makeup (Pappas et al., 2018). The stand was established post-fire in approximately 1879 (Barr et al., 2012). The understory is mainly comprised of wild rose (*Rosa Woodsii)* and Labrador tea (*Ledum groenlandieum*). The groundcover contains a mixture of feather mosses, sphagnum moss, and lichen. The soil is poorly drained, with a thick layer of peat (~20 cm) over waterlogged sand.

The BERMS Old Aspen (OA) site in Prince Albert National Park is an even-aged stand of trembling aspen naturally established after a forest fire in 1919 (Barr et al., 2012). The understory is mainly hazelnut (*Corylus cornuta*) with a few other shrubs. The topography is relatively level, with uniform fetch of at least 3 km in each direction from the tower. The soil is an Orthic Gray Luvisol (loam to clay loam).

3.4 Methods

3.4.1 Dendrometer data

DC2 type circumference band dendrometers (Ecomatik, 2019) were mounted to groups of four trees of each study species in 2015, including trembling aspen at OA, jack pine at OJP, and black spruce and eastern larch at OBS. Measurements from the four groups of four trees were fed to HOBO UX120-006M data loggers, for a total of 16 bands. In 2016, to increase the sample

depth and cover a wider spatial area within each site, an additional 12 trees of each species were added to the network using DC3 type band dendrometers (Ecomatik, 2019). Over the short-term observation period, the sites were visited regularly during the growing season to ensure the smooth running of these instruments and when necessary, to replace or repair dendrometers. Following the expansion of data collection efforts in 2016, there were always between 12 and 16 dendrometers logging measurements of stem size for each species at any given time.

Raw data were collected with 30-minute resolution, at equal time steps as the meteorological data collected at BERMS. An R-script, based on calculations provided by Ecomatik, was used to convert the raw dendrometer output to a measure of radius change from a starting point of 0μm. The resulting data were checked for errors resulting from sensor failure, or wildlife activity, and data were omitted accordingly. Under normal circumstances, variations in stem radius were synchronous between individuals of the same species. Species averages were therefore calculated and used as a site- and species-specific records of radius change. The only exception was for eastern larch in 2016, which produced two distinct records of ΔR which was dependent on the banded individuals location within the site. Half of the individuals being located in a wetter section of OBS, and the other half in an area with less standing water. I therefore produced two species averages for eastern larch in 2016, larch-wet and larch-dry.

To extract the growth signal from these high-resolution data, the stem-cycle approach described in Deslauriers et al. (2007) was applied using the dendrometeR software package in R (van der Maaten et al., 2016). Daily and weekly mean (Rmean), minimum (Rmin), and maximum (Rmax) stem radius for each of the study species were also calculated. From the observations comparing the four extraction methods (stem cycle, Rmean, Rmin, and Rmax) (Appendix B), the stem cycle approach had a tendency of over-represented large pulses in stem radius relating to moisture inputs, resulting in increased variability (Appendix B). The “daily mean approach” is known to produce similar results as the stem cycle approach and is similarly effective at extracting the growth signal (Deslauriers et al., 2007). Daily and weekly-resolved records of mean stem radius were therefore constructed before calculating the difference between each value of mean stem radius and the preceding one, resulting in records of stem radius change (ΔR).

3.4.2 Core Samples

Core samples were extracted using a 5.1 mm increment borer, from OJP in the fall of 2018, and from OA in the spring of 2019, following a plot-based sampling scheme based on the findings of Babst et al. (2014a). This sampling protocol is designed to yield ring-width data appropriate for the reconstruction of stand-level above-ground biomass accumulation. This sampling scheme is believed to better represent stand-level growth and stem-level biomass accumulation compared with traditional dendroclimatological sampling, which tends to introduce bias by oversampling the largest or oldest individuals (Babst et al., 2014a).

The appropriate sample size was determined by stand density, with dense stands requiring a greater sample size to achieve an accurate reconstruction of biomass accumulation (Babst et al., 2014a). I examined the existing permanent sampling plots at OJP and OA (Gower, 2001) and chose the one which most accurately represented overall stand density at each of the sites. I sampled every living individual within these two plots, and extended their length on a randomly chosen side to accommodate additional individuals and reach the required sample size based on stand density. OJP Gower plot 4 was extended by 2.5m (27.2 m x 25 m), and OA Gower plot 2 by 15m (40 m x 25 m). In total, a single core was extracted from 54 and 46 individuals at OJP and OA respectively.

OBS was sampled earlier, in 2015, for a separate study by Pappas et al. (2020). Here, a single core was extracted from 90+ black spruce and eastern larch trees located in two 5m-radius circular plots in random locations within the site. After excluding the larch cores and those which contained missing or heavily fragmented segments, the final chronology was made up of 73 black spruce trees (ITRDB site code CANA610; https://www.ncdc.noaa.gov/paleo-search/study/29612).

All samples were processed in the Mistik Askiwin Dendrochronology (MAD) Lab, after being mounted to slotted boards and sanded with progressively finer grits of sandpaper. Each ring was measured with 0.001 mm precision on a Velmex stage system, under a Nikon 63X stereomicroscope, and using ProjectJ2X software (VoorTech, 2017). The resulting ring-width series are crossdated using COFECHA software (Holmes, 1983; Speer, 2010) and reworked to minimize the amount of flagged problematic segments (Chapter 2; Table 2.1). The resulting

crossdated series were standardized using the detrend function in the dplR (Bunn, 2008). A negative exponential curve was fit to each series before species specific master chronologies were built.

3.4.3 Flux-tower measurements

Eddy-covariance measurements of the CO_2 flux density were made at 29 m (OJP), 25 m (OBS), and 39 m (OA) above the ground. At OJP and OBS, continuous flux measurements have been recorded since 1999 and are ongoing. At OA, flux measurements were continuously measured from January 1997 to November 2017 when decommissioning of the site began. Details of the eddy-covariance system and data processing at OA and OBS for the entire period and at OJP up to 2012 are given in Griffis et al. (2003). In 2012 at OJP, the original closed-path infrared gas (CO_2/H_2O) analyzer (model LI7000, LI-COR Inc., Lincoln, NE, USA, in a thermostated housing) was replaced (model LI7200 (LI-COR Inc., Lincoln, NE, USA) and the subsequent data were processed using the EddyPro software (LI-COR Inc., Lincoln, NE, USA). A short period of overlap of the two systems at OBS showed close agreement. The CO_2 flux density as measured by eddy-covariance plus storage (Barr et al. 2006) is a direct measurement of net ecosystem exchange NEE, the net exchange of CO_2 between an ecosystem and the atmosphere. NEE is positive for an atmospheric C sink. In situations where the loss of dissolved organic C via groundwater flow is negligible (Moore, 2003), a reasonable assumption at these sites, NEE provides a direct measure of net ecosystem production NEP (i.e., NEP = - NEE), which is positive for an ecosystem C sink. In turn, NEP results as the difference between C gains by gross ecosystem photosynthesis (GEP) and C losses by total ecosystem respiration R_E, i.e., $NEP = GEP - R_E$.

Gaps in the NEE time series were filled using a standard procedure. NEE values during calm periods at night were rejected using a u_*-threshold filter, with u_*-threshold values of 0.35 m s^{-1} at OA, 0.30 m s^{-1} at OBS, and 0.25 m s^{-1} at OJP (Barr et al., 2013). The procedures to fill gaps in NEE and to estimate GEP and R_E are described in Barr et al. (2004). The resulting high-resolution NEP, GEP, and R_E data were summed over daily, weekly, monthly, and annual scales to assess their relationship with radial growth and stem radius change across multiple temporal scales.

3.4.4 Statistical Analysis

All data analysis and preliminary visualization were done in R. A moving window correlation with 1000 bootstrap replicates was performed using the treeclim package (Zang and Biondi, 2015) to assess the relationship between ΔR and ecosystem C-fluxes at daily resolution during the short-term observation period (2015 – 2018). Bootstrapped Pearson's correlations were computed over a 30-day moving window offset by 1-day, and were limited to the growing season (May – September). Relationships were "flagged" if statistically significant at the 99% confidence level. Since this type of analysis is not often undertaken at the daily scale, I tested the high resolution records of stem radius variability for normality across each of the 30-day intervals using the Shapiro-Wilk test (Appendix C). To further ensure Pearson's correlations are appropriate, I also compared the results from the moving-window Pearson's correlation analysis in Chapter 2 to equivalent analyses using non-parametric tests, namely Kendall's tau and Spearman's rank correlations (Appendix C). To assess lag in the relationship between ΔR and ecosystem C-flux at daily resolution, records of NEP, R_E, and GEP were lagged backwards from the record of stem radius by 0 to 11 days, before repeating the bootstrapped moving window correlation analysis, as described above.

At weekly, monthly, and annual scales, bootstrapped Pearson's correlations were assessed contemporaneously rather than over a moving window. These were also performed using the treeclim package (Zang and Biondi, 2015) at the 99% confidence level. At weekly resolution, relationships were assessed over a minimum 12 and maximum 27 weeks centered around the spring and summer months during the short-term observation period (2015 – 2018) (See Figure 3.3 for more detail regarding the observation period). The assessment of relationships on an annual scale were limited only by the carbon flux data, and were assessed over the medium term (19, 17, and 21 years for jack pine, black spruce, and trembling aspen, respectively).

3.5 Results

3.5.1 Annual Scale

Among the three study sites and three C fluxes (NEP, R_E, and GEP), the only pertinent relationship between radial growth and EC flux measurements at annual scale resolution was a

positive association between jack pine radial growth (ring width) and annual NEP recorded at OJP from 1999 – 2018 (Figure 3.1). Relationships between monthly ecosystem C-flux values from the current and previous growing seasons and annual radial growth are depicted in Figure 3.2. Jack pine growth was significantly and positively related to same-year May NEP. The relationship between jack pine radial growth and late-summer to early-winter NEP (August to December) from the previous growing season was also generally positive, including statistically significant correlations with previous August and October NEP. As for the other study species, there was a significant positive relationship between black spruce ring width and current July GEP, while trembling aspen growth had a significant negative correlation with current January NEP, and a significant positive correlation with current January R_E. Previous growing season GEP (May – October) was also positively associated with aspen ring width, however this relationship was relatively weak (r-values < 0.5), with confidence levels below 99%.

3.5.2 Weekly Scale

There was only one noteworthy relationship between the ΔR of the study species, and ecosystem C-flux at weekly temporal resolution during the short-term observation period (2015 – 2018). This was a significant positive relationship between weekly trembling aspen ΔR and NEP ($r > 0.75$), present during the 2015 growing season (Figure 3.3). However, due to issues with site access, trembling aspen data during the 2015 growing season were limited to 12 weeks, from late-May to early-August. All other correlations at weekly resolution were assessed over a minimum of 18 weeks, most often over 20 to 23 weeks (Figure 3.3) from the beginning of May to the end of August. Because of to the limited sample size, caution should be exercised when interpreting this lone significant relationship.

3.5.3 Daily Scale

GEP and NEP had a negative relationship with ΔR at daily resolution (Figure 3.4). These two measures of ecosystem production are intrinsically linked. Therefore, when the negative relationship between ΔR and NEP increased in strength over a given period within the observation period, the relationship between ΔR and GEP often exhibited a similar trend (Figure 3.4). The negative relationship between ecosystem production (GEP and NEP) and ΔR was generally strongest and most persistent during intervals with start dates in June and July 2016

and 2018, and nearer the beginning and end of the growing season in 2017 (Figure 3.4). In general, correlations between ecosystem production and ΔR during the 2015 growing season were weak and inconsistent, except there remained a strong relationship between trembling aspen ΔR and ecosystem production during intervals with start dates in mid-June to early-July. Another exception, or divergence from a common interspecies trend occurred in 2017. While there were strong correlations between black spruce, eastern larch, and trembling aspen ΔR and ecosystem production in 2017, daily jack pine ΔR showed no significant associaton with ecosystem production over the course of this growing season.

The relationship between daily R_E and ΔR was always positive, with sporadic instances of statistical significance (Figure 3.4). Overall, correlations between these two variables were quite weak. The strongest associations between daily R_E and ΔR were observed in 2016 during intervals with start dates in early- to mid-July. During this time, R_E had a significant positive relationship with the ΔR of black spruce and eastern larch (Figure 3.4).

3.5.4 Daily Lag

Negative relationships between daily ΔR and values of ecosystem production (GEP and NEP) often persisted when the latter was lagged backwards from ΔR by one-day (lag = -1) (Figures 3.5 and 3.6). Days with high rates of ecosystem production therefore often corresponded with a decrease in stem radius since the previous day (lag = 0), and/or by the next day (lag = -1). When further lag was introduced between these variables, the relationship tended to transition from negative to positive (Figures 3.5 and 3.6). Positive correlations between ΔR and lagged ecosystem production were strongest at -2 days, but were weak and inconsistent when compared to negative correlations at 0 or -1 day. Note that relationships between ΔR and lagged GEP (Figure 3.5) were almost indistinguishable from those between ΔR and lagged NEP (Figure 3.6). It is for this reason that these variables were once again discussed together as ecosystem production.

The positive relationship observed between daily ΔR and R_E (Figure 3.4) often persisted or was enhanced slightly when one or two days of lag was introduced between these variables (Figure 3.7). There were however, a few instances where negative relationships emerged when further lag was introduced. Notably, these occured in 2016 towards the beginning of the growing

season for jack pine and trembling aspen, and during intervals with start dates in July 2016 for black spruce and eastern larch. There was also a negative relationship between ΔR and R_E towards the end of the 2017 growing season, which persisted regardless of lag (Figure 3.7).

3.6 Discussion

The only consistent relationship between radial growth and ecosystem C-flux (NEP, GEP, and R_E) on an annual scale was a significant positive correlation between jack pine and annual NEP (r = 0.55, n = 20, 1999 – 2018) (Figure 3.1). Similar relationships between annual tree growth and NEP were identified by Rocha et al. (2006) for black spruce, Zweifel et al. (2010) for Norway spruce (*Picea abies*), and Lempereur et al. (2015) for evergreen oak (*Quercus ilex*). The simplest link between these two variables is woody biomass production, which contributes both to ring width and NEP. One could therefore hypothesize that a relationship between annual radial growth and NEP would be more likely to exist if a significant proportion of ecosystem production is allocated to woody biomass annually. Interestingly, according to two studies, one by Gower et al. (2001), and another by Litton et al. (2007), jack pine at OJP was reported to have a lower proportion of total NPP allocated to woody biomass (15 – 29%), compared with black spruce at OBS (16 – 30%), and aspen at OA (23 – 45%). Based on this metric alone, one would expect trembling aspen radial growth to have a strong relationship with ecosystem production, at least compared with jack pine and black spruce.

Nonetheless, my findings agree with those from Gea-Izquierdo et al. (2014), which identified a considerably stronger relationship between jack pine growth and measures of ecosystem production compared with black spruce, as well as aspen in this case. This may be attributable to interspecies and interannual differences in the allocation of NSCs to long-term storage pools, with slow growing or stress-tolerant trees, such as black spruce, relying more heavily on stored NSCs to maintain cellular respiration or to support growth (Rocha et al., 2006; Gea-Izquierdo et al., 2014). Deciduous trees, such as trembling aspen, are also known to be more conservative with their non-structural carbohydrate reserves, which are generally older and larger compared with coniferous trees (Richardson et al., 2013), likely because they are entirely dependent on stored NSCs during the leafless period in the spring. Black spruce and trembling aspen are therefore more likely to rely on stored NSCs than jack pine. A reliance on stored NSCs to support growth has the potential to introduce lag and blur the relationship between ecosystem

production and radial growth, helping to explain some of the interspecies differences observed in this association.

Surprisingly, the radial growth of jack pine had a strong positive correlation with values of ecosystem production from the previous year. Monthly values of NEP from late in the previous growing season (August to December) had a strong positive relationship with the annual-radial growth of jack pine (Figure 3.2), suggesting that jack pine may consistently benefit from elevated carbohydrate storage during the previous fall (1999 – 2018). There were however no significant relationships between monthly ecosystem-C flux values from the previous growing season and the annual-radial growth of black spruce or aspen over the medium term (Figure 3.2). This could indicate that their reliance on stored NSCs, if one exists, may be situational. It is suggested that these two species may rely more heavily on stored NSCs to support growth during growing seasons with unfavourable environmental conditions (Richardson et al., 2013; Gea-Izquierdo et al., 2014), introducing inconsistency in the lagged relationship between ecosystem production and radial growth. Furthermore, the stored NSCs allocated to support growth during periods of need may be over a year old (Richardson et al., 2013). Between aspen and black spruce however, aspen would appear to have a more consistent relationship with ecosystem production from the previous growing season at the BERMS sites. This assessment is based on a weak positive correlation observed between previous growing season GEP and aspen radial growth.

The radial growth of jack pine, black spruce, and aspen had contrasting relationships with current growing season ecosystem C-flux values over the medium term (Figure 3.2). Firstly, like Gea-Izquierdo et al. (2014), the radial growth of jack pine was positively related to photosynthetic activity in the spring. However, compared to the findings from this same study, which identified an equivalent response of radial growth to both NEP and GEP (Gea-Izquierdo et al., 2014), I found that relationships between jack pine radial growth and NEP were much stronger than equivalent relationships with GEP. Current May NEP had a strong positive association with the annual radial growth of jack pine, whereas correlations between spring GEP (March – May) and jack pine radial growth, while still positive, were far weaker (Figure 3.2). In contrast, black spruce radial growth had a stronger relationship with measures of ecosystem production later in the growing season, exhibiting a significant positive correlation with current

July GEP, which was stronger than the equivalent correlation with July NEP (Figure 3.2). Lastly, aspen radial growth had a strong negative association with current January NEP, a strong positive association with current January R_E, and a weak positive association with late growing season (August and September) GEP. Each of the species in this study had a rather unique relationship with current growing season ecosystem C-flux variables, likely due to interspecies differences in phenology, and strategies for photosynthate assimilation, allocation, and storage (Gea-Izquierdo et al., 2014). Because the temporal and spatial scale of this study is limited, a complete interpretation of the significance of the relationships observed herein would be ill advised, at least until we develop a better understanding of the numerous and complex processes that govern both radial growth and ecosystem C-flux in a diverse set of forest ecosystems and climates.

At daily resolution during the short-term observation period (2015 – 2018), relationships between ΔR and values of ecosystem production (GEP and NEP) were always negative (Figure 3.4). A similar relationship was observed by Zweifel et al. (2010) and Lempereur et al. (2015), who identified a significant negative correlation between the radial increment and NEP at sub-daily to daily scales. Zweifel et al. (2010) hypothesized that this is expressed due to the nature of dendrometer data, which contains information regarding two competing signals that become increasingly difficult to disentangle as the rate of radial expansion decreases relative to the amplitude of the stem water signal (Deslauriers et al., 2007). During days where there are high levels of ecosystem production, it is likely for stem size to shrink due to transpiration and dehydration in warm sunny conditions (Zweifel et al., 2010). This is especially likely during extended dry periods when there is insufficient moisture to fully replenish stem water content overnight (Turcotte et al., 2011) and when radial growth processes may be impacted due to moisture limitations (Deslauriers et al., 2016). Conversely, during periods of increased precipitation under cloud cover, the inverse is true. Under these conditions, ecosystem production is likely to be low while stem water content is likely to increase (Zweifel et al., 2010). This mode is most likely to occur beyond the main period of stem expansion, when the growth signal is easily overshadowed by the water signal (Deslauriers et al., 2007), and during instances of stem water replenishment. My findings, as described in the following section, agree with this interpretation.

Negative relationships were observed between ΔR and ecosystem production (GEP and NEP) during periods with above average precipitation, towards the end of the growing season in 2015, during intervals with start dates in June and July 2016, and during the beginning of the growing season in 2017 (Figures 3.4 and 1.2). Negative relationships between ΔR and ecosystem production also occurred during extended periods of dryness, such as towards the beginning and end of the growing season in 2016, or near the end of the 2017 growing season (Figures 3.4 and 1.2). I also observed negative correlations between ΔR and ecosystem production during intervals with start dates in June and July 2018, a period that was neither wet nor dry, but during which variations in stem radius were particularly sensitive to precipitation (Chapter 2, Section 2.6.2). In fact, nearly every period during which there was a significant negative correlation between measures of ecosystem production and the ΔR of the study species corresponds with a period during which ΔR was particularly responsive to precipitation (Chapter 2; Figure 2.4). It is therefore extremely likely that the observed relationship between ecosystem production and ΔR was spurious, largely driven by co-occurring responses to precipitation and light availability.

The 2016 growing season appears to be the only growing season during which negative relationships between ecosystem production and ΔR didn't co-occur with a positive relationship between ΔR and precipitation. During this growing season, there were significant negative correlations between the ΔR of the study species and measures of ecosystem production at lag = 0, present during intervals with start dates in June and July (Figure 3.4). Unlike other instances where negative relationships between ΔR and ecosystem production were present, there is no evidence suggesting that the study species were particularly sensitive to precipitation during this time (Chapter 2, Figure 2.4). Note that this was a period of excessive moisture, with OJP and OBS receiving approximately twice the average amount of precipitation during the month of July 2016 (Figure 1.2). Beyond the presence of a negative relationship between ecosystem production and ΔR during this period, there was also a strong positive relationship between ΔR and R_E for black spruce and eastern larch at OBS, an association which co-occurs with a remarkably similar relationship between ΔR to lagged soil temperature in Chapter 2 (Figure 2.6). This is perhaps unsurprising considering that R_E is largely controlled by soil temperature (Sellers et al., 1997; Gaumont-Guay et al., 2006). Again, variables of ecosystem C-flux are not independent from one another, with NEP being the product of the difference between GEP and R_E – when R_E is high, NEP tends to be low. Therefore, while precipitation and its association with light availability

may be of primary importance in influencing spurious correlations observed between ΔR and ecosystem production, there are likely other factors, such as air and soil temperature, that represent a causal link in these perceived relationships. Based on these observations, the importance of secondary explanatory variables may increase during periods where moisture is not limiting, when I observed a strengthening relationship between ΔR and these environmental variables (Chapter 2).

Other perceived relationships that were either emergent or enhanced when lag is introduced between ΔR and measures of ecosystem C-flux during the short-term observation period (2015 – 2018) were inconsistent between species and over time. While the presence of these associations may represent brief periods during which assimilated carbon from several days prior is being allocated to the process of radial cell expansion, it is equally likely they are simply the result of offset responses of photosynthetic activity and stem size to the same environmental variables. Further research would be required to determine whether photosynthates stored short term are being used to support radial growth processes at these sites, and if so, under which set of circumstances.

3.7 Conclusion

At annual scale resolution, tree-ring data may provide much needed information regarding ecosystem production, however, consistent with Gea-Izquierdo et al. (2014), only the radial growth of jack pine was identified as having a significant relationship with annual NEP at the study sites over the medium term (1999 – 2018). Compared with black spruce and trembling aspen, which are more likely to rely situationally on stored carbohydrates (Rocha et al., 2006; Richardson et al., 2013; Gea-Izquierdo et al., 2014), radial growth in jack pine was more closely related to ecosystem C-fluxes, benefiting from elevated levels of ecosystem production during the spring and previous fall.

Conversely, high-resolution stem size data are likely not a good proxy for ecosystem production, or vice versa, due to complexities in this relationship such as lag (Richardson et al., 2013), changing carbohydrate allocation strategies (Lempereur et al., 2015; Deslauriers et al., 2016), and spurious correlation. It is suggested that negative relationships between ΔR and NEP at fine temporal resolutions may occur due to the nature of dendrometer data, which contain

information regarding stem water dynamics, as well as radial growth (Deslauriers et al., 2007; Zeifel et al., 2010). In this paper, tree water relations likely played a significant role in driving the negative relationship observed between stem radius and previous day measures of ecosystem production (NEP and GEP) at daily resolution, especially during periods when the ΔR of the study species was highly responsive to precipitation (Chapter 2). This most often occurred beyond the main period of growth, and during periods where moisture was limiting. The relationships between ΔR and NEP and GEP at daily resolution were likely spurious, influenced by a combination of factors, including, but not limited to, the confounding effects of precipitation and soil temperature.

Overall, the findings from this study are in good agreement with the current litterature. This is significant considering this is the first study to look at these relationships at this level of detail in the North American boreal forest. The fact that I was not able to identify any true relationships between active growth and ecosystem production over fine temporal scales does not signify that these associations do not exist, it simply highlights a widespread issue when working with slow growing and stress tolerant trees. The main issue is that dendrometer arrays remain the most convenient system for collecting high-resolution data of stem size, and until we develop alternative means of collecting high-resolution radial-growth data, more work is needed to develop a standardized method that more effectively disentangles the growth from the water signal in dendrometer data. This method may require the use of complementary instrumentation, to collect information regarding stem water dynamics with the use of sap flux sensors for example. In the meantime, this work may serve to highlight specific sets of conditions under which dendrometer data may be particularly influenced by the stem water signal, e.g. under moisture limited conditions.

3.8 References

Babst, F., Bouriaud, O., Alexander, R., Trouet, V., & Frank, D. (2014a). Toward consistent measurements of carbon accumulation: A multi-site assessment of biomass and basal area increment across Europe. *Dendrochronologia*, *32*(2), 153–161.

Babst, F., Bouriaud, O., Papale, D., Gielen, B., Janssens, I. A., Nikinmaa, E., Ibrom, A., Wu, J., Bernhofer, C., & Köstner, B. (2014b). Above-ground woody carbon sequestration

measured from tree rings is coherent with net ecosystem productivity at five eddy-covariance sites. *New Phytologist*, *201*(4), 1289–1303.

Bakker, J. D. (2005). A new, proportional method for reconstructing historical tree diameters. *Canadian Journal of Forest Research*, *35*(10), 2515–2520.

Baldocchi, D. D. (2003). Assessing the eddy covariance technique for evaluating carbon dioxide exchange rates of ecosystems: Past, present and future. *Global Change Biology*, *9*(4), 479–492.

Barr, A. G., Black, T. A., Hogg, E. H., Kljun, N., Morgenstern, K., & Nesic, Z. (2004). Inter-annual variability in the leaf area index of a boreal aspen-hazelnut forest in relation to net ecosystem production. *Agricultural and Forest Meteorology*, *126*(3), 237–255.

Barr, A. G., Morgenstern, K., Black, T. A., McCaughey, J. H., & Nesic, Z. (2006). Surface energy balance closure by the eddy-covariance method above three boreal forest stands and implications for the measurement of the CO2 flux. *Agricultural and Forest Meteorology*, *140*(1), 322–337.

Barr, A. G., van der Kamp, G., Black, T. A., McCaughey, J. H., & Nesic, Z. (2012). Energy balance closure at the BERMS flux towers in relation to the water balance of the White Gull Creek watershed 1999–2009. *Agricultural and Forest Meteorology*, *153*, 3–13.

Barr, A. G., Richardson, A. D., Hollinger, D. Y., Papale, D., Arain, M. A., Black, T. A., Bohrer, G., Dragoni, D., Fischer, M. L., Gu, L., Law, B. E., Margolis, H. A., McCaughey, J. H., Munger, J. W., Oechel, W., & Schaeffer, K. (2013). Use of change-point detection for friction–velocity threshold evaluation in eddy-covariance studies. *Agricultural and Forest Meteorology*, *171–172*, 31–45.

Bush, E. & Lemmen, D.S, editors (2019). Canada's changing climate report. *Government of Canada, Ottawa, ON,* 444p.

Chen, G., Yang, Y., & Robinson, D. (2013). Allocation of gross primary production in forest ecosystems: Allometric constraints and environmental responses. *New Phytologist*, *200*(4), 1176–1186.

Cuny, H. E., Rathgeber Cyrille, B. K., Frank, D., Fonti, P., Mäkinen, H., Prislan, P., Rossi, S., Campelo, F., Vavrčík, H., & Camarero, J. J. (2015). *Woody biomass production lags stem-girth increase by over one month in coniferous forests*.

Delpierre, N., Berveiller, D., Granda, E., & Dufrêne, E. (2016). Wood phenology, not carbon input, controls the interannual variability of wood growth in a temperate oak forest. *New Phytologist*, *210*(2), 459–470.

Deslauriers, A., Huang, J.-G., Balducci, L., Beaulieu, M., & Rossi, S. (2016). The contribution of carbon and water in modulating wood formation in black spruce saplings. *Plant Physiology*, pp–01525.

Deslauriers, A., Rossi, S., & Anfodillo, T. (2007). Dendrometer and intra-annual tree growth: What kind of information can be inferred? *Dendrochronologia*, *25*(2), 113–124.

Ecomatik (2019). *Circumference DC2, DC3*. Ecomatik Umweltmess- Und Datentechnik. Retrieved October 25, 2019, from https://ecomatik.de/en/products/dendrometer/circumference-dc2-dc3/

Gaumont-Guay, D., Black, T. A., Griffis, T. J., Barr, A. G., Jassal, R. S., & Nesic, Z. (2006). Interpreting the dependence of soil respiration on soil temperature and water content in a boreal aspen stand. *Agricultural and Forest Meteorology*, *140*(1), 220–235.

Gea-Izquierdo, G., Bergeron, Y., Huang, J.-G., Lapointe-Garant, M.-P., Grace, J., & Berninger, F. (2014). The relationship between productivity and tree-ring growth in boreal coniferous forests. *Boreal Environment Research*.

Gower, S. T., Krankina, O., Olson, R. J., Apps, M., Linder, S., & Wang, C. (2001). Net primary production and carbon allocation patterns of boreal forest ecosystems. *Ecological Applications*, *11*(5), 1395–1411.

Granier, A., Bréda, N., Longdoz, B., Gross, P., & Ngao, J. (2008). Ten years of fluxes and stand growth in a young beech forest at Hesse, North-eastern France. *Annals of Forest Science*, *7*(65), 704–704.

Griffis, T. J., Black, T. A., Morgenstern, K., Barr, A. G., Nesic, Z., Drewitt, G. B., Gaumont-Guay, D., & McCaughey, J. H. (2003). Ecophysiological controls on the carbon balances of three southern boreal forests. *Agricultural and Forest Meteorology*, *117*(1), 53–71.

Henderson, N., & Sauchyn, D. (2008). Climate change impacts on Canada's Prairie Provinces: A summary of our state of knowledge. *Prairie Adaptation Research Collaborative: Summary Document*, *08–01*, 20.

Holmes, R. L. (1983). Computer-assisted quality control in tree-ring dating and measurement. *Tree-Ring Bulletin*, *43*(1), 69–78.

Ilvesniemi, H., Levula, J., Ojansuu, R., Kolari, P., Kulmala, L., Pumpanen, J., Launiainen, S., Vesala, T., & Nikinmaa, E. (2009). Long-term measurements of the carbon balance of a boreal Scots pine dominated forest ecosystem. *Boreal Environ. Res*, *14*, 731–753.

Kljun, N., Black, T. A., Griffis, T. J., Barr, A. G., Gaumont-Guay, D., Morgenstern, K., McCaughey, J. H., & Nesic, Z. (2006). Response of net ecosystem productivity of three boreal forest stands to drought. *Ecosystems*, *9*(7), 1128–1144.

Lempereur, M., Martin-StPaul, N. K., Damesin, C., Joffre, R., Ourcival, J.-M., Rocheteau, A., & Rambal, S. (2015). Growth duration is a better predictor of stem increment than carbon supply in a Mediterranean oak forest: Implications for assessing forest productivity under climate change. *New Phytologist*, *207*(3), 579–590.

Litton, C. M., Raich, J. W., & Ryan, M. G. (2007). Carbon allocation in forest ecosystems. *Global Change Biology*, *13*(10), 2089–2109.

Misson, L., Baldocchi, D. D., Black, T. A., Blanken, P. D., Brunet, Y., Yuste, J. C., Dorsey, J. R., Falk, M., Granier, A., Irvine, M. R., Jarosz, N., Lamaud, E., Launiainen, S., Law, B.E., Longdoz, B., Loustau, D., McKay, M., Paw. K.T., Goldstein, A.H.. (2007). Partitioning forest carbon fluxes with overstory and understory eddy-covariance measurements: A synthesis based on FLUXNET data. *Agricultural and Forest Meteorology*, *144*(1), 14–31.

Moore, T. R. (2003). Dissolved organic carbon in a northern boreal landscape. *Global Biogeochemical Cycles*, *17*(4).

Pan, Y., Birdsey, R. A., Fang, J., Houghton, R., Kauppi, P. E., Kurz, W. A., Phillips, O. L., Shvidenko, A., Lewis, S. L., Canadell, J. G., Ciais, P., Jackson, R. B., Pacala, S. W., McGuire, A. D., Piao, S., Rautiainen, A., Sitch, S., & Hayes, D. (2011). A Large and Persistent Carbon Sink in the World's Forests. *Science*, *333*(6045), 988–993.

Pappas, C., Matheny, A. M., Baltzer, J. L., Barr, A. G., Black, T. A., Bohrer, G., Detto, M., Maillet, J., Roy, A., Sonnentag, O., & Stephens, J. (2018). Boreal tree hydrodynamics: Asynchronous, diverging, yet complementary. *Tree Physiology*, *38*(7), 953–964.

Pappas C., Maillet, J., Rakowski, S., Baltzer, J.L., Barr, A.G., Black, A., Fatichi, S., Matheny, A.M, Roy, A., Sonnentag, O., & Zha, T. (2020). Aboveground tree growth is a minor and decoupled fraction of boreal forest carbon input. *Agricultural and Forest Meteorology, 290.*

Richardson, A. D., Carbone, M. S., Keenan, T. F., Czimczik, C. I., Hollinger, D. Y., Murakami, P., Schaberg, P. G., & Xu, X. (2013). Seasonal dynamics and age of stemwood nonstructural carbohydrates in temperate forest trees. *New Phytologist*, *197*(3), 850–861.

Rocha, A. V., Goulden, M. L., Dunn, A. L., & Wofsy, S. C. (2006). On linking interannual tree ring variability with observations of whole-forest CO2 flux. *Global Change Biology*, *12*(8), 1378–1389.

Sellers, P. J., Hall, F. G., Kelly, R. D., Black, A., Baldocchi, D., Berry, J., Ryan, M., Ranson, K. J., Crill, P. M., & Lettenmaier, D. P. (1997). BOREAS in 1997: Experiment overview, scientific results, and future directions. *Journal of Geophysical Research: Atmospheres*, *102*(D24), 28731–28769.

Speer, J. H. (2010). *Fundamentals of Tree-ring Research*. University of Arizona Press.

Teets, A., Fraver, S., Hollinger, D. Y., Weiskittel, A. R., Seymour, R. S., & Richardson, A. D. (2018). Linking annual tree growth with eddy-flux measures of net ecosystem productivity across twenty years of observation in a mixed conifer forest. *Agricultural and Forest Meteorology*, *249*, 479–487.

Turcotte, A., Rossi, S., Deslauriers, A., Krause, C., & Morin, H. (2011). Dynamics of Depletion and Replenishment of Water Storage in Stem and Roots of Black Spruce Measured by Dendrometers. *Frontiers in Plant Science*, *2*.

van der Maaten, E., van der Maaten-Theunissen, M., Smiljanic, M., Rossi, S., Simard, S., Wilmking, M., Deslauriers, A., Fonti, P., von Arx, G., & Bouriaud, O. (2016). dendrometeR: Analyzing the pulse of trees in R. *Dendrochronologia*.

VoorTech. (2017). *The Tree Ring Measuring Program Project J2X*. http://www.voortech.com/projectj2x/

Zang, C., & Biondi, F. (2015). treeclim: An R package for the numerical calibration of proxy-climate relationships. *Ecography*, *38*(4), 431–436.

Zweifel, R., Eugster, W., Etzold, S., Dobbertin, M., Buchmann, N., & Häsler, R. (2010). Link between continuous stem radius changes and net ecosystem productivity of a subalpine Norway spruce forest in the Swiss Alps. *New Phytologist*, *187*(3), 819–830

3.9 Figures

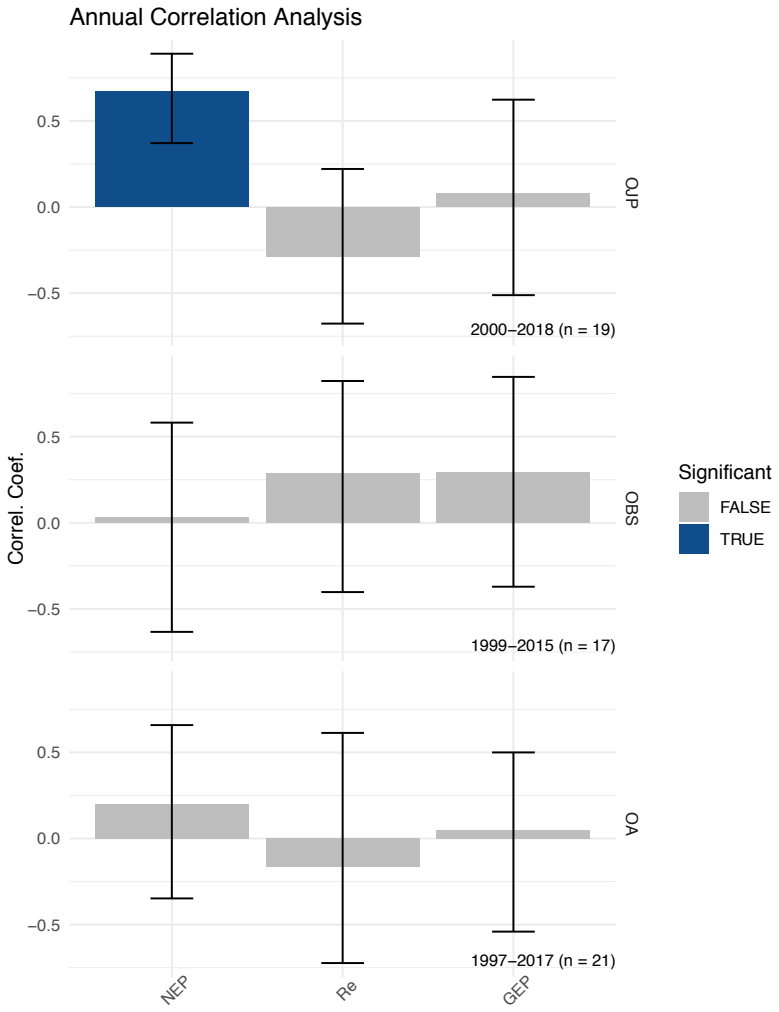

Figure 3.1: Bootstrapped correlation analysis between annual ring widths of jack pine at OJP, black spruce at OBS, and trembling aspen at OA, and annual summed NEP, Re, and GEP (x-axis). The height of each column represents the Pearson's correlation r-value from -1 to 1. Bootstrapped confidence intervals (99%) are depicted by each error bar and statistical significance is highlighted in blue. The site names are labeled on the right of each graph, which are arranged in a column-wise matrix.

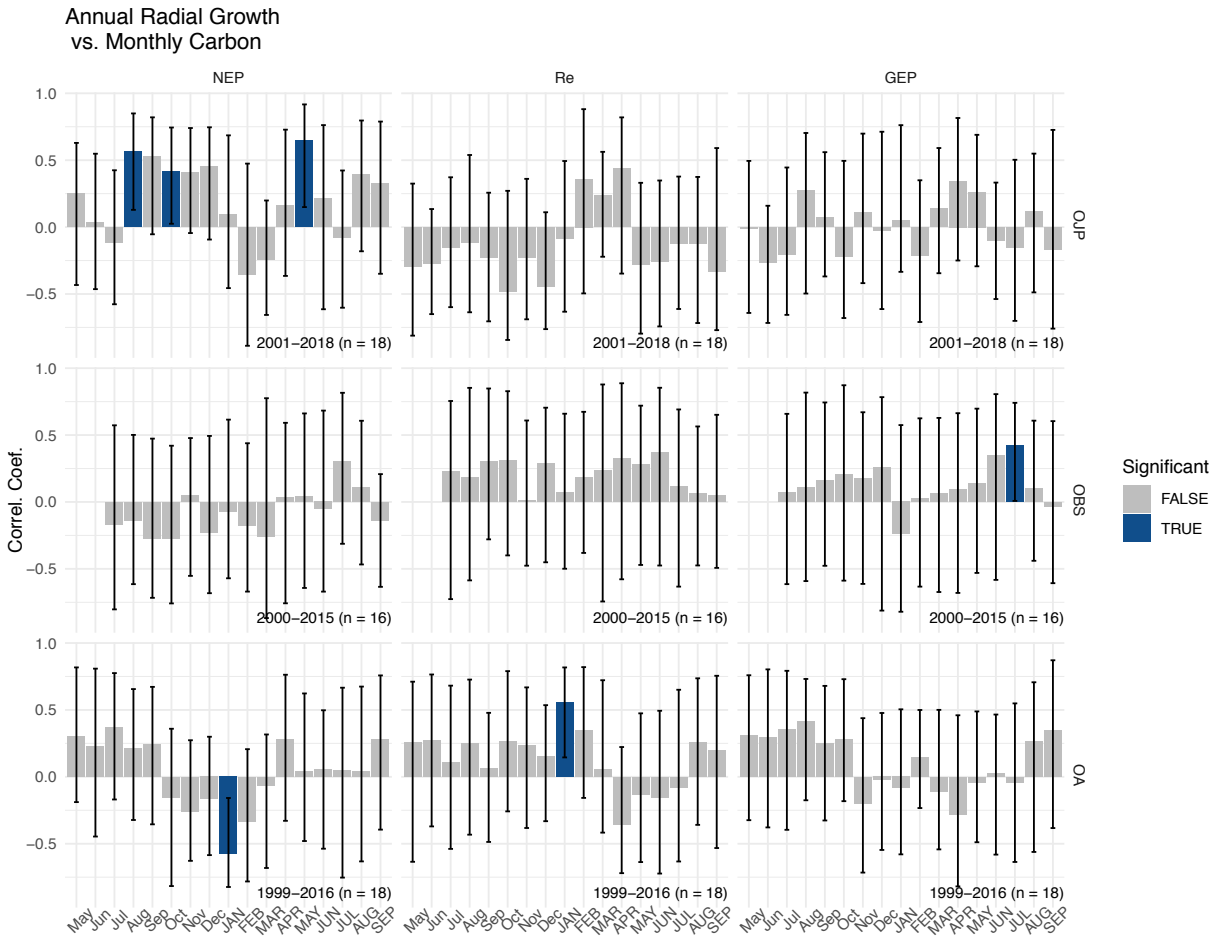

Figure 3.2: Bootstrapped correlation analysis between annual ring widths of jack pine at OJP, black spruce at OBS, and trembling aspen at OA, and monthly summed NEP, Re, and GEP. Relationships were assessed from previous May to current September (-5 to 9) for OJP and OA, and from previous July to current September (-7 to 9) at OBS (x-axis), due to a more restricted sample size at this site. The height of each column represents the Pearson's correlation r-value from -1 to 1. Bootstrapped confidence intervals (99%) are depicted by each error bar and statistical significance is highlighted in blue. Graphs are arranged in a two-dimensional matrix with ecosystem C-flux variables listed above each column, and site names labeled to the right of each row.

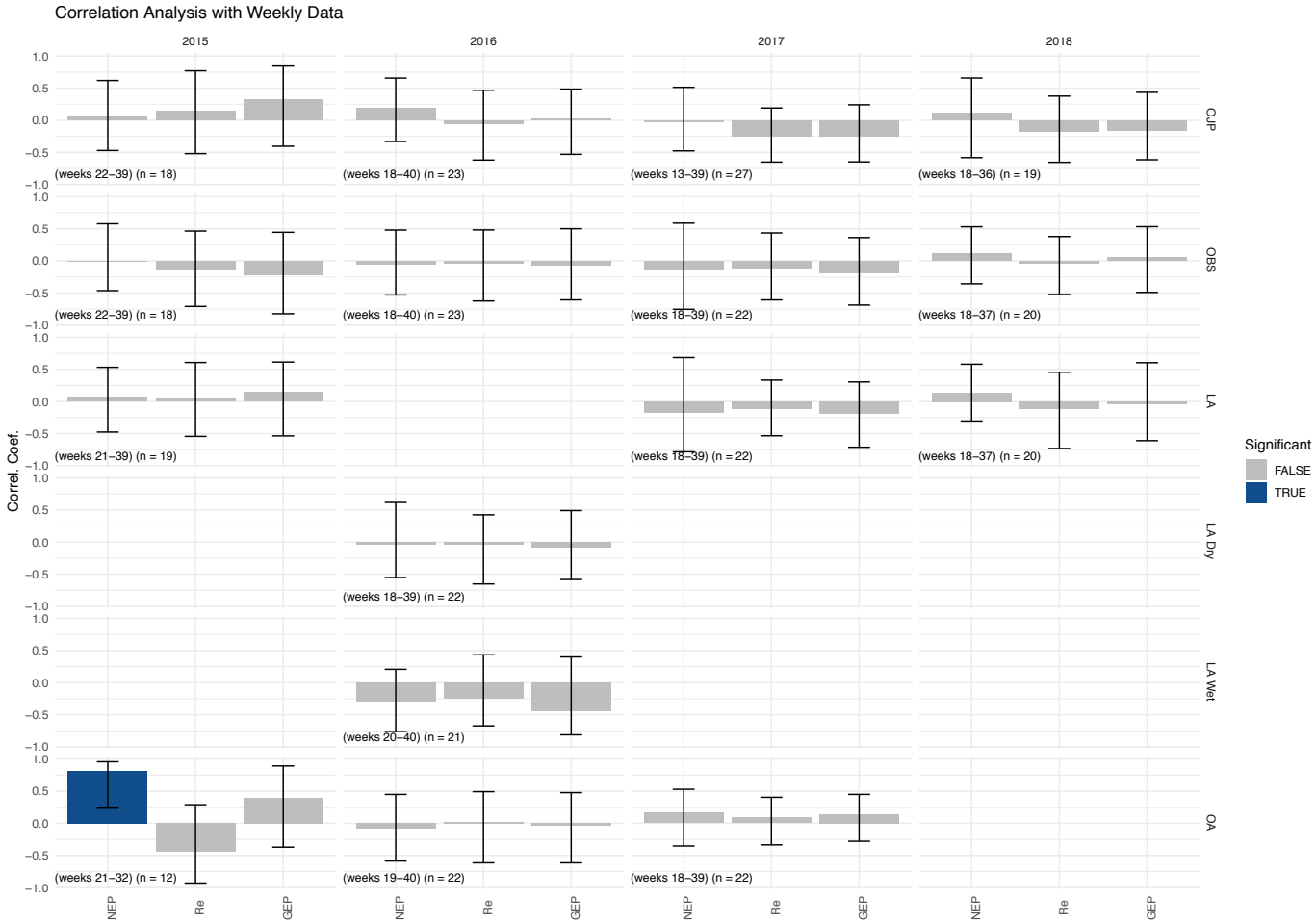

Figure 3.3: Bootstrapped correlation analysis between weekly ΔR and summed weekly NEP, Re, and GEP (x-axis). Relationships were assessed within each growing season over the course of the short-term observation period (2015 – 2018). The height of each column represents the Pearson's correlation r-value from -1 to 1. Bootstrapped confidence intervals (99%) are depicted by each error bar, and statistical significance is highlighted in blue. Graphs are arranged in a two-dimensional matrix with growing season year listed above each column, and site/species names labeled to the right of each row.

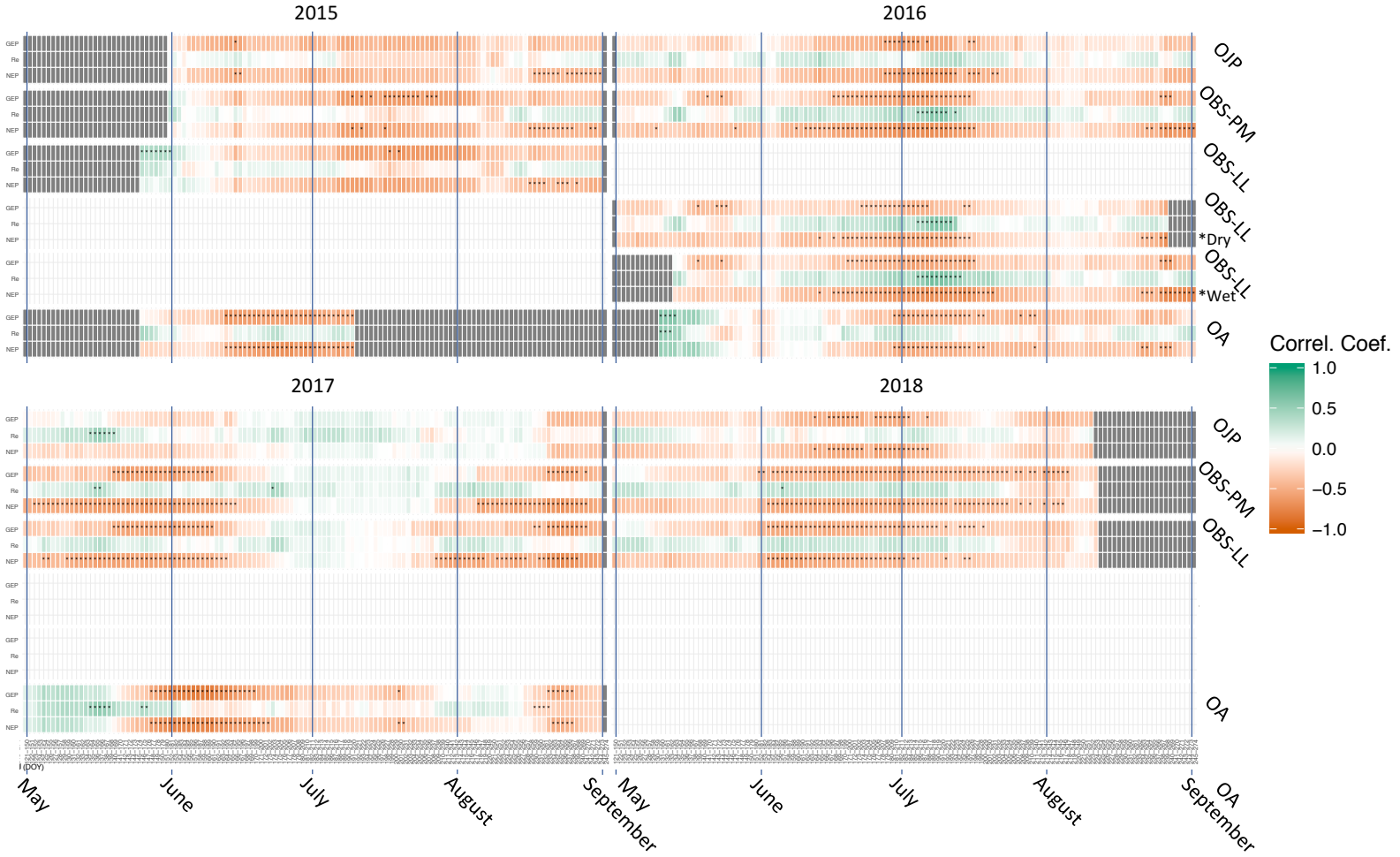

Figure 3.4: Moving window correlation functions of the relationship between daily resolved variations in stem radius and ecosystem C-flux (NEP, R_E, and GEP) within each of the four growing seasons during the observation period (2015 – 2018). Relationships were assessed over a 30-day moving window, jogged by 1-day, using bootstrapped Pearson's correlations (1000 iterations). The labels on the x-axis correspond with the start date of each 30-day interval. For example, intervals with start dates in May are found between the May and June x-axis labels. Significance at the 99% confidence level is flagged with *.

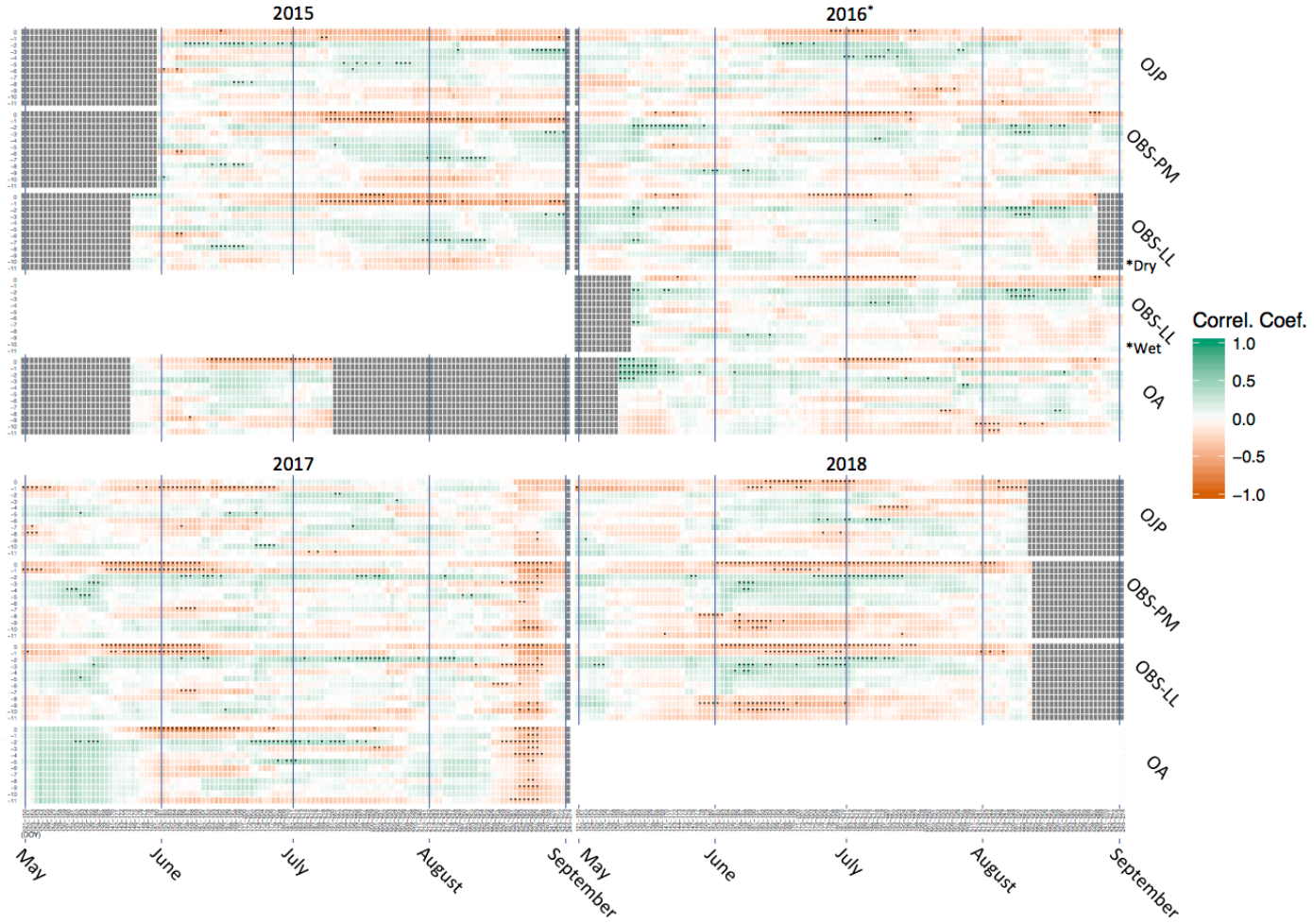

Figure 3.5: Moving window correlation functions assessing lag in the relationship between daily variations in stem radius and GEP, which is lagged from the stem radius data by 0 to 11-days (y-axis). As above, relationships were assessed over a 30-day moving window, jogged by 1-day, using bootstrapped Pearson's correlations. The labels on the x-axis correspond with the start date of each 30-day interval. Significance at the 99% confidence level is flagged with *.

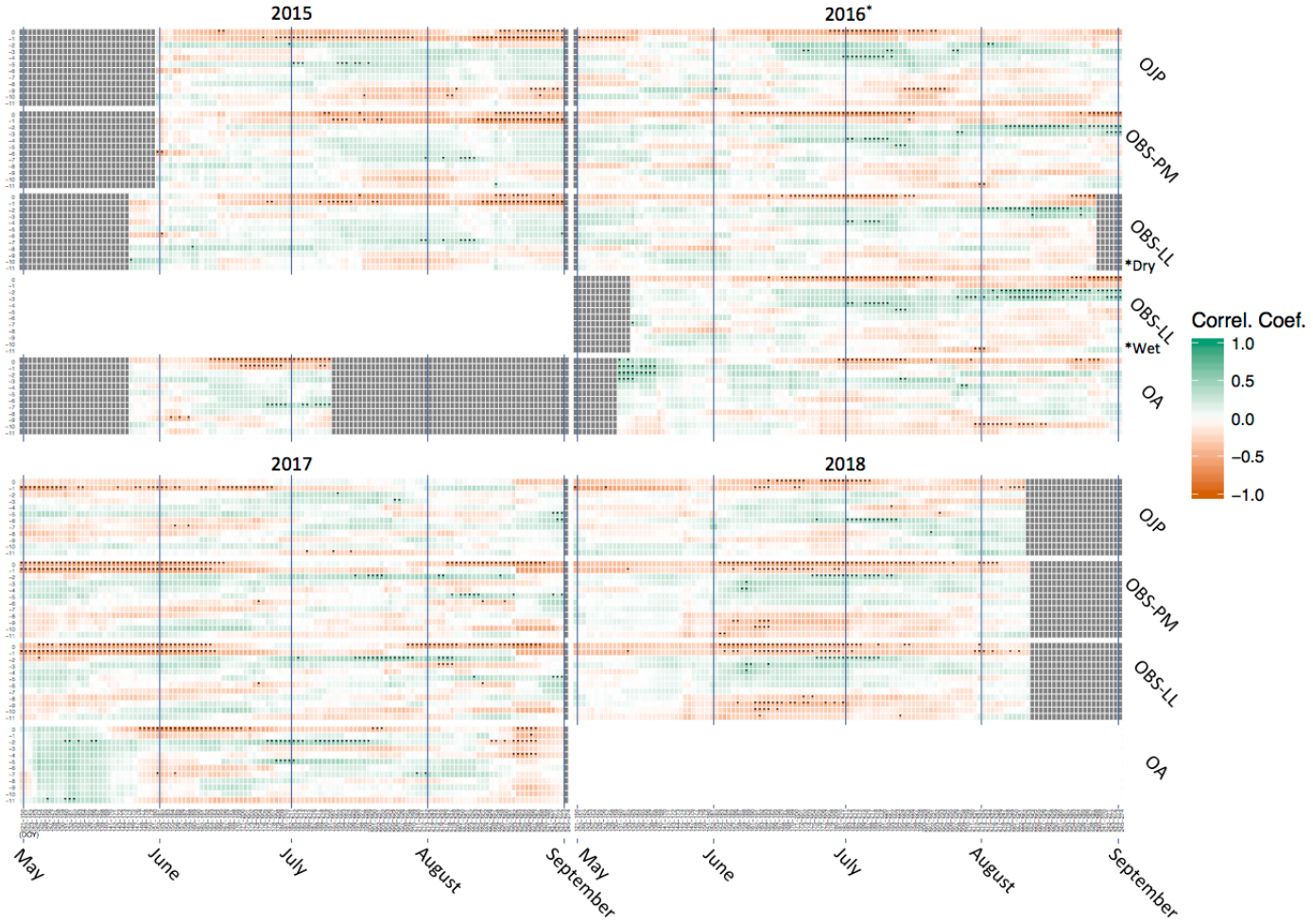

Figure 3.6: Moving window correlation functions assessing lag in the relationship between daily variations in stem radius and NEP, which is lagged from the stem radius data by 0 to 11-days (y-axis). As above, relationships were assessed over a 30-day moving window, jogged by 1-day, using bootstrapped Pearson's correlations. The labels on the x-axis correspond with the start date of each 30-day interval. Significance at the 99% confidence level is flagged with *

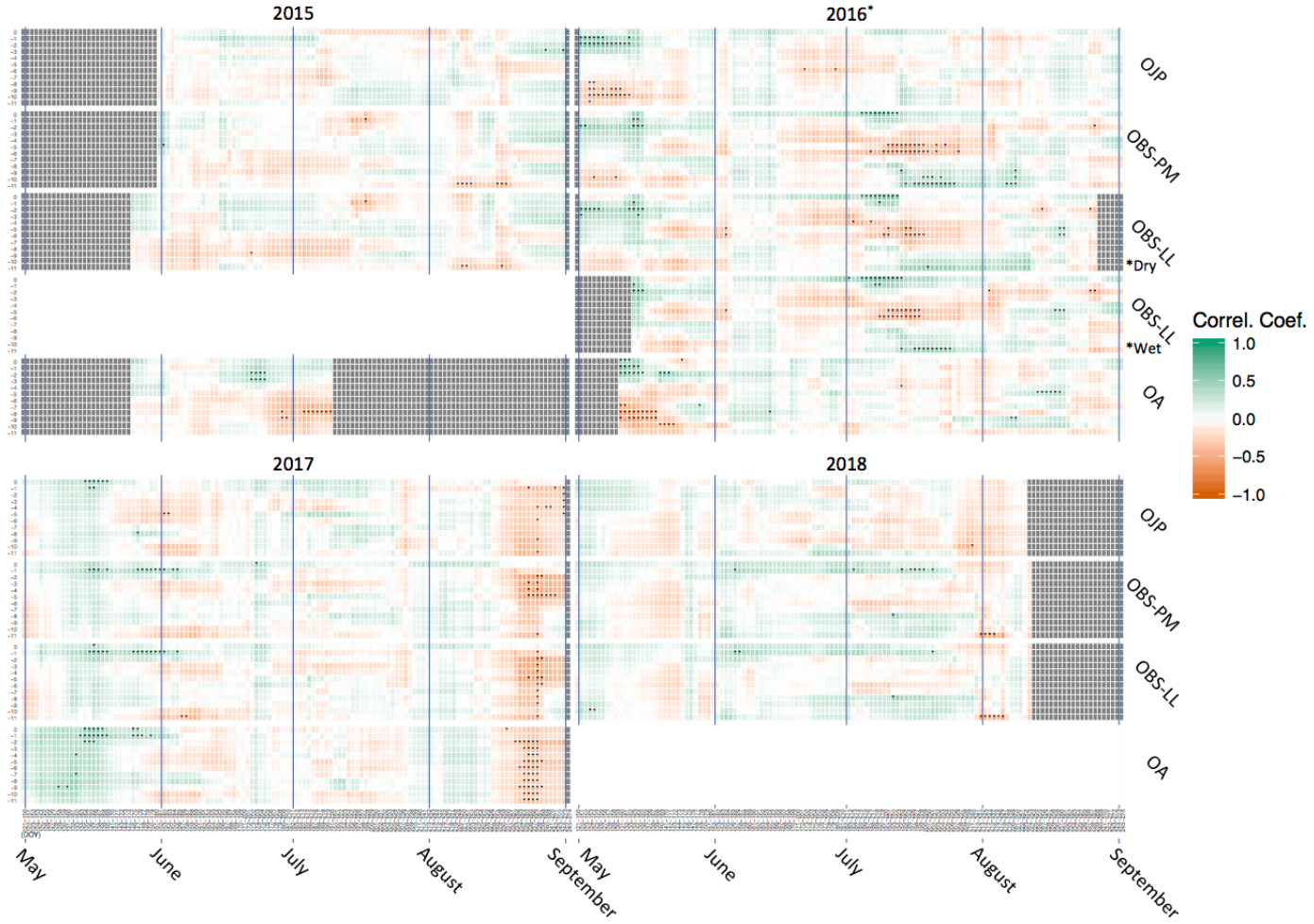

Figure 3.7: Moving window correlation functions assessing lag in the relationship between daily variations in stem radius and R_E, which is lagged from the stem radius data by 0 to 11-days (y-axis). As above, relationships were assessed over a 30-day moving window, jogged by 1-day, using bootstrapped Pearson's correlations. The labels on the x-axis correspond with the start date of each 30-day interval. Significance at the 99% confidence level is flagged with *.

CHAPTER 4

INSIGHTS FROM OVER TWENTY YEARS OF CARBON DYNAMICS IN BOREAL ASPEN AND JACK PINE STANDS

4.1 Abstract

This paper assesses the ecological mechanisms underlying trends in ecosystem production in the southern boreal forest. Eddy-covariance measurements of NEP and repeated biometric carbon (C) stock measurements were made over a 22-year period (1994 – 2016) at two mature (~100 year old) boreal forest stands in central Saskatchewan; Old Jack Pine (OJP), and Old Aspen (OA), two of the of the Boreal Ecosystem Research and Monitoring Sites (BERMS). There were several notable shifts in the distribution of carbon across the measured carbon pools at OJP and OA. The most notable fluxes at OJP occurred in response to an increase in tree mortality between 2010 and 2016, likely resulting from a vulnerability to high winds. The increase in tree mortality was accompanied by a decrease in tree level net primary production (NPP_{Tree}), from 90 ± 4 gC/m^2yr (1994 – 2004), and 89 ± 5 gC/m^2yr (2004 – 2008), to 66 ± 7 gC/m^2yr (2010 – 2016). However, during this same period net ecosystem production (NEP_{EC}) at OJP was maintained at a level near that of the 22-year average, 39 ± 11 gC/m^2yr (1994 – 2004), 38 ± 11 gC/m^2yr (2004 – 2008), and 42 ± 9 gC/m^2yr (2008 – 2016). At OA, the most significant recorded fluxes occurred during a wet subperiod (2004 – 2010), likely in response to moisture stress due to drought and/or subsequent flooding. Regardless of the increase in tree mortality and turbulent stock changes that occurred at OA during the wet subperiod, NPP_{Tree} was maintained at levels near 200 gC/m^2yr over the course of the observation period, 218 ± 12 gC/m^2yr (1994 – 2004), 199 ± 24 gC/m^2yr (2004 – 2010), and 228 ± 26 gC/m^2yr (2010 – 2016). There was however a notable decrease in NEP_{EC} during this same period at OA, 173 ± 27 gC/m^2yr (1994 – 2004), 89 ± 31 gC/m^2yr (2004 – 2010), and 145 ± 31 gC/m^2yr (2010 – 2016). Climate change will undoubtedly impact carbon dynamics in the boreal forest. We find evidence that aspen stands may react poorly to moisture stress, resulting in a redistribution of carbon and a notable decrease in annual NEP. We also find that wind may represent an important agent of change in mature jack pine stands. An increase in the incidence and intensity of extreme storms and high winds will likely lead to more frequent disturbance in a range of boreal forest stands.

4.2 Introduction

The boreal forest is a vital component of the global carbon cycle, as it represents the single largest reservoir of global terrestrial carbon (Sellers et al., 1995; Soja et al., 2007; Bradshaw and Warkentin 2015). Capable of storing just under twice as much carbon as tropical forests (Carlson et al., 2009), the circumpolar boreal forest currently contains an estimated 1041.5 ± 674.2 Pg of stored carbon (C) (Bradshaw and Warkentin 2015). While there is a high level of uncertainty associated with this value, even the most conservative of estimates (~300 Pg C) equates to approximately half of the carbon currently present in our atmosphere (Gower et al., 2001). Over the short term, the boreal forest has long been regarded as an overall sink for carbon, although there is evidence suggesting that the strength of that sink is decreasing significantly in response to rapid climate change, with some regions approaching carbon neutrality, and others expected to become an overall source of carbon in the foreseeable future (Kurz et al., 2008; Peng et al., 2011; Bradshaw and Warkentin 2015). In a recent spatial analysis of carbon flux across the circumpolar boreal zone, Canada yielded the lowest mean annual carbon flux overall, with a value just above zero. Temporally, there was an observed declining trend in annual carbon uptake since 1980 and projected persistent negative annual fluxes in Canada by 2050. It is also likely that some regions (e.g. western Canada) are already emitting more carbon than they are storing in response to changes in climate and the disturbance regime (Bradshaw and Warkentin 2015).

The boreal forest is particularly vulnerable to climate change, in part because of its location. The impacts of climate change are expected to be particularly severe at northern high latitudes. The most significant land surface warming is expected above 45° – 50° north latitude, where mean annual land surface temperature is likely to increase by upwards of 2°C by the last two decades of the century (2081-2100) (IPCC, 2013), regardless of steps taken to curtail this outcome (Huntingford and Mercado, 2016). In fact, much of northern Canada has already experienced an increase in annual average temperature surpassing 2°C since 1948 (Bush and Lemmen, 2019).

Modeling change in the distribution of moisture in response to climate change is quite difficult compared with projecting departures in global land surface temperature (Cook et al.,

2014). The most reliable models project an overall increase in precipitation in already moist environments (mid- to high-latitudes in North America), and a further decline in precipitation in dry environments (the subtropics) (Cook et al., 2014). However, an increase in precipitation does not necessarily equate to an increase in available moisture on the ground. Atmospheric warming raises the vapor pressure deficit by increasing the amount of moisture the air can hold, leading to an overall increase in evaporative demand (Cook et al., 2014). Both precipitation and potential evapotranspiration (PET) are expected to increase across much of North America (Cook et al., 2014; Jeong et al., 2014). One of the most marked increases in PET globally, is expected in the Central Plains of North America (105° – 90°W, 32° – 50°N) (Cook et al., 2014). In many instances, projected increases in precipitation will be insufficient to offset the increase in evapotranspiration (Wang et al., 2014). In Canada, over the last six decades (since 1951), there was a marked drying trend across much of central and western Canada, while northeastern Canada appeared to be trending towards wetter conditions (Wang et al., 2014). These historical trends are expected to carry forward over the next several decades (Wang et al., 2014). Overall, the frequency and severity of drought is expected to further increase in the boreal forests of western and central Canada (PARC Summary 2008; Jeong et al., 2014; Wang et al., 2014; Bush and Lemmen, 2019).

In response to an increase in temperature and moisture stress, tree mortality in western Canada has occured at 2.6 times the rate observed in eastern Canada (Peng et al., 2011). However, it has been shown that individual stands can have contrasting or even conflicting responses to climatic change (Goulden et al., 1998; Black et al., 2000). Trembling aspen, for example, is identified as being particularly sensitive to moisture stress (Kljun, 2007; Chen et al., 2017). There was an observed collapse in aspen growth over a large area of the aspen parkland region over several years following drought conditions in 2001 – 2002. During this time, several large patches of trembling aspen underwent widespread tree mortality, sometimes resembling the devastating effects of fire (Michaelian et al., 2011). Overall, forest response to drought depends on the distribution of moisture across the landscape, topography, soil characteristics, and stand composition (Kljun et al., 2007). Stand age may also play a role in determining how a forest responds to changing conditions. Increasing temperatures had an overall negative effect of on growth rates and mortality in all forest stands regardless of stand age and type; however, older forests were most susceptible to drying induced reductions in tree growth (Chen et al., 2016).

Large trees have greater maintenance costs and may therefore be disproportionally impacted by temperature and moisture stress (Chen et al., 2016). Understanding the impact of climate, disturbance, and stand ageing, in contrasting boreal forest stands, brings us closer to accurately anticipating the net effect of climate change on forest carbon dynamics in the Canadian boreal forest (Goulden et al., 1997; Chen and Luo 2015).

Eddy covariance (EC) represents the most common technique for measuring forest carbon (C) flux at the stand or ecosystem level (Baldocchi et al., 2003). Confidence in the EC method has increased over time as practitioners continue to produce reliable values for ecosystem production that hold up against independent values collected via other means (Baldocchi et al., 2003), and as techniques and equipment are refined (Aubinet et al., 2012). Bias in these data is further minimized when the method is deployed over several years, in which case there is a trend towards further convergence between EC derived values of production and those collected independently (Baldocchi et al., 2003). While the EC flux towers may very well provide the most reliable and accurate representation of ecosystem level C flux, the EC method cannot offer a breakdown of the component fluxes, beyond its main constituents of gross primary production (GPP), and total ecosystem respiration (R_E). To offer a further breakdown of the component fluxes, EC derived data are often supplemented with repeated biometric measures of in-situ carbon, stored in individual ecosystem components (Gower et al., 2001). This improves our capacity to interpret trends in ecosystem production and carbon allocation, which is needed if we are to formulate a mechanistic understanding of how a given ecosystem will respond to changing biotic and abiotic factors over the long term.

The goal of this paper is to better understand the ecological mechanisms responsible for ecosystem level change in forest carbon dynamics within two representative boreal forest stands in the southern boreal forests of western Canada. We will leverage a two-decade long record of forest C stocks and fluxes to examine the impacts of climate, natural disturbance, and stand ageing on the distribution of carbon within our study sites.

4.3 Study Sites

This study was conducted at three of the Boreal Ecosystem Research and Monitoring Sites (BERMS), located near the southern edge of the boreal forest in the Boreal Plains Ecozone

of central Saskatchewan (Figure 1.1). Site characteristics are given in Table 1.1. The climate of the study area is characterized by short, warm, dry summers and long, cold winters. Mean annual temperature In Prince Albert (PA), Saskatchewan, where the nearest and most complete long term record of climate is recorded, is currently 1.7°C (1989 – 2018). This represents a 1.9°C increase in annual average temperature over the last century, when compared to the 1890 – 1919 reference period (-0.2°C). Annual average precipitation in PA is 517 mm (1983 – 2012), a 60 mm increase since the 1890 – 1919 reference period (457 mm) (Figures D.1 and D.2; Appendix D).

The Old Jack Pine (OJP) site, located northeast of Candle Lake, Saskatchewan, is an even-aged stand of jack pine, naturally established post-fire in 1914 (Barr et al., 2012). The understory is composed of clumps of green alder (*Alnus crispa*), and the dominant ground cover includes some bearberry (*Arctostaphylos uva-ursi*), and a nearly continuous cover of reindeer lichen (*Cladina mitis*). The soil is a well-drained Orthic Eutric Brunisol (loamy sand). Water table depth is approximately ~6-7 m below the ground surface, and often decoupled from the root zone.

The BERMS Old Aspen (OA) site in Prince Albert National Park, is an even-aged stand of trembling aspen, naturally established after a forest fire in 1919 (Barr et al., 2012). The understory is mainly hazelnut (*Corylus cornuta*) with a few other shrubs. The topography is relatively level, with uniform fetch of at least 3 km in each direction from the tower. The soil is an Orthic Gray Luvisol (loam to clay loam). Water table may be as deep as 4 m below the soil surface at this site, at times impinging on the root zone.

4.4 Methods

4.4.1 Biometric C Stock Measurements

Repeated C stock measurements were made in 1994, 2004, 2010, and 2016 at OA, and 1994, 2004, 2008/2009, and 2016 at OJP. In 1994, Gower et al. (1997) established replicate 25 x 25 m allometry plots, four at OA and eight at OJP, immediately outside the footprint of the flux towers, in forest similar to that in the flux footprint. At the same time, Fournier et al. (1997) established a single 50 x 60 m plot at each site, also immediately outside the flux footprint but in a different part of the stand.

Each overstory tree within the plots was measured and permanently tagged in 1994. The Fournier plots at both sites along with three of four Gower plots at OA and four of eight Gower plots at OJP were re-measured in July 2004, July 2008 (OJP), and July 2010 (OA), and September 2016. The Fournier plot was subdivided into 25 x 30 m quadrants to create four plots of similar sizes to the Gower plots, producing a total of seven plots at OA and eight plots at OJP. Tree measurements included species, DBH, and status (live, standing dead, or broken for each tree that was standing, as well as fallen for snags that could be found). Tree mortality at both sites was determined by comparing the status of each tree among remeasurements. Trees or snags that could not be found were assumed to have fallen.

The living biomass (B), and standing dead (SD) necromass (including whole dead and broken trees) of the dominant tree species was determined from allometric equations based on stem diameter at breast height (DBH, 1.37 m). Allometric equations provided biomass estimates for coarse root, stem, branch, and foliage for live trees. In the case of broken stems, the height at which the tree broke was recorded, and taper was accounted for while estimating biomass in the remaining stem. We adopted the standard, Canada-wide DBH-based equations developed by Lambert et al. (2005) and Ung et al. (2008), which spanned the observed DBH ranges. Wood and foliage biomass were multiplied by 0.50 to estimate C content (Ajtay, 1977; Matthews, 1993).

Understory and fine root biomass were measured in 1994 and 2004, but were not re-measured in 2008/2010 or 2016. Total understory biomass was determined from the dry biomass of all components in three 1 x 1 m subplots randomly located in each of the replicate Gower plots. At the OA site, all vegetation in the plot was clipped and separated into annual herbs, woody tissue and new foliage. At OJP, where the understory consists of a few clumps of green alder and a nearly continuous ground cover of reindeer lichen, it was not feasible to separate the lichen from the forest floor, so lichen was pooled together with the forest floor following the protocol developed by Howard et al. (2004).

Coarse-root biomass was determined from DBH-based allometric equations developed by Ruark and Bockheim (1987) at OA and Steele et al. (1997, unpublished data) at OJP. Coarse root C content was assumed to be 50% (Kalyn & Van Rees, 2006). Fine root biomass in 1994 was measured by Steele at al. (1997), and again in 2004 by Kalyn & Van Rees (2006). The latter estimated fine root (< 2 mm) biomass from minirhizotron data using a plane intersect method

developed by Bernier and Robitaille (2004). Organic C content of fine roots at OA and OJP was 46% and 39 %, respectively (Kalyn and Van Rees, 2006).

4.4.2 Downed Woody Debris

Downed woody debris (DWD), defined as downed non-self-supporting woody material in various stages of decomposition, located above the soil and including sound and rotting logs and uprooted stumps, was measured using the line-intersect method (Halliwell and Apps, 1997). The DWD volume (V) per hectare was calculated as:

$$V = \frac{\pi}{2L} \sum_{i=1}^{n} A_i \qquad \text{(Eq. 3.1)}$$

where L is the length of the sample line and A_i is the cross-sectional area of the i^{th} piece at the intersection. Debris items were assigned to five diameter classes (<0.5, 0.5-<1.0, 1.0-<3.0, 3.0-<5.0 and ≥5.0 cm) using a go-no-go-gauge with notches at 0.5, 1, 3 and 5 cm. For items ≥5.0 cm, diameter was measured using either a diameter caliper or a standard diameter tape. Items were identified by species, if possible, and visually assessed for the degree of decomposition (sound, sloughing, punky or rotten). To calculate the detritus mass in diameter classes <5.0 cm using Equation 3.1, a mean diameter and specific gravity was assigned to each class (Halliwell and Apps, 1997). For items ≥5.0 cm, values of specific gravity were estimated as a function of the decomposition state. Halliwell and Apps (1997) assumed that rotten items have a specific gravity of 0.1 less than sound items, while sloughing and punky items were assigned specific gravities interpolated at equal intervals between sound and rotten values. DWD was assumed to be 50% C.

In 1994, DWD was measured in two plots at both sites by Halliwell and Apps (1997). Unfortunately, the plots were not marked and could not be found, so the DWD measurement was relocated to the Gower and Fournier allometric tree plots in 2004 and 2008/2010. The inconsistency in plot location adds uncertainty to the measured DWD change between 1994 and 2004. DWD measurements taken in the Fournier plots were weighted accordingly (2x) due to the difference in size between these and the Gower plots.

4.4.3 Forest Floor and Mineral Soil

Forest floor (FF) and mineral soil C stocks were measured in the Gower plots in 1994 and 2004, but the plots were not re-measured in 2008/2010 or 2016. The 1994 measurements (Gower et al. 1997) were based on soil samples from the replicate plots but only average values for each site were available to this study. In 2004, the soil C stocks were re-measured in the three plots at OA and four plots at OJP. To estimate uncertainty of the C stock change, we assumed that the variability among soil plots in 1994 was the same as measured in 2004. Three random locations within each plot were sampled. Total soil C content was calculated for each horizon from horizon depth, bulk density, and percent carbon data. At each of the three locations, four soil samples were collected from each horizon, averaged within horizon, then summed to a depth of 70 cm below the ground surface. Percent total and organic C data were obtained through dry combustion of each sample (LECO Carbon Determinator CR-12 analyzer). Total soil C content was calculated by taking the C content of the soil profiles and averaging among the three replicate plots.

The sampling of the FF C stocks required site-specific modifications to the sampling protocol at both sites. At OJP, it was not feasible to separate the lichen, bryophytes, and fine woody debris from the LFH horizon, therefore these components were pooled as FF. Each sample was air dried with all live vegetation and live coarse roots removed, and ground to pass through a 0.2 mm sieve. A sub-sample was oven-dried at 110 ºC to a constant mass and weighed to the nearest 0.1 g. The total FF C stock estimate was later divided back into its various components by assuming lichen, bryophytes and fine woody debris accounted for 41% of the FF C content as reported by Vogel et al. (1998) for OJP in 1994. At OA, the clearest visual division between the forest floor and mineral soil occurred at the interface between the Ah and Ae horizons, therefore the FF C stock measurement included both Ah and LFH horizons.

4.4.4 Total Ecosystem C-Stocks and Rates of Change

Ecosystem component C-stocks were calculated for each plot and averaged across plots for each measurement period. Each value is recorded with a value of uncertainty (±), which is the standard error of the mean among replicate plots.

C stock rates of change were computed over four periods: 1994 – 2004, 2004 – 2008/2010, 2008/2010 – 2016, and 1994 – 2016. We limited this analysis to three primary C stock components; tree biomass (ΔB), SD necromass (ΔSD), and DWD (ΔDWD) - based on these components' contributions to total ecosystem carbon and our confidence in the quality of these measurements. Of the three components used to estimate the change in total ecosystem carbon (ΔC), the tree biomass and SD necromass were measured most consistently, producing the highest subjective confidence in rate of change estimates for these components. The estimates of ΔDWD were more uncertain, due to inconsistencies in DWD transect location between the first and subsequent measurements. We will thus exercise caution in interpreting changes in DWD stocks. Rates of change in C stocks between measurement periods were also calculated individually for each plot and then averaged across the site. Each value is therefore, once again, recorded along with a value of uncertainty (±), representative of the standard error of the mean among replicate plots. In the case of DWD, because transect placement was inconsistent, rates of change were calculated from stand level averages. During periods where there was insufficient overlap between sampling locations, uncertainty (±) in ΔDWD is estimated based on the average.

4.4.5 C Fluxes

In addition to estimating C stocks and their rates of change, the allometric tree plots allowed for estimation of the living trees contribution to net primary production (NPP_{Tree}), and inter-stock C fluxes from living trees to SD, living trees to DWD and from SD to DWD necromass. For trees that died during the measurement period, their respective contribution to NPP_{Tree} and C flux to SD and ground pools was assessed in one of three ways. Firstly, if an updated DBH was recorded at the end of the measurement period for a given tree, and it was unchanged or smaller than the original DBH, we assumed that this tree died at the beginning of the measurement period. Secondly, if an updated DBH was recorded at the end of the measurement period for a given tree, and it was larger than the original DBH, this updated DBH measurement was used to assess its resulting contribution to each pool. Finally, if no updated DBH was available, we assumed that the tree died halfway through the period and grew at the same rate as surviving trees of a similar size.

4.4.6 Flux-Tower Measurements

Eddy-covariance measurements of the CO_2 flux density were made at 39 m (OA) and 29 m (OJP) above the ground from twin scaffold towers. At OA, fluxes were measured from February to September 1994 and continuously since March 1996. At OJP, fluxes were measured from May to Sept 1994 and continuously since September 1999. Details of the eddy-covariance systems and data processing used at OA throughout and at OJP until 2012 are given in Griffis et al. (2003). In October 2012, the LI-7000 closed-path infrared gas analyzer at OJP was replaced with model LI-7200 and the 30-min fluxes were computed using the EddyPro software (LI-COR Inc, Lincoln, NE, USA).

The CO_2 flux density as measured by eddy-covariance plus storage (Barr et al. 2006) is a direct measurement of net ecosystem exchange NEE, the net exchange of CO_2 between an ecosystem and the atmosphere. NEE is positive for an atmospheric C sink. In situations where the loss of dissolved organic C via groundwater flow is negligible (Moore, 2003), a reasonable assumption at these sites, NEE provides a direct measure of net ecosystem production NEP (i.e., NEP = - NEE), which is positive for an ecosystem C sink. In turn, NEP results as the difference between C gains by gross ecosystem photosynthesis (GEP) and C losses by total ecosystem respiration RE, i.e., NEP = GEP – RE.

Gaps in the NEE time series were filled using a standard procedure. NEE values during calm periods at night were rejected using a u_*-threshold filter, with u_*-threshold values of 0.37 m s^{-1} at OA and 0.25 m s^{-1} at OJP (Barr et al. 2013). The procedures to fill short (less than one month) gaps in NEE and to estimate GEP and R_E are described in Barr et al. (2004). Both sites had one long gap in NEE, from October 1994 to March 1996 at OA and Oct 1994 to July 1999 at OJP. The long gaps were filled using the ecosys model as configured for the jack pine site in Grant et al. (2007). The model was run for 1994 to 2004, then the simulated and measured fluxes were compared using least-squares linear regression based on the time of year, and gaps were filled with adjustments for model-measurement differences.

4.4.7 Calculation of Annual NEP

To provide the most representative and comparable measure of annual NEP, the 12-month period over which this metric is calculated is tailored to the GEP curve, which becomes

positive in April at both sites, signaling the onset of photosynthesis. Annual NEP is therefore summed from monthly data between April – March, representing one growing season and a subsequent period of dormancy. Average annual NEP was calculated for each measurement period and is presented along with a standard error (±), in this case representing interannual variability during the measurement period. In all other cases, uncertainty is based on the standard error of the mean among replicate plots.

4.5 Results

4.5.1 Precipitation and Soil Water

The 1994-2016 study period had normal, dry, and wet subperiods (Figure 4.1). Compared with mean annual precipitation and standard deviation (1980 – 2016) from two nearby climate stations (468 ± 81 and 442 ± 88 mm y^{-1} at Waskesiu Lake (53.92, -106.08) and Prince Albert A (53.22, -105.67) respectively, precipitation at the two sites was: near-normal, within one standard deviation between 1994 – 2000 (471 mm y^{-1} at OA and 436 mm y^{-1} at OJP); below-normal, well below one standard deviation, between 2001 – 2003 (257 mm y^{-1} at OA and 324 mm y^{-1} at OJP); above-normal, above one standard deviation between 2004 – 2010 (570 mm y^{-1} at OA and 568 mm y^{-1} at OJP); and again normal, within one standard deviation between 2011 – 2016 (504 mm y^{-1} at OA and 548 mm y^{-1} at OJP). There are therefore, normal and dry subperiods during the first measurement interval (‘94-04), a wet subperiod which corresponds to the second measurement interval (‘04-10), and another normal subperiod corresponding with the final measurement interval (’10-16).

The dry and wet subperiods were associated with changes in the soil-water status at both sites, however, the sites differed in two respects. First, their root-zone VWC varied on different scales (Figure 4.2). The OJP site, with its sandy soil and low water-holding capacity, had high and low VWC extremes in almost every year, whereas the OA site, with its higher water-holding capacity and shallower water table, had longer-term fluctuations in VWC including a prolonged period of extreme low VWC from 2001 – 2003 and a sustained high VWC extreme from 2005 – 2007. Second, the long-term fluctuations in water table depth affected the two sites differently. The water table at both sites fell during the dry subperiod (2001 – 2003) and rose during the wet subperiod (2004 – 2010). However, the deeper water table at OJP, ~6-7 m below the ground

surface, was decoupled from the root zone, whereas the shallower water table at OA at times impinged on the root zone, with root-zone soil water depletion coincident with the falling water table in 2001 – 2003, and high VWC and extended periods of flooding in the low-lying areas of the stand associated with the high water-table following 2004. These differences are ecologically significant: the OA stand underwent prolonged periods of water stress (drought then flooding), whereas the OJP stand experienced intermittent periods of drought stress each summer but never flooded. We will see in sections below that this difference had a profound effect on tree mortality and the component C stock changes.

4.5.2 Stand Density and Mortality

There was an increased rate of tree mortality that occurred at both study sites during different subperiods. Living stand density at OA was 964 ± 41 stems/ha in 1994, and decreased to 473 ± 47 by 2016 (Figure 4.3). The rate of tree mortality was 2.4% and 2.3% of living stems per year between 1994 – 2004 and 2010 – 2016 respectively. The rate was almost doubled to 4.3% between 2004 – 2010, during the wet subperiod that followed the 2001 – 2003 drought. Stand density at the OJP site was greater than at OA, starting at 1315 ± 118 living stems/ha in 1994, and decreasing to 887 ± 99 stems/ha by 2016 (Figure 4.3). The average annual rate of tree mortality at OJP was lesser than at OA, ranging from 1.3% – 2.1% per year between measurement periods. While the mortality rate remained relatively constant during the first 14 years of observation, decreasing only slightly (from 1.5%/yr to 1.3%/yr) between the 1994 – 2004 and 2004 – 2008 periods, it increased to 2.1%/yr during the 2008 – 2016 period.

4.5.3 C Stocks

At OA, living tree biomass C stocks were about twice as large per unit area compared with OJP, and they were remarkably constant over time, ranging from 94 ± 10 tC/ha to 100 ± 6 tC/ha (Table 4.1). The largest percent-change between two consecutive stock measurements is -6.5% (approximately -1.1% per year), occurring during the wet subperiod (2004 – 2010), resulting in a reported loss of 108 ± 73 gC/m^2 per year from living biomass C stocks (Table 4.2). Overall, additions of carbon to the living biomass from tree growth were largely counterbalanced by the flux of carbon exiting the pool via tree mortality, as demonstrated by the net-zero (5 ± 35

gC/m^2yr) average annual rate of change over the entire 22-year observation period (1994 – 2016) (Table 4.2).

Over the first ten years of observation (1994 – 2004) at OJP, *in-situ* C stocks held in the biomass of live trees increased at an average rate of 1.26% per year (12.6% total), from 41.9 ± 2.2 tC/ha to 47.2 ± 2.3 tC/ha (Table 4.1). The subsequent four-year period (2004 – 2008) saw a similar rate of increase of 1.1% per year (4.4% total), from 47.2 ± 2.3 tC/ha to 49.3 ± 2.5 tC/ha. This relatively stable increase resulted in additions of approximately 50 gC/m^2 per year to the biomass of living trees between 1994 – 2008, followed by a period of stasis. In the subsequent eight-year period (2008 – 2016), the rate of biomass gain by tree growth was in relative equilibrium with biomass loss by tree mortality, resulting in an average annual rate of biomass change near zero (-5 ± 10 gC/m^2 per year) (Table 4.2).

In terms of necromass, SD C stocks were also consistently greater at OA compared with OJP. The largest differences between the two sites were observed in 2004 and 2010, when OA SD C stocks were largest. Over the 22-year observation period, SD C stocks at OA increased from 9.3 ± 1.5 tC/ha in 1994, to 12.3 ± 1.6 tC/ha and 13.4 ± 3.0 tC/ha in 2004 and 2010 respectively, before dropping to 9.3 ± 2.5 tC/ha in 2016 (Table 4.1). SD C Stocks were far more consistent at OJP, with values of 6.2 ± 0.8 tC/ha and 6.2 ± 0.9 tC/ha in 1994 and 2004 respectively, followed by a slight decrease to 4.7 ± 0.7 tC/ha in 2008, before attaining its highest value of 6.9 ± 1.1 tC/ha by 2016 (Table 4.1). While both sites saw some fluctuation in SD C stocks, with higher than usual values in 2004 and 2010 at OA, and lower than usual values in 2008 at OJP, both sites returned to a relative equilibrium by 2016. This resulted in average annual rates of change of 0 ± 13 gC/m^2yr and 3 ± 5 gC/m^2yr over the 22-year observation period, at OA and OJP respectively (Table 4.2). Additions of carbon to SD necromass from tree mortality are therefore largely counterbalanced by losses to ground.

4.5.4 Net Ecosystem and Primary Production

NPP_{Tree} at OA was more than twice as high as at OJP, and regardless of the increase in tree mortality and stock changes, NPP_{Tree} remained remarkably constant throughout the 22-year period. NPP_{Tree} was 218 ± 12 gC/m^2yr, 199 ± 24 gC/m^2yr, and 228 ± 26 gC/m^2yr between 1994 –

2004, 2004 – 2010, and 2010 – 2016 respectively (Figure 4.4). At OJP, NPP_{Tree} was constant during the first two measurement periods, with values of 90 ± 4 gC/m^2yr, and 89 ± 5 gC/m^2yr between 1994 – 2004, and 2004 – 2008 respectively, then dropped to 66 ± 7 gC/m^2 per year in the subsequent period (2008 – 2016) (Figure 4.5).

Compared with NPP_{Tree}, NEP_{EC} demonstrated more variability between measurement periods at OA, with more marked depressed productivity between 2004 – 2010, co-occurring with the increase in tree mortality and SD C Stocks during the wet subperiod. Average annual NEP_{EC} decreased 48% from 173 ± 27 gC/m^2yr between 1994 – 2004, to 89 ± 31 gC/m^2yr between 2004 – 2010, followed by a recovery to 145 ± 31 gC/m^2yr between 2010 – 2016 (Figure 4.4). Ecosystem production at OJP was not impacted in the same way during the wet subperiod. Average annual NEP_{EC} at OJP remained rather constant over the course of the 22-year observation period, with approximately 39 ± 11 gC/m^2yr accumulating in the ecosystem between 1994 – 2004, 38 ± 11 gC/m^2yr between 2004 – 2008, and 42 ± 9 gC/m^2yr between 2008 – 2016 (Figure 4.5). Note that there is a considerable amount of interannual variability in NEP_{EC} at both sites, as expressed by the standard error of the mean annual NEP_{EC} for each measurement period.

4.5.5 Inter-Stock C Fluxes

During the period of increased mortality at OA (the wet subperiod, 2004 – 2010), there was a large flux of 191 ± 50 gC/m^2 per year from the living to the SD pool, and an even more substantial flux of 243 ± 25 gC/m^2 per year from the living and SD pools to ground (Table 4.2). This influx of woody debris was reflected in an independent measure of DWD, which was 250 gC/m^2 per year over the same six-years (Table 4.2). The above average rate of transfer from the living to the SD pool is mainly a result of trees going from living to whole dead, as indicated by a substantial increase in the rate of transfer between these two pools (Figure 4.4). However, there was also an increase in the rate of carbon transferred from the living to the broken pool compared with the preceding period (Figure 4.4). As for the marked flux of carbon to ground during this period, there were substantial influxes from living (109 ± 16 gC/m^2 yr), whole dead (95 ± 20 gC/m^2yr), and broken trees (38 ± 12 gC/m^2 yr). In fact, more carbon is transferred from the living pool straight to the ground in each subsequent period between measurements,

increasing from 56 ± 12 gC/m^{2}yr, to 109 ± 16 gC/m^{2}yr, and finally to 132 ± 29 gC/m^{2}yr (Figure 4.4).

During the last measurement period (2010 and 2016), there was very little carbon (34 ± 12 gC/m^{2}yr) transferred from the living pool to the SD pool (Table 4.2). However, as previously mentioned, there were huge additions from the living pool straight to ground (132 ± 29 gC/m^{2}yr). After accounting for further additions to ground from the dead pool (79 ± 25 gC/m^{2}yr), and the broken pool (11 ± 4 gC/m^{2}yr) (Figure 4.4), total additions to ground amounted to 222 ± 39 gC/m^{2}yr, which is similar in magnitude to that from the previous measurement period (Table 4.2). In this instance, the independent measure of DWD was far less effective at capturing the maintained high-level rate of transfer to ground. According to the DWD measurements, there was a negative rate of transfer of -78 gC/m^{2}yr between 2010 – 2016, representing a marked decrease in woody biomass present on the forest floor during this period. There was also an above average internal flux of carbon in the SD pool as a substantial amount of whole dead trees broke during this period, transferring 62 ± 22 gC/m^{2}yr from the whole dead to the broken pool, representing a near a four-fold increase in carbon flux between these two pools compared with the preceding periods (Figure 4.4). This however has little consequence on the overall distribution of carbon in the ecosystem since both pools are categorized as SD.

At OJP, the highest mortality rates were recorded during the 2008 – 2016 period. In response, the annual flux of carbon from biomass to necromass (from the living pool to SD and ground) also increased, from 36 ± 4 gC/m^{2}yr and 38 ± 8 gC/m^{2}yr during the 1994 – 2004 and 2004 – 2008 periods respectively, to 67 ± 11 gC/m^{2}yr during 2008 – 2016 (Table 4.2). During this same period, there was no notable increase in the rate of carbon transfer to the dead pool resulting from live trees remaining whole and standing as they die. Rather, this enhanced flux is a result of living trees being broken or felled entirely, as indicated by a marked increase in the amount of living biomass being transferred from the living pool to the broken pool in the form of stumps or taller broken stems (12 ± 3 gC/m^{2}yr), as well as from the living pool straight to ground in the form of broken tree tops and whole felled trees (17 ± 4 gC/m^{2}yr) (Figure 4.5). There was also a considerable increase in the rate of transfer from the dead pool to the broken pool during this period (14 ± 5 gC/m^{2}yr) (Figure 4.5).

The recorded decline in SD C stocks between 2004 and 2008 at OJP coincided with a doubling of the average flux from the living and SD pools to ground, from 30 ± 3 gC/m^{2}yr between 1994 – 2004 to 61 ± 12 gC/m^{2}yr between 2004 – 2008 (Table 4.2). This is almost entirely due to a significant transfer of carbon from whole dead trees to ground (55 ± 12 gC/m^{2}yr) (Figure 4.5). However, this increase in woody biomass on the ground was once again not reflected in an independent measure of DWD. Additions to DWD remained remarkably constant between measurement periods, ranging from 13.0 gC/m^{2}yr – 14.4 gC/m^{2}yr (Table 4.2).

4.6 Discussion

4.6.1 Moisture

Evidence suggests that variability in the moisture regime over the 22-year observation period may have played a significant role in driving the most notable stock changes at OA. There was an increase in the mortality rate of aspen during the wet subperiod (2004 – 2010), accompanied by a marked decline in living C stocks, with substantial variability between sample plots (-108 ± 73 gC/m^2). This is likely indicative of a spatially heterogeneous response of aspen to moisture stress associated with drought and/or subsequent flooding. The flux of carbon from the living to the dead pool (including SD and ground) was approximately 85% higher between 2004 – 2010 compared with the preceding period (1994 – 2004) (Table 4.2), and this considerable transfer of carbon from biomass to necromass did not occur uniformly across the landscape. One of the seven plots accounted for 39.6% of the measured flux from the living to the dead pool. At OA, which is not as well drained as OJP, there was water pooling in low lying areas across the landscape. It is therefore possible that the plot which disproportionally contributed to the elevated mortality rate during this period was situated in an area with standing water. Alternatively, this plot could have been disproportionally impacted by the 2001 – 2003 drought. Michaelian et al., (2011) show that drought can have prolonged impacts on tree mortality in western Canada. The observed increase in mortality during the wet subperiod may therefore be a legacy effect of recent drought, or the result of some combination of drought and subsequent flooding contributing to overall moisture stress.

While the mortality rate and the flux of carbon from the living to the dead pool fell back to pre-2004 levels following the wet subperiod at OA, the transfer of carbon to ground remained

high between 2010 and 2016 (Figure 4.4). Some of this maintained high flux can be attributed to an enhancement of the SD carbon pool during the wet subperiod, some of which would inevitably be transferred to ground in later years. However, the most substantial flux of carbon to ground was from the living pool. During this period (2010 – 2016), a single plot accounted for 31.5% of the measured carbon flux from the living pool to ground. It is unclear as to why the living trees in this plot were more susceptible to being felled or broken, and whether this was the result of a different type of disturbance, such as wind. Spatial heterogeneity in carbon flux between pools resulted in high values for standard error associated with several of the average annual fluxes recorded at OA. A larger number of plots may have helped to achieve a more accurate representation of the average annual carbon flux between pools at this site.

4.6.2 Wind

In a study of the impact of windthrow on tree mortality in southern boreal forest stands, the most vulnerable were identified as even-aged, mature stands (~90 years), of early successional species (Rich et al., 2007), an apt description for both of the study sites. Furthermore, of the nine tree-species studied, jack pine and aspen were identified as being "most susceptible to windthrow", with the 1st and 3rd highest mortality rates following wind disturbance, respectively (Rich et al., 2007). This characteristic vulnerability to wind could significantly impact the distribution of carbon across the landscape at either of the study sites, offering a potential explanation for some of the notable trends in carbon flux observed over the 22-year observation period, especially at OJP.

There is observational evidence of the potentially devastating effects of wind at OJP. Between September 2016 and April 2017, there was an estimated 14% loss of living trees at the site. In this time, approximately 414 ± 49 gC/m^2 was transferred from the living pool to SD or ground, and an additional 127 ± 31 gC/m^2 already in the SD pool was impacted, resulting in further additions to ground. Because we did not revisit the site between measurement in September 2016, and the following April, it is uncertain when these trees were felled, and whether a single event was responsible. During this period, there were high winds recorded at OJP on October 4th and 5th, March 7th and 8th, and March 19th. On these days, there were sustained winds > 30km/h recorded at both Prince Albert, and Waskesiu with gusts over 50km/h

on October 4th and 5th, and gusts over 70km/h on March 7th and 19th (ECCC climate station #4056241). While higher wind speeds were recorded on March 7th, and 19th, added weight from wet snow falling during the October 4th and 5th storm make this an equally likely candidate. Regardless of whether it was one of these events, or a combination of these and others, that were responsible for an estimated 900% increase in average annual mortality at OJP, this example shows the potential for a significant redistribution of carbon across the landscape in a very short period of time.

The notable flux of carbon from the dead and broken pools to ground observed between 2004 and 2008 at OJP (Figure 4.5) may have been a result of wind disproportionally impacting the weakened trees in the SD pool. In the decade preceding this period, the SD pool had been maintained at a relatively stable level (Tables 4.1 and 4.2). A large number of trees at various states of decay would have therefore accumulated in the SD pool, many of which would be especially vulnerable to windthrow.

Between 2008 and 2016, there was a notable increase in the mortality rate at OJP, accompanied by a marked increase in the amount of carbon transferred from the living and dead pools to broken, and from the living pool straight to ground (Figure 4.5). This may have also been the result of wind, breaking living and dead stems, and felling whole live trees. Unlike the preceding period, less carbon was transferred from the SD pool to ground, which is unexpected considering this group is likely to be most vulnerable to blowdown. This discrepancy could be due to the fact that there was less carbon present in the dead pool during this time period. At OJP, the number of individuals classified as whole dead went from 392 ± 61 in 2004 to 210 ± 53 by 2008. Therefore, the most vulnerable SD, tall individuals that had achieved more advanced states of decay, had likely already been selected for during the preceding period. The decrease in carbon flux from dead to ground may therefore be proportional to this decrease in the presence of SD, and especially vulnerable individuals.

4.6.3 Net Ecosystem and Primary Production

There was a decrease in the annual average rate of carbon uptake (NPP_{Tree}) at OJP to 66 gC/m^2yr between 2008 and 2016. This was the same period during which we observed an increase in tree mortality. Prior to this, NPP_{Tree} was maintained at about 90 gC/m^2yr since 1994.

It appears that the loss of living individuals impacted the trees ability to fix carbon within the stand. There was an even more substantial increase in tree mortality at OA between 2004 – 2010. However, unlike OJP, the loss of living individuals was not accompanied by a meaningful decrease in NPP_{Tree}. The forest at OA appears to be better at taking advantage of openings in the canopy. This is a characteristic trait of deciduous species like trembling aspen, which are effective at increasing their photosynthetic capacity in response to an increase in light availability (Stuart-Haëntjens et al., 2015).

This study suggests that NEP is relatively insensitive to changes in NPP_{Tree} at these sites. Annually averaged NEP_{EC} over the 22-year observation period was 40 ± 6 gC/m^2yr at OJP and 142 ± 18 gC/m^2yr at OA. At OJP, NEP_{EC} was quite consistent between measurement periods, with values hovering around the 22-year average, ranging from 38 ± 11 to 42 ± 9 gC/m^2yr, regardless of the drop in NPP_{Tree} toward the end of the observation period. At OA, NEP_{EC} fell considerably during the wet subperiod, to 89 ± 31 gC/m^2yr, 37% lower the 22-year average. In this case, it was NPP_{Tree} which was maintained at a steady level, irrespective of the trend in NEP_{EC}. While the recorded decrease in NEP at OA may have been an ecosystem wide response to moisture stress during the wet subperiod, the specific nature of this response remains unclear due to the lack of reliable data for all component stocks in the ecosystem.

It is difficult to compare NEP_{EC} to anything calculated from the biometric inventory data. The closest approximation to a biometric measure of NEP (NEP_{Bio}) provided by this study is the change in total C stocks between measurement periods as expressed by ΔC (Total) in Table 4.2. However, this is an incomplete picture without reliable and repeated measures of carbon in all components of the ecosystem, understory, fine root, and soil (forest floor and mineral soil). Such measurements were attempted in 1994 and 2004 but were discontinued due to questions regarding their reliability. Nonetheless, if we are to consider the impact of these measurements on our estimate of NEP_{Bio} for the period between 1994 and 2004, ΔC (Total) decreases slightly, from 67.2 to 59.2 gC/m^2yr at OJP, and more than doubles at OA, increasing from 111.4 to 302.4 gC/m^2yr (Table 4.3). Compared with NEP_{EC} over this same period (Table 4.2), the adjustment caused an incremental improvement in ΔC (Total) at OJP. Nonetheless, this metric overestimated NEP_{EC} by approximately 50% at OJP and 75% at OA. What is clear is that ground and soil level

processes have a considerable impact on boreal ecosystem carbon dynamics (Sellers et al., 1997; Litton et al., 2007; Misson et al., 2007).

At OJP, ΔC (Total) is positive throughout the observation period, representing a net accumulation of carbon within the ecosystem. At OA, there is a loss in total carbon between 2010 and 2016, due to a reduction in the SD and DWD carbon pools (Table 4.2). The result is a negative value for ΔC (Total) during this period. NEP_{EC} is however positive throughout the observation period at both sites, raising the question of whether the missing carbon at OA could have ended up in one of the unmeasured components of the ecosystem. If we were to assume that additions to understory, fine root, forest floor, and soil between 2010 – 2016 are comparable to those from the period between 1994 – 2004 (Table 4.3), ΔC (Total) would increase from -101 ± 39 to 90 ± 39 gC/m^2yr, inching closer to the value of 145 ± 31 gC/m^2yr recorded for NEP_{EC} over this same period (Table 4.2).

Our values of ΔC (Total) for the periods 2004 – 2010, and 2010 – 2016 at OA were however largely driven by stock changes in the DWD pool between measurement in 2004, 2010, and 2016, and there is a great deal of uncertainty associated with these measurements. The locations where the DWD measurements were first taken in 1994 were not marked. Sampling locations were therefore relocated in 2004 to within the permanent sampling plots established in 1994 by Gower and Fournier (Fournier et al., 1997; Gower et al., 1997) in 2004. Further inconsistencies in the number and location of plots sampled for DWD were introduced during later field campaigns. These inconsistencies along with the uncertainty associated with the DWD line-intersect method in general (Waddell, 2002; Woldendorp et al., 2004) have likely contributed to the observed discrepancies between measures of DWD and estimates of carbon input to ground, and to the high variability of ΔC (Total) between measurement periods at OA.

4.7 Conclusion

Over the 22-year observation period, several notable changes in C stocks were recorded at our two study sites. large scale changes in the distribution of carbon across the landscape occurred during periods of elevated tree mortality, likely resulting from shifts in the moisture regime at OA, and windthrow at OJP. There is evidence that ecosystem level production was also impacted by the increase in tree mortality and the flux of carbon between pools, however

this differed between the two sites. NPP_{Tree} decreased at OJP in response to enhanced mortality, yet it was maintained at a relatively stable level at OA regardless of the increased rate of tree mortality. The deciduous trees here were likely more capable of taking advantage of holes in the canopy by upping their production efficiency. As for NEP_{EC}, the opposite pattern was observed. NEP_{EC} was maintained at a stable level at OJP, and was notably depressed during the wet subperiod at OA.

Future studies of this nature should focus on developing a protocol to reliably and accurately measure C stocks in the components of the ecosystem that were neglected in this study (Table 4.3), and on reducing uncertainty in the DWD carbon pool. This is especially important considering soil level processes can represent a vital component of boreal forest carbon dynamics. If a more extensive data collection campaign were launched, a more accurate estimate of NEP_{Bio} could be achieved, helping to better understand the mechanisms behind the decrease in NEP at OA during the wet subperiod.

There is also opportunity to further explore the impact of windfall on NPP_{Tree} and NEP in mature jack pine stands, with further study of the hypothesized windthrow event(s) occurring post-measurement in 2016. As a result of this disturbance, we could expect an immediate and substantial influx of carbon to the DWD pool, and a subsequent increase in the rate of heterotrophic respiration. Further measures of DWD and EC flux in the coming years would be required to confirm whether these expectations are met and to better appreciate the impact of this type of disturbance on jack pine stand and carbon dynamics.

Climate change will undoubtedly have several impacts on carbon dynamics in the boreal forest. Here we find evidence that trembling aspen stands may react poorly to excessive moisture and flooding. At OA, flooding likely contributed to moisture stress, ultimately resulting in a redistribution of carbon across the landscape, and a notable decrease in annual NEP. An increase in moisture is expected in the eastern Canadian boreal forest (Wang et al., 2014). We may therefore observe similar negative impacts on mature aspen stands found here. However, it remains unclear whether it was drought, flooding, or some combination of the two which contributed most to overall moisture stress at our study site. While there is a considerable body of knowledge concerning the impacts of drought on trembling aspen growth, the potential impacts of flooding have not yet been studied to this same extent and warrant further

examination. We also found that wind may represent an important agent of change in mature jack pine stands. An increase in the incidence and intensity of extreme storms and high winds (IPCC, 2013), will likely lead to more frequent high impact disturbance in both jack pine and aspen stands across the boreal (Rich et al., 2007).

Our two study sites were in close proximity to one another, separated by only about 100 kms. Carbon dynamics within these sites were nonetheless driven by drastically different ecological mechanisms. We thus caution against painting the southern boreal forest with too wide a brush. It is vitally important that we first gain a broad understanding of the mechanisms responsible for governing carbon and stand dynamics in a range of representative boreal forest stands, before we can reliably interpret or forecast change.

4.8 References

Ajtay, G. L. (1979). Terrestrial primary production and phytomass. *The Global Carbon Cycle, SCOPE 13*, 129–181.

Aubinet, M., Vesala, T., & Papale, D. (2012). *Eddy covariance: A practical guide to measurement and data analysis*. Springer Science & Business Media.

Baldocchi, D. D. (2003). Assessing the eddy covariance technique for evaluating carbon dioxide exchange rates of ecosystems: Past, present and future. *Global Change Biology*, *9*(4), 479–492.

Barr, A. G., Morgenstern, K., Black, T. A., McCaughey, J. H., & Nesic, Z. (2006). Surface energy balance closure by the eddy-covariance method above three boreal forest stands and implications for the measurement of the CO2 flux. *Agricultural and Forest Meteorology*, *140*(1), 322–337.

Barr, A. G., Richardson, A. D., Hollinger, D. Y., Papale, D., Arain, M. A., Black, T. A., Bohrer, G., Dragoni, D., Fischer, M. L., Gu, L., Law, B. E., Margolis, H. A., McCaughey, J. H., Munger, J. W., Oechel, W., & Schaeffer, K. (2013). Use of change-point detection for friction–velocity threshold evaluation in eddy-covariance studies. *Agricultural and Forest Meteorology*, *171–172*, 31–45.

Barr, Alan G., Black, T. A., Hogg, E. H., Kljun, N., Morgenstern, K., & Nesic, Z. (2004). Inter-annual variability in the leaf area index of a boreal aspen-hazelnut forest in relation to net ecosystem production. *Agricultural and Forest Meteorology*, *126*(3), 237–255.

Barrow, E. (2009). Climate scenarios for Saskatchewan. *A Report Prepared for the Prairie Adaptation Research Collaborative (PARC)*.

Bernier, P. Y., & Robitaille, G. (2004). A plane intersect method for estimating fine root productivity of trees from minirhizotron images. *Plant and Soil*, *265*(1), 165–173.

Black, T. A., Chen, W. J., Barr, A. G., Arain, M. A., Chen, Z., Nesic, Z., Hogg, E. H., Neumann, H. H., & Yang, P. C. (2000). Increased carbon sequestration by a boreal deciduous forest in years with a warm spring. *Geophysical Research Letters*, *27*(9), 1271–1274.

Bradshaw, C. J., & Warkentin, I. G. (2015). Global estimates of boreal forest carbon stocks and flux. *Global and Planetary Change*, *128*, 24–30.

Bush, E. & Lemmen, D.S, editors (2019). Canada's changing climate report. *Government of Canada, Ottawa, ON,* 444p.

Carlson, M., Wells, J., & Roberts, D. (2009). *The carbon the world forgot: Conserving the capacity of Canada's Boreal Forest region to mitigate and adapt to climate change.* Boreal Songbird Initiative and Canadian Boreal Initiative, Seattle, WE, USA and Ottawa, Canada.

Chen, H. Y., & Luo, Y. (2015). Net aboveground biomass declines of four major forest types with forest ageing and climate change in western Canada's boreal forests. *Global Change Biology*, *21*(10), 3675–3684.

Chen, H. Y., Luo, Y., Reich, P. B., Searle, E. B., & Biswas, S. R. (2016). Climate change-associated trends in net biomass change are age dependent in western boreal forests of Canada. *Ecology Letters*, *19*(9), 1150–1158.

Chen, L., Huang, J.-G., Alam, S. A., Zhai, L., Dawson, A., Stadt, K. J., & Comeau, P. G. (2017). Drought causes reduced growth of trembling aspen in western Canada. *Global Change Biology*.

Cook, B. I., Smerdon, J. E., Seager, R., & Coats, S. (2014). Global warming and 21 st century drying. *Climate Dynamics*, *43*(9–10), 2607–2627.

Fournier, R. A., Rich, P. M., & Landry, R. (1997). Hierarchical characterization of canopy architecture for boreal forest. *Journal of Geophysical Research: Atmospheres*, *102*(D24).

Goulden, M. L., Wofsy, S. C., Harden, J. W., Trumbore, S. E., Crill, P. M., Gower, S. T., Fries, T., Daube, B. C., Fan, S.-M., & Sutton, D. J. (1998). Sensitivity of boreal forest carbon balance to soil thaw. *Science*, *279*(5348), 214–217.

Gower, S. T., Krankina, O., Olson, R. J., Apps, M., Linder, S., & Wang, C. (2001). Net primary production and carbon allocation patterns of boreal forest ecosystems. *Ecological Applications*, *11*(5), 1395–1411.

Gower, S. T., Vogel, J. G., Norman, J. M., Kucharik, C. J., Steele, S. J., & Stow, T. K. (1997). Carbon distribution and aboveground net primary production in aspen, jack pine, and black spruce stands in Saskatchewan and Manitoba, Canada. *Journal of Geophysical Research: Atmospheres*, 29029–29041.

Grant, R. F., Black, T. A., Humphreys, E. R., & Morgenstern, K. (2007). Changes in net ecosystem productivity with forest age following clearcutting of a coastal Douglas-fir forest: Testing a mathematical model with eddy covariance measurements along a forest chronosequence. *Tree Physiology*, *27*(1), 115–131.

Griffis, T. J., Black, T. A., Morgenstern, K., Barr, A. G., Nesic, Z., Drewitt, G. B., Gaumont-Guay, D., & McCaughey, J. H. (2003). Ecophysiological controls on the carbon balances of three southern boreal forests. *Agricultural and Forest Meteorology*, *117*(1), 53–71.

Halliwell, D. H., & Apps, M. J. (1997). *BOReal Ecosystem-Atmosphere Study (BOREAS) biometry and auxiliary sites: Soils and detritus data*.

Howard, E. A., Gower, S. T., Foley, J. A., & Kucharik, C. J. (2004). Effects of logging on carbon dynamics of a jack pine forest in Saskatchewan, Canada. *Global Change Biology*, *10*(8), 1267–1284.

Huntingford, C., & Mercado, L. M. (2016). High chance that current atmospheric greenhouse concentrations commit to warmings greater than 1.5 C over land. *Scientific Reports*, *6*,

Jeong, D. I., Sushama, L., & Khaliq, M. N. (2014). The role of temperature in drought projections over North America. *Climatic Change*, *127*(2), 289–303.

Kalyn, A. L., & Van Rees, K. C. J. (2006). Contribution of fine roots to ecosystem biomass and net primary production in black spruce, aspen, and jack pine forests in Saskatchewan. *Agricultural and Forest Meteorology*, *140*(1), 236–243.

Kljun, N., Black, T. A., Griffis, T. J., Barr, A. G., Gaumont-Guay, D., Morgenstern, K., McCaughey, J. H., & Nesic, Z. (2007). Response of net ecosystem productivity of three boreal forest stands to drought. *Ecosystems*, *10*(6), 1039–1055.

Kurz, W. A., Stinson, G., Rampley, G. J., Dymond, C. C., & Neilson, E. T. (2008). Risk of natural disturbances makes future contribution of Canada's forests to the global carbon cycle highly uncertain. *Proceedings of the National Academy of Sciences*, *105*(5).

Lambert, M.-C., Ung, C.-H., & Raulier, F. (2005). Canadian national tree aboveground biomass equations. *Canadian Journal of Forest Research*, *35*(8), 1996–2018.

Litton, C. M., Raich, J. W., & Ryan, M. G. (2007). Carbon allocation in forest ecosystems. *Global Change Biology*, *13*(10), 2089–2109.

Matthews, G. (1993). The carbon content of trees. *Technical Paper - Forestry Commission (United Kingdom)*.

Michaelian, M., Hogg, E. H., Hall, R. J., & Arsenault, E. (2011). Massive mortality of aspen following severe drought along the southern edge of the Canadian boreal forest. *Global Change Biology*, *17*(6), 2084–2094.

Misson, L., Baldocchi, D. D., Black, T. A., Blanken, P. D., Brunet, Y., Yuste, J. C., Dorsey, J. R., Falk, M., Granier, A., Irvine, M. R., Jarosz, N., Lamaud, E., Launiainen, S., Law, B. E., Longdoz, B., Loustau, D., McKay, M., Paw U, K. T., Goldstein, A. H. (2007). Partitioning forest carbon fluxes with overstory and understory eddy-covariance measurements: A synthesis based on FLUXNET data. *Agricultural and Forest Meteorology*, *144*(1), 14–31.

Moore, T. R. (2003). Dissolved organic carbon in a northern boreal landscape. *Global Biogeochemical Cycles*, *17*(4).

Peng, C., Ma, Z., Lei, X., Zhu, Q., Chen, H., Wang, W., Liu, S., Li, W., Fang, X., & Zhou, X. (2011). A drought-induced pervasive increase in tree mortality across Canada's boreal forests. *Nature Climate Change*, *1*(9), 467–471.

Rich, R. L., Frelich, L. E., & Reich, P. B. (2007). Wind-throw mortality in the southern boreal forest: Effects of species, diameter and stand age. *Journal of Ecology*, *95*(6), 1261–1273.

Ruark, G. A., & Bockheim, J. G. (1987). Below-ground biomass of 10-, 20-, and 32-year-old Populus tremuloides in Wisconsin. *Pedobiologia*, *30*(3), 201–217.

Sellers, P., Hall, F., Ranson, K. J., Margolis, H., Kelly, B., Baldocchi, D., den Hartog, G., Cihlar, J., Ryan, M. G., & Goodison, B. (1995). The Boreal Ecosystem–Atmosphere Study (BOREAS): An overview and early results from the 1994 field year. *Bulletin of the American Meteorological Society*, *76*(9), 1549–1577.

Sellers, P. J., Hall, F. G., Kelly, R. D., Black, A., Baldocchi, D., Berry, J., Ryan, M., Ranson, K. J., Crill, P. M., & Lettenmaier, D. P. (1997). BOREAS in 1997: Experiment overview, scientific results, and future directions. *Journal of Geophysical Research: Atmospheres*, *102*(D24), 28731–28769.

Soja, A. J., Tchebakova, N. M., French, N. H., Flannigan, M. D., Shugart, H. H., Stocks, B. J., Sukhinin, A. I., Parfenova, E. I., Chapin, F. S., & Stackhouse, P. W. (2007). Climate-induced boreal forest change: Predictions versus current observations. *Global and Planetary Change*, *56*(3), 274–296.

Steele, S. J., Gower, S. T., Vogel, J. G., & Norman, J. M. (1997). Root mass, net primary production and turnover in aspen, jack pine and black spruce forests in Saskatchewan and Manitoba, Canada. *Tree Physiology*, *17*(8–9), 577–587.

Stocker, T. F., Qin, D., Plattner, G. K., Tignor, M., Allen, S. K., Boschung, J., Nauels, A., Xia, Y., Bex, B., & Midgley, B. M. (2013). *IPCC, 2013: Climate change 2013: the physical science basis. Contribution of working group I to the fifth assessment report of the intergovernmental panel on climate change*.

Stuart-Haëntjens, E. J., Curtis, P. S., Fahey, R. T., Vogel, C. S., & Gough, C. M. (2015). Net primary production of a temperate deciduous forest exhibits a threshold response to increasing disturbance severity. *Ecology*, *96*(9), 2478–2487.

Ung, C.-H., Bernier, P., & Guo, X.-J. (2008). Canadian national biomass equations: New parameter estimates that include British Columbia data. *Canadian Journal of Forest Research*, *38*(5), 1123–1132.

Vogel, J. G., & Gower, S. T. (1998). Carbon and Nitrogen Dynamics of Boreal Jack Pine Stands With and Without a Green Alder Understory. *Ecosystems*, *1*(4), 386–400.

Waddell, K. L. (2002). Sampling coarse woody debris for multiple attributes in extensive resource inventories. *Ecological Indicators*, *1*(3), 139–153.

Wang, Y., Hogg, E. H., Price, D. T., Edwards, J., & Williamson, T. (2014). Past and projected future changes in moisture conditions in the Canadian boreal forest. *The Forestry Chronicle*, *90*(5), 678–691.

Woldendorp, G., Keenan, R. J., Barry, S., & Spencer, R. D. (2004). Analysis of sampling methods for coarse woody debris. *Forest Ecology and Management*, *198*(1), 133–148.

4.9 Tables and Figures

Table 4.1: In-situ C stocks in the biomass, necromass, and on the forest floor in the form of downed woody debris, calculated from repeated inventory data. Values for above ground carbon in both pools include allometrically derived estimates for wood, bark, branches, and foliage (when appropriate). All values are in tonnes of carbon per hectare (tC/ha) and are representative of the mean and standard error among replicate plots.

Biomass C Stocks	**OJP**					**OA**			
	1994	**2004**	**2008**	**2016**		**1994**	**2004**	**2010**	**2016**
Tree Above Ground	35.6 ± 1.9	40.1 ± 2.0	41.8 ± 2.1	41.4 ± 2.2		84.7 ± 4.9	89.7 ± 5.9	84.2 ± 9.3	86.8 ± 9.9
Tree Coarse Root	6.3 ± 0.3	7.2 ± 0.4	7.5 ± 0.4	7.5 ± 0.4		10.4 ± 0.5	10.4 ± 0.6	9.4 ± 1.0	9.4 ± 1.0
Tree Total	41.9 ± 2.2	47.2 ± 2.3	49.3 ± 2.5	48.9 ± 2.6		95.1 ± 5.4	100.1 ± 6.4	93.6 ± 10.3	96.2 ± 10.9
Necromass C Stocks									
Standing Dead Above Ground	5.3 ± 0.7	5.2 ± 0.7	3.9 ± 0.6	5.7 ± 0.9		8.1 ± 1.3	9.9 ± 1.4	11.2 ± 2.6	7.1 ± 1.9
Standing Dead Coarse Root	1.0 ± 0.1	1.0 ± 0.1	0.8 ± 0.1	1.2 ± 0.2		1.2 ± 0.2	2.3 ± 0.3	2.2 ± 0.4	2.2 ± 0.6
Standing Dead Total	6.2 ± 0.8	6.2 ± 0.9	4.7 ± 0.7	6.9 ± 1.1		9.3 ± 1.5	12.3 ± 1.6	13.4 ± 3.0	9.3 ± 2.5
Downed Woody Debris (DWD)	1.6 ± 0.1	2.9 ± 0.4	3.5 ± 0.5	4.6 ± 0.6		9.7 ± 4.7	12.9 ± 1.2	27.9 ± 3.7	23.2 ± 4.2

Table 4.2: The rate of change in C stocks, and fluxes between pools, occurring during the periods between repeated measurements. Estimates for NPP_{Tree}, derived from the contribution of living trees to biomass between measurements, and EC derived values of whole ecosystem production (NEP_{EC}) are also included. All values are in grams of carbon per m^2 per year (gC/m^2yr) and are representative of the mean and standard error among replicate plots. In the case of NEP, the mean and standard error are calculated from annual values between each measurement period. *Due to inconsistencies in DWD sampling at OJP, uncertainty associated with ΔDWD between 1994-2004 and 1994-2016 are estimated as the mean standard error from the remaining two periods.

C Stock Rates of Change	OJP					OA			
	94-04	04-08	08-16	94-16		94-04	04-10	10-16	94-16
ΔB (Tree Biomass)	54.0 ± 6.8	51.0 ± 9.8	-4.7 ± 9.8	32.1 ± 6.6		49.5 ± 30	-108.5 ± 72.7	44.2 ± 20.2	5.0 ± 34.8
ΔSD (Standing Dead)	0.2 ± 4.7	-39.5 ± 14.5	27.6 ± 10.5	2.9 ± 5.3		29.5 ± 17.1	18.2 ± 45.2	-67.2 ± 19.1	0.0 ± 13.1
ΔDWD (Downed Woody Debris)	13.0 ± 5.4*	14.4 ± 5.9	14.0 ± 4.8	13.6 ± 5.4*		32.4 ± 15.0	250.2 ± 37.3	-78 ± 28.8	61.7 ± 1.0
ΔC (Total)	67.2 ± 9.9	25.9 ± 18.5	36.9 ± 15.1	48.6 ± 10.0		111.4 ± 37.6	159.9 ± 93.4	-101 ± 40.0	66.7 ± 37.2
C Fluxes									
NPP_{Tree}	90.2 ± 4.2	88.8 ± 4.6	66 ± 6.8	81.2 ± 4.5		218 ± 12.1	199.3 ± 24.3	228.3 ± 25.7	215.7 ± 18.5
NEP_{EC}	39.1 ± 11.4	38.5 ± 11.5	42.1 ± 8.9	40.1 ± 6.2		172.7 ± 27.2	89.5 ± 31.5	144.8 ± 31.2	142.4 ± 18.1
Living (B) --> Standing Dead (SD)	31.4 ± 4	33.9 ± 8.1	46.3 ± 10.1	37.3 ± 5.1		106.2 ± 14.1	191.3 ± 49.9	34.1 ± 12	109.7 ± 20
Living + Standing Dead (B + SD) --> Ground (G)	30.0 ± 3.2	61.5 ± 12.4	29.8 ± 7.3	35.6 ± 4.5		120.5 ± 14.8	242.7 ± 25.4	222.1 ± 38.6	181.5 ± 13.8
Living (B) --> Dead (SD + G)	36.1 ± 3.9	37.6 ± 8.5	66.9 ± 11.2	47.6 ± 5.6		166.3 ± 24.5	307.5 ± 52.2	178 ± 28.4	208 ± 24.2

Table 4.3: C stock measurements of other ecosystem components taken in 1994 and 2004. The rates of change occurring between 1994 and 2004 (94-04) are also provided. The values for total ecosystem C-stocks, as well as the updated value for the rate of change in total C stocks (ΔC Total) includes C stocks in the ecosystem components listed in this table and those contained in the biomass, necromass, and DWD, in Table 4.1. All C stocks (under 1994 and 2004) are in tonnes of carbon per hectare (tC/ha), and the rates of change (under 94-04) are in grams of carbon per m^2 per year (gC/m^2yr).

Additional C Stock Measurements	OJP				OA		
	1994	2004	94-04		1994	2004	94-04
Understory	0.2	0.1	-1		0.7	3.3	26
Fine Root	0.7	1.6	9		0.2	1.7	15
Forest Floor	4.4	4.8	4		19.4	34.0	146
Mineral Soil	18.2	16.2	-20		36.0	36.4	4
Total Ecosystem Carbon Stocks	73.2 ± 2.3	79.0 ± 2.5	59.2 ± 9.9		170.4 ± 7.3	200.7 ± 6.7	302.4 ± 37.6

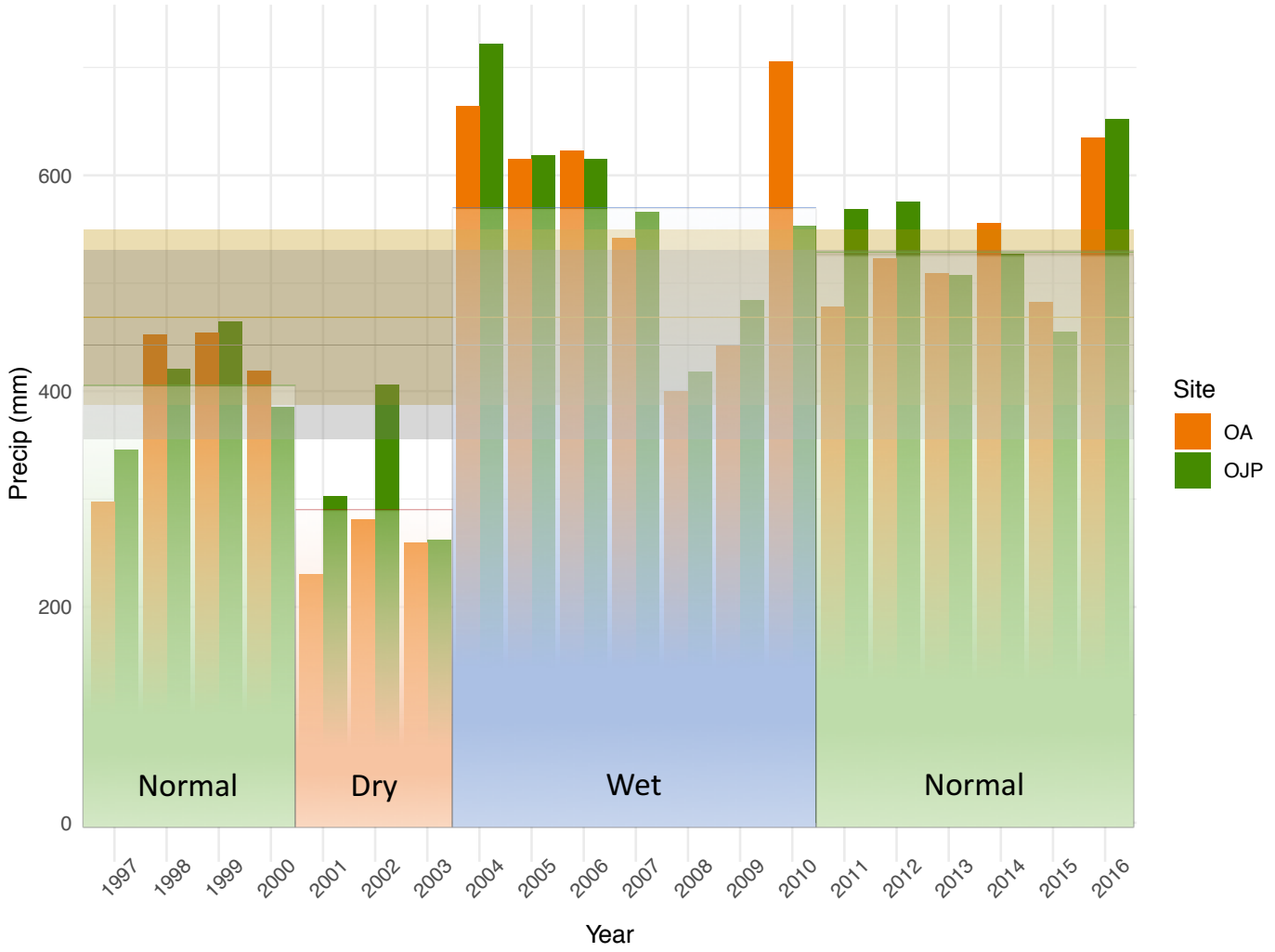

Figure 4.1: Annual precipitation totals at BERMS sites OJP (green bars) and OA (orange bars) from 1997 to 2016. Average precipitation (1980 – 2016) along with one standard deviation is shown in yellow for Waskesiu Lake and gray for Prince Albert. Average precipitation during select subperiods (1997 – 2000, 2001 – 2003, 2004 – 2010, and 2011 – 2016) are shown in green if within one standard deviation from the norm, in red if below one standard deviation, and in blue if above one standard deviation.

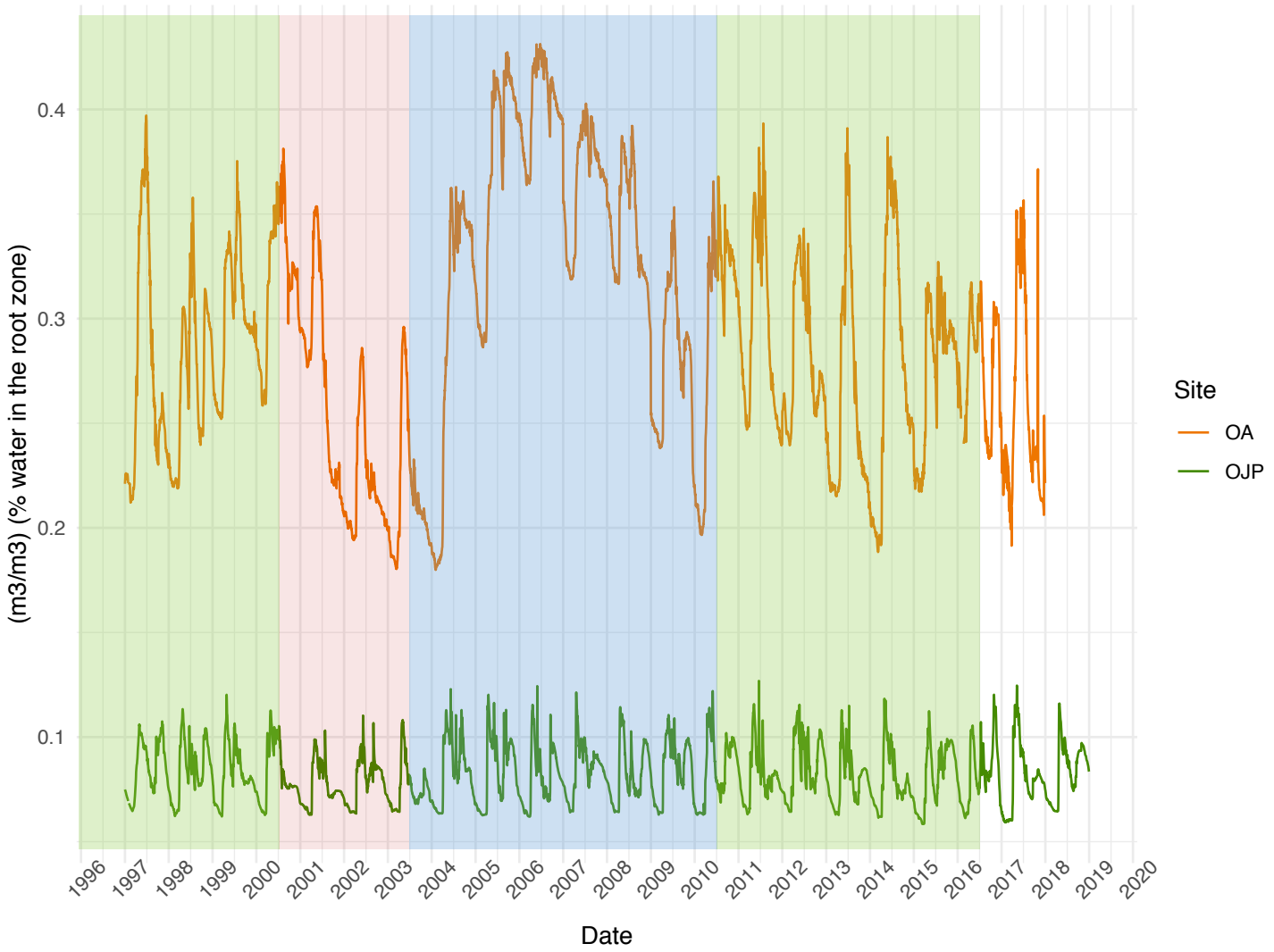

Figure 4.2: Volumetric Soil Water Content (VWC) from 1997 to 2019 at OA (orange) and OJP (green). The normal, dry, and wet subperiods are shown here in green, red, and blue, respectively.

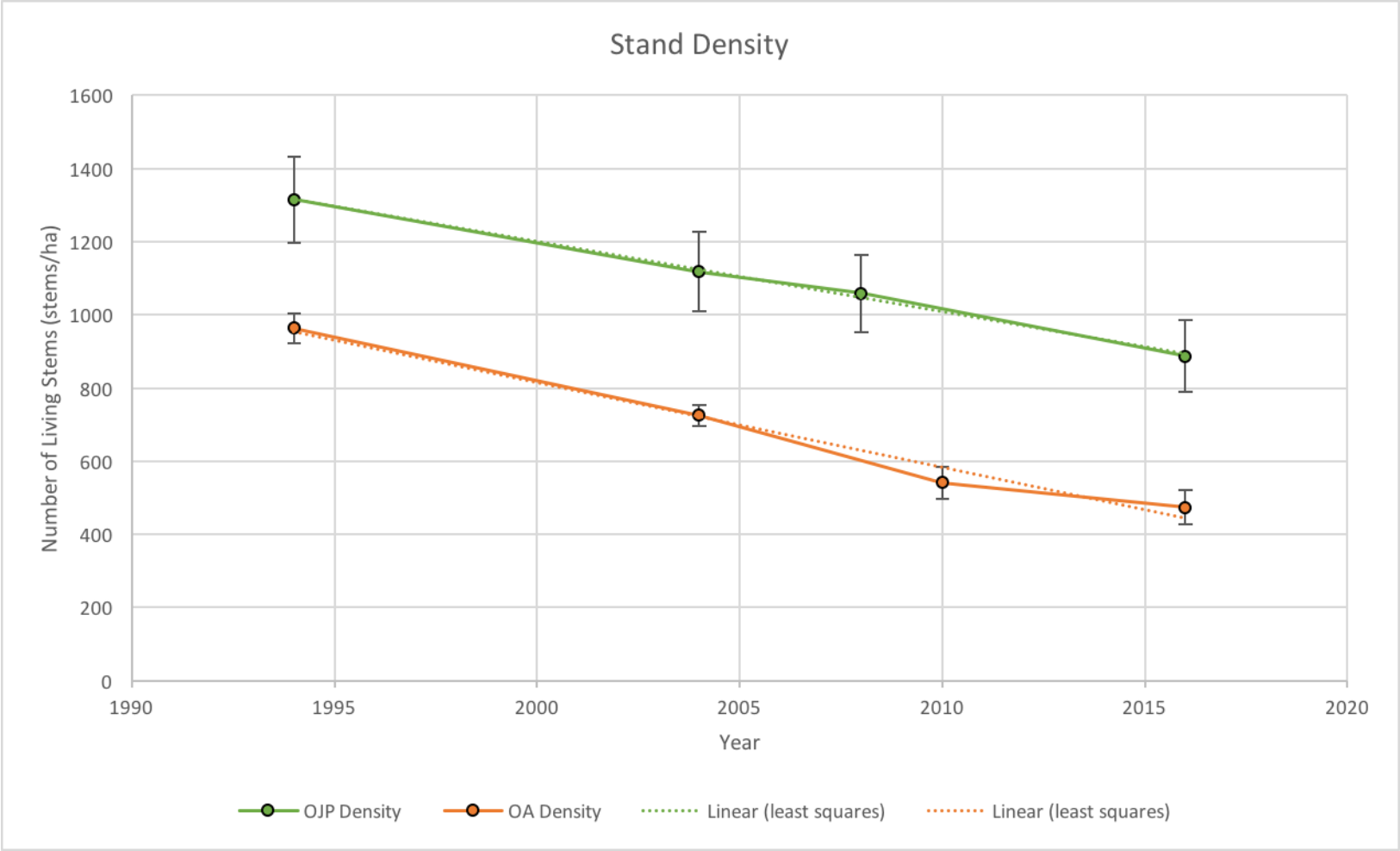

Figure 4.3: The change in stand density at OJP and OA. A linear least squares regression line is included to show periods of divergence from the trend over time.

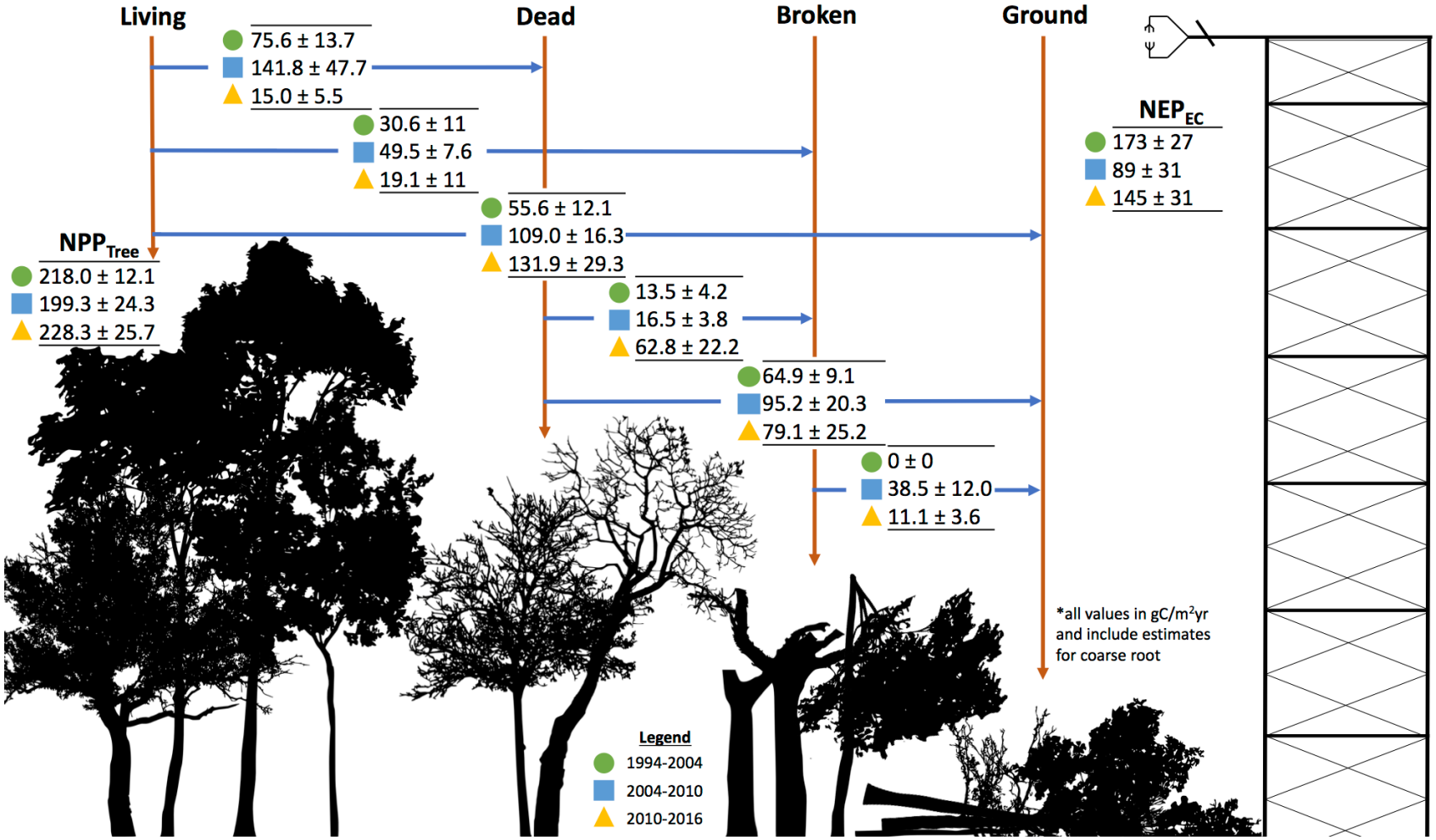

Figure 4.4: Conceptual diagram of C fluxes between pools at OA during each measurement period. The green circle represents the period between measurement in 1994 and 2004, the blue square, the period between 2004 and 2010, and the yellow triangle, the period between 2010 and 2016. Values for NPP_{Tree} and NEP_{EC} are also depicted on this figure. All values listed are in grams of carbon per m^2 per year (gC/m^2yr).

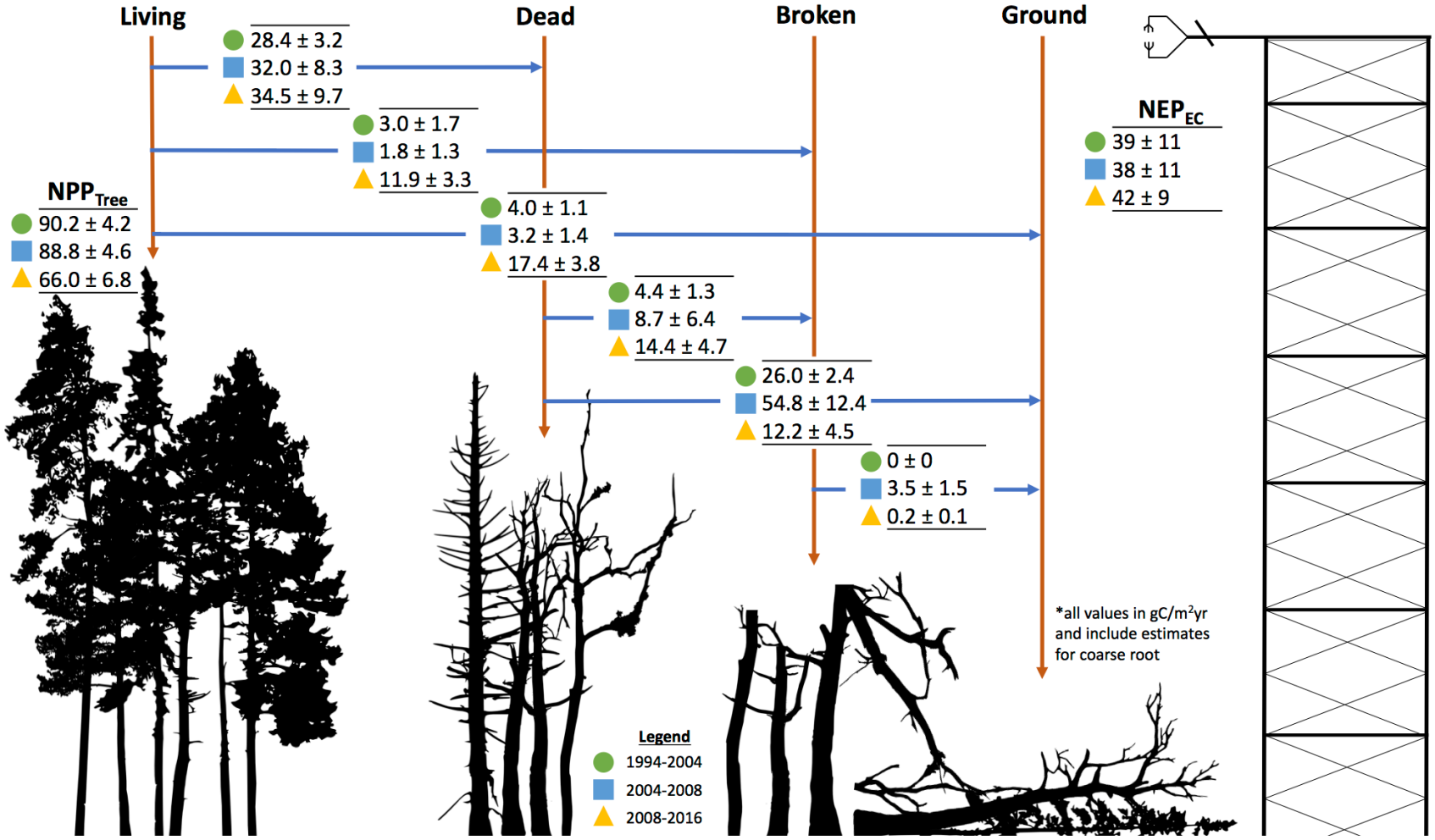

Figure 4.5: Conceptual diagram of C fluxes between pools at OJP during each measurement period. The green circle represents the period between measurement in 1994 and 2004, the blue square, the period between 2004 and 2008, and the yellow triangle, the period between 2008 and 2016. Values for NPP_{Tree} and NEP_{EC} are also depicted on this figure. All values listed are in grams of carbon per m^2 per year (gC/m^2yr).

CHAPTER 5

CONCLUSIONS

The main goal of this research was to better understand the interface between radial growth, climate, and carbon in the Canadian southern boreal forest, and to ultimately improve our understanding of how climate change may impact radial-tree growth and carbon dynamics in this region. Over the course of the three manuscripts contained herein, the main environmental drivers of radial-tree growth and forest-stand level carbon flux were identified over the short-, medium-, and long-term, and comparisons were made between the species examined (jack pine, black spruce, eastern larch, and trembling aspen). Based on these results, I offer a summary of my main findings and discuss their implications in the context of climate change.

5.1 Synthesis of Dendrochronological Findings

One of the main strengths associated with this compendium of research is the extensive collection of data and observations regarding the dominant drivers of ring widths and stem size across multiple temporal scales. For this reason, I would like to begin by offering a synthesis of my main findings related to this comprehensive examination of relationships in the context of the southern boreal forest.

5.1.1 Jack Pine

In this region over the long term (approx.100 years), there were no statistically significant relationships between monthly temperature and precipitation variables and the annual radial growth of jack pine. At best, it can be said that jack pine radial growth had a weak negative association with current October temperature over the long term. In recent decades however, since about the late 1970s, I observed emergent positive relationships between jack pine radial growth and previous spring temperature (April), previous winter temperatures (November – January), current spring temperature (April), and current late summer temperatures (July – September). In terms of relationships with precipitation, over the long term, jack pine radial growth had a relatively consistent positive relationship with May precipitation. Since about the late 1970s, relationships with precipitation have become muted, with a significant decrease in the strength of relationships between annual radial growth and monthly adjusted precipitation.

Over the medium term (2000 – 2018) jack pine had a strong positive relationship with annually resolved measures of NEP (summed over the calendar year, from January to December). At monthly scale resolution, jack pine radial growth was positively associated with previous fall NEP (August – December), with statistically significant relationships with previous August and October NEP, as well as with current May NEP.

5.1.2 Black Spruce

The annual radial growth of black spruce was negatively associated with spring and early summer temperatures over the long term (100+ years), this includes a significant negative relationship with current maximum June temperature. In recent decades, again since about the late 1970s, negative relationships between annual black spruce radial growth and monthly temperature variables have weakened, while positive relationships with current late summer / fall temperatures (July – September) have emerged. Black spruce has had a strong positive relationship with several monthly precipitation variables over the long term, including significant positive relationships with previous May and August precipitation, as well as with current spring / early summer precipitation (March – June). Like with jack pine, relationships with precipitation have become muted since about the late 1970s, with a significant decrease in the strength of relationships between the radial growth of black spruce and monthly precipitation.

Over the medium term (1999 – 2015), there were no relationships between black spruce radial growth and annual measures of ecosystem carbon (NEP, GEP, and R_E). However, when exploring relationships between annual radial growth and monthly ecosystem C-flux, a significant positive relationship between black spruce radial growth and current July GEP was observed.

5.1.3 Trembling Aspen

Over the long term observation period (approx. 100 years), trembling aspen had a positive relationship with late-spring / early-summer temperatures (May – July). These positive relationships have been fairly consistent in terms of their quality, remaining generally positive over the lifetime of this stand. In recent decades, since about the late 1970s, I observed emergent positive relationships with previous growing season temperatures (May – September), suggesting that previous growing season conditions, specifically air temperature, is becoming increasingly

important for the growth of trembling aspen in this region. Trembling aspen has had a relatively weak relationship with monthly precipitation in this region over the long term. I did however, observe a strong positive relationship with previous September precipitation which persisted from approximately the early 1930s to the mid-1970s. Like with jack pine and black spruce, It can be said that the relationship between trembling aspen and precipitation has weakened in recent decades but this trend is not as clear cut as with these other species. Perhaps a weakening of the relationship between annual radial growth and precipitation has been ongoing longer for trembling aspen than it has for jack pine or black spruce. It is difficult to make this determination concidering relationships with precipitation have been relatively weak over the lifetime of this forest stand.

Over the medium term (1997 – 2017) there were no relationships between the annual radial growth of trembling aspen and annually resolved measures of ecosystem carbon. When exploring relationships with monthly C-flux variables however, the annual radial growth of trembling aspen had a significant negative relationship with current January NEP, and a significant positive relationship with current January R_E.

5.1.4 Common Physiological Responses Amongst Study Species

Over intra-annual timescales during the short term observation period (2015 – 2018), nearly all observed relationships between the stem radius variability (ΔR) of the study species and local environmental variables, including eddy covariance C-flux variables, can be attributed to short-term physiological responses of stem size to meteorological conditions. For example, the four study species for which I have collected high-resolution stem size data (jack pine, black spruce, eastern larch, and trembling aspen) all had a strong positive relationship with precipitation over daily and weekly timescales. This is attributed to stem water replenishment in response to the input of moisture during periods with low vapor pressure deficit (VPD) under cloud cover. Additionally, observed negative relationships between daily variations in stem size and air temperature are attributed to increased transpiration rates and an immediate decrease in stem water volume in response to sunny conditions and warm air temperatures. While these physiological responses to inputs of moisture and fluctuations in daily temperature and light availability were common between species, I did note subtle inter-species differences in their responses. Compared with the other three species, jack pine stem size appeared to be most

sensitive to the input of moisture from precipitation. The stem size of black spruce and larch were less sensitive to precipitation than jack pine overall, but more responsive to precipitation when they had lesser access to root zone water resources, during periods when water table fell below the root zone. Finally, trembling aspen appeared to be least susceptible to stem radius fluctuations in response to precipitation.

The only relationships observed over intra-annual scales that may be associated with tracheid cell production or enlargement, processes which contribute to active ring development and radial growth, were positive relationships between air and soil temperature and the ΔR of the study species. This occured during the 2016, 2017, and 2018 growing seasons, during periods of enhanced moisture availability, when positive relationships between ΔR and air temperature from 1 to 3 days prior (lag = -1 to -3), as well as with soil temperature (lag = 0) were observed.

Relationships between the ΔR of the study species and ecosystem C-flux variables over intra-annual scales were likely spurious, driven by co-occuring responses of stem size and ecosystem C-flux to the same meteorological variables discussed above, namely temperature and precipitation, as well as their interactions with cloud cover and light availability.

5.2 Radial Growth/Climate Relationship

Climate at the nearby ECCC climate station in Prince Albert, Saskatchewan, has been warming and wetting since 1890 (Appendix D). Relative to the reference period (1890-1919), temperature has increased during every month except October, which experienced little change. The most marked increase in temperature, occurred in January, February, and March, months during which there was roughly a 4°C increase in mean monthly temperature. The remaining months (April – December) experienced an increase in temperature nearer 1°C relative to the reference period. Months with the most marked increase in precipitation include April and October. However, there was also an increase in precipitation throughout the spring and summer months (May, June, July) and early fall (September) (Appendix D).

It has been suggested that some boreal forest trees may end up benefitting from spring warming, providing there is sufficient moisture to support growth (Boisvenue & Running, 2006; Zhang et al., 2008; D'Orangeville et al., 2018). Trees in the southern boreal forest of Saskatchewan may be particularly well positioned to take advantage of the observed climatic

changes, considering that moisture is the dominant limiting factor controlling the distribution and growth of trees in this region (Sellers et al., 1995; Ireson et al., 2015), and that the dominant tree species found here may benefit from moderate climate warming (D'Orangeville et al., 2018).

The results from Chapter 2 provide support for this hypothesis. Here, I report on shifting growth/climate relationships over the long term (~100 years) at annual-scale resolution. These shifts include a weakening of the relationship between radial growth and precipitation, since the mid-1950s for aspen, and since the late-1970s for jack pine and black spruce, and an overall enhanced positive response of these three species to spring and summer air temperature. Like the divergence problem, which highlights issues of non-stationarity in the growth/climate relationship in trees further north, I attribute the cause of this dynamic relationship to changing limitations. More specifically, the shifting growth/climate relationships observed here are likely signalling a decrease in moisture limitations, and a positive response to recent warming. Over intra-annual scales, I also find evidence of a positive relationship between daily stem radius change (ΔR) and air temperature within the growing season during the short-term observation period (2015 – 2018). However, this relationship was only significant when moisture requirements were met, again calling reference to the importance of moisture and its role in supporting the relationship between radial growth and temperature.

Changes in moisture conditions in the Canadian boreal forest, both historically (over the last several decades), and moving forward, are spatially variable across the landscape (Jeong et al., 2014; Wang et al., 2014). It is likely that the Boreal Ecosystem Research and Monitoring Sites (BERMS) are situated in a region where an increase in evaporative demand in response to the recent warming trend has, to date, been successfully offset by a co-occurring increase in precipitation, resulting in a net increase in available moisture. It is unclear whether this trend will carry forward for much longer, as it is likely for the balance to tip in the opposite direction, as rates of evapotranspiration are expected to overshadow any gains in moisture related to an increase in precipitation over the long term (Jeong et al., 2014; Wang et al., 2014). This is likely already occurring to the west and to the north of the BERMS sites (Wang et al., 2014), where we find evidence of reduced radial growth and increased tree mortality (Barber et al., 2000; Michaelian et al., 2011; Walker & Johnstone 2014). While the findings from this and other studies help to improve our understanding of the impacts of climate change on boreal forest

trees, more work is needed. Relationships between radial-tree growth and climate in the Canadian boreal forest are regionally defined and species specific, requiring widespread and comprehensive study.

5.3 Carbon Dynamics

My next goal was to assess the relationship between radial-tree growth and carbon, to better understand how the direct impact of climate change on boreal forest tree growth may translate to an impact on forest carbon dynamics. To date, dendrochronological techniques have been underutilized in the context of forest carbon research. However, tree rings hold great potential in this field of study, as they are an *in situ* representation of forest wood production over time, one of the largest components of forest ecosystem production. Recent work in this area has yielded mixed results, highlighting significant gaps in our understanding of tree level primary production and its role in the process of active ring development (or xylogenesis). My goal in Chapter 3 was to assess relationships between forest carbon and radial growth across the temporal scale, over the medium- and short-terms. I applied analytical techniques analogous to those from the dendroclimatological assessment completed in Chapter 2, in this case applying them in a relatively novel context. Overall my findings are similar to those from other recent studies and help us to better understand the nature of observed relationships.

At annual-scale resolution, only the radial growth of jack pine was significantly and positively influenced by ecosystem level carbon (net ecosystem production; NEP) over the medium term (~20 years). Comparatively, black spruce and trembling aspen are more likely to rely situationally on stored non-structural carbohydrates (Rocha et al., 2006; Richardson et al., 2013; Gea-Izquierdo et al., 2014), introducing the potential for inconsistency in the relationship between ecosystem production (uptake) and radial growth (allocation). As evidenced by my comparison of static and dynamic correlation analyses in Chapter 2, even a slight inconsistency in the relationship between ecosystem production and radial growth over time has the potential to influence the result of a static correlation analysis. It can therefore be said that jack pine had a consistent relationship with ecosystem carbon during the observation period (2000 – 2018), during which this species consistently benefited from carbohydrate storage from the previous fall, and from elevated levels of ecosystem production during the current spring.

Over intra-annual scales (2015 – 2018), correlation between stem radius change (ΔR) and values of ecosystem carbon flux (NEP, R_E, GEP) were likely spurious, and driven by co-occurring responses to precipitation and light availability, as well as soil temperature. As identified by Zweifel et al. (2010), perceived negative relationships between ΔR and measures of ecosystem production (NEP and GEP) are more likely to do with tree/water relations than with radial growth. These represent two competing signals in high-resolution stem size data that become increasingly difficult to disentangle as temporal resolution increases. The likely reason for the inverse relationship between ΔR and measures of ecosystem production (NEP and GEP) observed in this study at daily resolution is as follows: Days where there are high levels of ecosystem production, under warm sunny conditions, manifest in stem shrinkage due to high transpiration and dehydration. Conversely, during rain events, and under cloud cover, the inverse is true, ecosystem production is more likely to be low while stem water content is being replenished. The likelihood that this perceived negative relationship is associated with stem water dynamics at daily resolution is further evidenced by the fact that these relationships are significant almost exclusively during periods when the ΔR of my study species were particularly responsive to precipitation, as observed in the previous chapter of this dissertation (Chapter 2).

Similar overlap was observed between the positive relationship between ΔR and R_E in Chapter 3, and the positive relationship between ΔR and soil temperature in Chapter 2, pointing to the likelihood that this relationship likely results from a common response to a third variable, in this case soil temperature. Based on these findings, there was effectively no evidence of a true relationship between stem size and measures of ecosystem carbon over fine-scale temporal resolution. Perceived relationships were likely spurious, driven by a combination of factors, including but not limited to combinations of precipitation and soil temperature.

My findings point to the likelihood that radial growth and ecosystem carbon are independent from one another. Therefore, the impact of climate change on the radial growth of widespread boreal forest species may not result in an impact on overall ecosystem carbon dynamics, as initially hypothesized. It is however still possible that there exists a connection between radial growth and ecosystem carbon variables and that it is simply undetectable by means of standard dendrochronological analysis. This would likely be due to the complexity and inconsistency in a relationship where variable lags and changing carbohydrate allocation

strategies are occurring in response to environmental conditions, mechanisms that are often site and species specific (Richardson et al., 2013; Gea-Izquierdo et al., 2014; Lempereur et al., 2015; Deslauriers et al., 2016). Our understanding of the process of carbon uptake and allocation to woody biomass will only improve over time, as datasets of eddy covariance flux continue to increase in breadth, length, and accuracy. Future research should also look to improve current methods of isolating the growth signal from the water signal in dendrometer data, perhaps using complementary datasets, like those collected with the use of sapflux sensors.

By taking a slightly different approach in Chapter 4 of this dissertation, I identify important agents of change, responsible for a conciderable redistribution of carbon and impacts to stand level carbon dynamics in jack pine and trembling aspen stands. For this study, I contributed the latest in a series of repeated inventory style measurements which make up a two-decade long record (1994 – 2016) of forest carbon stocks and fluxes at BERMS Old Jack Pine (OJP) and Old Aspen (OA). Conciderable changes in the distribution of carbon across the landscape occurred at both sites over the course of the observation period. The most notable stock changes occurred during periods of enhanced tree mortality, likely resulting from moisture stress at OA, and windthrow at OJP. There is evidence that ecosystem level production was also impacted during periods of enhanced tree mortality, however this differed between the two sites. NPP_{Tree} decreased at OJP in response to enhanced mortality, yet it was maintained at a relatively stable level at OA regardless of the mortality rate. The deciduous trees here were likely more capable of taking advantage of holes in the canopy by maintaining LAI and increasing production efficiency. As for NEP_{EC}, the opposite pattern was observed. NEP_{EC} was maintained at a stable level at OJP, and was notably depressed during a period of increased mortality at OA.

While moisture stress may have been responsible for an increase in tree mortality and a significant redistribution of carbon across the landscape at OA, considering the maintenance of overall NPP_{Tree}, the radial growth of surviving trees may have been impacted positively. This positive impact is likely due to trembling aspen's ability to take advantage of an increase in light availability through newly formed holes in the canopy. Therefore, if the radial growth/climate relationship were assessed for the trees within OA, as they were in Chapter 2, we may identify that an increase in moisture positively impacted radial growth within the site, which is not indicative of the whole story. In reality, an increase in moisture may have benefit the trees in

well drained sections of the site, due to an increase in water and light resources, while simultaneously causing flooding in nearby sections of the site, resulting in additional moisture stress and high levels of mortality for nearby trees. This has implications for those undertaking dendroclimatological studies in trembling aspen and perhaps other deciduous dominated stands.

5.4 Final Thoughts

In summary, over the near term, warming and wetting may benefit the radial growth of several tree species in the southern boreal forest of Saskatchewan, where moisture is the main limiting factor (Ireson et al., 2015). I see evidence of this in shifting growth/climate relationships, and in the positive response of radial growth to temperature during periods when moisture requirements are met. However, in mature trembling aspen dominated stands, an increase in available moisture may result in small- to medium-scale disturbance, resulting in enhanced tree mortality and a significant flux of carbon from biomass to necromass. Based on my observations at OA, wetting simultaneously contributed to enhanced mortality and enhanced growth. The end result was a net decrease in ecosystem production.

Moving forward, increased rates of evapotranspiration are expected to overshadow any gains in moisture related to an increase in precipitation, a trend which is likely already occurring to the west and to the north of the BERMS sites (Wang et al, 2014). Under these circumstances, and based on my results, species in the southern boreal forest will need to rely more heavily on effective precipitation and root-zone soil moisture to support their growth. Under extreme water limitations, we are likely to see a negative response to warm air temperature, reduced growth rates, and enhanced tree mortality (Barber et al., 2000; Michaelian et al., 2011; Peng et al., 2011; Walker & Johnstone 2014; Chen & Luo 2015).

Lastly, I identified that wind likely represents an important agent of disturbance in mature jack pine stands. An increase in the incidence and intensity of extreme storms and high winds (IPCC, 2013) will likely lead to more frequent high-impact disturbance in the boreal forest. While mature jack pine stands may be particularly vulnerable to this type of disturbance, this is likely to have widespread impact in a range of boreal forest stands (Rich et al., 2007). At OJP wind throw resulted in a decrease in tree-level primary production (NPP_{Tree}), however overall ecosystem production (NEP_{EC}) was not impacted.

Overall, climate change will have a varied impact on radial growth and carbon dynamics in the boreal forest. In this study, I observed contrasting drivers of radial growth and carbon dynamics in sites situated within a 50 km radius in the southern boreal forest of Saskatchewan. Further work is needed to better understand how climate change will impact radial growth and carbon dynamics in this region of Canada and beyond. It is vitally important that we first gain a broad understanding of the mechanisms responsible for governing radial growth and carbon dynamics in a range of characteristic boreal forest stands, before we can reliably interpret or forecast change. In the meantime, we must be careful not to paint the boreal forest with too wide a brush.

5.5 References

Barber, V. A., Juday, G. P., & Finney, B. P. (2000). Reduced growth of Alaskan white spruce in the twentieth century from temperature-induced drought stress. *Nature*, *405*(6787), 668–673.

Boisvenue, C., & Running, S. W. (2006). Impacts of climate change on natural forest productivity – evidence since the middle of the 20th century. *Global Change Biology*, *12*(5), 862–882.

Chen, H. Y., & Luo, Y. (2015). Net aboveground biomass declines of four major forest types with forest ageing and climate change in western Canada's boreal forests. *Global Change Biology*, *21*(10), 3675–3684.

Deslauriers, A., Huang, J.-G., Balducci, L., Beaulieu, M., & Rossi, S. (2016). The contribution of carbon and water in modulating wood formation in black spruce saplings. *Plant Physiology*, pp–01525.

D'Orangeville, L., Houle, D., Duchesne, L., Phillips, R. P., Bergeron, Y., & Kneeshaw, D. (2018). Beneficial effects of climate warming on boreal tree growth may be transitory. *Nature Communications*, *9*.

Gea-Izquierdo, G., Bergeron, Y., Huang, J.-G., Lapointe-Garant, M.-P., Grace, J., & Berninger, F. (2014). The relationship between productivity and tree-ring growth in boreal coniferous forests. *Boreal Environment Research*.

Ireson, A. M., Barr, A. G., Johnstone, J. F., Mamet, S. D., van der Kamp, G., Whitfield, C. J., Michel, N. L., North, R. L., Westbrook, C. J., DeBeer, C., & others. (2015). The

changing water cycle: The Boreal Plains ecozone of Western Canada. *Wiley Interdisciplinary Reviews: Water*, *2*(5), 505–521.

Jeong, D. I., Sushama, L., & Khaliq, M. N. (2014). The role of temperature in drought projections over North America. *Climatic Change*, *127*(2), 289–303.

Lempereur, M., Martin-StPaul, N. K., Damesin, C., Joffre, R., Ourcival, J.-M., Rocheteau, A., & Rambal, S. (2015). Growth duration is a better predictor of stem increment than carbon supply in a Mediterranean oak forest: Implications for assessing forest productivity under climate change. *New Phytologist*, *207*(3), 579–590.

Michaelian, M., Hogg, E. H., Hall, R. J., & Arsenault, E. (2011). Massive mortality of aspen following severe drought along the southern edge of the Canadian boreal forest. *Global Change Biology*, *17*(6), 2084–2094.

Peng, C., Ma, Z., Lei, X., Zhu, Q., Chen, H., Wang, W., Liu, S., Li, W., Fang, X., & Zhou, X. (2011). A drought-induced pervasive increase in tree mortality across Canada's boreal forests. *Nature Climate Change*, *1*(9), 467–471.

Rich, R. L., Frelich, L. E., & Reich, P. B. (2007). Wind-throw mortality in the southern boreal forest: Effects of species, diameter and stand age. *Journal of Ecology*, *95*(6), 1261–1273.

Richardson, A. D., Carbone, M. S., Keenan, T. F., Czimczik, C. I., Hollinger, D. Y., Murakami, P., Schaberg, P. G., & Xu, X. (2013). Seasonal dynamics and age of stemwood nonstructural carbohydrates in temperate forest trees. *New Phytologist*, *197*(3), 850–861.

Rocha, A. V., Goulden, M. L., Dunn, A. L., & Wofsy, S. C. (2006). On linking interannual tree ring variability with observations of whole-forest CO2 flux. *Global Change Biology*, *12*(8), 1378–1389.

Sellers, P., Hall, F., Ranson, K. J., Margolis, H., Kelly, B., Baldocchi, D., den Hartog, G., Cihlar, J., Ryan, M. G., & Goodison, B. (1995). The Boreal Ecosystem–Atmosphere Study (BOREAS): An overview and early results from the 1994 field year. *Bulletin of the American Meteorological Society*, *76*(9), 1549–1577.

Stocker, T. F., Qin, D., Plattner, G. K., Tignor, M., Allen, S. K., Boschung, J., Nauels, A., Xia, Y., Bex, B., & Midgley, B. M. (2013). *IPCC, 2013: Climate change 2013: the physical science basis. Contribution of working group I to the fifth assessment report of the intergovernmental panel on climate change*.

Walker, X., & Johnstone, J. F. (2014). Widespread negative correlations between black spruce growth and temperature across topographic moisture gradients in the boreal forest. *Environmental Research Letters*, *9*(6), 064016.

Wang, Y., Hogg, E. H., Price, D. T., Edwards, J., & Williamson, T. (2014). Past and projected future changes in moisture conditions in the Canadian boreal forest. *The Forestry Chronicle*, *90*(5), 678–691.

Zhang, K., Kimball, J. S., Hogg, E. H., Zhao, M., Oechel, W. C., Cassano, J. J., & Running, S. W. (2008). Satellite-based model detection of recent climate-driven changes in northern high-latitude vegetation productivity. *Journal of Geophysical Research: Biogeosciences*, *113*(G3).

Zweifel, R., Eugster, W., Etzold, S., Dobbertin, M., Buchmann, N., & Häsler, R. (2010). Link between continuous stem radius changes and net ecosystem productivity of a subalpine Norway spruce forest in the Swiss Alps. *New Phytologist*, *187*(3), 819–830.

APPENDIX A

REGRESSION ANALYSIS BETWEEN PRINCE ALBERT, WASKESIU, AND BERMS

A regression analysis was undertaken to assess the relationship between meteorological conditions at the three BERMS sites and those from nearby Environment and Climate Change Canada (ECCC) climate stations, Prince Albert (stations #4056240 and #4056241) and Waskesiu Lake (station #4068559). I compared daily mean, minimum, and maximum temperature, as well as daily precipitation at OJP, OBS, and OA, with equivalent measures from Prince Albert and Waskesiu over the 22-year data collection period at BERMS (1997 – 2018). This was done for conditions within each month independently, resulting in a series of linear models describing the relationship between monthly conditions at the BERMS sites, and those from Prince Albert and Waskesiu (Tables A.1 to A.6).

Between 1997 – 2018, conditions at Waskesiu closely resembled conditions at the BERMS sites (Tables A.4 to A.6). However, the long-term climate record only begins in 1966, and contains missing data. Comparatively, climate records from the ECCC station in Prince Albert yielded slightly weaker relationships when compared with equivalent conditions at BERMS (Tables A.1 to A.3), yet the long-term record is far more extensive, beginning in 1884 and near continuous since 1890.

Overall, mean and maximum daily temperature at the BERMS sites are closely related to equivalent conditions from both ECCC climate stations. The relationship between minimum daily temperatures at the BERMS and ECCC sites is comparatively weaker, especially during the spring and summer months (Tables A.1 to A.6).

I went on to build long-term monthly climate records for the three BERMS sites modeled from conditions at Prince Albert and Waskesiu (See Figure A.1, and Example Code below). However, relationships were close enough to justify the use of the climate record collected from Prince Albert for the annual climate analysis in Manuscript 2, allowing us to avoid introducing unnecessary uncertainty into the analysis by using modeled data.

I did not attempt to model precipitation, it is regionally defined, and thus did not yield strong relationships between the BERMS and ECCC sites. Even Waskesiu and OA, which are near one-another, had significant differences in daily rainfall (Table A.6).

Table A.1: Regression between daily conditions at Prince Albert and OJP (1997-2018)

Month	MeanAirTemp	R^2	MinAirTemp	R^2	MaxAirTemp	R^2	Precip	R^2
Jan	y = -0.927 + 0.916x	0.880	y = -1.798 + 0.826x	0.795	y = -1.659 + 0.931x	0.887	y = 0.387 + 0.581x	0.291
Feb	y = -0.467 + 0.894x	0.852	y = -1.663 + 0.797x	0.768	y = -0.565 + 0.954x	0.851	y = 0.234 + 0.628x	0.424
Mar	y = -0.120 + 0.879x	0.859	y = -1.266 + 0.790x	0.800	y = 0.067 + 0.973x	0.878	y = 0.212 + 0.884x	0.490
Apr	y = -0.331 + 0.966x	0.877	y = 0.178 + 0.889x	0.736	y = -1.136 + 0.934x	0.914	y = 0.430 + 0.614x	0.476
May	y = -1.047 + 1.039x	0.815	y = 1.489 + 0.770x	0.603	y = -2.658 + 0.990x	0.903	y = 0.432 + 0.733x	0.411
Jun	y = -0.259 + 0.993x	0.777	y = 3.341 + 0.720x	0.601	y = -1.547 + 0.975x	0.869	y = 1.330 + 0.547x	0.304
Jul	y = 0.685 + 0.949x	0.705	y = 4.322 + 0.697x	0.552	y = -1.383 + 0.989x	0.827	y = 1.398 + 0.546x	0.251
Aug	y = -0.792 + 1.031x	0.819	y = 4.137 + 0.718x	0.583	y = -2.205 + 1.007x	0.903	y = 0.640 + 0.563x	0.390
Sep	y = -0.789 + 1.015x	0.867	y = 2.413 + 0.774x	0.642	y = -2.134 + 0.978x	0.919	y = 0.464 + 0.812x	0.549
Oct	y = -0.668 + 0.989x	0.887	y = 0.747 + 0.815x	0.655	y = -1.830 + 0.959x	0.928	y = 0.402 + 0.691x	0.538
Nov	y = -1.056 + 0.935x	0.916	y = -0.854 + 0.862x	0.815	y = -1.870 + 0.962x	0.928	y = 0.259 + 0.823x	0.573
Dec	y = -0.714 + 0.948x	0.884	y = -1.136 + 0.865x	0.802	y = -1.912 + 0.937x	0.883	y = 0.277 + 0.949x	0.463

Table A.2: Regression between daily conditions at Prince Albert and OBS (1997-2018)

Month	MeanAirTemp	R^2	MinAirTemp	R^2	MaxAirTemp	R^2	Precip	R^2
Jan	y = -0.337 + 0.910x	0.774	y = -1.373 + 0.803x	0.652	y = -1.316 + 0.939x	0.828	y = 0.382 + 0.534x	0.257
Feb	y = -0.306 + 0.894x	0.831	y = -1.545 + 0.781x	0.736	y = -0.648 + 0.960x	0.843	y = 0.315 + 0.549x	0.282
Mar	y = -0.216 + 0.870x	0.854	y = -1.395 + 0.767x	0.779	y = -0.087 + 0.969x	0.872	y = 0.299 + 0.623x	0.494
Apr	y = 0.128 + 0.938x	0.679	y = 0.756 + 0.850x	0.510	y = -0.676 + 0.908x	0.768	y = 0.437 + 0.612x	0.522
May	y = -0.667 + 1.036x	0.633	y = 2.493 + 0.729x	0.334	y = -2.322 + 0.974x	0.794	y = 0.598 + 0.674x	0.382
Jun	y = 0.837 + 0.935x	0.532	y = 5.263 + 0.592x	0.247	y = -0.857 + 0.940x	0.735	y = 1.337 + 0.540x	0.314
Jul	y = 1.507 + 0.905x	0.499	y = 6.811 + 0.540x	0.205	y = -1.257 + 0.972x	0.741	y = 1.595 + 0.536x	0.216
Aug	y = -0.821 + 1.017x	0.800	y = 5.074 + 0.652x	0.482	y = -2.600 + 0.999x	0.904	y = 0.945 + 0.569x	0.280
Sep	y = -0.924 + 1.009x	0.855	y = 2.870 + 0.733x	0.556	y = -2.491 + 0.967x	0.921	y = 0.576 + 0.666x	0.537
Oct	y = -0.830 + 0.994x	0.886	y = 0.827 + 0.781x	0.609	y = -2.229 + 0.956x	0.937	y = 0.402 + 0.685x	0.632
Nov	y = -1.127 + 0.926x	0.909	y = -0.958 + 0.837x	0.802	y = -2.168 + 0.954x	0.932	y = 0.381 + 0.645x	0.436
Dec	y = -0.610 + 0.939x	0.876	y = -1.158 + 0.845x	0.785	y = -1.909 + 0.939x	0.891	y = 0.328 + 0.785x	0.346

Table A.3: Regression between daily conditions at Prince Albert and OA (1997-2018)

Month	MeanAirTemp	R^2	MinAirTemp	R^2	MaxAirTemp	R^2	Precip	R^2
Jan	y = 1.011 + 0.953x	0.903	y = 0.171 + 0.843x	0.804	y = -0.293 + 0.975x	0.929	y = 0.272 + 0.657x	0.492
Feb	y = 0.674 + 0.908x	0.886	y = -0.474 + 0.776x	0.766	y = -0.116 + 0.986x	0.934	y = 0.171 + 0.703x	0.518
Mar	y = 0.367 + 0.884x	0.905	y = -0.059 + 0.776x	0.815	y = -0.448 + 0.972x	0.948	y = 0.306 + 0.651x	0.460
Apr	y = -0.116 + 0.998x	0.897	y = 1.242 + 0.865x	0.697	y = -1.671 + 0.954x	0.958	y = 0.401 + 0.620x	0.537
May	y = -0.470 + 1.035x	0.839	y = 2.726 + 0.741x	0.546	y = -2.070 + 0.972x	0.951	y = 0.405 + 0.768x	0.493
Jun	y = -0.043 + 0.975x	0.777	y = 4.781 + 0.629x	0.464	y = -1.495 + 0.950x	0.935	y = 0.848 + 0.645x	0.507
Jul	y = 0.664 + 0.933x	0.730	y = 6.253 + 0.587x	0.393	y = -1.046 + 0.939x	0.898	y = 1.103 + 0.611x	0.269
Aug	y = -0.366 + 0.998x	0.792	y = 5.890 + 0.613x	0.408	y = -2.071 + 0.971x	0.928	y = 0.596 + 0.631x	0.387
Sep	y = -0.321 + 1.001x	0.843	y = 3.663 + 0.692x	0.500	y = -2.047 + 0.968x	0.945	y = 0.320 + 0.849x	0.698
Oct	y = -0.297 + 1.046x	0.901	y = 1.669 + 0.828x	0.594	y = -1.773 + 0.983x	0.962	y = 0.223 + 0.739x	0.531
Nov	y = -0.240 + 0.933x	0.922	y = 0.127 + 0.845x	0.816	y = -1.429 + 0.954x	0.948	y = 0.339 + 0.637x	0.301
Dec	y = 0.477 + 0.948x	0.901	y = -0.149 + 0.841x	0.798	y = -0.802 + 0.954x	0.927	y = 0.173 + 0.928x	0.616

Table A.4: Regression between daily conditions at Waskesiu and OJP (1997-2018)

Month	MeanAirTemp	R^2	MinAirTemp	R^2	MaxAirTemp	R^2	Precip	R^2
Jan	y = -1.354 + 0.948x	0.952	y = -1.734 + 0.906x	0.921	y = -1.517 + 0.958x	0.954	y = 0.167 + 0.931x	0.498
Feb	y = -0.946 + 0.945x	0.943	y = -1.064 + 0.907x	0.904	y = -1.132 + 0.973x	0.948	y = 0.163 + 0.626x	0.459
Mar	y = -0.497 + 0.942x	0.948	y = -0.702 + 0.897x	0.905	y = -0.732 + 0.992x	0.959	y = 0.314 + 0.554x	0.282
Apr	y = 0.169 + 0.989x	0.938	y = 0.454 + 0.937x	0.852	y = -0.622 + 0.988x	0.954	y = 0.327 + 0.683x	0.487
May	y = -0.351 + 1.044x	0.911	y = 0.823 + 0.918x	0.806	y = -1.088 + 0.997x	0.937	y = 0.471 + 0.620x	0.421
Jun	y = -0.070 + 1.016x	0.876	y = 1.609 + 0.891x	0.792	y = -0.461 + 0.987x	0.906	y = 1.486 + 0.530x	0.265
Jul	y = 0.088 + 1.010x	0.842	y = 1.921 + 0.886x	0.723	y = -0.298 + 0.994x	0.887	y = 1.400 + 0.472x	0.270
Aug	y = -0.554 + 1.039x	0.905	y = 1.198 + 0.934x	0.786	y = -0.407 + 0.997x	0.918	y = 0.613 + 0.546x	0.389
Sep	y = -0.644 + 1.031x	0.934	y = 0.487 + 0.965x	0.826	y = -0.854 + 1.005x	0.947	y = 0.423 + 0.693x	0.492
Oct	y = -0.620 + 0.991x	0.939	y = -0.023 + 0.972x	0.838	y = -0.833 + 0.986x	0.955	y = 0.454 + 0.516x	0.510
Nov	y = -0.897 + 0.980x	0.962	y = -0.665 + 0.976x	0.922	y = -1.024 + 0.989x	0.964	y = 0.165 + 0.809x	0.542
Dec	y = -0.973 + 0.975x	0.954	y = -1.035 + 0.944x	0.927	y = -1.553 + 0.957x	0.942	y = 0.201 + 0.815x	0.483

Table A.5: Regression between daily conditions at Waskesiu and OBS (1997-2018)

Month	MeanAirTemp	R^2	MinAirTemp	R^2	MaxAirTemp	R^2	Precip	R^2
Jan	y = -0.631 + 0.950x	0.851	y = -0.91 + 0.901x	0.790	y = -1.205 + 0.962x	0.883	y = 0.206 + 0.814x	0.412
Feb	y = -0.693 + 0.952x	0.933	y = -0.732 + 0.902x	0.890	y = -1.225 + 0.979x	0.938	y = 0.311 + 0.449x	0.202
Mar	y = -0.548 + 0.939x	0.954	y = -0.741 + 0.879x	0.899	y = -0.880 + 0.995x	0.966	y = 0.364 + 0.395x	0.287
Apr	y = 0.653 + 0.956x	0.714	y = 1.068 + 0.901x	0.589	y = -0.163 + 0.959x	0.799	y = 0.315 + 0.706x	0.574
May	y = -0.077 + 1.049x	0.726	y = 1.675 + 0.931x	0.512	y = -0.811 + 0.983x	0.828	y = 0.557 + 0.623x	0.454
Jun	y = 0.548 + 0.989x	0.635	y = 3.144 + 0.809x	0.397	y = -0.089 + 0.966x	0.787	y = 1.320 + 0.585x	0.344
Jul	y = 0.292 + 0.999x	0.649	y = 3.574 + 0.801x	0.366	y = -0.574 + 0.993x	0.827	y = 1.364 + 0.525x	0.306
Aug	y = -0.816 + 1.040x	0.908	y = 2.012 + 0.884x	0.707	y = -1.217 + 1.007x	0.952	y = 0.852 + 0.556x	0.307
Sep	y = -0.892 + 1.035x	0.938	y = 0.837 + 0.951x	0.771	y = -1.324 + 1.000x	0.961	y = 0.490 + 0.591x	0.534
Oct	y = -0.806 + 1.002x	0.949	y = 0.109 + 0.958x	0.821	y = -1.265 + 0.987x	0.972	y = 0.539 + 0.447x	0.456
Nov	y = -0.937 + 0.976x	0.966	y = -0.688 + 0.956x	0.925	y = -1.330 + 0.982x	0.972	y = 0.234 + 0.725x	0.548
Dec	y = -0.773 + 0.973x	0.959	y = -0.866 + 0.932x	0.928	y = -1.525 + 0.961x	0.954	y = 0.233 + 0.731x	0.425

Table A.6: Regression between daily conditions at Waskesiu and OA (1997-2018)

Month	MeanAirTemp	R^2	MinAirTemp	R^2	MaxAirTemp	R^2	Precip	R^2
Jan	y = 0.425 + 0.978x	0.967	y = 0.155 + 0.920x	0.936	y = -0.385 + 0.981x	0.959	y = 0.259 + 0.732x	0.313
Feb	y = 0.037 + 0.950x	0.954	y = 0.209 + 0.889x	0.909	y = -1.098 + 0.955x	0.936	y = 0.190 + 0.486x	0.295
Mar	y = -0.043 + 0.933x	0.964	y = 0.528 + 0.877x	0.917	y = -1.229 + 0.956x	0.953	y = 0.370 + 0.398x	0.271
Apr	y = 0.572 + 0.990x	0.949	y = 1.529 + 0.894x	0.840	y = -0.846 + 0.984x	0.971	y = 0.369 + 0.612x	0.454
May	y = 0.276 + 1.035x	0.935	y = 2.042 + 0.918x	0.789	y = -0.313 + 0.964x	0.968	y = 0.285 + 0.786x	0.688
Jun	y = -0.02 + 1.009x	0.893	y = 2.679 + 0.847x	0.720	y = -0.173 + 0.947x	0.955	y = 0.745 + 0.744x	0.575
Jul	y = 0.109 + 0.993x	0.878	y = 3.471 + 0.812x	0.624	y = 0.414 + 0.926x	0.930	y = 0.594 + 0.745x	0.535
Aug	y = -0.475 + 1.028x	0.908	y = 2.431 + 0.886x	0.679	y = -0.625 + 0.974x	0.958	y = 0.285 + 0.749x	0.572
Sep	y = -0.354 + 1.031x	0.937	y = 1.453 + 0.941x	0.750	y = -0.736 + 0.992x	0.975	y = 0.198 + 0.781x	0.715
Oct	y = -0.213 + 1.046x	0.956	y = 0.931 + 1.011x	0.816	y = -0.675 + 1.000x	0.970	y = 0.369 + 0.464x	0.359
Nov	y = -0.097 + 0.979x	0.972	y = 0.296 + 0.959x	0.931	y = -0.607 + 0.977x	0.974	y = 0.218 + 0.695x	0.339
Dec	y = 0.194 + 0.971x	0.966	y = 0.018 + 0.919x	0.932	y = -0.482 + 0.965x	0.964	y = 0.163 + 0.699x	0.481

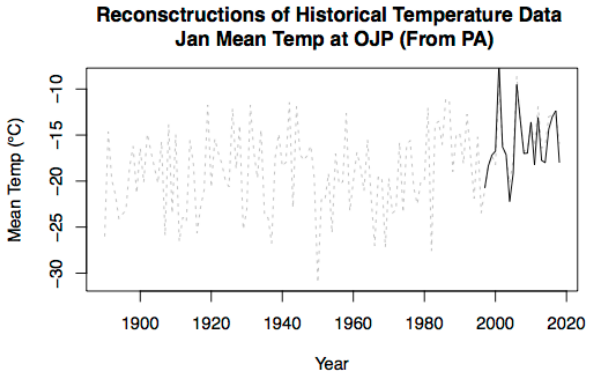
Reconsctructions of Historical Temperature Data
Jan Mean Temp at OJP (From PA)
Mean Temp (°C)
−10
−15
−20
−25
−30
1900
1920
1940
1960
1980
2000
2020
Year

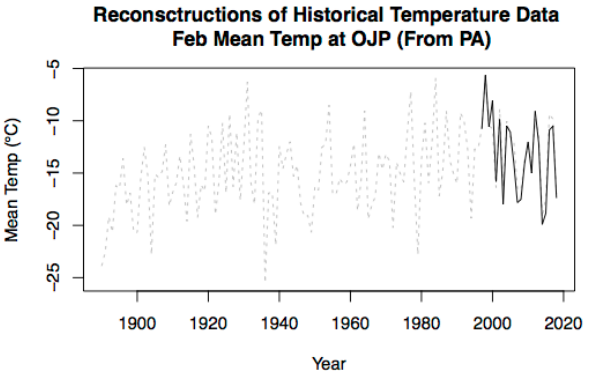
Reconsctructions of Historical Temperature Data
Feb Mean Temp at OJP (From PA)
Mean Temp (°C)
−5
−10
−15
−20
−25
1900
1920
1940
1960
1980
2000
2020
Year

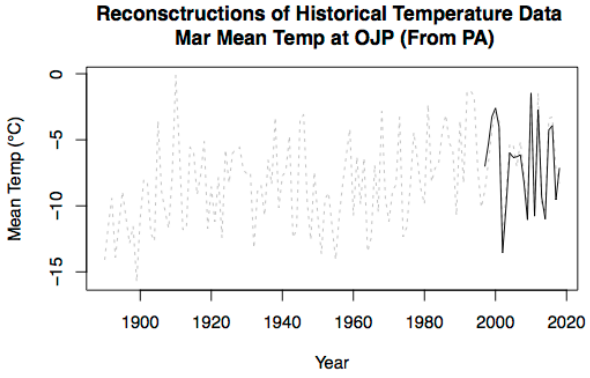
Reconsctructions of Historical Temperature Data
Mar Mean Temp at OJP (From PA)
Mean Temp (°C)
0
−5
−10
−15
1900
1920
1940
1960
1980
2000
2020
Year

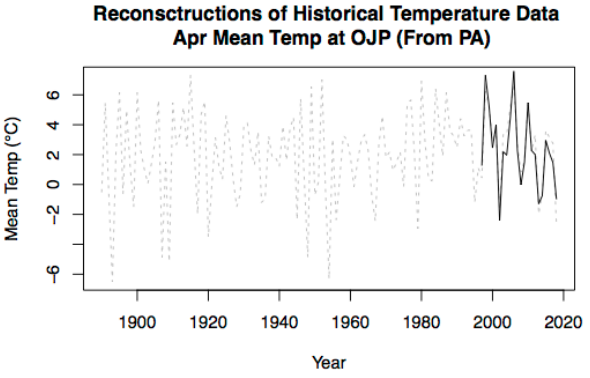
Reconsctructions of Historical Temperature Data
Apr Mean Temp at OJP (From PA)
Mean Temp (°C)
6
4
2
0
−2
−6
1900
1920
1940
1960
1980
2000
2020
Year

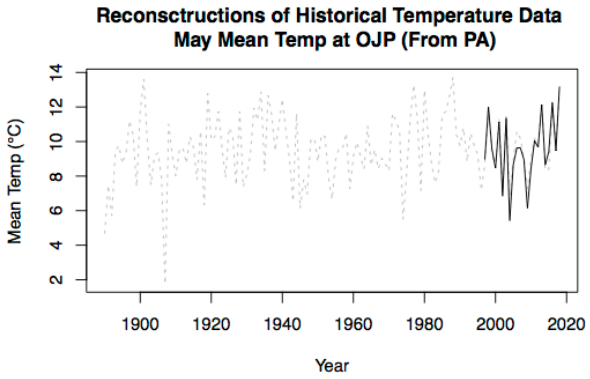
Reconsctructions of Historical Temperature Data
May Mean Temp at OJP (From PA)
Mean Temp (°C)
14
12
10
8
6
4
2
1900
1920
1940
1960
1980
2000
2020
Year

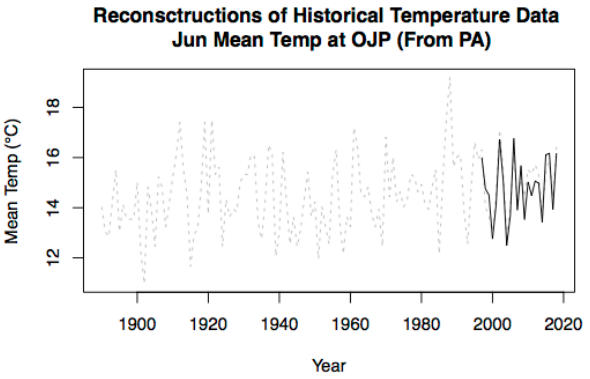
Reconsctructions of Historical Temperature Data
Jun Mean Temp at OJP (From PA)
Mean Temp (°C)
18
16
14
12
1900
1920
1940
1960
1980
2000
2020
Year

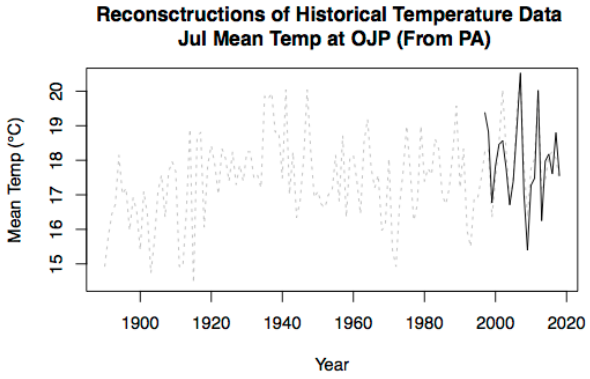
Reconsctructions of Historical Temperature Data
Jul Mean Temp at OJP (From PA)
Mean Temp (°C)
20
19
18
17
16
15
1900
1920
1940
1960
1980
2000
2020
Year

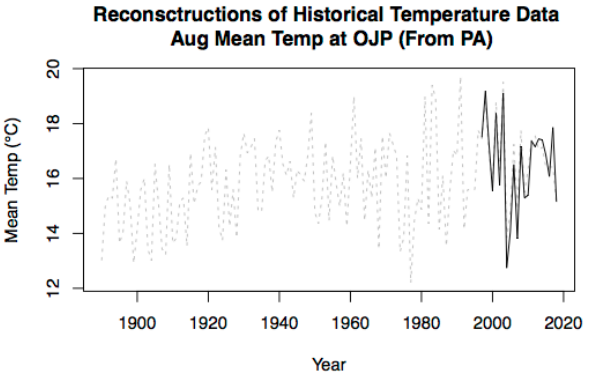
Reconsctructions of Historical Temperature Data
Aug Mean Temp at OJP (From PA)
Mean Temp (°C)
20
18
16
14
12
1900
1920
1940
1960
1980
2000
2020
Year

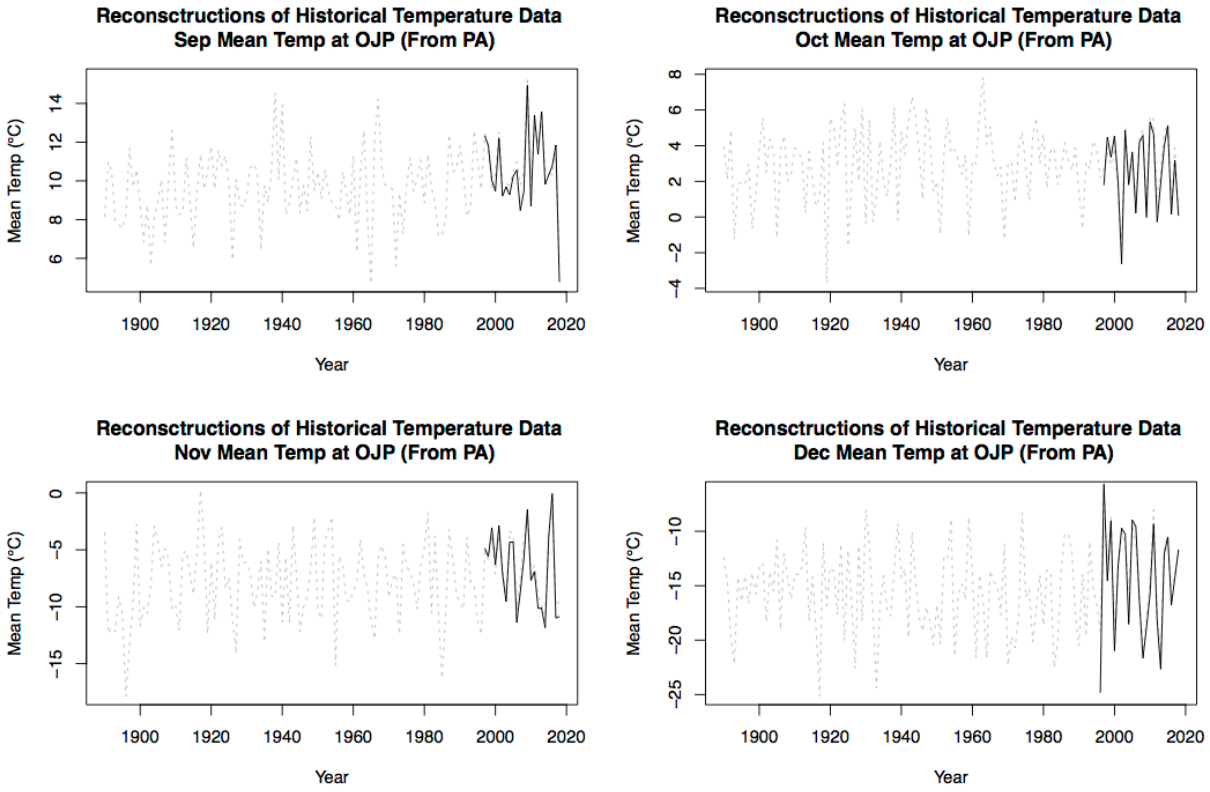

Figure A.1: Monthly mean temperature at OJP modeled from ECCC climate data from Prince Albert station # 4056241 (grey dotted line), compared with instrumental temperature from BERMS OJP 1997-2018 (solid black line).

Example Code

```
#Modeled monthly temperature at OJP from PA.

### Read in daily data

filesPA <- dir(file.path("data/climatePA"), pattern = "*.csv", full.names = T) # Folder containing raw output from https://climate.weather.gc.ca/historical_data/search_historic_data_e.html (daily conditions at Prince Albert from 1997 - 2018)

daily.clim.PA <- filesPA %>%
  map_df(~read_csv(.x, col_types = cols(.default = "d", `Date/Time` = col_character()), skip = 24)) %>%
  mutate(`Date` = ymd(`Date/Time`, tz = "America/Regina")) %>%
  mutate(AirTempPA = `Mean Temp (°C)`) %>%
  mutate(minAirTempPA = `Min Temp (°C)`) %>%
  mutate(maxAirTempPA = `Max Temp (°C)`) %>%
  mutate(PrecipPA = `Total Precip (mm)`) %>%
  select(Date, Year, Month, Day, AirTempPA, minAirTempPA, maxAirTempPA, PrecipPA)
daily.climate.OJP <- read_csv("~/Desktop/BERMS Analysis/Climate Daily/daily.climate.OJP.csv") %>%
  mutate(`Date` = ymd(`Date`, tz = "America/Regina")) %>%
  mutate(AirTempOJP = AirTemp) %>%
  mutate(minAirTempOJP = minAirTemp) %>%
  mutate(maxAirTempOJP = maxAirTemp) %>%
  mutate(PrecipOJP = Precip) %>%
  select(Date, Year, Month, Day, AirTempOJP, minAirTempOJP, maxAirTempOJP, PrecipOJP)

daily.climate.OBS <- read_csv("~/Desktop/BERMS Analysis/Climate Daily/daily.climate.OBS.csv") %>%
  mutate(`Date` = ymd(`Date`, tz = "America/Regina")) %>%
  mutate(AirTempOBS = AirTemp) %>%
  mutate(minAirTempOBS = minAirTemp) %>%
  mutate(maxAirTempOBS = maxAirTemp) %>%
  mutate(PrecipOBS = Precip) %>%
  select(Date, Year, Month, Day, AirTempOBS, minAirTempOBS, maxAirTempOBS, PrecipOBS)

daily.climate.OA <- read_csv("~/Desktop/BERMS Analysis/Climate Daily/daily.climate.OA.csv") %>%
  mutate(`Date` = ymd(`Date`, tz = "America/Regina")) %>%
  mutate(AirTempOA = AirTemp) %>%
  mutate(minAirTempOA = minAirTemp) %>%
  mutate(maxAirTempOA = maxAirTemp) %>%
  mutate(PrecipOA = Precip) %>%
  select(Date, Year, Month, Day, AirTempOA, minAirTempOA, maxAirTempOA, PrecipOA)
### Join
```

```
Daily.Climate <- daily.clim.PA %>%
  left_join(daily.climate.OJP) %>%
  left_join(daily.climate.OBS) %>%
  left_join(daily.climate.OA)

### Subset by month

Jan.Daily.Climate <- Daily.Climate %>%
  filter(Month == 1)
Feb.Daily.Climate <- Daily.Climate %>%
  filter(Month == 2)
Mar.Daily.Climate <- Daily.Climate %>%
  filter(Month == 3)
Apr.Daily.Climate <- Daily.Climate %>%
  filter(Month == 4)
May.Daily.Climate <- Daily.Climate %>%
  filter(Month == 5)
Jun.Daily.Climate <- Daily.Climate %>%
  filter(Month == 6)
Jul.Daily.Climate <- Daily.Climate %>%
  filter(Month == 7)
Aug.Daily.Climate <- Daily.Climate %>%
  filter(Month == 8)
Sep.Daily.Climate <- Daily.Climate %>%
  filter(Month == 9)
Oct.Daily.Climate <- Daily.Climate %>%
  filter(Month == 10)
Nov.Daily.Climate <- Daily.Climate %>%
  filter(Month == 11)
Dec.Daily.Climate <- Daily.Climate %>%
  filter(Month == 12)

### Build linear models

Jan.OJPvPA.AT <- lm(Jan.Daily.Climate$AirTempOJP ~ Jan.Daily.Climate$AirTempPA)
Feb.OJPvPA.AT <- lm(Feb.Daily.Climate$AirTempOJP ~ Feb.Daily.Climate$AirTempPA)
Mar.OJPvPA.AT <- lm(Mar.Daily.Climate$AirTempOJP ~ Mar.Daily.Climate$AirTempPA)
Apr.OJPvPA.AT <- lm(Apr.Daily.Climate$AirTempOJP ~ Apr.Daily.Climate$AirTempPA)
May.OJPvPA.AT <- lm(May.Daily.Climate$AirTempOJP ~ May.Daily.Climate$AirTempPA)
Jun.OJPvPA.AT <- lm(Jun.Daily.Climate$AirTempOJP ~ Jun.Daily.Climate$AirTempPA)
Jul.OJPvPA.AT <- lm(Jul.Daily.Climate$AirTempOJP ~ Jul.Daily.Climate$AirTempPA)
Aug.OJPvPA.AT <- lm(Aug.Daily.Climate$AirTempOJP ~ Aug.Daily.Climate$AirTempPA)
Sep.OJPvPA.AT <- lm(Sep.Daily.Climate$AirTempOJP ~ Sep.Daily.Climate$AirTempPA)
Oct.OJPvPA.AT <- lm(Oct.Daily.Climate$AirTempOJP ~ Oct.Daily.Climate$AirTempPA)
Nov.OJPvPA.AT <- lm(Nov.Daily.Climate$AirTempOJP ~ Nov.Daily.Climate$AirTempPA)
```

```
Dec.OJPvPA.AT <- lm(Dec.Daily.Climate$AirTempOJP ~ Dec.Daily.Climate$AirTempPA)

Jan.OJPvPA.mT <- lm(Jan.Daily.Climate$minAirTempOJP ~
Jan.Daily.Climate$minAirTempPA)
Feb.OJPvPA.mT <- lm(Feb.Daily.Climate$minAirTempOJP ~
Feb.Daily.Climate$minAirTempPA)
Mar.OJPvPA.mT <- lm(Mar.Daily.Climate$minAirTempOJP ~
Mar.Daily.Climate$minAirTempPA)
Apr.OJPvPA.mT <- lm(Apr.Daily.Climate$minAirTempOJP ~
Apr.Daily.Climate$minAirTempPA)
May.OJPvPA.mT <- lm(May.Daily.Climate$minAirTempOJP ~
May.Daily.Climate$minAirTempPA)
Jun.OJPvPA.mT <- lm(Jun.Daily.Climate$minAirTempOJP ~
Jun.Daily.Climate$minAirTempPA)
Jul.OJPvPA.mT <- lm(Jul.Daily.Climate$minAirTempOJP ~
Jul.Daily.Climate$minAirTempPA)
Aug.OJPvPA.mT <- lm(Aug.Daily.Climate$minAirTempOJP ~
Aug.Daily.Climate$minAirTempPA)
Sep.OJPvPA.mT <- lm(Sep.Daily.Climate$minAirTempOJP ~
Sep.Daily.Climate$minAirTempPA)
Oct.OJPvPA.mT <- lm(Oct.Daily.Climate$minAirTempOJP ~
Oct.Daily.Climate$minAirTempPA)
Nov.OJPvPA.mT <- lm(Nov.Daily.Climate$minAirTempOJP ~
Nov.Daily.Climate$minAirTempPA)
Dec.OJPvPA.mT <- lm(Dec.Daily.Climate$minAirTempOJP ~
Dec.Daily.Climate$minAirTempPA)
Jan.OJPvPA.MT <- lm(Jan.Daily.Climate$maxAirTempOJP ~
Jan.Daily.Climate$maxAirTempPA)
Feb.OJPvPA.MT <- lm(Feb.Daily.Climate$maxAirTempOJP ~
Feb.Daily.Climate$maxAirTempPA)
Mar.OJPvPA.MT <- lm(Mar.Daily.Climate$maxAirTempOJP ~
Mar.Daily.Climate$maxAirTempPA)
Apr.OJPvPA.MT <- lm(Apr.Daily.Climate$maxAirTempOJP ~
Apr.Daily.Climate$maxAirTempPA)
May.OJPvPA.MT <- lm(May.Daily.Climate$maxAirTempOJP ~
May.Daily.Climate$maxAirTempPA)
Jun.OJPvPA.MT <- lm(Jun.Daily.Climate$maxAirTempOJP ~
Jun.Daily.Climate$maxAirTempPA)
Jul.OJPvPA.MT <- lm(Jul.Daily.Climate$maxAirTempOJP ~
Jul.Daily.Climate$maxAirTempPA)
Aug.OJPvPA.MT <- lm(Aug.Daily.Climate$maxAirTempOJP ~
Aug.Daily.Climate$maxAirTempPA)
Sep.OJPvPA.MT <- lm(Sep.Daily.Climate$maxAirTempOJP ~
Sep.Daily.Climate$maxAirTempPA)
Oct.OJPvPA.MT <- lm(Oct.Daily.Climate$maxAirTempOJP ~
Oct.Daily.Climate$maxAirTempPA)
```

```
Nov.OJPvPA.MT <- lm(Nov.Daily.Climate$maxAirTempOJP ~
Nov.Daily.Climate$maxAirTempPA)
Dec.OJPvPA.MT <- lm(Dec.Daily.Climate$maxAirTempOJP ~
Dec.Daily.Climate$maxAirTempPA)

### Read in monthly climate data

MonthlyMeanTempPA <- read_csv("~/Desktop/BERMS Analysis/Annual
Data/meanTempPA.csv")
MonthlyMinTempPA <- read_csv("~/Desktop/BERMS Analysis/Annual
Data/minTempPA.csv")
MonthlyMaxTempPA <- read_csv("~/Desktop/BERMS Analysis/Annual
Data/maxTempPA.csv")

### Model monthly temperature at OJP

MeanTempOJPfromPA <- MonthlyMeanTempPA %>%
  mutate(Year = Year) %>%
  mutate(Jan = Jan*coef(Jan.OJPvPA.AT)[[2]] + coef(Jan.OJPvPA.AT)[[1]]) %>%
  mutate(Feb = Feb*coef(Feb.OJPvPA.AT)[[2]] + coef(Feb.OJPvPA.AT)[[1]]) %>%
  mutate(Mar = Mar*coef(Mar.OJPvPA.AT)[[2]] + coef(Mar.OJPvPA.AT)[[1]]) %>%
  mutate(Apr = Apr*coef(Apr.OJPvPA.AT)[[2]] + coef(Apr.OJPvPA.AT)[[1]]) %>%
  mutate(May = May*coef(May.OJPvPA.AT)[[2]] + coef(May.OJPvPA.AT)[[1]]) %>%
  mutate(Jun = Jun*coef(Jun.OJPvPA.AT)[[2]] + coef(Jun.OJPvPA.AT)[[1]]) %>%
  mutate(Jul = Jul*coef(Jul.OJPvPA.AT)[[2]] + coef(Jul.OJPvPA.AT)[[1]]) %>%
  mutate(Aug = Aug*coef(Aug.OJPvPA.AT)[[2]] + coef(Aug.OJPvPA.AT)[[1]]) %>%
  mutate(Sep = Sep*coef(Sep.OJPvPA.AT)[[2]] + coef(Sep.OJPvPA.AT)[[1]]) %>%
  mutate(Oct = Oct*coef(Oct.OJPvPA.AT)[[2]] + coef(Oct.OJPvPA.AT)[[1]]) %>%
  mutate(Nov = Nov*coef(Nov.OJPvPA.AT)[[2]] + coef(Nov.OJPvPA.AT)[[1]]) %>%
  mutate(Dec = Dec*coef(Dec.OJPvPA.AT)[[2]] + coef(Dec.OJPvPA.AT)[[1]])

MinTempOJPfromPA <- MonthlyMinTempPA %>%
  mutate(Year = Year) %>%
  mutate(Jan = Jan*coef(Jan.OJPvPA.mT)[[2]] + coef(Jan.OJPvPA.mT)[[1]]) %>%
  mutate(Feb = Feb*coef(Feb.OJPvPA.mT)[[2]] + coef(Feb.OJPvPA.mT)[[1]]) %>%
  mutate(Mar = Mar*coef(Mar.OJPvPA.mT)[[2]] + coef(Mar.OJPvPA.mT)[[1]]) %>%
  mutate(Apr = Apr*coef(Apr.OJPvPA.mT)[[2]] + coef(Apr.OJPvPA.mT)[[1]]) %>%
  mutate(May = May*coef(May.OJPvPA.mT)[[2]] + coef(May.OJPvPA.mT)[[1]]) %>%
  mutate(Jun = Jun*coef(Jun.OJPvPA.mT)[[2]] + coef(Jun.OJPvPA.mT)[[1]]) %>%
  mutate(Jul = Jul*coef(Jul.OJPvPA.mT)[[2]] + coef(Jul.OJPvPA.mT)[[1]]) %>%
  mutate(Aug = Aug*coef(Aug.OJPvPA.mT)[[2]] + coef(Aug.OJPvPA.mT)[[1]]) %>%
  mutate(Sep = Sep*coef(Sep.OJPvPA.mT)[[2]] + coef(Sep.OJPvPA.mT)[[1]]) %>%
  mutate(Oct = Oct*coef(Oct.OJPvPA.mT)[[2]] + coef(Oct.OJPvPA.mT)[[1]]) %>%
  mutate(Nov = Nov*coef(Nov.OJPvPA.mT)[[2]] + coef(Nov.OJPvPA.mT)[[1]]) %>%
  mutate(Dec = Dec*coef(Dec.OJPvPA.mT)[[2]] + coef(Dec.OJPvPA.mT)[[1]])
```

```
MaxTempOJPfromPA <- MonthlyMaxTempPA %>%
  mutate(Year = Year) %>%
  mutate(Jan = Jan*coef(Jan.OJPvPA.MT)[[2]] + coef(Jan.OJPvPA.MT)[[1]]) %>%
  mutate(Feb = Feb*coef(Feb.OJPvPA.MT)[[2]] + coef(Feb.OJPvPA.MT)[[1]]) %>%
  mutate(Mar = Mar*coef(Mar.OJPvPA.MT)[[2]] + coef(Mar.OJPvPA.MT)[[1]]) %>%
  mutate(Apr = Apr*coef(Apr.OJPvPA.MT)[[2]] + coef(Apr.OJPvPA.MT)[[1]]) %>%
  mutate(May = May*coef(May.OJPvPA.MT)[[2]] + coef(May.OJPvPA.MT)[[1]]) %>%
  mutate(Jun = Jun*coef(Jun.OJPvPA.MT)[[2]] + coef(Jun.OJPvPA.MT)[[1]]) %>%
  mutate(Jul = Jul*coef(Jul.OJPvPA.MT)[[2]] + coef(Jul.OJPvPA.MT)[[1]]) %>%
  mutate(Aug = Aug*coef(Aug.OJPvPA.MT)[[2]] + coef(Aug.OJPvPA.MT)[[1]]) %>%
  mutate(Sep = Sep*coef(Sep.OJPvPA.MT)[[2]] + coef(Sep.OJPvPA.MT)[[1]]) %>%
  mutate(Oct = Oct*coef(Oct.OJPvPA.MT)[[2]] + coef(Oct.OJPvPA.MT)[[1]]) %>%
  mutate(Nov = Nov*coef(Nov.OJPvPA.MT)[[2]] + coef(Nov.OJPvPA.MT)[[1]]) %>%
  mutate(Dec = Dec*coef(Dec.OJPvPA.MT)[[2]] + coef(Dec.OJPvPA.MT)[[1]])

write.csv(MeanTempOJPfromPA, "~/Desktop/BERMS Analysis/Annual
Data/meanTempOJPPA.csv")
write.csv(MinTempOJPfromPA, "~/Desktop/BERMS Analysis/Annual
Data/minTempOJPPA.csv")
write.csv(MaxTempOJPfromPA, "~/Desktop/BERMS Analysis/Annual
Data/maxTempOJPPA.csv")

### Plot against instrumental temperature (1997-2018)

plot(meanTempOJPPA$Year, meanTempOJPPA$Jan,
    main = "Reconsctructions of Historical Temperature Data \n Jan Mean Temp at OJP (From
PA)",
    xlab = "Year",
    ylab = "Mean Temp (°C)",
    type = "l",
    lty = 2,
    col = "Grey")
lines(MeanTempOJP$Year, MeanTempOJP$Jan,
     col = "Black")
```

APPENDIX B

A COMPARISON OF TECHNIQUES FOR EXTRACTING AND REPRESENTING HIGH RESOLUTION RADIAL INCREMENT DATA

Automatic dendrometers produce high resolution records of stem size, capturing both reversible and irreversible variation associated with water and growth dynamics. In this dissertation, a comprehensive assessment of radial growth and its interactions with climate and carbon across the temporal scale, it is important to effectively disentangle the growth signal from the water signal. The stem-water signal functions on sub-daily to daily scales, largely driven by diurnal fluctuations in temperature and transpiration, as well as precipitation and soil moisture (Herzog et al., 1995). The finest resolution one can hope to achieve, in describing the radial increment, is therefore daily.

The most common methods for extracting radial growth records from high-resolution dendrometer data are the "stem cycle approach" and the "daily approach" discussed and compared at length in Deslauriers et al. (2007). In this section, these methods are compared. For the stem cycle approach, the dendrometeR package (van der Maaten et al., 2016) was used to breakdown each cycle into its distinct phases, contraction (phase 1), expansion (phase 2), and the radial increment (phase 3). The radial increment phase is only present when the previous cycles' maximum is surpassed during the current cycle. Therefore, each cycle does not necessarily contain a phase 3. The dendrometeR package also produces data regarding a phase 4, which describes the properties of each complete cycle, and contains information regarding cycle maxima regardless of whether peak stem size from the previous day was surpassed. The daily approach involves extracting a daily mean, maximum, and minimum for each 24h period. A simple R-script was written to extract these values. Data for both the stem cycle and daily approaches are calculated for each tree individually before calculating a site average (Figures B.1 – B.4).

The main difference between the stem cycle approach and the daily approach is the way the dataset is broken up, with one governed by the length of each stem cycle, and the other governed by the hours in a day. The stem cycle may therefore last longer than 24 hours in response to a long expansion phase, or if there is no discernable contraction phase. This would

result in an exaggerated radial increment or cycle maxima that is more likely to be related to an input of moisture, rather than a pulse of radial growth. The other difference is the level of complexity associated with each extraction method. For the stem cycle approach, before the data can be broken down into cycles and cycle phases, a gap filling procedure must be run in the presence of missing data. This was necessary in several instances with my data, due to gaps resulting from sensor malfunction, and issues with wildlife. The added complexity associated with the stem cycle approach may result in a higher level of uncertainty.

Due to the potential for the stem cycle approach to produce exaggerated stem size data in response to precipitation (Figures B.1 – B.4), and due to uncertainty introduced by the gap filling procedure, records of mean daily stem size are used for analysis in Manuscripts one and two (Chapters 2 and 3). This is further justified considering the findings from Deslauriers et al. (2007), which found a tight correlation between records of mean daily stem size, and increment data produced using the stem cycle approach.

When it comes to representing stem size data, there are a few options. Radial increment data are often recorded as stem radius variations, based on the change in stem size between subsequent days or cycles (Deslauriers et al., 2007). This produces a "flat" dataset of stem radius that fluctuates around zero. Stem radius change (ΔR) is exactly zero when there is no change in stem radius between two subsequent days or cycles. It is positive ($\Delta R+$) if there is an increase in stem size, or negative ($\Delta R-$) if there is a decrease in stem size, compared with the previous day or cycle. Another option is to construct radial increment time series that are cumulative, beginning from an initial DBH, or from zero (See Figure B.5 for a comparison). This is often used as a simple depiction of radial growth, which is cumulative by nature. Data of ΔR are used for statistical analysis.

References

Deslauriers, A., Rossi, S., & Anfodillo, T. (2007). Dendrometer and intra-annual tree growth: What kind of information can be inferred? *Dendrochronologia*, *25*(2), 113–124.

Herzog, K. M., Häsler, R., & Thum, R. (1995). Diurnal changes in the radius of a subalpine Norway spruce stem: Their relation to the sap flow and their use to estimate transpiration. *Trees*, *10*(2), 94–101.

van der Maaten, E., van der Maaten-Theunissen, M., Smiljanic, M., Rossi, S., Simard, S., Wilmking, M., Deslauriers, A., Fonti, P., von Arx, G., & Bouriaud, O. (2016). dendrometeR: Analyzing the pulse of trees in R. *Dendrochronologia*, 40.

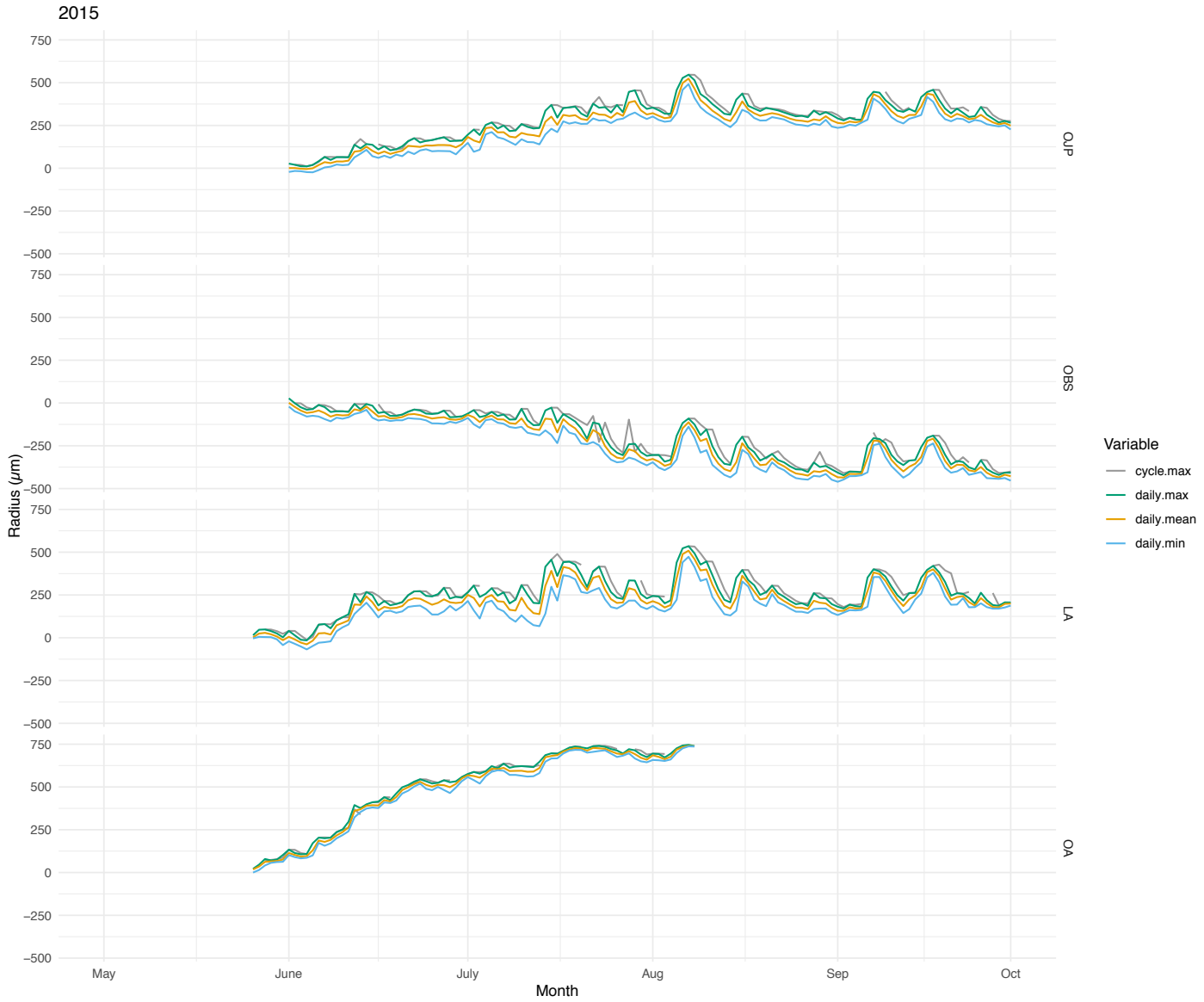

Figure B.1: Comparing records of daily stem size from the 2015 growing season extracted using the daily approach (daily.max, daily.mean, daily.min), and the stem cycle approach (cycle.max), representative of each cycle's peak (phase 4, max).

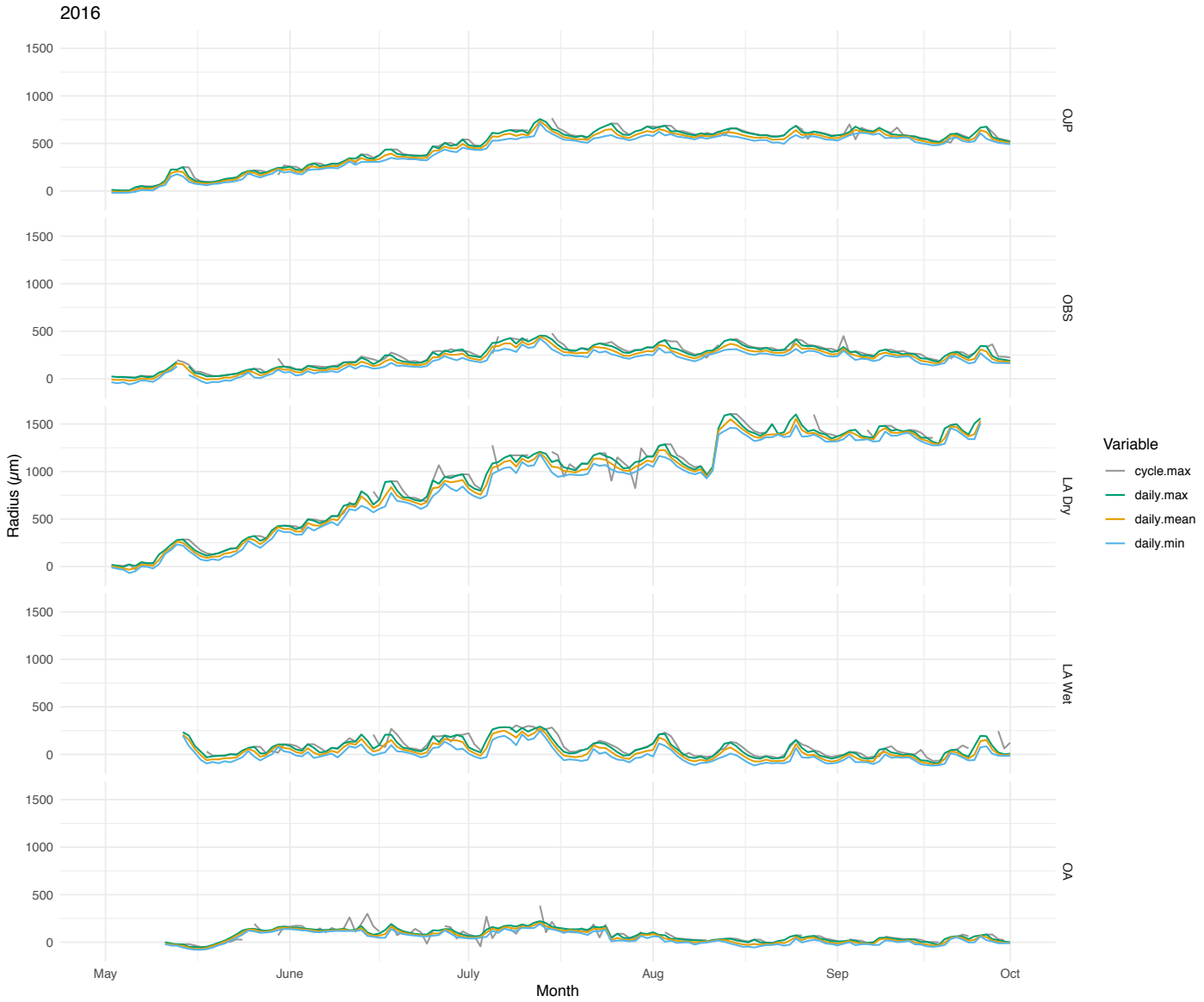

Figure B.2: Comparing records of daily stem size from the 2016 growing season extracted using the daily approach (daily.max, daily.mean, daily.min), and the stem cycle approach (cycle.max), representative of each cycle's peak (phase 4, max).

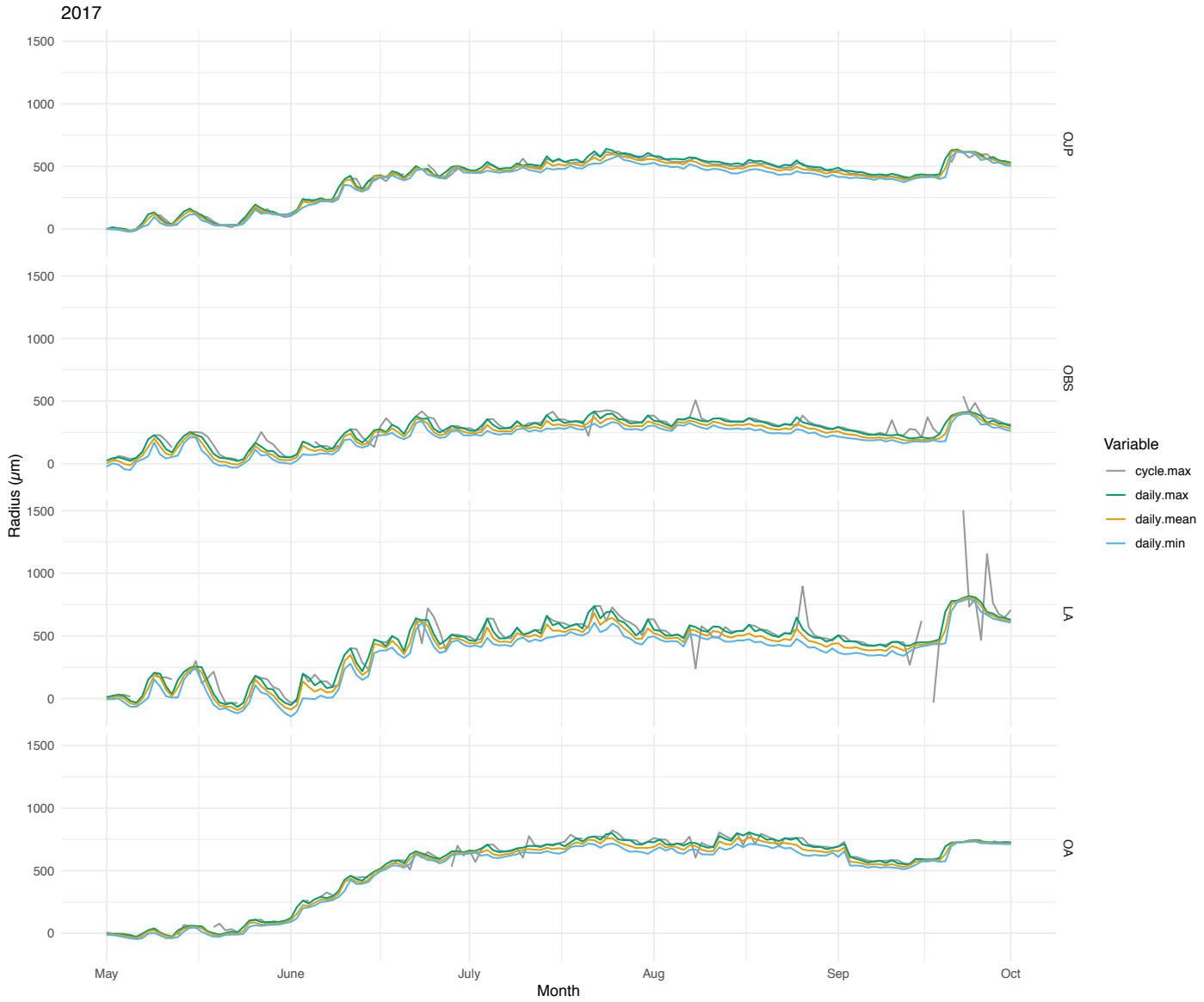

Figure B.3: Comparing records of daily stem size from the 2017 growing season extracted using the daily approach (daily.max, daily.mean, daily.min), and the stem cycle approach (cycle.max), representative of each cycle's peak (phase 4, max).

Figure B.4: Comparing records of daily stem size from the 2018 growing season extracted using the daily approach (daily.max, daily.mean, daily.min), and the stem cycle approach (cycle.max), representative of each cycle's peak (phase 4, max).

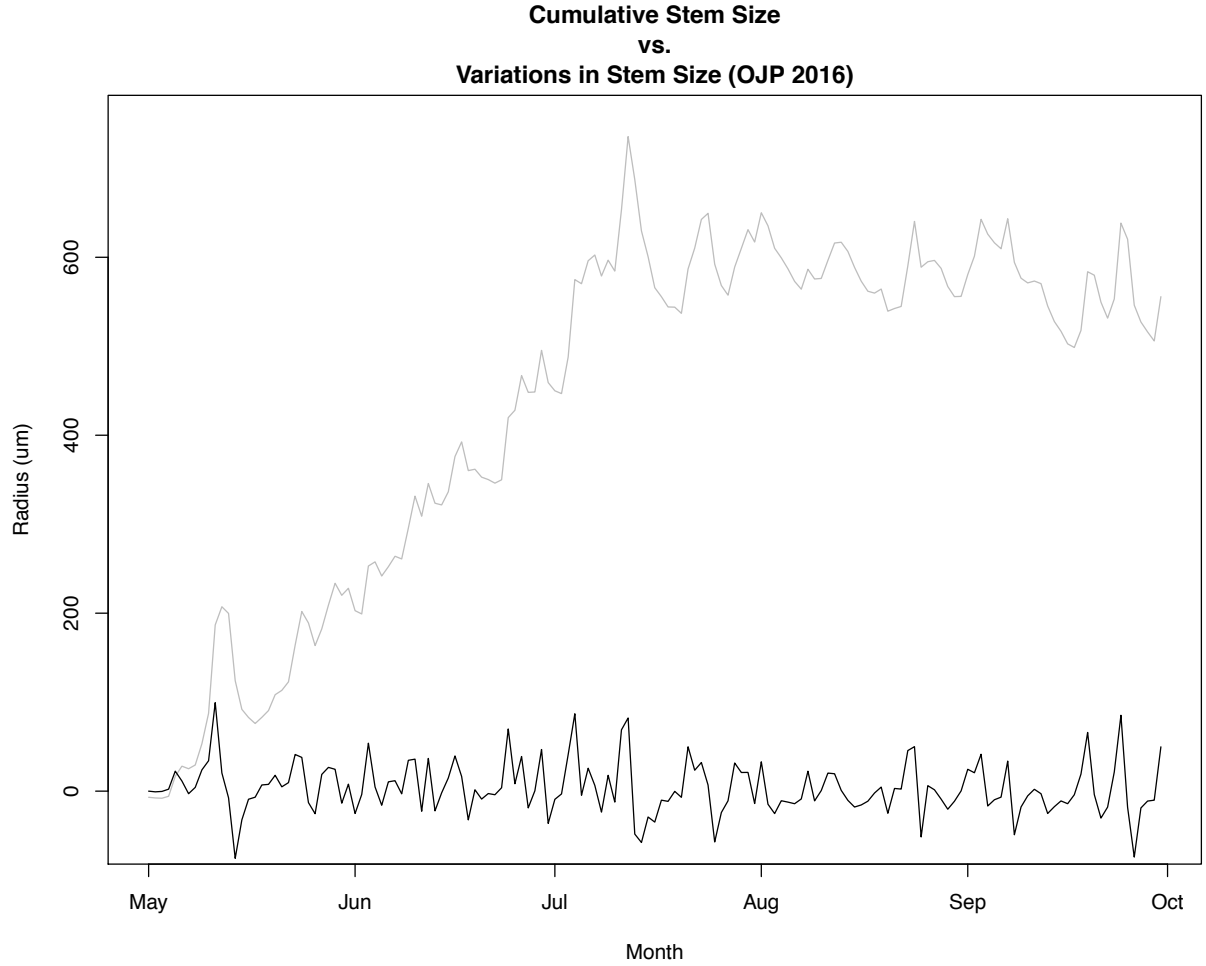

Figure B.5: A comparison of representation techniques for mean daily stem size data. Cumulative mean daily stem size is shown in grey, and variations in mean daily stem size in black. This example data were collected in 2016 at the OJP site.

APPENDIX C

TESTING FOR NORMALITY IN THE TREE RING DATA AND COMPARING PARAMETRIC AND NON-PARAMETRIC CORRELATION COEFICIENTS

Pearson's correlation is a widely used and common test for assessing the linear relationship between two variables. One of the main assumptions underlying this test is that the data are normally distributed. It is often said that this assumption must be met if we are to draw accurate conclusions from hypothesis testing. However, it has been shown that Pearson's correlation coefficient (r) is relatively insensitive to data non-normality, and that the rate of type 1 and type 2 errors only increases when data are exceptionally non-normal, with a "highly kurtotic" shape (Bishara & Hittner, 2012). While bootstrapping or other resampling procedures may help further reduce the possibility for error in hypothesis testing, in cases where we are dealing with non-normal data, a nonparametric test for correlation may still be favored (Bishara & Hittner, 2012). The most common nonparametric tests for correlation are Spearman's rho, and Kendall's tau.

The Shapiro-Wilk test is used to assess normality in the daily stem size change (ΔR) data. This is done over a moving window to test for data normality within each of the 30-day intervals over which dynamic relationships between ΔR and local meteorological variables are assessed in Chapter 2, and dynamic relationships between ΔR and ecosystem carbon are assessed in Chapter 3 (Figure C.1). Furthermore, non-bootstrapped versions of the moving-window correlation analyses undertaken in Chapters 2 and 3, are computed using Pearson's r, Spearman's rho, and Kendall's tau, and the results and conclusions drawn from these independent analyses are compared (Figure C.2).

Data normality varies significantly between species and growing seasons (Figure C.1). The percentage of intervals that contain normal data in each growing season and for a given species varies from 12% (jack pine in 2015) to 90% (jack pine in 2016). In general, the 2015 growing season contains the largest proportion of intervals containing non-normal ΔR data, and the 2016 growing season contains the largest proportion of intervals containing normally distributed ΔR data. Intervals during the 2017 and 2018 growing seasons are more likely to contain normal data, however the percentage of intervals containing normally distributed data

relative to the total is often not far above 50%. The only conclusion that can be drawn here is that normality in the ΔR data over a given 30-day window within the growing season is haphazard.

Repeating the same moving-window correlation analysis using parametric (Pearson's r) and nonparametric (Spearman's rho, and Kendall's tau) correlation coefficients yields results that, in most cases, are practically identical (Figure C.2). The 2015 growing season is the only growing season during which results between parametric and non-parametric tests differ significantly. During the second half of the 2015 growing season, Pearson's correlations highlight statistically significant negative relationships between the ΔR of jack pine (OJP), black spruce (OBS), and eastern larch (LA), and ecosystem production (GEP and NEP). A relationship which becomes insignificant when nonparametric tests for correlation are applied (Figure D.2). When Pearson's correlations are bootstrapped however, as they are in Chapter 3 (Figure 3.4), the results more closely resemble those from the non-parametric tests. Therefore, the potential for type 1 error, in this case the identification of potentially false relationships by Pearson's r during the growing season with the highest proportion of intervals containing non-normal data, would seem to have been mitigated through the process of bootstrapping. During the three remaining growing seasons in the observation period (2016, 2017, and 2018), it can be said that there are minor differences in the presence and persistence of significant relationships highlighted by each test, but none that would impact the observations made, or conclusions drawn in Chapters 2 or 3. Therefore, due to its widespread application in dendroclimatology, and due to the proven ability of bootstrapping to minimize type 1 error in response to data non-normality, Pearson's r remains the most desirable test for correlation, allowing for the use of relatively standard methodology, which increases ease of application and replicability.

Reference

Bishara, A., & Hittner, J. (2012). Testing the Significance of a Correlation with Nonnormal Data: Comparison of Pearson, Spearman, Transformation, and Resampling Approaches. *Psychological Methods*, *17*(3), 399–417. https://doi.org/10.1037/a0028087

Figure C.1: Intervals containing non-normal ΔR data are identified with 95% confidence and are indicated with a pink box in the bottommost portion of each graph, intervals which contain normally distributed ΔR data are indicated by a blue box in the topmost portion of each graph. The percentage of intervals containing normal data relative to the total number of intervals is recorded in the top right corner of each graph. Graphs are arranged in a two-dimensional matrix with growing season year listed above each column, and site/species names labeled to the right of each row.

Pearson's

Spearman's

Kendall Tau

Figure C.2: Comparing results from Pearson's, Spearman's, and Kendall's tests for correlation. Relationships are flagged (*) if correlation coefficients surpass critical values required for statistical significance.

APPENDIX D

LONG-TERM CLIMATIC TRENDS IN PRINCE ALBERT

To get a sense of how conditions have changed in Prince Albert over a timeframe relevant to the research presented in this dissertation, an analysis of trends in monthly precipitation (Figure B.1) and temperature (Figure B.2) was undertaken. Data of monthly total adjusted precipitation, and homogenized mean monthly temperature, from the Environment and Climate Change Canada (ECCC) climate stations in Prince Albert (#4056240 and #4056241), were acquired online at https://www.canada.ca/en/environment-climate-change/services/climate-change/science-research-data/climate-trends-variability/adjusted-homogenized-canadian-data.html. These climate records are complete from 1890 – 2012 for precipitation, and from 1890 – 2018 for temperature. For each month, trends in the temperature and precipitation data, since 1890, and since 1950, were assessed by plotting time series fit with linear trend-lines using the least-squares method, and by comparing the first and last 30-year mean from each time series as a measure of change. The earliest 30-year means, the two reference periods, span periods from 1890 – 1919, and from 1950 – 1979, for both temperature and precipitation. The latest 30-year means span the period from 1983 – 2012 for precipitation, and 1989 – 2018 for temperature. Percent change in precipitation was calculated as the difference between the last and first 30-year means divided by the first 30-year mean.

The months with the most marked increases in total precipitation are April and October, with respective increases of 64% and 47% relative to the 1890 reference period (the 30-year mean between 1890 – 1919). Compared with this period, nearly all months saw increases in precipitation, except August and November. Other months with notable increases in precipitation include January, May, June, July, and September.

Relative to both reference periods (1890 – 1919, and 1950 – 1979), temperature has increased during every month except October, which experienced little change. The most significant changes in temperature occurred in January, with a 4.4°C and 5.2°C increase relative to the 1890 and 1950 reference periods respectively. There were also marked increases in temperature in February (4.6°C, and 2.3°C) and March (3.8°C and 3.1°C). The remainder of the increases in mean monthly temperature were around the 1°C mark.

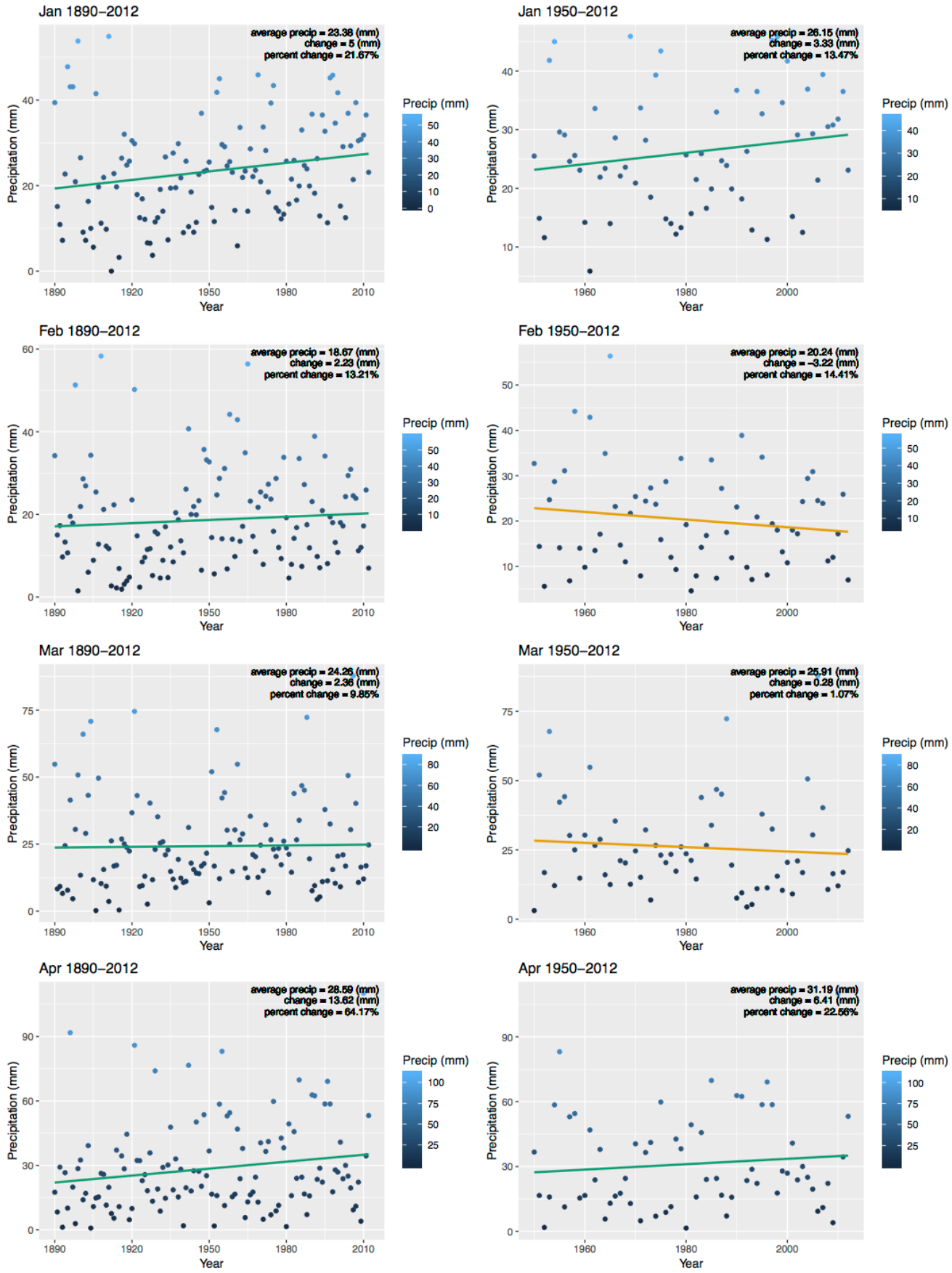
Jan 1890–2012
average precip = 23.38 (mm)
change = 5 (mm)
percent change = 21.67%
Jan 1950–2012
average precip = 26.15 (mm)
change = 3.33 (mm)
percent change = 13.47%
Feb 1890–2012
average precip = 18.67 (mm)
change = 2.23 (mm)
percent change = 13.21%
Feb 1950–2012
average precip = 20.24 (mm)
change = −3.22 (mm)
percent change = 14.41%
Mar 1890–2012
average precip = 24.26 (mm)
change = 2.36 (mm)
percent change = 9.85%
Mar 1950–2012
average precip = 25.91 (mm)
change = 0.28 (mm)
percent change = 1.07%
Apr 1890–2012
average precip = 28.59 (mm)
change = 13.62 (mm)
percent change = 64.17%
Apr 1950–2012
average precip = 31.19 (mm)
change = 6.41 (mm)
percent change = 22.56%
Precipitation (mm)
Year
Precip (mm)

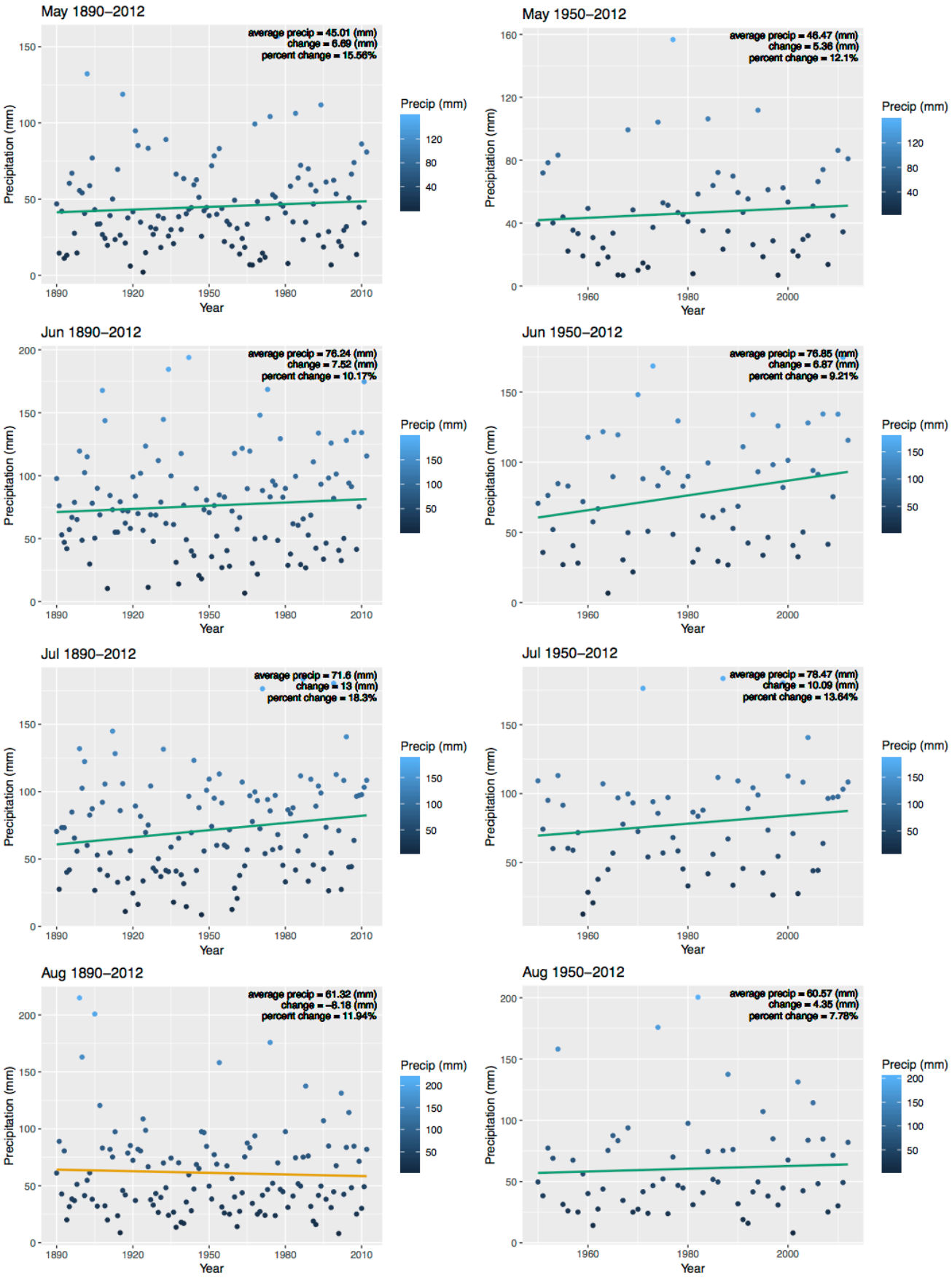
May 1890–2012
average precip = 45.01 (mm)
change = 6.69 (mm)
percent change = 15.56%
May 1950–2012
average precip = 46.47 (mm)
change = 5.36 (mm)
percent change = 12.1%
Jun 1890–2012
average precip = 76.24 (mm)
change = 7.52 (mm)
percent change = 10.17%
Jun 1950–2012
average precip = 76.85 (mm)
change = 6.87 (mm)
percent change = 9.21%
Jul 1890–2012
average precip = 71.6 (mm)
change = 13 (mm)
percent change = 18.3%
Jul 1950–2012
average precip = 78.47 (mm)
change = 10.09 (mm)
percent change = 13.64%
Aug 1890–2012
average precip = 61.32 (mm)
change = −8.18 (mm)
percent change = 11.94%
Aug 1950–2012
average precip = 60.57 (mm)
change = 4.35 (mm)
percent change = 7.78%
Precipitation (mm)
Year
Precip (mm)

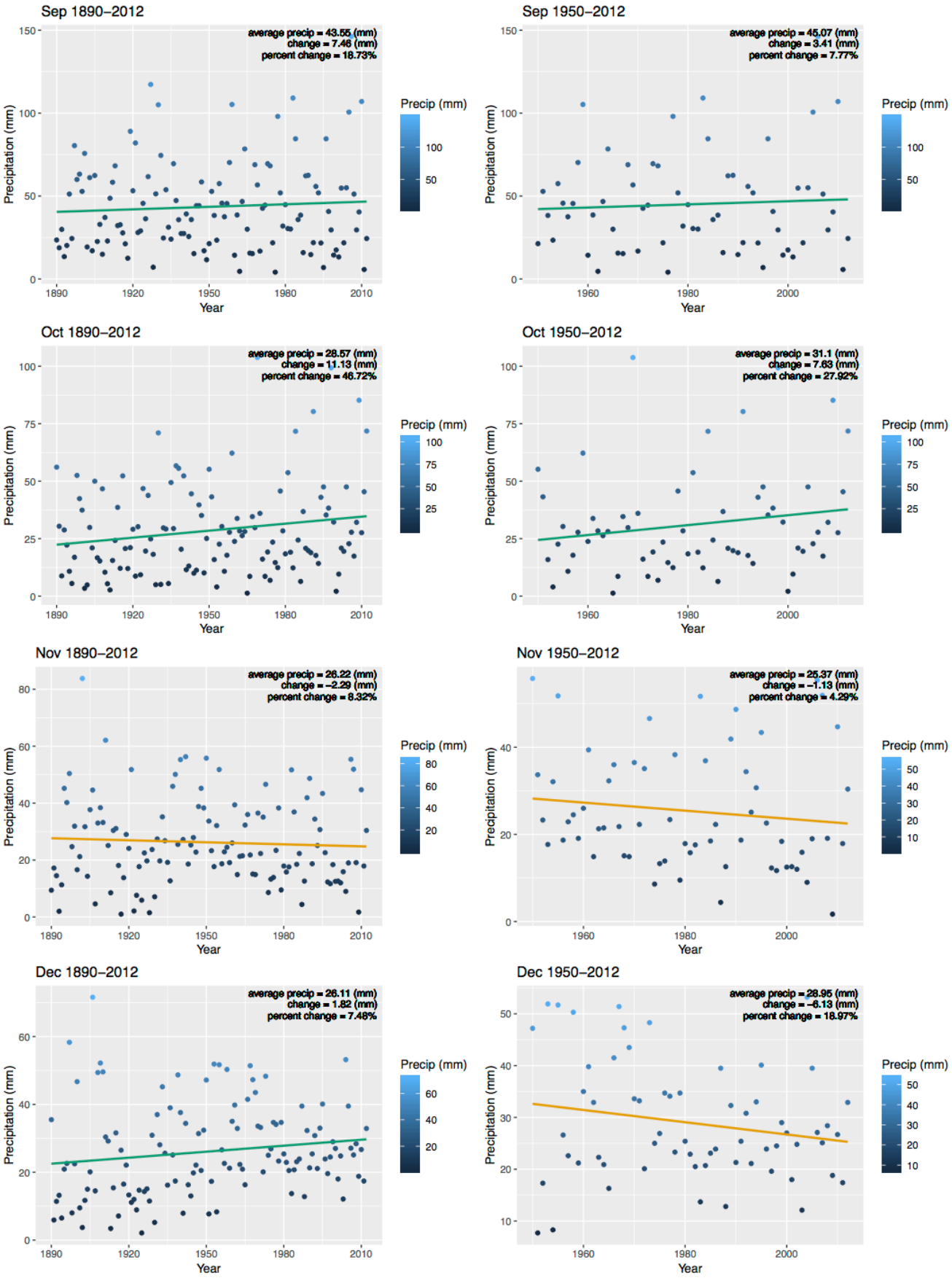
Sep 1890–2012
average precip = 43.55 (mm)
change = 7.46 (mm)
percent change = 18.73%
Sep 1950–2012
average precip = 45.07 (mm)
change = 3.41 (mm)
percent change = 7.77%
Oct 1890–2012
average precip = 28.57 (mm)
change = 11.13 (mm)
percent change = 46.72%
Oct 1950–2012
average precip = 31.1 (mm)
change = 7.63 (mm)
percent change = 27.92%
Nov 1890–2012
average precip = 26.22 (mm)
change = −2.29 (mm)
percent change = 8.32%
Nov 1950–2012
average precip = 25.37 (mm)
change = −1.13 (mm)
percent change = 4.29%
Dec 1890–2012
average precip = 26.11 (mm)
change = 1.82 (mm)
percent change = 7.48%
Dec 1950–2012
average precip = 28.95 (mm)
change = −6.13 (mm)
percent change = 18.97%
Precip (mm)
Precipitation (mm)
Year

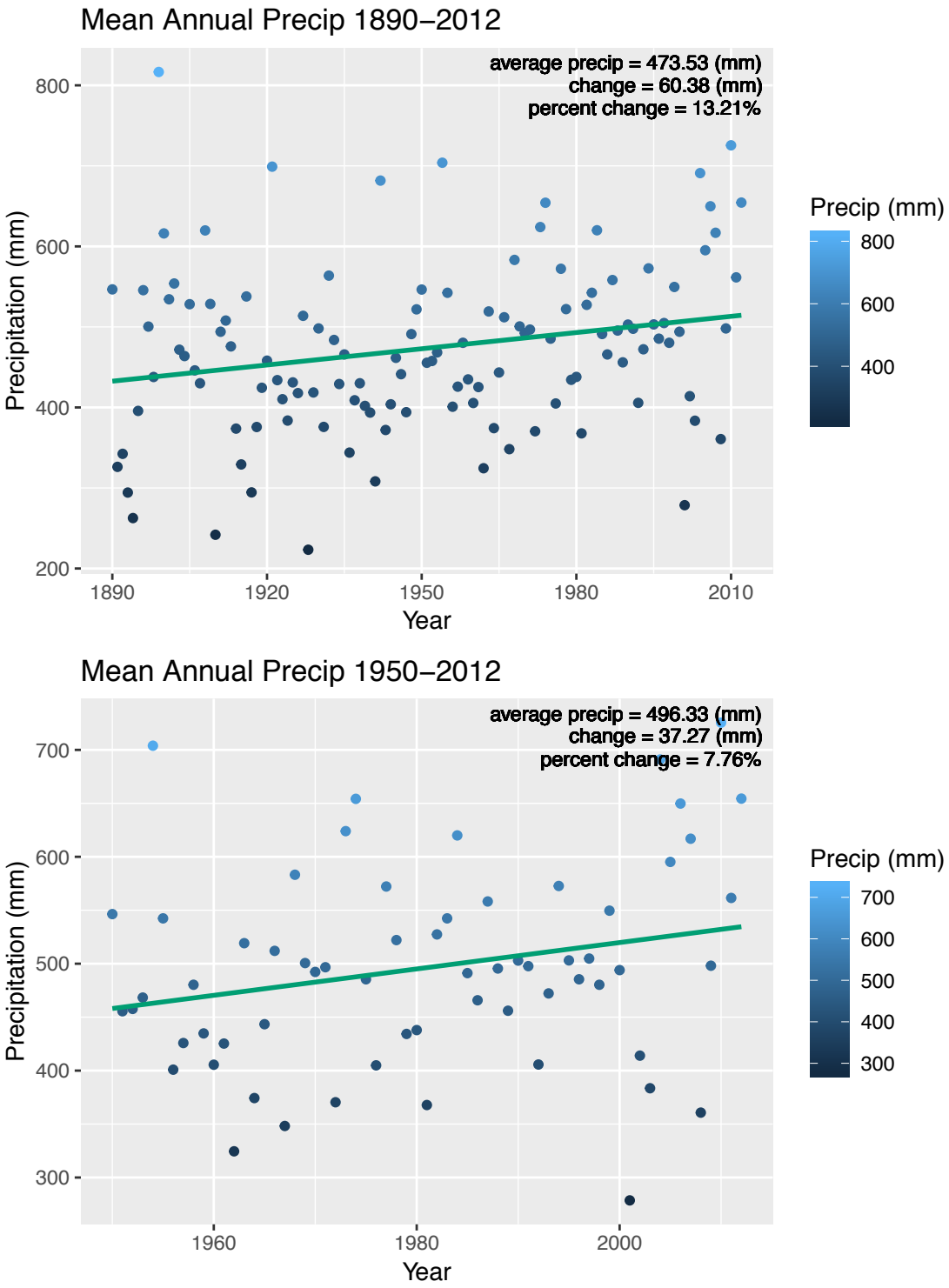

Figure D.1: Long-term trends in total monthly precipitation from 1890-2012 (left column) and from 1950-2012 (right column), as well as mean annual precipitation (bottommost two graphs). The linear trend line was fit using the least-squares method and is green if positive and yellow if negative. The change reported in the top right corner of each graph represents the difference between the first and last 30-year mean of each record. Percent change is calculated as the difference of the last and first 30-year means divided by the first 30-year mean.

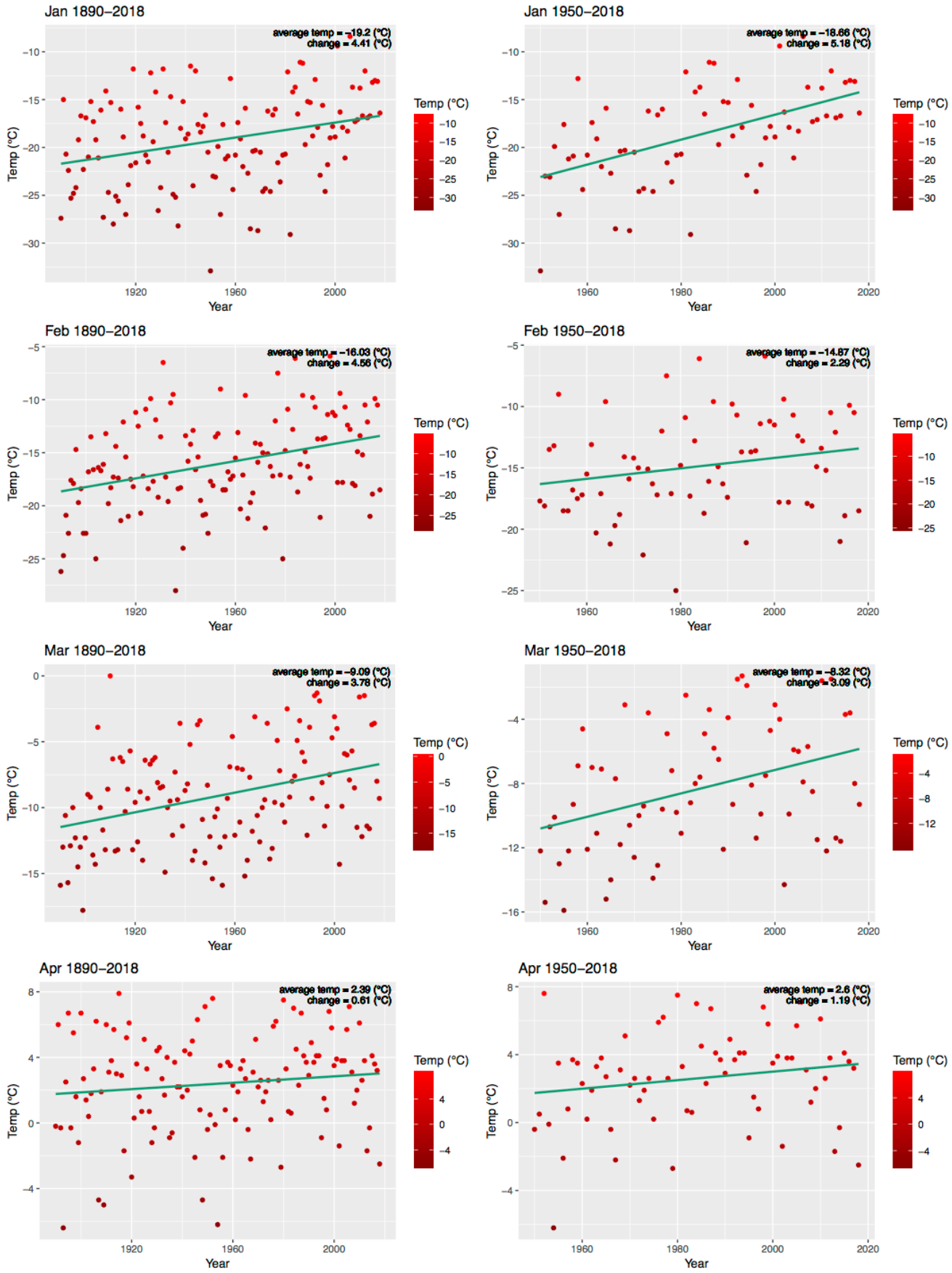
Jan 1890–2018
average temp = −19.2 (°C)
change = 4.41 (°C)
Jan 1950–2018
average temp = −18.66 (°C)
change = 5.18 (°C)
Feb 1890–2018
average temp = −16.03 (°C)
change = 4.56 (°C)
Feb 1950–2018
average temp = −14.87 (°C)
change = 2.29 (°C)
Mar 1890–2018
average temp = −9.09 (°C)
change = 3.78 (°C)
Mar 1950–2018
average temp = −8.32 (°C)
change = 3.09 (°C)
Apr 1890–2018
average temp = 2.39 (°C)
change = 0.61 (°C)
Apr 1950–2018
average temp = 2.6 (°C)
change = 1.19 (°C)
Temp (°C)
Year

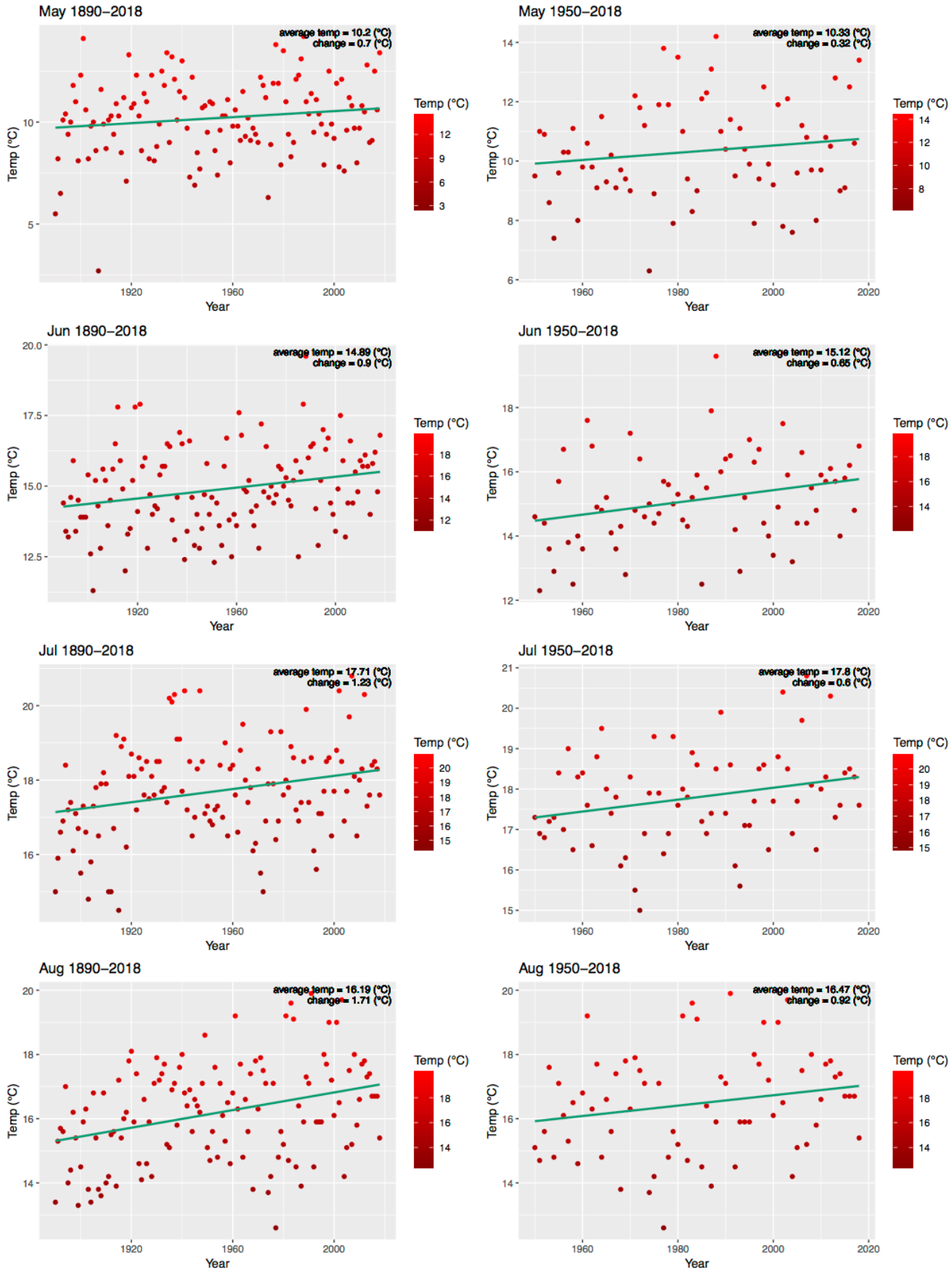
May 1890–2018
average temp = 10.2 (°C)
change = 0.7 (°C)
May 1950–2018
average temp = 10.33 (°C)
change = 0.32 (°C)
Jun 1890–2018
average temp = 14.89 (°C)
change = 0.9 (°C)
Jun 1950–2018
average temp = 15.12 (°C)
change = 0.65 (°C)
Jul 1890–2018
average temp = 17.71 (°C)
change = 1.23 (°C)
Jul 1950–2018
average temp = 17.8 (°C)
change = 0.6 (°C)
Aug 1890–2018
average temp = 16.19 (°C)
change = 1.71 (°C)
Aug 1950–2018
average temp = 16.47 (°C)
change = 0.92 (°C)
Temp (°C)
Year

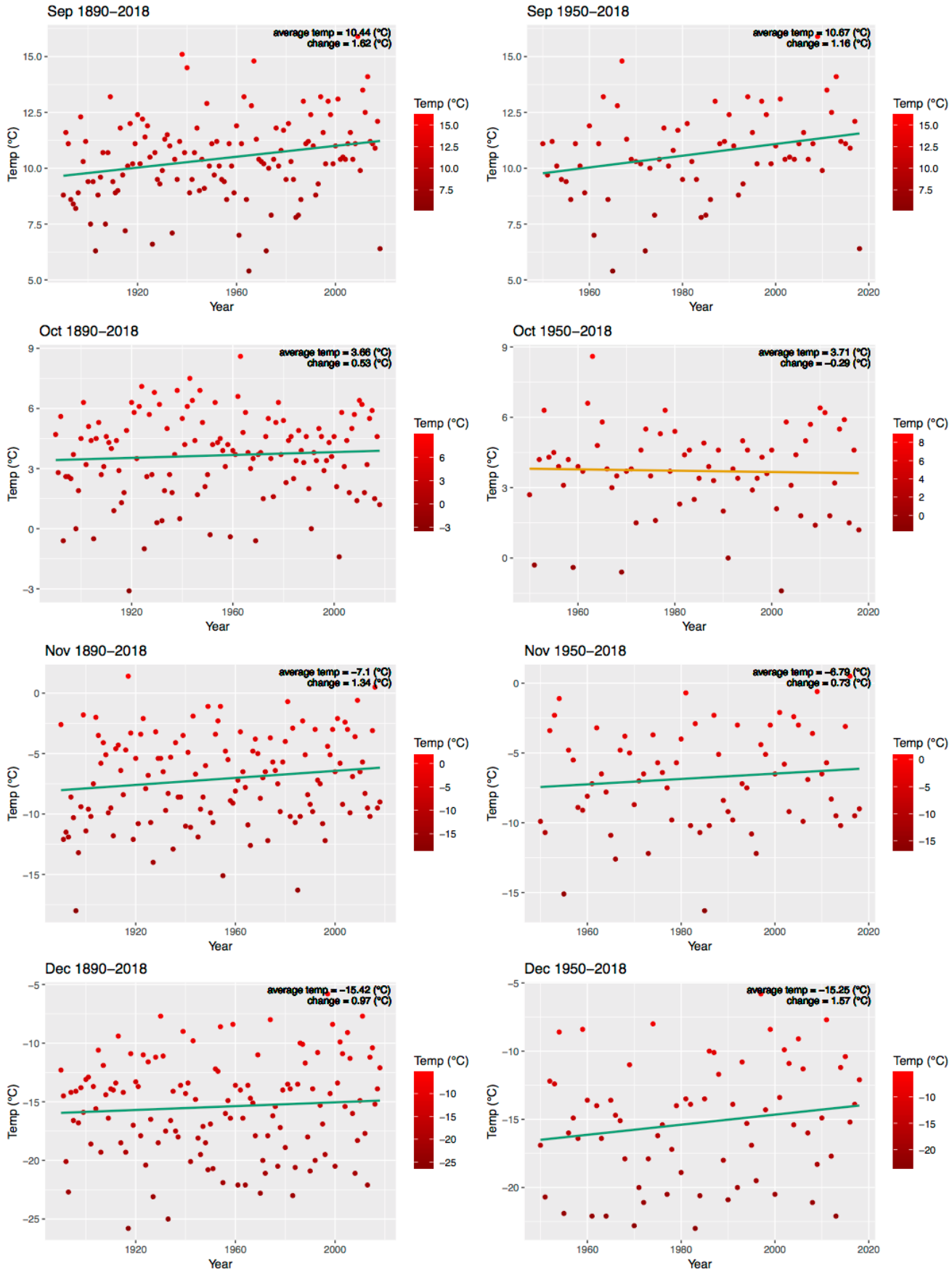
Sep 1890–2018
average temp = 10.44 (°C)
change = 1.62 (°C)
Sep 1950–2018
average temp = 10.67 (°C)
change = 1.16 (°C)
Oct 1890–2018
average temp = 3.66 (°C)
change = 0.53 (°C)
Oct 1950–2018
average temp = 3.71 (°C)
change = −0.29 (°C)
Nov 1890–2018
average temp = −7.1 (°C)
change = 1.34 (°C)
Nov 1950–2018
average temp = −6.79 (°C)
change = 0.73 (°C)
Dec 1890–2018
average temp = −15.42 (°C)
change = 0.97 (°C)
Dec 1950–2018
average temp = −15.25 (°C)
change = 1.57 (°C)
Temp (°C)
Year

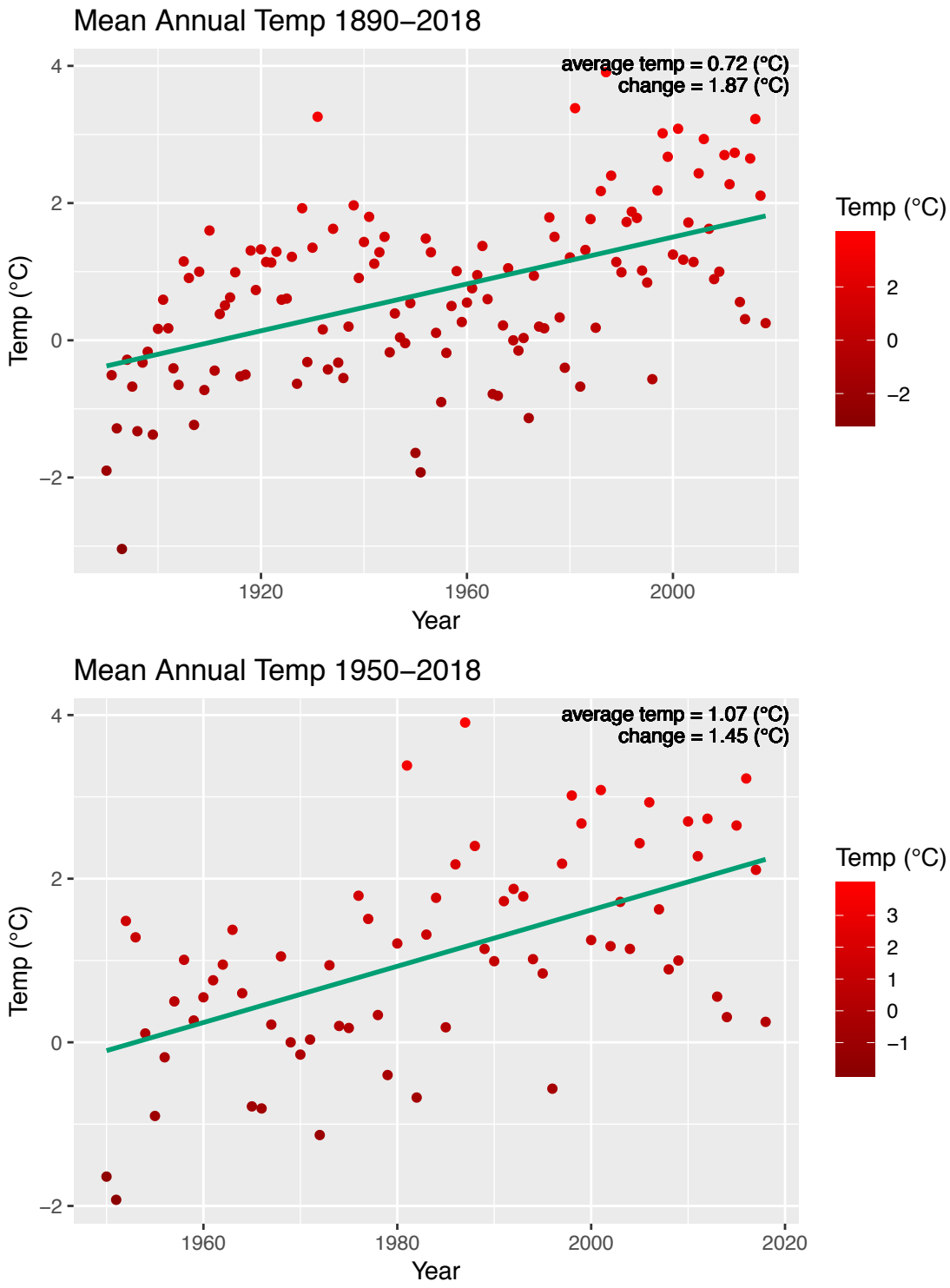

Figure D.2: Long-term trends in mean monthly temperature from 1890-2018 (left column) and from 1950-2018 (right column), as well as total annual temperature (bottommost two graphs). The linear trend line was fit using the least-squares method and is green if positive and yellow if negative. The change reported in the top right corner of each graph represents the difference between the first and last 30-year mean of each record. Percent change is calculated as the difference of the last and first 30-year means divided by the first 30-year mean.